DIRECT AND INDIRECT EVIDENCE FOR THE ENDOSOMOLYTIC PROPERTIES OF POLY(AMIDOAMINE)S

by

N. G. Pattrick B.Sc. (Hons)

A thesis submitted to the University of London in partial fulfillment of the requirements for the degree of Doctor of Philosophy

Center for Polymer Therapeutics
School of Pharmacy
Faculty of Medicine
University of London

December 2002

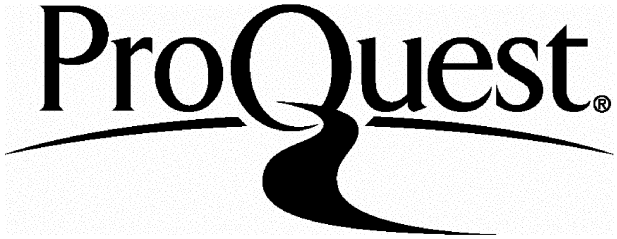

This work is dedicated to my family, whom I love dearly

Acknowledgements

Firstly I would like to thank Professor Ruth Duncan for her help, support and belief in me throughout my Ph.D. I would also like to acknowledge Dr Steve Brocchini for his patience, help and support, especially during the move to Cardiff. I would also like to thank the collaborator Professor Paolo Ferruti, for giving me the opportunity to study in Milan, and supplying me with large amounts of PAAs.

Many thanks are also due to my fellow work colleagues at CPT, who not only provided me with intellectual stimulation, but gave me emotional support, happiness and many laughs. I would especially like to thank Elinor, for having a positive attitude to life and for showing me the delights of Cardiff nightlife. I would also like to thank Ruthie, for being there with me through thick and thin. Thanks are also due to Richard, for his common sense, Ryan, for his cheeky sense of humour, and Myrto, for her enthusiasm and constant willingness to help others. I would also like to acknowledge Sam, for her continued friendship and endless supply of gossip, and Rhian for taking me in. I would also like to thank Michelle and Peli for helpful discussions on PAA work and Maria for helping me with chemistry.

Finally, I would like to thank my family, for their love and constant support during my Ph.D, which I am forever grateful. Thanks also to Maria, who has always been there, and to Nolan, for sticking with me.

Abstract

Many potential therapeutics (such as genes, antisense and protein drugs) have their targets in a variety of intracellular compartments and thus it is essential to develop intracytoplasmic delivery vectors to mediate this process, in particular, escape of the therapeutic from endosomal vesicles to the cytoplasm. It is in this context that amphoteric, biocompatible, biodegradable poly(amidoamine) (PAA) polymers were studied. These polymers are able to display pH-dependent conformational changes in response to pH, thus displaying membrane-permeabilising properties at endosomal but not physiological pH. In this thesis different methods were used to demonstrate their endosomolytic properties.

The ability of PAAs to mediate transfection of the plasmid pSV-β-galactosidase in HepG2 cells provided first direct evidence for their endosomolytic ability. For the first time it was shown that the PAAs termed ISA 1 and 4 were able to mediate delivery of the non-permeant toxins ricin A-chain (RTA) and gelonin to the cytoplasm of B16F10 cells. Toxin cytosolic delivery was indicated by a decrease in the IC_{50} value from > 1.8mg/mL to ≤ 0.65mg/mL. To investigate the intracellular trafficking of PAAs alone and in combination with gelonin, fluorescent-labelled PAAs and gelonin were prepared for fluorescence microscopy. Uptake studies showed that the intracellular fate of the PAA and toxin differed according to the PAA structure used.

Direct evidence for PAA-mediated intracellular membrane disrupting capability was investigated using isolated rat liver lysosomes as a model membrane system. After intravenous (i.v.) administration of ISA 1 (50mg/kg), nearly a 3-fold increase in the lysosomal enzyme N-acetyl-β-D-glucosaminidase (NAGase) was observed compared to the control. Morphologically ISA 1-containing lysosomes appeared less densely stained compared to the control.

Finally, an ISA 1-gelonin construct was examined for endosomolytic ability. However conjugation of gelonin alleviated the pH-dependent membrane rupturing ability of the parent PAA.

In conclusion, evidence for the endosomolytic properties of PAAs was demonstrated. However in order for a successful PAA-conjugate to be developed, it is important that the activity of PAAs and/or the drug is maintained upon conjugation.

Contents

List of Figures

List of Tables

Abbreviations

ALL	acute lymphocytic leukaemia
AIDS	acquired immune deficiency syndrome
APS	ammonium persulphate
bp	base pairs
BDMA	benzyldimethylamne
BCA	bicinchoninic acid
BSA	bovine serum albumin
CCV	claithrin-coated vesicle
CLSM	confocal laser scanning microscopy
CCC	covalently closed circular
Dc-Chol	3β-(N-[N-(dimethylaminoethane)carbamoyl] cholesterol
DDSA	dodecenyl succinic anhydride
DDW	double distilled water
DMSO	dimethyl sulphoxide
DMEAMA	poly(2-dimethyl amino ethyl) methacrylate
DNA	deoxyribonucleic acid
DOGS	dioctadecylamidoglycylspermine
DOPE	dioleoyl phosphatidylethanolamine
DOTAP	dioleoyl(trimethylammonio)propane
DOTMA	(N[1-(2,3-dioleyloxy)propyl]-*N,N,N*-trimethyl ammonium)
EDTA	ethylenediaminetetraacetic acid
EGF	epidermal growth factor
EM	electron microscopy
EPR	Enhanced Permeability and Retention Effect
EtBr	ethidium bromide
FCS	foetal calf serum
FDA	Food and Drug Adminstration
FITC	fluorescein
GPC	gel permeation chromatography
h	hour(s)
HPMA	N-(2-hydroxypropyl)methacrylamide
IPEC	interpolyelectrolyte complex
i.v.	intravenous
mRNA	messenger ribonucleic acid
MTT	3-(4,5-dimethylthiazol-2-yl)-2,5-diphenyltetrazolium bromide
Mw	molecular weight
NAGase	N-acetyl-β-D-glucosaminidase
OG	oregon green
OG-SE	oregon green 488 succinimidyl ester
OG-COOH	oregon green 488 carboxylic acid
PAAs	poly(amidoamine)s
PBS	phosphate buffered saline
PCI	photochemical internalisation
PEAAc	poly(ethyl acrylic acid)
PEG	poly(ethylene glycol)
PEI	poly(ethylenimine)

PPAAc	poly(propyl acrylic acid)
RBC	red blood cell
RES	reticulo-endothelial system
RNA	ribonucleic acid
RSA	relative specific activity
RTA	ricin A-chain
RTB	ricin B-chain
S.D.	standard deviation
SDS	sodium dodecyl sulphate
SDS-PAGE	sodium dodecyl sulphate polyacrylamide gel electrophoresis
SEM	scanning electron microscopy
SMANCS	styrene-co-maleic anhydride-neocarzinostatin
TEM	transmission electron microscopy
TEMED	N,N,N,N'-tetramethyethylenediamine
TLC	thin layer chromatography
TR-COOH	texas red carboxylic acid
TR-SE	texas red succinimidyl ester
VLS	vascular leak syndrome
(v/v)	volume for volume
(w/v)	weight for volume
(w/w)	weight for weight

CHAPTER 1

INTRODUCTION

1.1 Intracytoplasmic Delivery

The emergence of molecular biology and the recent completion of the Human Genome Project have led to the identification of many new disease targets that have the possibility to be treated at the molecular level. Gene therapy, which acts to replace missing or defective genes, is one such therapeutic strategy, however, more recently, other methods have been examined (discussed in section 1.6). In practise, the efficacy of these macromolecular therapeutics is limited due to their inability to enter the intracellular compartments where their targets lie. For example genes have their target in the cell nucleus and antisense oligonucleotides have their targets in the cell cytoplasm.

Thus, the main challenge at present is the design of a safe, efficient vector capable of large-scale manufacture, with the ability to deliver macromolecules not only to target cells but also to the appropriate intracellular location. Targeting, transport across biological membranes and trafficking of the vector to the designated organelle have all been shown to be rate-limiting steps for the cytosolic delivery of macromolecular therapeutics (Ferruti et al, 2002; Tan et al, 2000, Renes, et al, 2000). Therefore, a potential intracytoplasmic delivery system must be able to overcome all these obstacles if it is to be used successfully in the clinic. Although many different intracytoplasmic delivery systems are being explored (section 1.7), this study has focused on the use of PAA polymers as vectors to mediate intracytoplasmic delivery.

Systematic evaluation of PAAs over the last 20 years has shown that structures can be synthesised to include properties such as low toxicity, non-immunogenicity, ability to passively target solid tumours by the Enhanced Permeability and Retention Effect (EPR) effect (section 1.4), and membrane permeabilising properties in response to a decrease in pH (reviewed in Ferruti et al, 2002). This property in particular has conferred PAAs with potential endosomolytic properties and thus has made them attractive agents for the delivery of genes and proteins.

Initial experiments using the PAA termed MBI conjugated to triton X-100 indicated the bioresponsiveness of PAAs, (Duncan et al, 1994), and therefore it was considered important to verify and quantitate this property by obtaining direct and indirect evidence for PAA-mediated intracytoplasmic delivery. In addition, with the overall aim of this project being the utilisation of PAAs to deliver macromolecular therapeutics such as proteins to the cell cytoplasm, PAA bioresponsiveness was tested after conjugation to proteins.

In order to appreciate and understand this work, it is important to have background knowledge on the topics of drug delivery systems, endocytosis, polymer chemistry particularly in relation to PAAs, and endosomolytic polymers in general. Thus each of these topics will be reviewed below.

1.2 Targeted Drug Delivery Vehicles

Targeting of a substance to specific regions in the body can be divided into three levels. First order targeting describes targeting to a specific organ; second order targeting is associated with cell/tissue specific targeting; and third order targeting describes targeting at the organelle level (figure 1.1). The idea of drug targeting to a specific region in the body was first proposed by Ehrlich who put forward the concept of the "magic bullet" in 1906. Since then a number of different vector targeting systems have been described, which can target either actively or passively.

Active targeting, which relies on ligand-receptor interactions, facilitates the selective localisation of a drug-construct carrying the ligand to a specific target, increasing its local concentration at that particular site. Recently, vectors for intracytoplasmic delivery that utilise active targeting are being developed. Antibody-drug conjugates (reviewed in Dubowchik and Walker, 1999), polymeric vectors such as N-(2-hydroxypropyl)methacrylamide (HPMA) copolymer doxorubicin-galactosamine (PK2) (Seymour et al, 2002) and polyethylenimine (PEI) which has been conjugated to various ligands, (reviewed in Kircheis et al, 2001a) are examples of such systems.

Passive targeting exploits the "natural" (passive) distribution pattern of a drug carrier *in vivo*, without an additional targeting moiety (Crommelin et al, 2001). An example of passive targeting affects particulate systems (0.1-7μm) and charged molecules. These molecules can passively accumulate in cells of the reticulo-endothelial system (RES) (also known as the mononuclear phagocyte system). This system is part of the body's immune defence, comprising circulating blood monocytes and both fixed and free macrophages responsible for the removal of particulate antigens. These molecules are readily phagocytosed by these types of macrophages and thus accumulate in the liver and spleen as a result of an abundance of mononuclear phagocytes and a rich blood supply in these organs. This RES capture of molecules has big implications in the efficacy of many therapeutics (reviewed in Davis, 2002) and thus much research has focused on conferring "stealth" properties onto them, which effectively shield them from macrophages (Kircheis et al, 2001b).

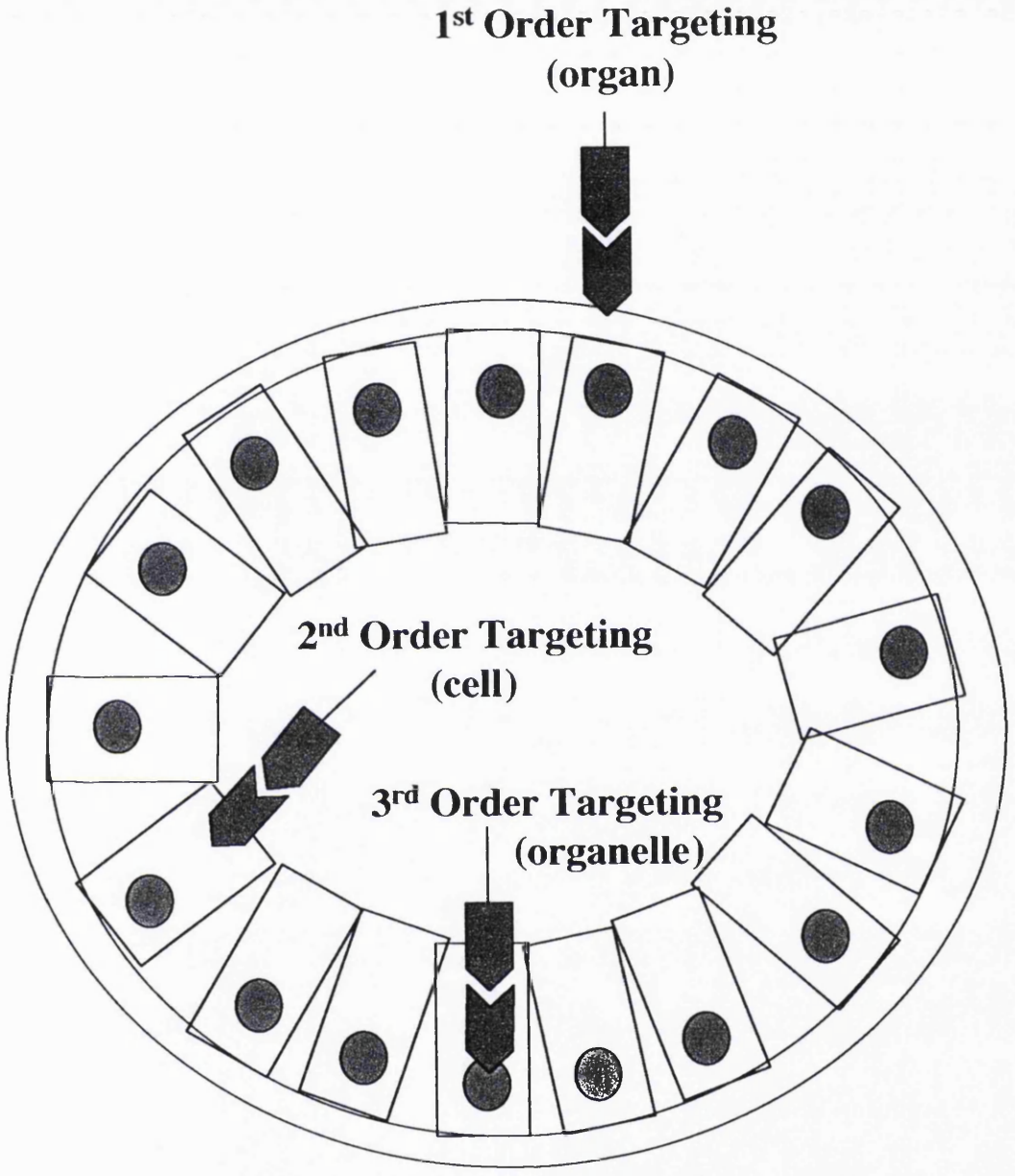

Figure 1.1 Levels of targeted delivery

Another example of passive targeting which is of relevance in this study is passive accumulation of macromolecules (which do not exceed 0.2 μm in size) to regions of inflammation or tumour sites by the EPR effect. This is discussed in more detail in section 1.4.

As PAAs are part of a growing field known as polymer therapeutics, a brief introduction to this will be given including examples of polymers which exhibit both active and passive targeting.

1.3 Polymer Therapeutics

The use of polymeric drug delivery systems became widely established through the development of depot formulations. Depot formulations usually consist of an insoluble, biodegradable polymer which is implanted into the body and releases drug in a sustained manner over a period of time. Gliadel® (Gilford Pharmaceuticals), is a commercially available depot formulation which is used for the treatment of glioblastoma multiforme. As this implant provides local delivery of the anticancer agent, it can be implanted in the brain during surgery, post- removal of the primary tumour (Brem et al, 1995). The success of these types of systems led to the design and development of water-soluble polymers which are now the core element of an emerging field known as polymer therapeutics.

Polymer therapeutics (reviewed in Duncan et al, 1996) encompasses the field of water-soluble polymeric drugs (reviewed in Shaunak et al, 1998), polymer-drug conjugates (reviewed in Duncan et al, 2001), polymer-protein conjugates (reviewed in Nucci et al, 1991; reviewed in Maeda, 2001), polymeric intracytoplasmic delivery vehicles (Richardson et al, 1999a; Boussif et al, 1995) and polymeric micelles (reviewed in Jones and Leroux, 1999) that entrap drugs by covalent linkage.

The use of polymers in cancer therapy has proved to have advantages over other types of therapies for a number of reasons. Firstly, synthetic polymers are already used daily for a wide array of biomedical applications including contact lenses, plasma expanders, prostheses and pharmaceutical excipients (Duncan, 1985). Additionally, polymeric structures can be tailor-made to optimise required features for drug delivery such as molecular weight and inclusion of targeting moieties. Conjugation of polymers to drugs also offers an increase in drug solubility, improves pharmacokinetics, decreases drug-related systemic toxicity and in the instance of polymer conjugation to

proteins, reduces immunogenicity (reviewed in Nucci et al, 1991). Importantly, circulating macromolecules such as polymers offer passive tumour targeting by the EPR effect (discussed in section 1.4).

Polymer-drug conjugates were first proposed by Helmut Ringsdorf and fellow colleagues 20-30 years ago who put forward the Ringsdorf model, in which a biostable or biodegradable polymeric backbone is used as a carrier for a drug, which is attached to the polymer via a biodegradable spacer. Additionally, a targeting moiety can be attached to the polymeric backbone to achieve specific localisation of the carrier in the body (Ringsdorf, 1975). Synthetic polymers typically exist as a range of molecular masses and this is characterised by polydispersity. Polydispersity is expressed as M_w/M_n. Weight-average molar mass (M_w) is defined as the sum of the products of the molar mass of each fraction multiplied by its weight fraction. Number-average molar mass (M_n) is defined as the sum of the products of the molar mass of each fraction multiplied by its mole fraction. Therefore the closer the polydispersity is to 1.0 the more uniform the polymer molecular weight (Young and Lovell, 1996).

1.3.1 Polymer-Protein Conjugates

One of the main aims of this thesis was to design PAA-protein conjugates with potential anti-cancer activity, whereby PAA intracytoplasmic ability would be utilised to deliver the conjugated cytotoxic protein to its destination in the cytosol. Therefore, it is important to understand the literature surrounding other polymer-proteins, in order to realise the advantages and limitations to this approach. Thus, an introduction to this topic is given below.

The study of the properties of polymer-protein conjugates such as antibodies and cytokines that occurred along with the development of polymer-drug conjugates, has led to several polymer-protein conjugates becoming commercially available or in late phase clinical testing (table 1.1).

Conjugation of proteins to polymers has been shown to provide many advantages including: a) prolonged protein circulation time (aiding tumour targeting by the EPR effect); b) reduced protein immunogenicity; c) increased protein stability and d) improved protein solubility (reviewed in Ulbrich et al, 2000; reviewed in Seymour et al, 1991; reviewed in Duncan, 2000).

Table 1.1 Polymer-protein conjugates on the market and in late phase development

Polymer-protein	Company	Use	Status	Reference
PEG-adenosine deaminase (ADAGEN®)	Enzon, Inc.	Severe combined immunodeficiency syndrome	Market	Hershfield et al, 1987
PEG-L-asparaginase (ONCASPAR®)	Enzon, Inc.	Acute lymphoblastoid leukaemia	Market	Ho and Frei, 1970
SMANCS Zinostatin stimulator	Yamanouchi	Hepatocellular carcinoma	Market	Maeda, 2001
PEG-interferon 2α (PEGASYS®)	Hoffman-La Roche	Hepatitis C	Market	Perry and Jarvis, 2001
PEG-filgrastim (PEGylated Neulasta)	Amgen	Febrile Neutropenia	Market	Curran and Goa, 2002
PEG-interferon 2β (PEG-INTRON™)	Schering-Plough	Cancer (various)	Phase III	Glue et al, 2000

The first polymer-protein drugs for treating cancer became available in the early 1990's. An example of this is PEG-L-asparaginase, which represents the class of PEGylated-protein conjugates. L-asparaginase is a protein used to treat acute lymphocytic leukaemia (ALL) in children, however, as with many proteins, itsuse is limited by its immunogenicity, short plasma half-life and a requirement for multiple daily injections. Poly(ethylene glycol) (PEG) has a number of characteristics that hasmade it attractive for conjugation to proteins. These include high water-solubility, itshigh degree of hydration resulting in a very large hydrodynamic volume, non-toxicity, non-immunogencity and ability to be cleared rapidly from the body (reviewed in Zalipsky and Lee, 1992). In addition, it has been approved by the Food and Drug Administration (FDA) for human administration topically, by mouth, or injection. Conjugation of L-asparaginase to PEG increased plasma half-life, reduced protein immunogenicity and reduced the dosing schedule to weekly injections. PEG-L-asparaginase is now been approved for the treatment of pediatric ALL, adult ALL and Non Hodgkins Lymphoma (Harris et al, 2001).

Although polymer conjugation to proteins offers distinct advantages, there are some drawbacks to this approach. One main disadvantage is that the conjugate is often considered as a new chemical entity by regulatory authorities, which can hinder its progress through clinical trials. Additionally, conjugation of a polymer to a protein can block or sterically hinder the active site of the protein, or, if the polymer is bioactive, result in loss in activity of the polymer (Rungsardthong et al, 2001). Thus it is essential that these factors are considered carefully if this approach is to be used.

1.3.2 Lysosomotropic vs endosomotropic delivery

Following the advancement and success of lysosomotropic polymer-drug conjugates into clinical trials (Vasey et al, 1999; Seymour et al, 2002), we are now applying the design criteria used previously to optimise these conjugates to develop PAAs for intracytoplasmic delivery. This has been possible because the requirements for a lysosomotropic delivery system are nearly identical to that required for an endosomotropic delivery system such as PAAs as shown in table 1.2. As the lysosomotropic drugs and PAAs are designed to accumulate in tumours by the EPR effect, this phenomenon will be discussed below.

Table 1.2 Requirements for lysosomotropic and endosomotropic drug delivery systems

Vector requirement for lysosomotropic delivery	Vector requirement for endosomotropic delivery
Biocompatible	Biocompatible
Carry the payload	Carry the payload
Protect the payload from degradation	Protect the payload from degradation
Avoid liver uptake	Avoid liver uptake
Target appropriate cell type	Target appropriate cell type
Enter cell by endocytosis	Enter cell by endocytosis
Trafficking to lysosome	Exit the endosome
Release of payload	Appropriate organelle trafficking
	Release of payload

1.4 The Enhanced Permeability and Retention (EPR) Effect as a means of Tumour Targeting

The EPR effect has been studied in depth by Maeda and co-workers, and is based on the fact that many different macromolecules passively accumulate in solid tumours (reviewed in Maeda and Matsumura, 1989). This phenomenon has been attributed to two factors; the discontinuous endothelium as often displayed by tumour vasculature which allows macromolecular extravasation to a greater extent than seen with most other endothelial barriers, and additionally lack of effective lymphatic drainage in tumours preventing clearance of extravasating macromolecules resulting in tumour accumulation by passive diffusion (reviewed in Maeda, 1994). This effect has been documented in many solid tumours, and it is now widely accepted that this phenomenon is crucial to the observed pharmacological effect of many macromolecular drug delivery systems (Duncan, 1992). A schematic of this concept can be seen in figure 1.2.

1.5 Endocytosis and Intracellular Trafficking in the Context of Drug Delivery

Understanding the endocytic pathway in cells and the complex mechanisms involved in the intracellular transport of internalised membrane components is paramount if efficient drug delivery systems utilising the endocytic pathway are to be successful. Although some vesicle trafficking events still remain controversial, there is fundamental agreement on the most important features of the pathway which will be described below.

All cells internalise extracellular material during the process of endocytosis. This can broadly be divided into two categories;

(1) Phagocytosis (cell eating), refers to the binding and internalisation of large (>0.75μm diameter) particles such as apoptotic cells. This mechanism was mainly established by the pioneering work of Elie Metchnikoff in the 1880's. (A detailed review on phagocytic mechanisms is beyond the scope of this thesis).

(2) Pinocytosis, (cell drinking), refers to the constitutive formation of smaller (< 0.2μm diameter) vesicles carrying extracellular fluid and macromolecules specifically or non-specifically bound to the plasma membrane (reviewed in Mellman, 1996).

Pinocytosis can be divided into three categories; fluid-phase pinocytosis, non-specific adsorptive pinocytosis and receptor-mediated pinocytosis (figure 1.3).

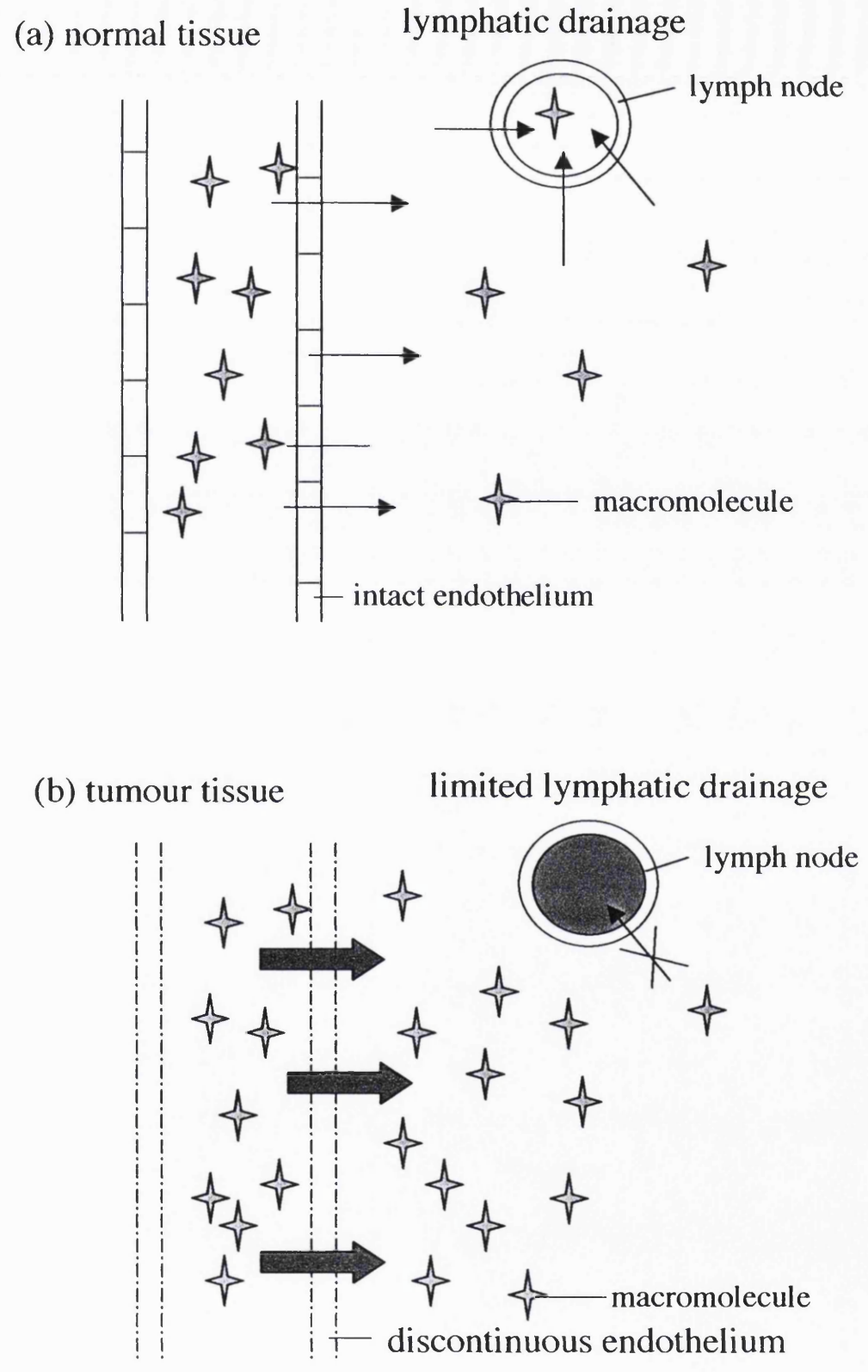

Figure 1.2 The EPR effect, adapted from Duncan, 1992. Panel (a) The endothelial barrier limits macromolecules from passing through. Lymphatic drainage ensures that any which have passed through are removed; (b) macromolecules can pass through leaky vasculature of endothelium and poor lymphatic drainage leads to their accumulation in tumours.

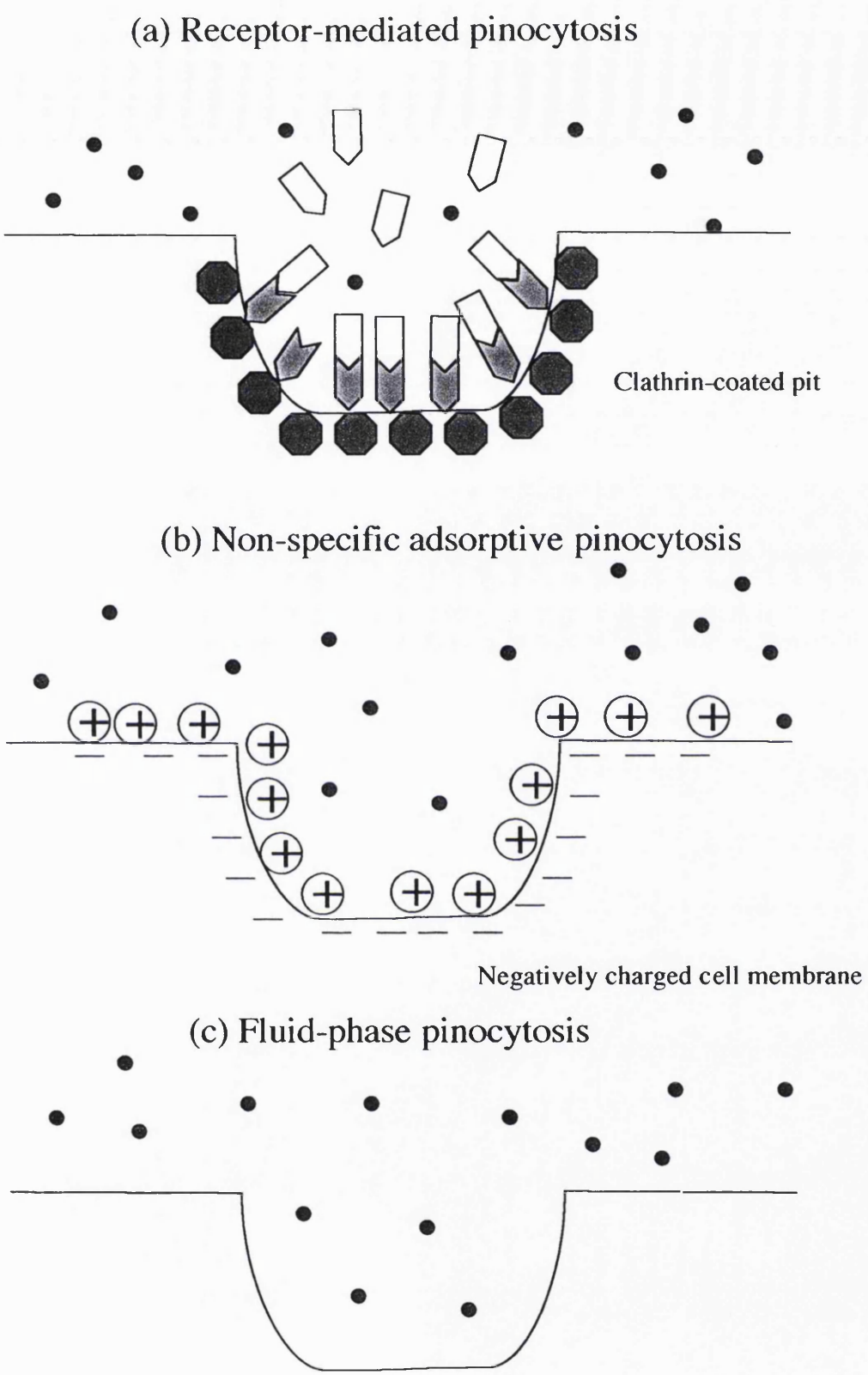

Figure 1.3 Diagram showing the three categories of pinocytosis. Panel (a) shows receptor-mediated pinocytosis: receptor ligands bind to cell-surface receptors and are concentrated on the clathrin-coated pit; (b) Non-specific adsorptive pinocytosis:positively charged molecules bind electrostatically to the negatively charged cell membrane; (c) fluid-phase pinocytosis: non-diffusable uncharged molecules are internalisedAs a result of ongoing membrane invagination
Key: clathrin-coated pit; receptor molecule; receptor ligand; uncharged molecule; positively charged molecule

(1) Fluid-phase pinocytosis is a constitutive phenomenon that is characterised by ongoing membrane invagination and capture of any non-diffusable molecule present in the extracellular medium.

(2) Non-specific adsorptive pinocytosis is mediated via the binding of a molecule to the cell surface non-specifically by ionic interactions between the molecule and theplasma membrane or through hydrophobic/hydrophilic interactions between non-polar moieties and the lipid bilayer. As a result of membrane binding, non-specific absorptive pinocytosis is more efficient at substrate capture than fluid-phase.

(3) Receptor-mediated pinocytosis requires the presence in the plasma membrane of specific receptors that link the molecule destined to be endocytosed. As a large number of receptors can be concentrated in localised regions along the plasma membrane, this can be a very efficient method of ligand uptake.

Different types of endocytic pathways are known to exist within the cell to mediate the processes of non-specific absorptive, receptor-mediated and fluid-phase pinocytosis. These pathways will be discussed below.

Clathrin-dependent pinocytosis

The best-defined pathway of extracellular fluid and receptor-bound ligand uptake is the clathrin-coated vesicle (CCV) pathway. CCVs are found in virtually all cell types and form from domains at the plasma membrane known as clathrin-coated pits. CCVs comprise a protein clathrin coat, which forms lattices of hexagons and pentagons, forming a cage-like structure. These coats are linked to a heterotetrameric adaptin complex known as AP-2 (reviewed in Clague, 1998). AP-2 provides two functions; firstly it attaches clathrin to membranes via interaction of AP-2 with a high affinity receptor (Zhang et al, 1994), and secondly it recruits cargo-bearing receptors (bearing the appropriate signals) that are destined for incorporation into CCVs (Ohno et al, 1995). Invagination of CCVs occurs at the plasma membrane, under the control of a number of accessory/regulatory proteins until a mature vesicle is 'pinched off' the parent membrane by the action of GTPase dynamin (Owen and Luzio, 2000). Although this pathway is mainly responsible for receptor-mediated endocytosis by concentrating different receptors within coated-pits, it is also implicated in fluid-phase pinocytosis.

Caveolae

Caveolae are small (~ 50nm-80nm diameter) specialised invaginations of the plasma membrane seen in many cell types, especially capillary endothelial cells, smooth muscle cells and adipocytes (Peters et al, 1985). The cholesterol-binding protein caveloin 1 (Vip21) is required for caveolae formation (Peters et al, 1985; Rothberg et al, 1992). In endothelium, the formation of caveolae is associated with the transcytosis of solutes across the cell, however, the contribution of caveolae to total endocytic activity is unclear (reviewed in Mellman, 1996).

Clathrin-independent pinocytosis

There is increasing evidence for pinocytosis that is independent of clathrin (Lamaze and Schmid, 1995). Although caveolae formation is a dynamin-dependent, clathrin-independent form of pinocytosis, studies have shown that another type of clathrin-independent pinocytosis can also occur, which is not dependent on dynamin, although the mechanisms concerning this pathway are not clear.

Vesicles formed at the cell surface undergo a series of fusion events with other organelles during the process of pinocytosis. The principal components of these intracellular sorting compartments are discussed below.

Endosomes

Early endosomes are often located on the cell periphery and receive most types of vesicles coming in from the cell surface. Although the initial sorting event occurs at the plasma membrane, many more sorting events occur in sorting endosomes, including the discharge of internalised ligands from their receptors, targeting of membrane proteins to their correct plasma membrane domains and transfer of ligands to late endosomes or back to the plasma membrane via recycling endosomes (reviewed in Mellman, 1996).

Different endosomes have characteristic pH values that are essential for their proper functioning. An H^+ v-ATPase pump in the vesicle membrane which is driven by the organelle membrane potential ensures that these vesicles maintain an acidic pH. Acidification is essential for sorting endosomes in order to allow receptor dissociation from ligands and plays a role in membrane traffic. Typically, the pH of sorting endosome is in the range 5.9-6.0, however recycling endosomes have characteristically

higher pH values, in the range 6.4-6.5 depending on the cell type (reviewed in Mukherjee et al, 1997).

Late endosomes

Late endosomes are defined as vesicular structures that accumulate and concentrate internalised contents after passage through early endosomes, and are thought to mediate a final set of sorting events prior to delivery of material to lysosomes (reviewed in Mellman 1996; reviewed in Clague, 1998). These endosomes contain primary inward invaginations of the membrane (known as multi-vesicular bodies) and contain the highest concentration of the cation-independent mannose 6-phosphate receptor, and also degradative enzymes. Late endosomes undergo extensive vesicular traffic with the Trans Golgi network to acquire these newly synthesised lysosomal enzymes and to return the mannose 6-phosphate receptor back to the Trans Golgi network. These vesicles have a lower pH than early endosomes, characteristically in the range 5.0-6.0, as they contain degradative enzymes with pH optima within this range (reviewed in Mukherjee et al, 1997).

Lysosomes

Transfer of material between late endosomes and lysosomes appears to be a direct fusion event resulting in a hybrid organelle (Luzio et al, 2000). Lysosomes are distinguished from late endosomes by virtue of their higher density on Percoll gradients and their lack of the cation-independent mannose 6-phosphate receptor. A lower lumenal pH of around 4.5-5.5 exists in these organelles (Asokan and Cho, 2002). Lysosomes represent the final step of traffic for macromolecules, as once transferred to this compartment, they are digested by a battery of lysosomal enzymes to small molecules (typically < 1kDa). As a result of this digestion, the luminal concentration of nutrients rises above that of the cytoplasm. This leads to a concentration gradient across the vacuolar membrane which drives diffusion of these small molecules through specific channels or carriers in the lysosome membrane. These small molecules (amino acids, sugars) are then utilised in the cytoplasm for cell sustenance and growth (reviewed in Mukherjee et al, 1997).

A schematic diagram of the endocytosis pathway can be seen in figure 1.4.

There are many limiting factors associated with the cytosolic delivery of substances via the endocytic pathway. The first of these are the vast array of lysosomal

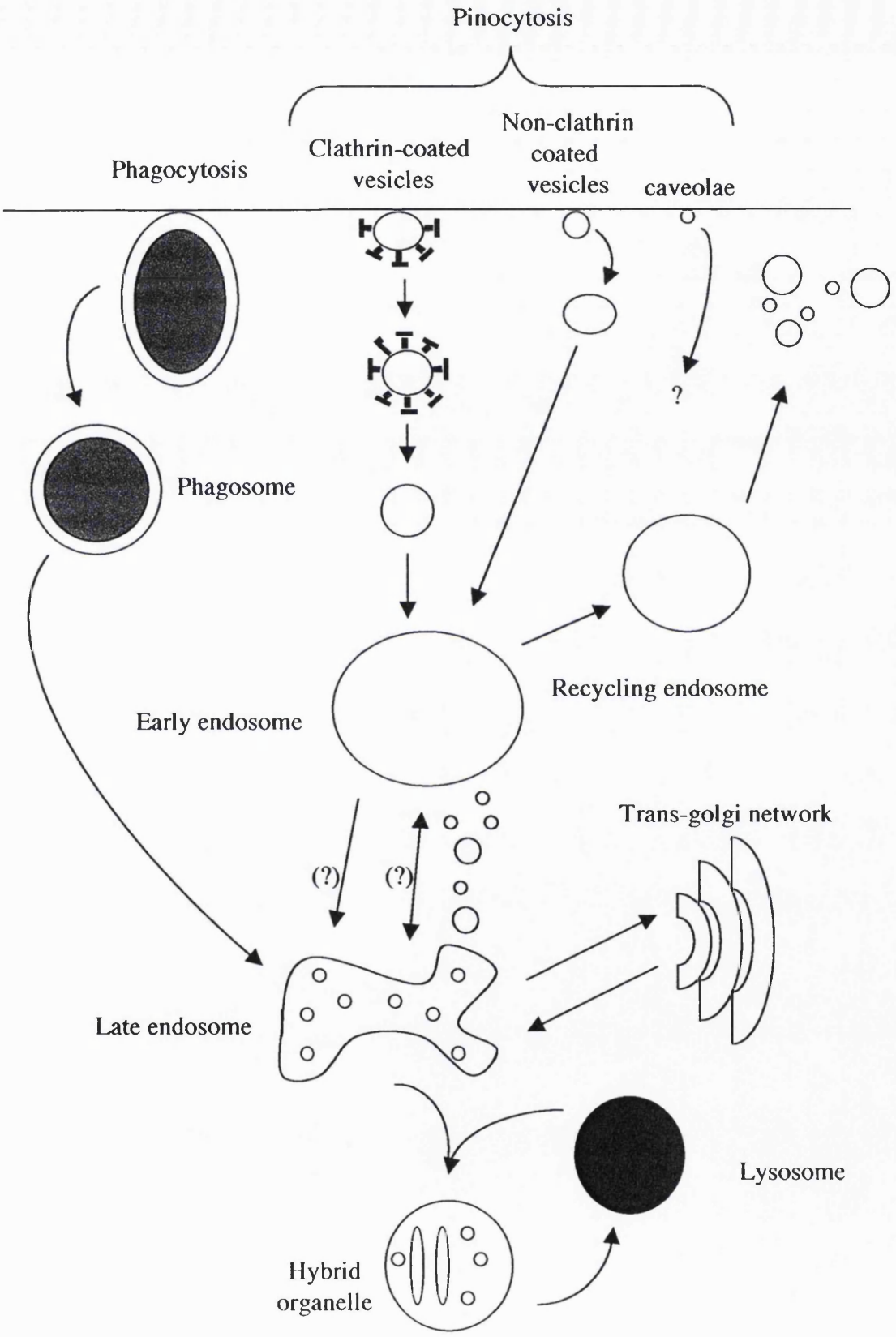

Figure 1.4 The endocytic pathway in a non-polarised cell. (?) these pathways are speculatory.

enzymes that may degrade therapeutic substances which are trafficked to the lysosome. In addition, the physical constraint of crossing the membranes of the endocytic pathway have also been reported to limit cytosolic access (Klemm et al, 1998; Lucas et al, 1999; Kircheis et al, 2001a).

1.5.1 Intracellular Trafficking of Toxins

The mechanisms of intracellular trafficking of ricin and gelonin toxins will be discussed below and are of relevance to this thesis for a number of reasons: a) conjugates of these toxins with antibodies against tumour cell-surface antigens are currently being investigated as potential intracytoplasmic delivery systems (section 1.6); b) some plant and bacterial toxins are able to inherently enter the cytoplasm, and understanding the mechanism of cytosolic access has implications for the future design of intracytoplasmic delivery systems; c) both RTA and gelonin have been delivered to the cytosol using endosomolytic systems.

The plant toxin ricin, has been particularly well documented as a marker for endocytosis and intracellular transport steps (reviewed in Sandvig and van Deurs, 1996). This protein (derived from *Ricinus communis*), is a highly cytotoxic, dimeric glycoprotein composed of RTA with molecular weight ~ 29,500 and a B-chain (RTB) of molecular weight 34,000, which are linked by a disulphide bridge (Lord et al, 1994).

RTB is the cell-binding moiety, which acts to promote binding and endocytosis of the protein by binding to glycolipids and glycoproteins with terminal galactose residues. The holotoxin is then taken up by both clathrin-dependent and independent endocytosis with about 95% of ricin subsequently transported to lysosomes. Of the remaining amount, about 75% is transported to the Golgi apparatus (reviewed in Sandvig and van Deurs, 1996). Once inside the cell, the toxin undergoes retrograde transport from the Golgi to the endoplasmic reticulum, where it is thought that the inter-chain disulphide bond linking the A- and the B-chains is broken. Free RTA, the catalytic moiety, then interacts with Sec61p translocon and is perceived as a substrate for the ER-associated protein degradation pathway. It is then translocated to the cytosol in a partially unfolded state (Argent et al, 2000). Once in the cytosol, ribosomal inactivation occurs by cleavage of the N-glycosidic bond of adenosine^{4324} nucleoside in 28S RNA of the 60S ribosomal subunit, leading to inhibition of protein synthesis (Endo et al, 1987, Simpson et al, 1999). RTA alone displays a much higher IC_{50} value *in vitro* compared to ricin holotoxin due to its inability to bind efficiently to cells and to gain access to the cytoplasm.

Gelonin is another ribosome inactivating toxin derived from the seeds of *Gelonium multiflorum.* This toxin consists of a single polypeptide chain with 251 amino acid residues with molecular weight 30,500 (Stirpe et al, 1980). It has similar properties to RTA, by catalytically inactivating the 60S subunit of ribosomes in eukaryotic cells, however this only occurs in cell free systems as gelonin lacks the cell-binding domain equivalent to RTB. As a result of this, gelonin is non-toxic to intact cells (Stirpe, 1980; Selbo et al, 2000a), due to its poor uptake and subsequent trafficking to lysosomes.

As cytosolic access of macromolecules such as proteins (toxins) and genes is crucial for many therapeutic strategies (reviewed in Plank et al, 1998, Lackey et al, 1999a), there is a requirement for an intracytoplasmic delivery vehicle to mediate membrane translocation and avoid lysosomal degradation (Murthy et al, 1999, Mönkkönen and Urtti, 1998). The challenges faced by a potential intracytoplasmic delivery system in terms of use of these toxins and other therapeutic strategies will be discussed below.

1.6 Challenges of Intracytoplasmic Delivery

The most widely researched therapeutic strategy which requires the intracytoplasmic delivery and nuclear trafficking of macromolecules is gene therapy. The classical definition of gene therapy is defined as the transfer of genetic material into cell nuclei to alter their function, usually for the benefit of the entire organism (Godbey and Mikos, 2001). This concept was first envisioned around 13 years ago and since then this field has expanded (encouraged by the recent completion of the Human Genome Project). Although gene therapy was initially envisioned for the treatment of monogenic disorders such as cystic fibrosis (Bellon et al, 1997), it is also currently being studied for a wide range of diseases including cancer, arthritis, neurodegenerative disorders and infectious diseases such as acquired immune deficiency syndrome (AIDS) (reviewed in Mhashilkar et al, 2001).

Although many genetic targets have been identified that could be corrected or altered by introduced deoxyribonucleic acid (DNA), DNA alone cannot be used for this purpose. In order to achieve a therapeutic effect DNA must enter the nucleus. However alone, it is either degraded by nucleases present in extracellular fluid, or is

endocytosed and trafficked to lysosomes where again degradation will occur (reviewed in Wattiaux et al, 2000, Murthy et al, 1999).

Increasing stability of DNA to nucleases has been addressed by synthesising oligonucleotide analogues (phosphorothioate oligomers, methylphosphonate oligonucleotides, morpholino-oligonucleotides and peptide nucleic acids) (reviewed in Lebedeva et al, 2000; Hamilton et al, 1999), which are reported to resist rapid nuclease degradation. However, these analogues still require an intracytoplasmic delivery system, because when administered alone they display a similar pharmacokinetic profile as DNA (reviewed in Dokka et al, 2000, reviewed in Wattiaux et al, 2000).

At present, a safe, efficient vector capable of delivering DNA to the nucleus has yet to be synthesised (Brown et al, 2001). The main reason for this is because a non-viral intracytoplasmic gene delivery system requires many complex features and intracellular trafficking steps in order to deliver its payload to the nucleus. These requirements are set out in table 1.3. Although it is not unfeasible that a vector which possesses all these characteristics will eventually be developed, it is likely that it will involve a multi-component system to accommodate all these features.

Ribozymes are ribonucleic (RNA) structures that catalyse the cleavage of many forms of RNA (reviewed in Helene and Toulme, 1990). Their ability to cleave and deactivate messenger RNA (mRNA) means that they can be used to down-regulate gene expression. Ribozymes have advantages over conventional DNA delivery because they are smaller in size than plasmids and do not require delivery into the nucleus to exert biological activity (Merdan et al, 2002a). Thus, intracytoplasmic delivery vehicles are attractive agents for their delivery.

In addition to DNA and RNA, many therapeutic proteins require intracytoplasmic delivery (Lackey et al, 1999a). Research groups are currently examining using immunotoxins as a new approach to cancer chemotherapy. Immunotoxins are comprised of a protein toxin connected to a binding ligand such as an antibody or growth factor. These molecules then selectively bind to cells bearing the target antigen and antibody internalisation occurs.

Although success with immunotoxin therapy has been reported (reviewed in Frankel et al, 2000), some are limited in their efficacy as a result of conjugate degradation in lysosomes following internalisation (reviewed in Frankel et al, 2000; reviewed in Rhíová, 1998), or lack of translocation efficiency to the cytosol, as

Table 1.3 Characteristics required for a non-viral intracytoplasmic gene delivery system

Property	Reference
Protection of DNA from degradation by extracellular nucleases	Godbey and Mikos, 2001; Zelphati et al, 1996; Wattiaux et al, 2000
Appropriate organ and cell targeting/biodistribution	Lui et al, 1997
Minimal toxicity to target cells	Godbey and Mikos, 2001
Endocytic uptake/membrane fusion	Zelphati et al, 1996
Exit from the endosome	Kyriakides et al, 2002; Wattiaux et al, 2000
Release of DNA from complex	Lucas et al, 1999
Nuclear trafficking/traversal through the nuclear pore	Lucas et al, 1999; reviewed in Tachibana et al, 2001, Kamiya et al, 2001; reviewed in Pouton, 1998; reviewed in Zuber et al, 2001
Stable, controlled expression of gene	Wu and Wu, 1998

displayed by certain toxins. Probably the most common limitation to immunotoxin therapy which confers dose-limiting toxicity is Vascular Leak Syndrome (VLS) (Baluna et al, 2000; reviewed in Kreitman, 1999) which is caused by toxin-mediated damage to endothelial cells. The problems associated with immunotoxin therapy leave a niche in the market which intracytoplasmic delivery vehicles could utilise. Degradation of the conjugate in lysosomes has been shown to be a rate-limiting step in immunotoxin therapy, which would not occur for intracytoplasmic delivery systems which lyse endomembranes before degradation occurs. Additionally, an intracytoplasmic delivery system alleviates the need for naturally cell permeant proteins, thus leaving a much wider choice of cytotoxic molecule to be delivered. Finally, chemical conjugation of a synthetic polymer to a protein such as a toxin can reduce its immunogenicity (Ulbrich et al, 2000; Seymour et al, 1991; Duncan, 2000).

Discussed below are the intracytoplasmic delivery systems currently being developed to utilise these therapeutic strategies. To date, the majority of these are being developed for gene delivery and therefore this will be the main focus of this section. It must be noted that as well as intracytoplasmic delivery vehicles, physical methods are also being developed for the delivery of genes into cells, which are not directly relevant to this thesis. These include electroporation, particle bombardment, microinjection and calcium phosphate precipitation (for reviews see Dokka and Rojanasakul, 2000; Chang, 1994).

1.7 Intracytoplasmic Delivery Systems

1.7.1 Non-Polymeric Intracytoplasmic Delivery Systems

1.7.1.1 Viral Vectors

In order to take advantage of the natural processes of viral transfection, modified viral vectors are currently being developed as gene delivery vehicles because they display high levels of transgene expression (Robins et al, 1998). Among these, retrovirus and adenovirus are the two most commonly used viral vectors that have been tested in phases I/II clinical trials.

Although viruses are able to induce high and stable expression of the transgene, their main disadvantages include the limitation on the size of the DNA insert, difficulty in large-scale production, cellular toxicity, immunogenicity (Murthy et al, 1999; Yang et al, 1994; Schofield and Caskey, 1995) and recombination events leading to reactivation of the virus (Provoda and Lee, 2000). It is crucial that the safety issues

associated with these vectors are addressed. Overlooking these problems led to the death of a research subject caused by a severe adverse reaction to a dose of over trillion modified adenovirus particles (Kielian and Hickey, 1999). For these reasons, an increasing amount of research has been focused towards developing non-viral systems for gene delivery.

1.7.1.2 Cationic lipids and liposomes

The potential of liposomes as drug carriers was first realised 25 years ago due to their ability to entrap solutes (reviewed in Gregoriadis et al, 1976). Hydrophilic drugs can be entrapped in the aqueous channels separating the hydrophobic lipid bilayers or in the liposomal lumen. Hydrophobic drugs can be sequestered in the acyl chains of phospholipid molecules within the bilayer (reviewed in Gregoriadis, 1990).

Oligonucleotides or plasmid DNA can be delivered with liposomes into cells either in encapsulated form or as a lipid-DNA complex (reviewed in Mönkkönen and Urtti, 1998). Of the non-viral gene delivery methods, liposomes have been the most widely tested vehicle to date (reviewed in Mhashilkar et al, 2001; Mönkkönen and Urtti, 1998). There are three common types of cationic lipids employed in lipid-based DNA delivery which are described below.

a) Lipids containing quaternary ammonium salts with long mono-unsaturated aliphatic chains. e.g. (N[1-(2,3-dioleyloxy)propyl]-*N,N,N*-trimethyl ammonium) (DOTMA). A 1:1 mixture of DOTMA and the fusogenic lipid dioleoyl phosphatidylethanolamine (DOPE) make up the commercially available transfection agent LipofectIN™ (Felgner et al, 1987).
b) Cationic derivatives of cholesterol e.g. 3β-(N-(N-(dimethylaminoethane)carbamoyl) cholesterol (Dc-Chol).
c) Lipids with multivalent headgroups (lipospermines) e.g. dioctadecylamidoglycylspermine (DOGS). This is available commercially as Transfectam® (Remy et al, 1998).

The structures of these lipids are shown in figure 1.5. As they are positively charged, they are able to form a polyelectrolyte complex with DNA, which is thus protected from nuclease degradation (Zelphati et al, 1996). The exact steps taken during lipid-mediated gene delivery remain unclear, however it is widely accepted that these lipid/DNA complexes bind to the cell membrane surface by charge interaction and are taken up by endocytosis (Kichler et al, 1997; Xu and Szoka, 1996; Zelphati et al,

Transfectam®

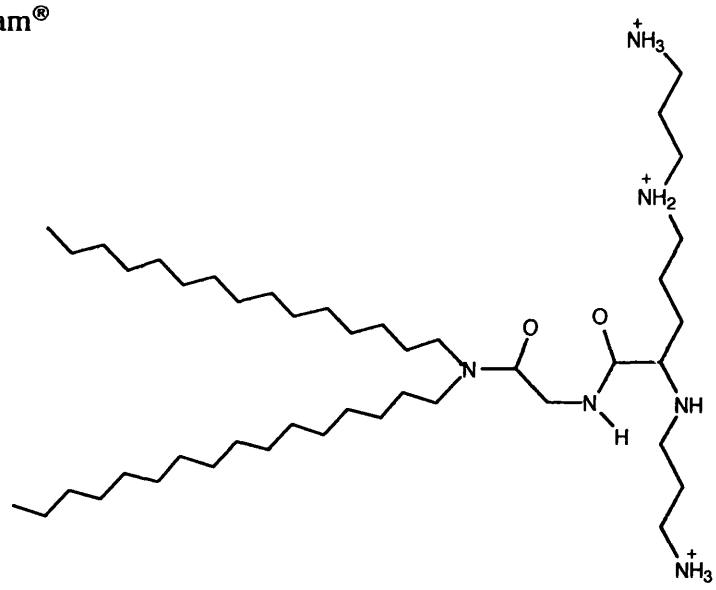

Components of LipofectIN™

DOTMA

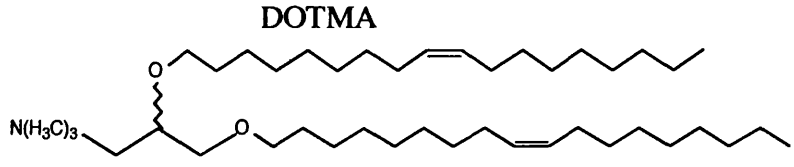

DOPE

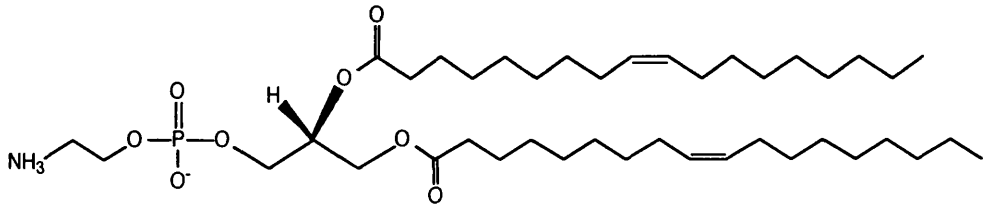

Figure 1.5 Structures of lipidic vectors

1996). Much work has been done to elucidate the mechanism of subsequent oligonucleotide release from cationic lipids once in the endosome. It has been proposed that cationic lipid fusion with the endosomal membrane occurs as a result of initial endosomal membrane destabilisation resulting in flip-flop of the anionic lipids located on the cytoplasmic face of the membrane. Membrane destabilisation could be initiated by close proximity of cationic and anionic lipids and the high radius of membrane curvature found in intracellular vesicles (Xu and Szoka, 1996). Anionic lipids can then diffuse laterally into the complex to form charge-neutralised ion-pairs with the cationic lipids. Neutralisation releases the oligonucleotide from its electrostatic interaction with lipids leading to its release into the cell cytoplasm (Zelphati et al, 1996).

Many cationic lipid formulations include the neutral co-lipid DOPE to promote membrane fusion (Mönkkönen and Urtti, 1998). This fusogenic lipid forms a stable lipid bilayer at pH 7, while in the acidic pH range of 5-6, a hexagonal–II structure is formed, which destabilises the membrane (reviewed in Kamiya et al, 2001).

In order to design more effective lipic vectors, lipid formulations have included cholesterol (Gao and Hui, 2001), PEG (reviewed in Kilbanov et al, 1990) and amphipathic peptides (Kichler et al, 1997). Additionally it was found that altering the liposome composition can result in pH-sensitive liposomes designed to undergo efficient fusion within the acidic environment of the endosome (Chu et al, 1990). Targeted liposomes have also been designed, which include immunoliposomes targeted to tumour cells over-expressing antigens (reviewed in Lebedeva et al, 2000).

A main disadvantage associated with DNA/lipid complexes includes instability in the extracellular environment due to interaction with serum proteins, leading to premature release of DNA (Zelphati et al, 1996; Moret et al, 2001). Serum protein interaction is most substantial with cationic liposomes, with opsonization of the liposome surface resulting in uptake of the complexes by the RES (Mönkkönen and Urtti, 1998; Finisinger et al, 2000; reviewed in Mahato et al, 1995).

1.7.1.3 Thiol-activated cytolysins

These are a group of pore-forming toxins produced from a variety of gram-positive bacteria, including species within the genera *Clostridium*, *Streptococcus*, *Listeria* and *Bacillus*. These toxins are secreted as water-soluble single polypeptide chains ranging from 50-80kDa with 40-80% sequence homology. They bind to cells with cholesterol-containing membranes, which leads to membrane insertion and homo-

oligomerisation of approximately 50 monomers to form pores in the lipid bilayer (reviewed in Provoda and Lee, 2000).

These transmembrane channels have been utilised for the delivery of antisense oligonucleotides to human leukaemia KY01 cells using the pore-forming toxin, Streptolysin-O (Giles et al, 1998). Although an antisense effect was seen, it is questionable as to whether the pore formation is reversible, as a non-reversible effect would ultimately result in cell death.

1.7.1.4 Photosensitizers

($AlPcS_{2a}$) is a photosensitive compound that is able to localise and rupture endosomes and lysosomes upon light exposure. This novel method is denoted photochemical internalisation (PCI) and involves the release of highly reactive oxygen species upon light exposure, which are able to destroy membranes (Selbo et al, 2000a).

Photochemical treatment of human melanoma cells after incubation of ($AlPcS_{2a}$) substantially improved the efficiency of transfection mediated by poly-L-lysine and PEI (Prasmickaite et al, 2000). However, the inclusion of cationic polymers to complex and prevent premature degradation of the DNA has drawbacks in terms of vector toxicity and intravenous administration. In addition, the requirement of light exposure to induce membrane rupture limits this technique to *in vitro* mechanistic studies.

PCI has recently been utilised to demonstrate the translocation of gelonin toxin to the cytosol from endosomes and lysosomes. This study demonstrated the importance of endosomal escape, as in the absence of inhibition of endosome to lysosome transport, degradation of gelonin occurred prior to cytosolic translocation (Selbo et al, 2000a).

1.7.2 Polymeric Intracytoplasmic Delivery Systems

1.7.2.1 Cationic polymers

A variety of polymeric vectors are also currently being investigated as gene-delivery vectors. The advantages of using polymeric systems has already been discussed in section 1.3. Among these vectors, cationic polymers such as PEI, chitosans, poly-L-lysine, and PAMAM dendrimers have been the most widely documented (reviewed in Garnett, 1999). Although many of these polymers are not strictly endosomolytic, details of their mechanism of action will be discussed before the focus is moved to endosomolytic vectors.

Polycation-mediated gene delivery is based on electrostatic interactions of the polycation with the negatively charged phosphate groups of DNA to form IPECs. As

with cationic lipid-mediated gene delivery, condensation protects the DNA from degradation by nucleases and results in compact particles which can be taken up by cells via endocytosis. The positive surface charge of polycation/DNA complexes produced with high polycation/DNA ratios usually serves to bind cells via electrostatic interactions to sulphated proteoglycans on the cell membrane (Mislick and Baldeschwieler, 1996), which could be essential for complex internalisation.

In vitro cationic polymers are membranolytic (Nevo et al, 1955; reviewed in Garnett, 1999), and thus could act upon the endosomal membrane causing destabilisation leading to release of the polyplex into the cytosol. In practise, however, cell membrane destabilisation also occurs, resulting in concentration-dependent cytotoxicity for many cationic polymers (Godbey and Mikos, 2001). IC_{50} values for the most widely used cationic gene delivery polymers are shown in table 1.4.

Efficiency of transfection is probably dependent on the rate of intracellular degradation of plasmid DNA (reviewed in Wattiiaux et al, 2000) and for many polyplexes, inability to promote endosomal membrane destabilisation results in degradation in the lysosome (Lucas et al, 1999). Many groups include membrane destabilising compounds such as fusogenic peptides in the transfection mixture which promote endosomal membrane destabilisation (Kircheis et al, 2001a). In addition weak bases such as chloroquine have been included during transfection which can increase transfection efficiency (Lucas et al, 1999).

Although high levels of transfection have been obtained *in vitro* for cationic polymeric delivery systems, it is important to note that most systems are being developed for *in vivo* use for systemic administration. This poses another set of problems such as anatomical size constraints, interactions with biological fluids and non-specific binding to non-target cells (Kircheis et al, 2001a). A major drawback of cationic systems is coating of the complexes with plasma components such as albumin and complement (reviewed in Plank et al, 1996). Opsonization causes rapid clearance of the foreign particles as well as interaction with cells of the RES resulting in high liver uptake (Godbey and Mikos, 2001; Kircheis et al, 2001a). Shielding the positive charge of polyplexes by PEG has been shown to efficiently shield polyplexes from these non-specific interactions (reviewed in Godbey et al, 1999a). Additionally surface modification of polymers by epidermal growth factor (EGF) (Schaffer et al, 1998; Schaffer et al, 2000) transferrin (Kircheis et al, 2001b; Godbey and Mikos, 2001) and asialoglycoprotein (Wu and Wu, 1998) receptor-ligands has been developed to

Table 1.4 Cytotoxicity of polymeric gene delivery vehicles

Polymer	Molecular weight (kDa)	IC_{50} value (μg/ml)	Cell lines	Incubation time (h)	Reference
PLL	56.5	50	L132	72	Richardson et al,1999a,
	56.5	50	CCRF	72	Richardson et al,1999a
	56.5	50	B16F10	72	Ferruti et al, 2000
	25	40	HepG2	4	Choi et al, 1998
PEI	25 (branched)	6	293T	2h	Lee et al, 2001
	25 (branched)	40	NIH 3T3	48	Jeong et al, 2001
DMAEMA	550	4.5	OVCAR	48	Van de Wettering et al, 1999
Chitosan	5	> 1,000	L132,	72	Richardson et al, 1999b
	5	> 1,000	CCRF	72	Richardson et al, 1999b
β-cyclodextrin	6.1	380	BHK-21	24	Hwang et al, 2001
PAMAM dendrimers	14.2	50	CCRF	72	Malik et al, 2000
	14.2	50	HepG2	72	Malik et al, 2000

introduce cell-specific targeting and to improve efficiency of uptake into cells.

1.7.2.2 Endosomolytic Polymers

Endosomal escape has been documented to be a major barrier to non-viral mediated gene delivery. In the recent years, a number of polymeric systems have been developed with the ability to lyse endosomal membranes. A schematic demonstrating the advantages of endosomolytic delivery is shown in figure 1.6. A brief review of endosomolytic polymers is discussed below and their structures can be seen in figure 1.7.

1.7.2.2.1 Polyethylenimine (PEI)

PEI is a polymer that has been used for years in the paper industry and in water purification (reviewed in Godbey et al, 1999a, reviewed in Kircheis et al, 2001a). The polymer, made up of an ethylamine repeating unit, is available in two main forms, branched or linear. The most important feature of this polymer is its high cationic charge density, as every third atom is a potentially protonable amino nitrogen, and the overall protonation level increases from 20-45% between pH values of 7 and 5 (Remy et al, 1998). Endosomal membrane rupture has been proposed by Behr and colleagues to occur as a result of the proton sponge mechanism, although evidence and understanding of the release mechanism of PEI from endosomal/lysosomal compartments is limited (Godbey et al, 1999a; Godbey and Mikos, 2001; Godbey et al, 1999b). This mechanism is thought to occur as follows; within endosomes, the influx of protons by v-ATPases is coupled to an accumulation of chloride ions. In the presence of PEI, a net increase in the ionic concentration occurs within the endosome due to the buffering capacity of PEI. In response to this, polymer swelling occurs due to internal charge repulsion. In addition, influx of water into the endosome occurs due to the increase in ionic concentration. It is proposed that these two mechanisms occurring simultaneously lead to endosomal rupture. A schematic of this mechanism is shown in figure 1.8.

Previously, PEI was shown to disrupt isolated rat liver lysosomes in an *in vitro* assay, as indicated by the release of the lyososmal enzyme NAGase (Klemm et al, 1998). The concentrations required for effective lysosomal disruption were significantly greater than those required for gene transfection. This discrepancy was explained by the fact in gene delivery experiments, PEI is endocytosed and concentrated in the inner lumen of acidic vesicles, whereas in experiments documenting

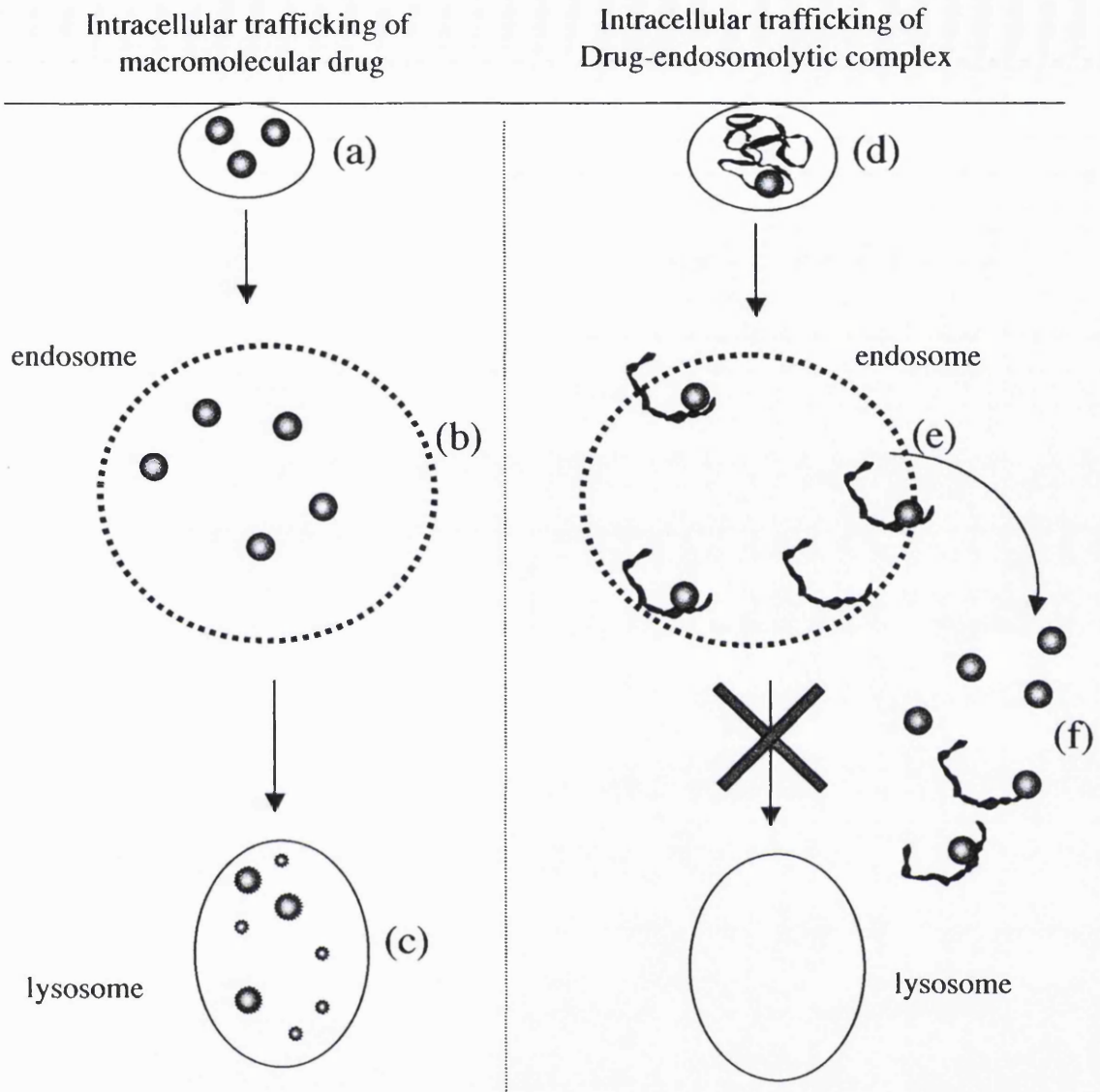

(a) Uptake of macromolecular drug into endocytic vesicle	(d) Uptake of macromolecular drug-endosomolytic polymer complex into endocytic vesicle
(b) Trafficking of drug to endosome	(e) Trafficking of complex to endosome; polymer-mediated membrane destabilisation occurs
(c) Trafficking of drug to lysosome where degradation by lysosomal enzymes occurs	(f) Drug and complex are delivered to cytoplasm, avoiding degradation

Figure 1.6 Alteration of intracellular trafficking of macromolecules by endosomolytic polymers

Poly(2-dimethyl amino ethyl) methacrylate (DMAEMA)

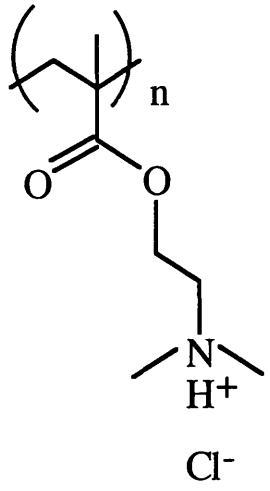

(a) Poly(ethyl acrylic acid) (PEAAc)
(b) Poly(propyl acrylic acid) (PPAAc)

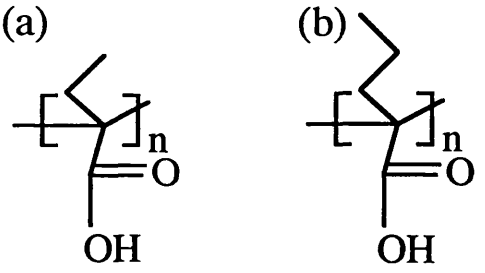

Poly(ethyleneimine) (PEI) (a) branched; (b) linear

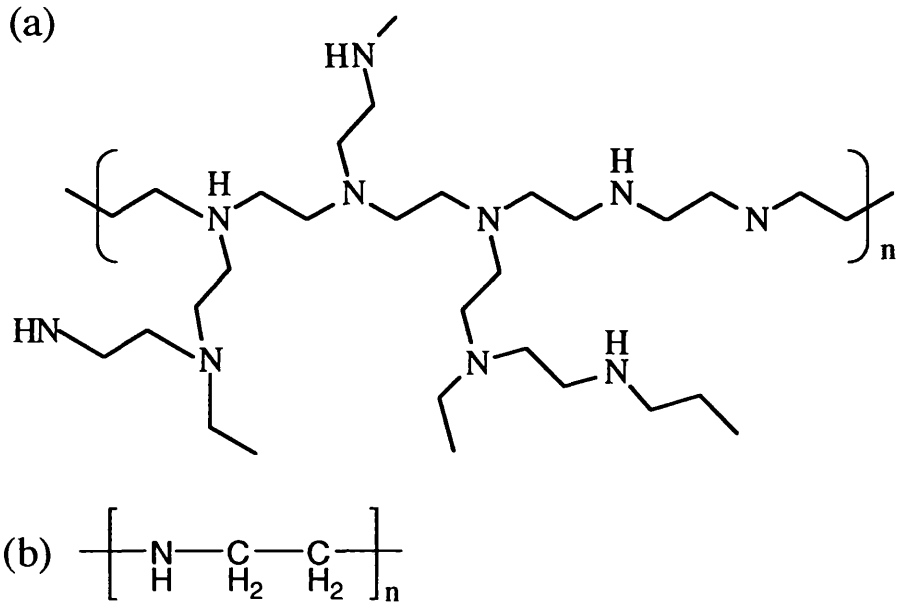

Figure 1.7 Structures of endosomolytic polymers

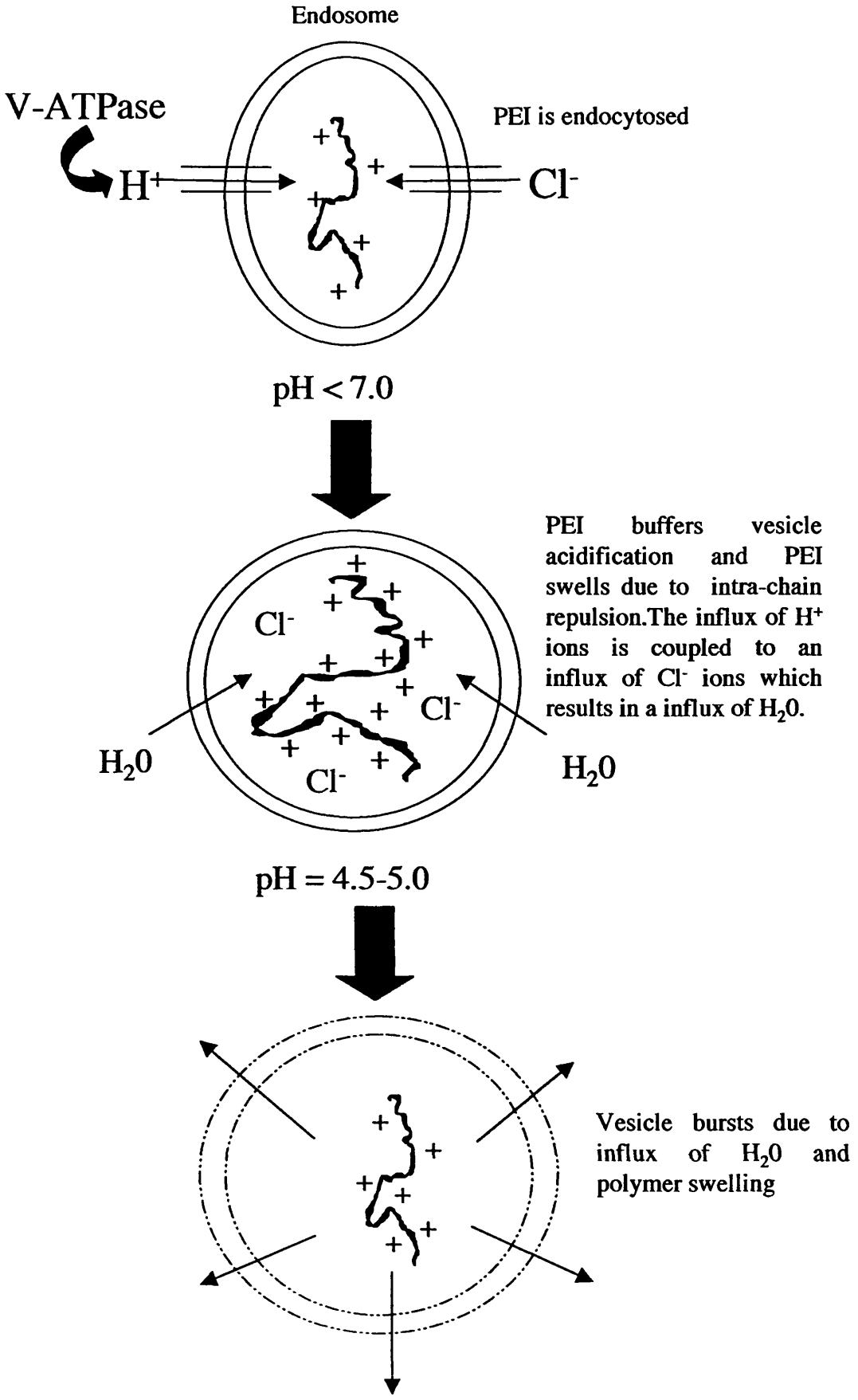

Figure 1.8 Proposed proton-sponge mechanism as occurs in endocytic vesicles after uptake of PEI.

lysosomal disruption, PEI interacts with the outer, cytoplasmic face of these vesicles, where the opportunity for concentration is lessened (Klemm et al, 1998).

A great deal of research is being carried out to elucidate the mechanism for PEI-mediated membrane rupture and its intracellular trafficking. At present there is controversy regarding this matter. A study in 1999 by Godbey and colleagues showed that the majority of PEI/DNA complexes localise to the nucleus of EA.hy 926 cells after 3.5-4.5h post-transfection (Godbey et al, 1999b). In contrast, a later study by Rémy-Kristensen and colleagues showed that fluorescent-labelled PEI/DNA complexes remained largely sequestered in late endosomes or lysosomes in L929 cells. No evidence of endosome disruption was seen and very few cells showed nuclear localisation of the complexes suggesting that endosomal escape was a major barrier for transfection (Rémy-Kristensen et al, 2001). A recent study has shown that fluorescent-labelled poly(ethylenimine)/ribozyme complexes are released from burst vesicles of SW13 adrenal gland cells using living cell confocal microscopy. After release, these complexes spread throughout the cell, including the nucleus (Merdan et al, 2002a). The conflicting results in these studies may be due to different intracellular trafficking routes taken by PEI in different cell-types.

Although PEI is the most widely researched polymeric gene delivery vector, it must be noted that it is highly cationic, thus problems of vector toxicity (Godbey et al, 1999a) and a hepatotropic pharmacokinetic profile (Lecocq et al, 2000) limit the application of this polymer in *in vivo* situations.

1.7.2.2.2 Poly[2-(dimethylamino)ethyl methacrylate] p(DMAEMA)

This synthetic polymer contains tertiary amino groups with pK_a values ~7.5, thus is partially protonated at physiological pH. It is reported to possess amine buffering capacity (as demonstrated by potentiometric titration) and to lyse endosomes by the proton sponge mechanism (Rungsardthong et al, 2001). Although transfection *in vitro* has been demonstrated with DMAEMA/DNA complexes, a relationship between the transfection efficiency and their cytotoxicity was found. A maximum number of transfected cells was observed when cytotoxicity was 40-80% (Van de Wetering et al, 1997). This suggests that like other cationic polymers, part of DMAEMA transfection efficiency could be attributed to local cell membrane destabilisation as well as an endosomolytic effect (Van de Wetering et al, 1999). In addition, cellular association and internalisation of DMAEMA/DNA complexes was only possible when the complexes displayed a positive zeta potential (Zuidam et al, 2000). Both electron

microscopy (EM) and confocal scanning laser microscopy (CSLM) analysis did not reveal the presence of polyplexes or plasmid alone outside endocytic vesicles or within the nucleus, suggesting that intracellular trafficking from the endosomes to the nucleus is a very inefficient process for this polymer (Zuidam et al, 2000).

In vivo administration of DMAEMA/[^{32}P]-pLuc complexes to mice resulted in distribution primarily to the lungs (Verbaan et al, 2001). PEGylation of the polymer with a view to improve vector toxicity and lung localisation resulted in a 20-fold loss in transfection activity, most probably due to the shielding effect conferred by PEG resulting in lower degree of cellular interaction (Rungsardthong et al, 2001; Zuidam et al, 2000).

1.7.2.2.3 Poly(ethyl acrylic acid) (PEAAc) and related polymers

PEAAc is a synthetic polymer designed to mimic certain key structural elements found in endosomal disrupting peptides (Kyriakides et al, 2002). These structural elements include a carboxyl side chain intermixed with alkyl side chains. While the precise molecular mechanism by which PEAAc disrupts lipid bilayers below pH 6.0 is not known, activity is thought to occur as a result of carboxylate ion protonation in response to a decrease in pH, as would be encountered in the acidic vesicles of the endocytic pathway. This protonation results in an increased hydrophobic character and a greater partitioning of the polymer into the endosomal membrane leading to bilayer disruption (Murthy et al, 1999).

Red blood cell haemolysis assays showed PEAAc to be inactive to red blood cells at physiological pH, but more haemolytic below pH 6.3 (Murthy et al, 1999). Interestingly, by adding a single methylene unit to PEAAc, to create PPAAc, a 15 fold increase in red blood cell lysis occurred in comparison to PEAAc, probably due to the increased hydrophobicity of the polymer. Increased hydrophobicity also conferred PPAAc with a higher pK_a value, thus maximum haemolysis was reached at pH 6 and below, whereas the maximum for PEAAc occurred at pH 5.0 and below (Stayton et al, 2000). It was also demonstrated that when the protein streptadividin was conjugated to PPAAc, the conjugate retained its haemolytic ability, which was similar to the free PPAAc (Lackey et al, 1999b).

Red blood cell haemolysis by PEAAc and PPAAc is proposed to occur through the colloid osmotic mechanism. In this mechanism, aqueous pores are formed in the red blood cell membrane permitting equilibration of the extracellular buffer solutes with those in the red blood cell cytosol. Low molecular weight solutes in the cytoplasm are

able to diffuse out of the pores of the cell, whilst cytoplasmic macromolecules are unable to permeate. This results in a net influx of solutes, leading to an osmotic imbalance within the cell and finally red blood cell lysis (Murthy et al, 1999). (A schematic of this mechanism can be viewed in figure 1.9). However, although experiments were able to prove that this mechanism occurs in red blood cells, it is unknown if such a mechanism applies to endosomes.

PPAAc has recently been used in a mouse wound healing model and it has been demonstrated that topical application of PPAAc/DOTAP/DNA complexes enhanced expression of thrombospondin 2 (Kyriakides et al, 2002). It is of importance to note that as PPAAc is negatively charged, a cationic vector must be used in combination with the polymer in order to mediate condensation of DNA. However inclusion of a cationic vector will have implications on the overall pharmacokinetic and toxicity profile of the complex.

In addition to gene delivery, PPAAc has been shown to enhance endosomal escape of the ribosome inactivating toxin RTA when complexed to this polymer *in vitro*, as demonstrated by inhibition of protein synthesis in Ramos cells after incubation of the complex for 6h (Lackey et al, 1999a).

1.7.2.2.4 Poly(amidoamine)s (PAA)s

PAAs first emerged into the biomedical field as heparin-complexing agents during haemodialysis, as a result of their ability to form polyelectrolyte complexes with this highly anionic anticoagulant (reviewed in Ferruti et al, 1985; reviewed in Ferruti, 1996).

In the early 1970's, several PAA structures were shown to display inherent antitumour activity (Ferruti et al, 1973). Following this, their potential as drug carriers was proposed as PAAs display several advantageous properties to suit this application. Water-solubility and hydrolyzable bonds in their main backbone allowing degradation in aqueous media were two such attributes (Ranucci et al, 1991). Since then, water-soluble PAA carriers for anticancer drugs such as platinates and mitomycin C were developed. *In vivo* studies of the PAA-drug conjugates demonstrated reduced toxicity compared to the parent compounds and displayed activity against mouse L1210 tumour models (reviewed in Ferruti et al, 2002). Although these conjugates have potential for further development, extensive research is now being carried out on PAAs for use as bioresponsive, endosomolytic polymers. The key physico-chemical parameters conferring PAAs with this property are discussed below.

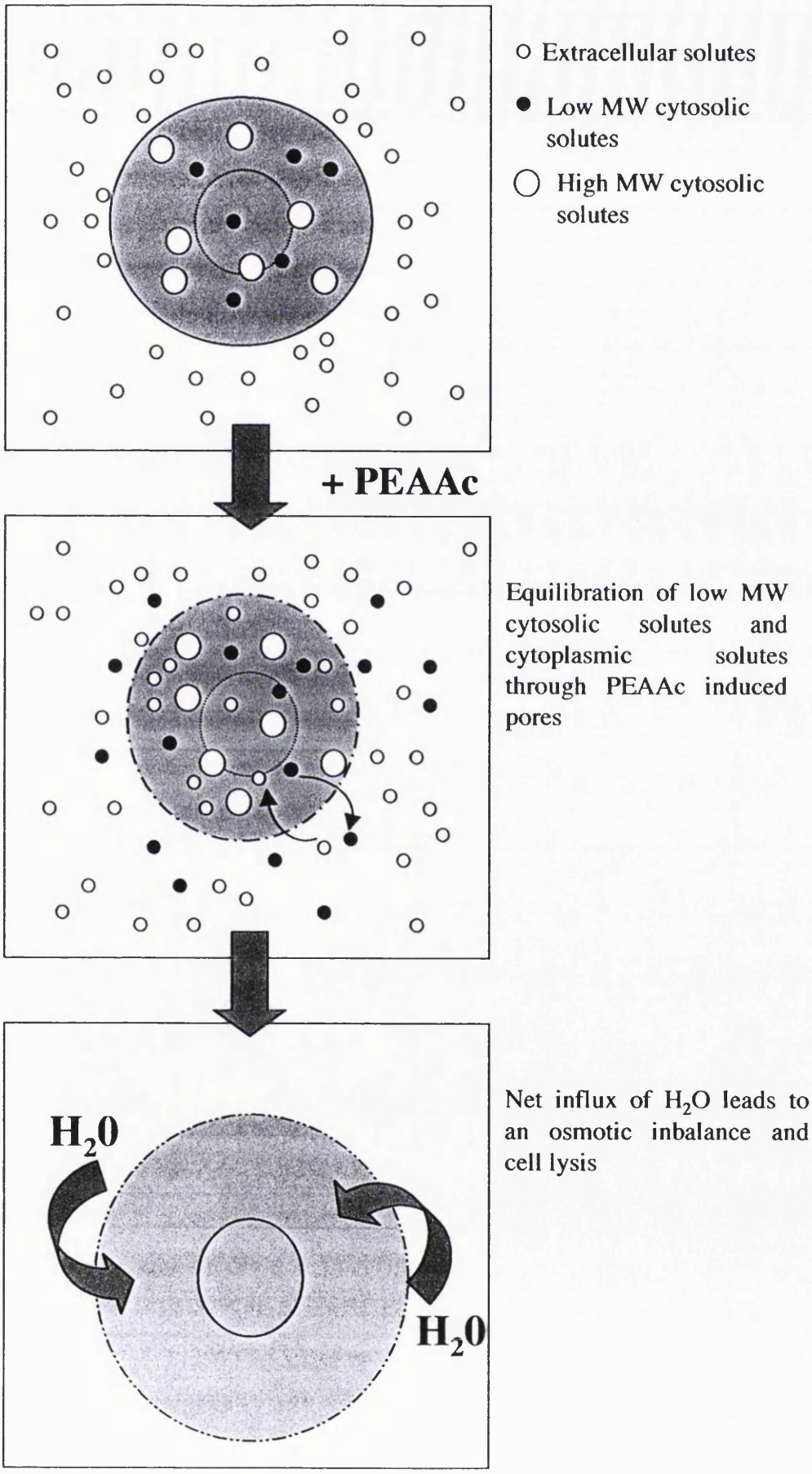

Figure 1.9 Proposed colloid osmotic mechanism to explain PEAAc-mediated RBC rupture

Linear PAAs are obtained by hydrogen transfer polyaddition of primary mono(amine)s and secondary bis(amine)s to bis-acrylamides as shown in figure 1.10. The resultant water-soluble polymers are characterised by the presence of amido- and tertiary amino-groups arranged regularly along the macromolecular chain (reviewed in Ferruti et al, 1998). Potentiometric titration experiments have shown that the basicity of the aminic nitrogens of each repeating unit does not depend on the degree of protonation of the whole macromolecule. Consequently, real basicity constants can be determined. This characteristic means that PAAs bearing two aminic nitrogen atoms show a marked conformational change in response to a decrease in pH. Following the first protonation, strong hydrogen bonds are formed between ammonium ions and carbonyl groups in the same monomeric unit. Protonation of the second aminic nitogen leads to electrostatic repulsion between ammonium ions, resulting in a rigid more extended conformation (reviewed in Ferruti, 1984).

This conformational change was further demonstrated using a hydroxylated PAA-triton X-100 conjugate (MBI-triton X-100). At pH 7.4, incubation of the conjugate with red blood cells did not cause lysis due to hiding of the detergent within the PAA coil. However, at pH 5.5, concentration-dependent lysis was observed. This was attributed to a pH-dependent conformational change occurring within the polymer coil exposing the detergent to red blood cells (Duncan et al, 1994). The structure of the MBI-triton X-100 conjugate and a schematic demonstrating its pH-responsiveness is shown in figure 1.11.

This unique physico-chemical property provided the opportunity to design bioresponsive polymers which could act as a potential substitute to the fusogenic peptides of viruses and allow delivery of macromoleuclar therapeutics to the cell cytosol. However, although the PAA-triton X-100 conjugate experiments demonstrated the bioresponsive properties of PAAs, the polymer itself did not display membrane permeabilising properties at a reduced pH. Therefore PAA structures were then synthesised (table 1.5) to cause pH-dependent haemolysis without the need for a pendant detergent as shown in figure 1.12 (Richardson et al, 1999a). From their protonation constants, the PAA ISA 23 (and ISA 22) is amphoteric, and thus has a net neutral charge at physiological pH. The PAA ISA 1 (and ISA 4) however is not amphoteric, and therefore displays a net positive charge at physiological pH. The pH-dependent haemolytic activity of these PAA structures can be attributed to their et al, 1999a) protonation constants. At pH $\leq$ 7.4, protonation of aminic nitrogens in the PAA backbone occurs leading to a conformational change within the polymer coil and an

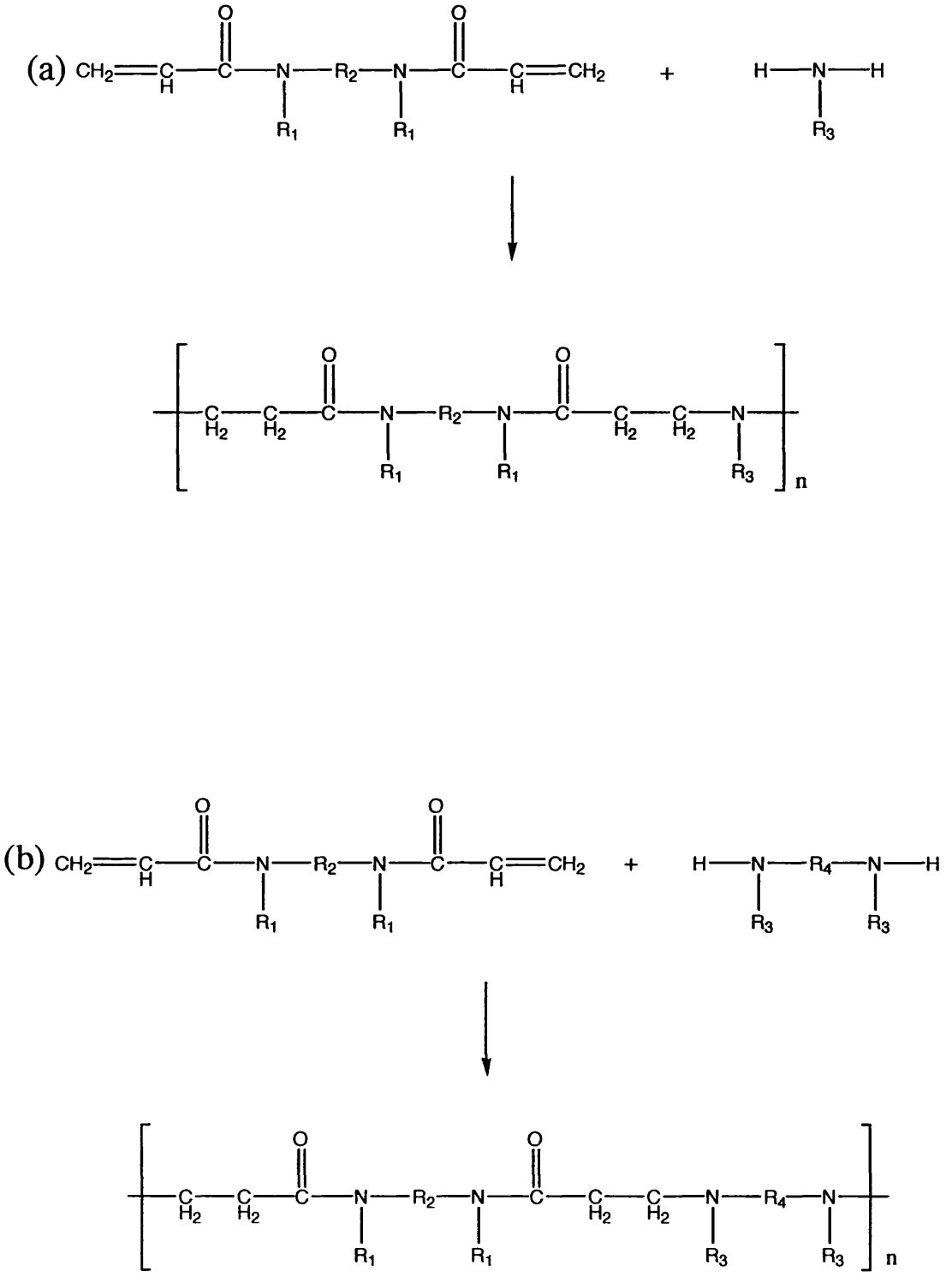

Figure 1.10 Synthesis of PAAs. Stepwise polyaddition of (a) primary or (b) secondary aliphatic amines to bis(acrylamide)s.

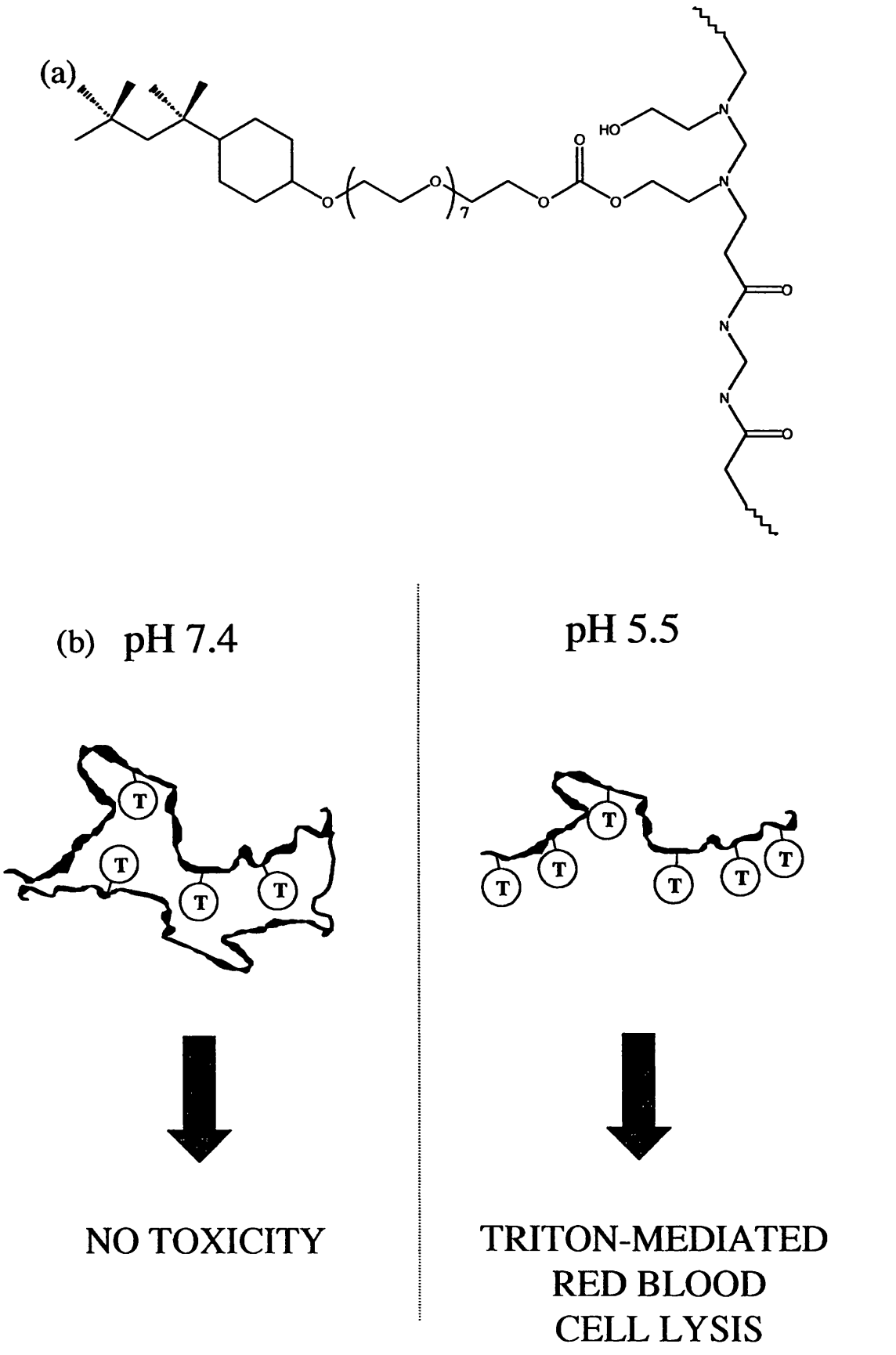

Figure 1.11 Characteristics of an MBI-triton X-100 conjugate. Panel (a) shows structure; (b) a schematic demonstrating the pH-responsiveness of PAAs using the MBI-triton X-100 conjugate.

Table 1.5 Structure and chemical characteristics of the PAAs under evaluation

ISA 1

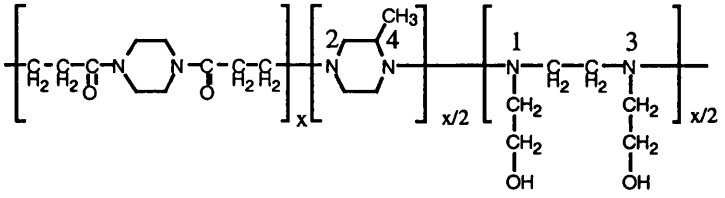

ISA 4

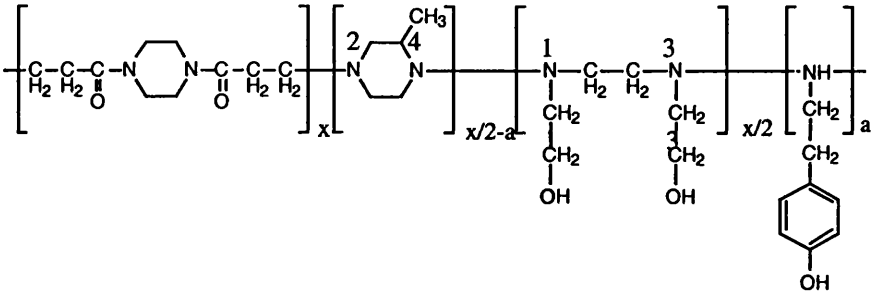

ISA 22

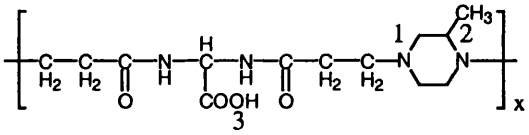

ISA 23

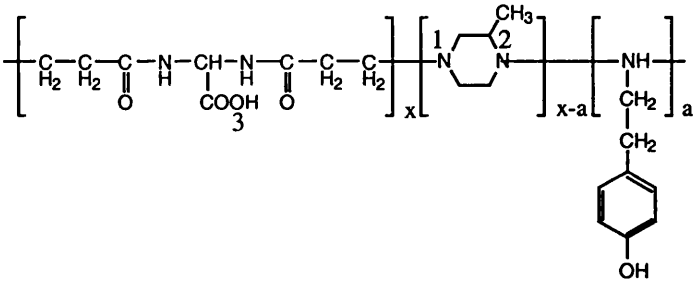

Polymer	pK_a1,	pK_a2,	pK_a3,	pK_a4	Mw[a] (g/mol)	Mn[a] (g/mol)
ISA 1	8.1,	6.9,	3.8,	3.0	12,300	5, 000
ISA 4	8.1,	6.9,	3.8,	3.0	15,000	10, 500
ISA 23	7.5,	3.25,	2.1		16,500	10, 500
ISA 22	7.5,	3.25,	2.1		14,900	8, 500

[a]Mw (weight-average molecular weight) and Mn (number-average molecular weight) were calculated by gel permeation chromatography against PAA standards (Richardson et al, 1999a).

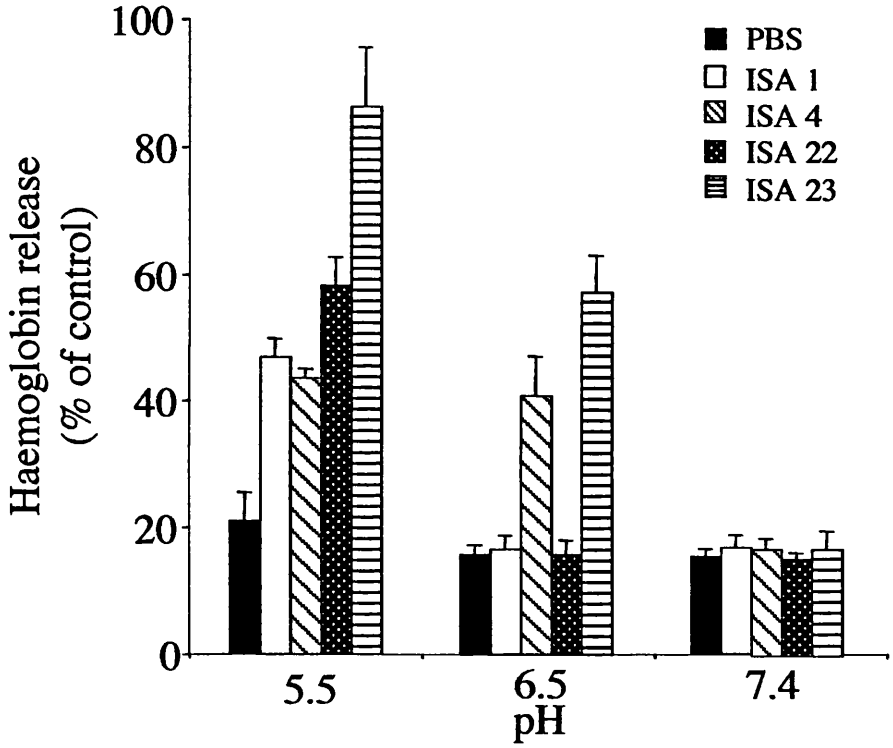

Figure 1.12 Haemolysis of rat RBC's after incubation with polymers (1mg/mL) for 24h. PBS was used as a control. Data represent mean ± S.D. (n=12). (Richardson et al, 1999a)

increase in positive charge. Although the mechanism for PAA-mediated membrane rupture has not been fully elucidated, polycation-mediated membrane damage has been well documented (Nevo et al, 1955; Godbey and Mikos, 2001). As aminic nitrogen protonation within PAAs increases at low pH, membrane damage occurs in acidic vesicles such as endosomes and lysosomes as opposed to the cell membrane. The efficiency of transfection is probably dependent on the rate of intracellular degradation of plasmid DNA (reviewed in Wattiiaux et al, 2000) and for many polyplexes, inability to promote endosomal membrane destabilisation results in degradation in the lysosome (Lucas et al, 1999). Many groups include membrane destabilising compounds such as fusogenic peptides in the transfection mixture which promote endosomal membrane destabilisation (Kircheis et al, 2001a). In addition weak bases such as chloroquine have been included during transfection which can increase transfection efficiency (Lucas et al, 1999).

Although high levels of transfection have been obtained *in vitro* for cationic polymeric delivery systems, it is important to note that most systems are being developed for *in vivo* use for systemic administration. This poses another set of problems such as anatomical size constraints, interactions with biological fluids and non-specific binding to non-target cells (Kircheis et al, 2001a). A major drawback of cationic systems is coating of the complexes with plasma components such as albumin and complement (reviewed in Plank et al, 1996). Opsonization causes rapid clearance of the foreign particles as well as interaction with cells of the RES resulting in high liver uptake (Godbey and Mikos, 2001; Kircheis et al, 2001a). Shielding the positive charge of polyplexes by PEG has been shown to efficiently shield polyplexes from these non-absence of damage to the cell membrane caused by PAAs has been demonstrated from cytotoxicity studies. All PAAs tested displayed IC_{50} values > 2 mg/mL towards B16F10, Mewo and HepG2 cell lines (Richardson et al, 1999a).

The lack of intrinsic toxicity of these PAAs suggested potential for parenteral administration and use as polymer-based therapeutics, however, it was essential to monitor their pharmacokinetic profile before further studies were undertaken. For these studies 2-(*p*-hydroxyphenyl)ethylamine analogues of ISA 23 and ISA 1 (denoted ISA 22 and ISA 4 respectively) were synthesised in order to allow their radioiodination and subsequent body distribution in male Wistar rats. After i.v. administration, ^{125}I-labelled ISA 4 was immediately taken up by the liver (> 80% recovered dose at 1h) (Richardson et al, 1999a). This is in agreement with pharmacokinetic studies using other cationic polymers (Lecocq et al, 2000; Verbaan et al, 2001; reviewed in Godbey and Mikos,

2001), and is due to surface opsonisation and rapid clearance by the RES. ^{125}I-labelled ISA 22 however, displayed a longer circulation time and reduced liver uptake (< 10% recovered dose at 5h) thus displays so called "stealth properties" (Richardson et al, 1999a).

As ISA 22 was able to display a long circulation time, preliminary experiments were performed to investigate whether it could be used to target tumours passively by the EPR effect as detailed in section 1.4. Biodistribution studies in male C57 mice bearing subcutaneous B16F10 melanoma showed that ^{125}I-labelled ISA 22 was still accumulating in tumour tissue after 5h (2.5% dose/g) (Richardson et al, 1999a).

1.8 Aims

PAA biocompatibility, body distribution and tumour accumulation have previously been documented (Richardson et al, 1999). However, as PAAs are being developed as intracytoplasmic delivery vehicles due to their proposed endosomolytic ability, it was considered important to collect evidence to support this and to investigate the feasibility of developing a PAA-protein conjugate for clinical testing.

Therefore the experimental aims of this thesis were to firstly provide evidence for the endosomolytic ability of PAAs. In chapter 3 (evaluation of the ability of PAAs to form IPECs and transfect cells *in vitro*), the ability of PAAs to form stable IPECs with DNA was evaluated. PAA-mediated endosomolytic ability was then explored by evaluating the ability of PAAs to mediate transfection of a β-galactosidase plasmid. However, as transfection efficiency is governed by many factors in addition to endosomal escape, it is difficult to assess for PAA-mediated endosomal breakage using only gene delivery as a model. Thus in chapter 4 (evaluation of the ability of PAAs to mediate intracytoplasmic delivery of RTA and gelonin toxins), the ability of PAAs to deliver the non-permeant toxins RTA and gelonin to the cell cytoplasm was also assessed. These systems only indirectly point to PAA-mediated endosomal rupture. To understand better the full potential of PAAs for intracytoplasmic delivery it was decided to seek direct evidence of their mechanisms of action. Therefore chapter 5 (direct evidence for PAA-induced lysosomal membrane rupture) reports experiments that sought direct evidence for PAA-mediated intracellular vesicle damage.

The long-term aim of this programme is to develop a PAA-toxin conjugate for clinical testing. Therefore in chapter 6 (synthesis and characterisation of PAA and gelonin fluorescent probes and visualisation of their endocytic capture) fluorescence microscopy was used to understand better the intracellular trafficking of both PAAs and

the gelonin toxin. In order to optimise the biological properties of these polymers for clinical applications, it was important to initially understand the polymer physico-chemical criteria required to achieve optimum PAA-mediated endosomolysis. In chapter 7, (evaluating the endosomolytic ability of modified PAA structures) the membrane lytic capability of different Mw analogues of ISA 23 were examined and this was compared to the parent ISA 23 polymer. In addition, the cytotoxic effect of a PAA-toxin construct was investigated *in vitro*.

CHAPTER 2

MATERIALS AND METHODS

2.1 Materials

2.1.1 General Chemicals

Phosphate buffered saline (PBS) Dulbecco A BR14 tablets were from Oxoid (Hampshire, UK). Sucrose, triton X-100, ethylenediaminetetraacetic acid (EDTA), sodium-citrate, bovine serum albumin (BSA), bicinchoninic acid (BCA) and copper II pentahydrate (4% (w/v)) were all supplied by Sigma (Dorset, UK). Glacial acetic acid and ethanol were from BDH (Poole, UK). Isofluorane was from Abbot labs (Kent, UK).

2.1.2 Polymers

PEG (Mw 8,000Da), dextran (Mw 72,000Da), PEI (Mn 70,000Da), Poly-L-lysine (56,500Da) were all from Sigma (Dorset, UK). All PAAs were supplied by Professor P. Ferruti (Milan, Italy) and their structures. The structures and chemical characteristics of the PAAs ISA 1, 4, 22 and 23 are listed in chapter 1, table 1.7. The PAAs ISA 1-NH_2 (Mw 16,700; Mn 9,800) and ISA 23-NH_2 (Mw 22,700; Mn 11,500) were synthesised to allow their conjugation to fluorescent probes. ISA 23 polymers of different Mw (A Mw 33,100 Mn 20,300; B Mw 23,800 Mn 18,200; C Mw 12,000 Mn 9,000) were synthesised to study the effect of Mw on their endosomolytic properties. A gelonin-ISA 1 conjugate (Mw 37,405) was synthesised to examine whether ISA 23 retains its endosomolytic properties when conjugated to a protein.

2.1.3 Tissue culture

RPMI 1640 media with Hepes (25mM) and L-glutamine, MEM media, foetal calf serum (FCS), trypsin (0.25%)-ETDA (1mM), non-essential amino acids and trypan blue were obtained from Gibco BRL (Scotland, UK). B16F10 cells were a kind gift from Professor Ian Hart, St. Thomas' Hospital (London, UK). HepG2 cells were purchased from ECACC (Wiltshire, UK).

2.1.4 Cytotoxicity assays

3-(4,5-Dimethylthiazol-2-yl)-2,5-diphenyltetrazolium bromide (MTT), sterile, optical grade dimethyl sulphoxide (DMSO), ricin, RTA and gelonin were purchased from Sigma (Dorset, UK).

2.1.5 Fluorescence microscopy

Oregon green 488 succinimidyl ester (OG-SE), texas red succinimidyl ester (TR-SE) and lysotracker red were all obtained from Molecular Probes (Leiden, The Netherlands). Anhydrous DMSO was obtained from Aldrich (Dorset, UK). $NaHCO_3$ and methanol were both supplied by BDH (Poole, UK). Paraformaldehyde was supplied by Fisher (Fisher Scientific Laboratories (Leicestershire, UK) and Vectashield® with DAPI was supplied by Vector Laboratories (California, USA).

2.1.6 IPEC formation

Calf thymus DNA, DNA gel loading solution, sodium acetate, potassium chloride, DNase II, perchloric acid, agarose, ethidium bromide (EtBr) and tris-base were from Sigma (Dorset, UK). Gel loading buffer was from Bio-Rad Laboratories (Hertfordshire, UK). λ Hind III DNA was obtained from Gibco BRL (Paisley, UK).

2.1.7 Amplification and transfection using pSV-β-galactosidase

E. coli DH5α cells were supplied by Gibco BRL (Paisley, UK). pSV-β-galactosidase, the β-galactosidase assay kit, restriction enzymes Vsp I and Bam HI, react 2 and react 3 buffers were all supplied by Promega (Southampton, UK). Agar, ampicillin, LipofectACE™ and LipofectIN™ were obtained from Gibco BRL (Paisley, UK). Glucose, isopropanol, tris-HCl, chloroform, lithium chloride, glycerol, sodium hydroxide, sodium chloride, phenol:chloroform:isoamyl alcohol, sodium dodecyl sulphate (SDS), RNase A, and lysozyme were all purchased from Sigma (Dorset, UK). LB broth was supplied by Anachem Ltd. (Bedfordshire, UK).

2.1.8 N-acetyl-β-D-glucosaminidase (NAGase) assays

4-Methylumbelliferyl-N-acetyl-β-D-glucosaminidase, 4-methylumbelliferone and sodium bicarbonate were obtained from Sigma (Dorset, UK).

2.1.9 Sodium dodecyl sulphate polyacrylamide gel electrophoresis (SDS-PAGE)

Broad range molecular weight standards, bis-acrylamide (30% (w/v)), ammonium persulphate (APS), N,N,N,N'-tetramethyethylenediamine (TEMED), β-mercaptoethanol, bromophenol blue, Siver stain plus kit and glycine were all obtained from Bio-Rad Laboratories (Hertfordshire, UK).

2.1.10 Transmission electron microscopy (TEM) and scanning electron microscopy (SEM)

Sodium cacodylate, gluteraldehyde, and osmium tetroxide, were supplied by Sigma, (Dorset, UK). Uranyl acetate, araldite CY212, benzyldimethylamne (BDMA), dodecenyl succinic anhydride (DDSA), propylene oxide and lead citrate were all purchased from Agar Scientific (Essex, UK).

2.2 Apparatus

2.2.1 General laboratory equipment

The Varifuge 3.0R centrifuge was obtained from Heraeus Instruments (UK). The Cary UV-visible and UV-1601 UV-visible spectrophotometers were purchased from Varian (Australia) and Shimadzu (Japan) respectively. The Tecan Sunrise micro-titre UV-Vis spectrophotometer was obtained from Tecan (Austria). The Micro Centaur mini-centrifuge was purchased from Sanyo Gallenkamp (UK). The AMINCO Bowman series 2 luminescence spectrophotometer was obtained from Spectronic Instruments (USA). The Avanti J-25 centrifuge, Optima™ LE-80K ultracentrifuge, JA-25.50 centrifuge rotor and SW28 centrifuge rotor were from Beckman Coulter (USA). The Potter-Elvehjem homogeniser was from Jencons Scientific (Bedfordshire, UK). PD10 gel permeation chromatography (GPC) columns were from Amersham Pharmacia Biotech (Hertfordshire, UK).

2.2.2 Tissue culture

The Neubauer haemocytometer was obtained from Weber Scientific (Sussex, UK). Serological pipettes were from Elkay (Hampshire, UK). Sterile tissue-culture 96-well and 6-well plates were obtained from Costar (New York, USA). BD Plastipak syringes were obtained from Becton Dickenson (Madrid, Spain). The Galaxy S CO_2 incubator was from Wolf Labs (UK). The class II type A-B3 microbiological safety cabinet AURA B was purchased from Bio Air s.c.r.l., (Milan, Italy).

2.2.3 Fluorescence microscopy

The Flexi-dry lyophiliser was from FTS systems (New York, USA). The Spectra/Por® dialysis membrane (2,000Mw cut-off) was obtained from Spectrum Laboratories (USA). The DRAM2 fluorescence microscope was from Leica Microsystems (Cambridge, UK). The FLUOstar OPTIMA fluorescence microtitre plate reader was from BMG (Offenburg, Germany). Alugram® SIL G/UV TLC plates were

from Macherey-Nagel (Düren, Germany). The UVGL-58 Mineralight® UV lamp was from UYP, (California, USA).

2.2.4 Agarose gel electrophoresis

The Horizon® horizontal agarose gel electrophoresis tank and the polaroid gel documenting system were from Gibco BRL (Paisley, UK). The UV transilluminator was obtained from UVP (California, USA).

2.2.5 IPEC formation

The Malvern ZetaSizer 3 was from Malvern Instruments Ltd, (Malvern, UK).

2.2.6 SDS-PAGE

The Power Pac 300 was from Bio-Rad Laboratories (Hertfordshire, UK). The Mini PROTEAN II® gel electrophoresis tank and accessories and the gel drying system including cellulose sheets and assembly table were from Bio-Rad Laboratories (Hertfordshire, UK).

2.2.7 TEM and SEM

BEEM® capsules, copper grids and holding chambers were from Agar Scientific (Essex, UK). The Philips 201 transmission electron microscope and the Philips 208 scanning electron microscope were supplied from Philips (The Netherlands).

2.3 Methods

2.3.1 Maintenance of cells

B16F10 cells were grown in RPMI 1640 media containing Hepes (25mM) and L-glutamine supplemented with foetal calf serum (10%). HepG2 cells were grown in MEM media supplemented with foetal calf serum (10%) and non-essential amino acids (5%). Cells were maintained in an atmosphere of 5% CO_2 (v/v) in a humidified CO_2 incubator and were grown in 75cm^2 tissue culture-treated, cantered neck flasks with vented tops (0.2μm).

2.3.2 Passaging of cells

All cell culture procedures were carried out in a class II laminar flow cabinet, where aseptic conditions were employed. Cells were passaged when they showed 70-80% confluency, in order to ensure an exponential growth phase. A 75cm^2 flask was

washed twice in 10mL PBS (0.1M) (in order to remove cell adhesion proteins) and 1mL pre-warmed trypsin (0.25%)-ETDA (1mM) was added. After a 5min incubation at 37°C, the cells became a suspension and 9mL pre-warmed media was added to the flask to dilute the trypsin. The cell suspension was then passed through a 20-gauge needle attached to a syringe to break up any cell aggregates and minimise cell clumping. 1mL was removed from this flask and used to seed a fresh tissue culture 75cm^2 flask containing 9mL pre-warmed media (1:10 split ratio). Flasks were then returned to the incubator and until cell growth reached 60-70% confluence or used in an experimental procedure. Passage numbers were recorded after every cell passage, and the maximum cell passage number used was 40.

B16F10 cells were passaged twice every week. HepG2 cells were passaged once every week.

2.3.3 Evaluation of cell number and cell viability

For quick cell counting a haemocytometer slide was used. The grid on this glass slide acts as a cell counting chamber. Cell viability can additionally be assessed using trypan blue dye. Trypan blue is only able to penetrate dead cells, thus viable cells are not stained and can be counted.

In order to prepare a Neubauer haemocytometer slide for cell counting, the edges of a precision ground coverslip were wet slightly and the coverslip pressed firmly onto the haemocytometer slide until Newton's rings appeared. Next, a cell suspension (20μL) was mixed with an equal volume of 2% (v/v) trypan blue dye (supplied as 4% (v/v) and diluted in PBS at a 1:1 ratio) and a drop (10μL) was placed at the edge of the coverslip using a pipette. The slide was then placed under an inverted light microscope and all viable cells counted (dead cells were stained blue) in a quadrant of known volume (0.1mm^3). The number of viable cells was then determined by the following formula:

Total number of viable cells/mL = mean number of cells per quadrant x dilution factor (2) x 10^4.

2.3.4 Freezing-down cells

A cell bank where cells were stored either frozen at -80^{0}C or in liquid nitrogen vapour, was created to ensure that when cell passage numbers reached over 40, new viable cells of low passage number could be easily recovered and used in subsequent assays.

First, sterile freezing media made from FCS (90% (v/v)) and DMSO (10% (v/v)) was filter sterilised (0.2μm filter) and warmed to 37^{0}C in a water-bath. Trypsinised cells diluted with media were then counted using a Neubauer haemocytometer. The number was recorded and the remaining cells transferred to a sterile centrifuge tube and spun at 1,500g x 5min at 37^{0}C. Following this, the supernatant was removed and cells were resuspended in the appropriate volume of freezing media to give a cell number of 1x10^6 cells/mL and disaggregated using a 20-gauge needle. Next, 1mL of the cell suspension was transferred into a sterile cryogenic vial. In order to ensure that cells were frozen slowly at a rate of 1°C/min, vials were wrapped in tissue paper, placed in a polystyrene box, placed at -20^{0}C for 1h and then at -80^{0}C overnight. The next morning, cells were placed in liquid nitrogen (-196^{0}C) for long term storage.

2.3.5 Cell recovery from cell banks

To recover the cryogenically frozen cells, the lids of the cryogenic vials were turned one-quarter and placed in a sterile 30mL universal bottle at 37°C. Once the preparation started to thaw (~ 3min), the preparation was centrifuged at 1,500g x 5min at 22^{0}C and the supernatant removed. Cells were resuspended in 1mL of the appropriate cell culture media for the cell line and used to seed a 25cm^2 tissue culture-treated, cantered neck flask with vented top (0.2μm) which contained 4mL of the appropriate cell culture medium. Once cells were confluent (~ 4 days), cells were passaged and seeded into 75cm^2 flasks.

2.3.6 Evaluation of cell viability using the colourimetric tetrazolium-based 3-[4,5-dimethylthiazol-2-yl]-2,5-diphenyltetrazolium bromide (MTT) assay

To ascertain the effect of potential toxicity of polymers on cells, a cytotoxicity assay was performed. Sterile, flat-bottomed 96-well plates were seeded with B16F10 or HepG2 cells to a density of 1 x 10^4 cells/well and incubated at 37°C in an atmosphere of CO_2 (5% (v/v)) for 24h. Polymers were dissolved in media to give stock solutions (0.05 and 2mg/mL) and were filter sterilised and then added to the cells to give a final concentration range of 0-2mg/mL as described in table 2.1.

After incubation for 67 h, cell viability was assessed using the MTT assay (Sgouras and Duncan, 1990). This assay is based on the ability of mitochondrial dehydrogenase enzymes in viable cells to metabolise a water-soluble tetrazolium dye (MTT) into an insoluble formazan salt as seen in figure 2.1. MTT (20μL of a 5mg/mL solution in PBS) was added to each well and the plates were subject

Table 2.1. Polymer concentrations used in the cytotoxicity assay

Polymer concentration (mg/mL)	Amount polymer (μL)	Amount media (μL)	Stock (mg/mL)
2	100	0	2
1	50	50	2
0.5	25	75	2
0.1	5	95	2
0.05	100	0	0.05
0.01	20	80	0.05
0.005	10	90	0.05
0.001	2	98	0.05
0	0	100	0

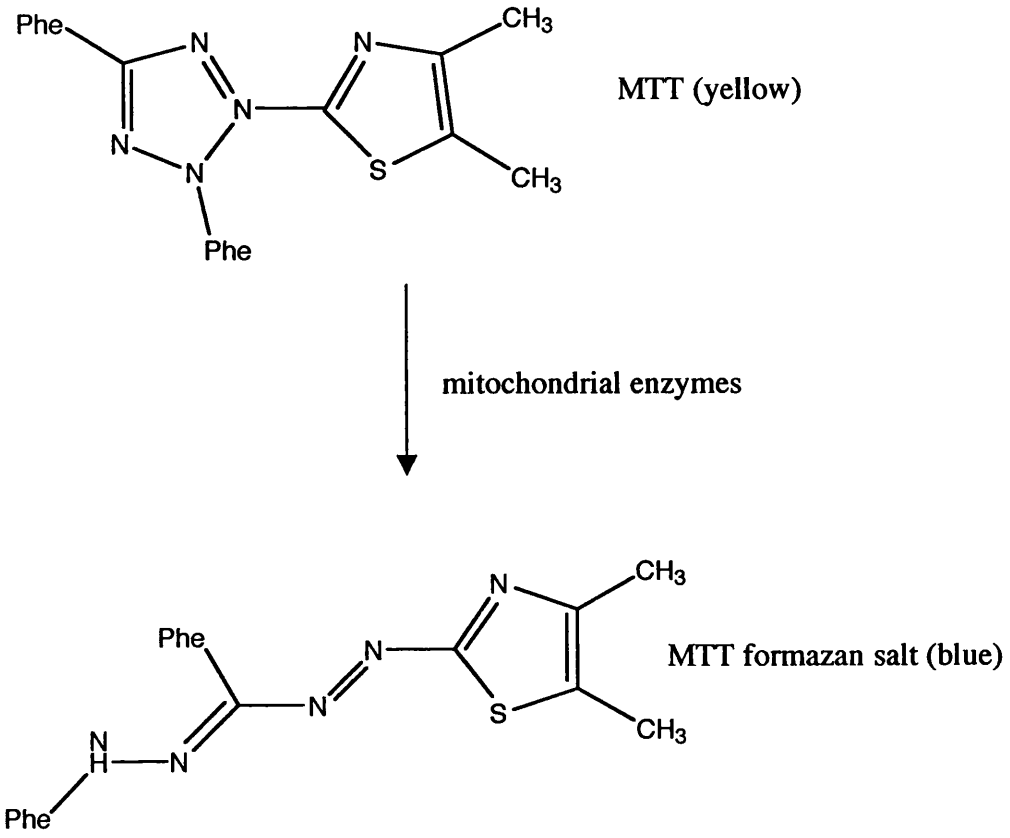

Figure 2.1 Schematic showing the reduction of MTT to an MTT formazan salt

to a further incubation of 5h at 37^{0}C in 5% CO_2. After this time, the plates were gently tipped and the media aspirated, taking care not to disturb the layer of formazan crystals at the base of each well. Spectrophotometric grade DMSO (100μL) was then added to each well and the plates incubated at 37°C for 30min to dissolve the crystals. The plates were then read spectrophotometrically at 550nm using a microtitre plate reader.

Cells incubated in cell culture medium alone were used as a control to assess 100% viability. Viability of cells exposed to test compounds was expressed as a percentage of the viability seen in the control untreated cells (mean ± S.D.) (n=18).

To establish the rate of growth of B16F10 and HepG2 cells, the MTT assay was repeated at 24h intervals for 10 days. A growth curve was constructed as a function of optical density (OD) against time for each cell line and shown in figures 2.2 and 2.3.

2.3.7 Toxin cytotoxicity

B16F10 or HepG2 cells were exposed to either RTA or gelonin (0-10μg/mL, 100μL) (stock concentrations made and determined by the bicinchoninic acid protein (BCA) assay, section 2.3.12) for 67h and viability assessed using the MTT assay as described above.

2.3.8 Evaluation of cytotoxicity of polymer/toxin combinations

The ribosome inactivating toxins RTA and gelonin were used in combination with polymers to test polymer-mediated endosomolytic ability. RTA and gelonin were dissolved in media at concentrations of 250ng/mL and 1.4μg/mL respectively for B16F10 cells and 0.1ng/mL and 0.1μg/mL for HepG2 cells respectively (non-toxic concentrations were determined by the toxin cytotoxicity assay outlined in section 2.3.7). The polymers used were then dissolved in the appropriate amount of these media to give polymer stock concentrations of 2mg/mL and 0.05mg/mL and filter sterilised. Pre-seeded 96-well plates were then dosed with polymers (100μL), ranging in concentration from 0-2mg/mL (obtained by diluting polymer stock solutions with media containing toxin) as outlined in table 2.2. In order to ensure that no toxin-related cytotoxicity occurred to cells at the pre-determined non-toxic concentration, media alone (no toxin) was also added to cells and included in the experiment. B16F10 or HepG2 cells were exposed to polymer/toxin combinations for 67h and cell viability measured by the MTT assay as described above.

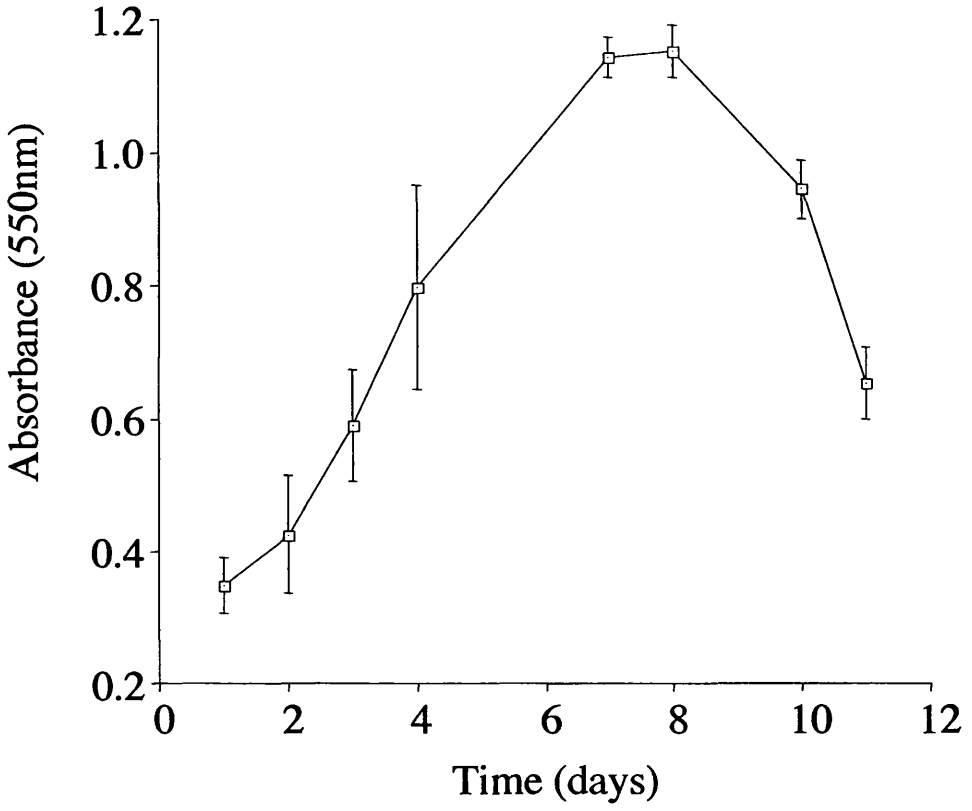

Figure 2.2 B16F10 growth curve of cells seeded to a density of 1 x 10^4 cells/mL. Data represent mean ± S.D. (n=18).

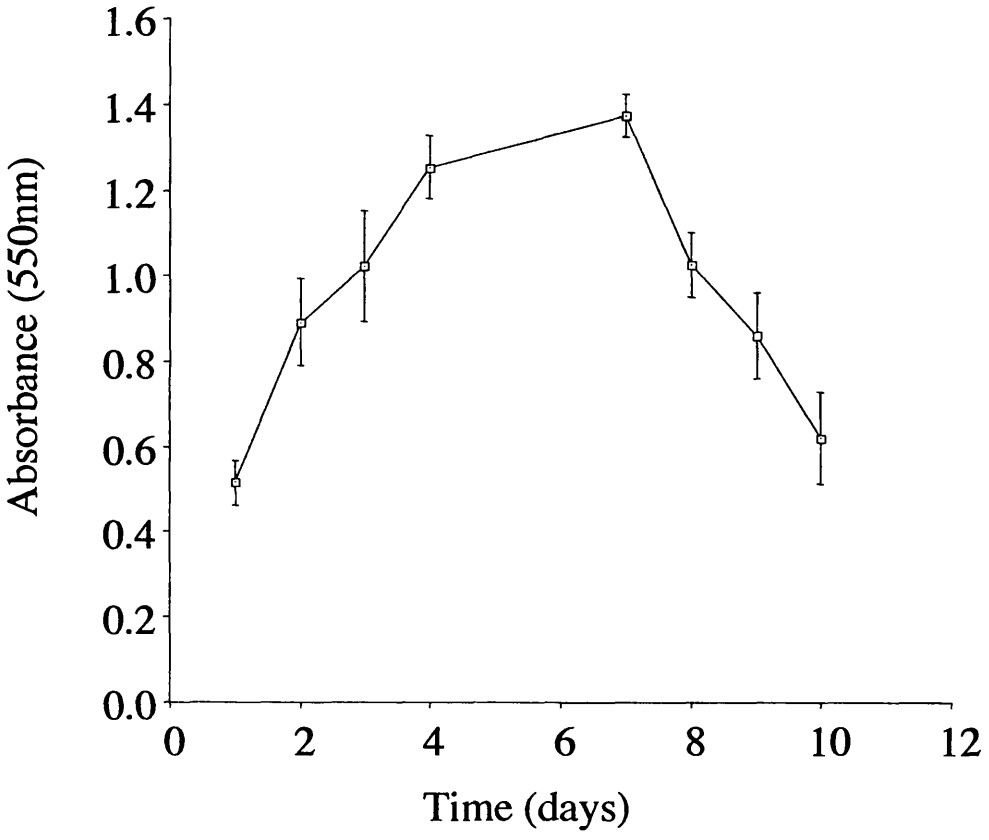

Figure 2.3 HepG2 growth curve of cells seeded to a density of 1 x 10^4 cells/mL. Data represent mean ± S.D. (n=18).

Table 2.2 Polymer concentrations used in the cytotoxicity assay with a fixed concentration of toxin

Polymer concentration (mg/mL)	Amount polymer (+ toxin) (μL)	Amount media (+ toxin) (μL)	Stock (mg/mL)
2	100	0	2
1	50	50	2
0.5	25	75	2
0.1	5	95	2
0.05	100	100	0.05
0.01	20	80	0.05
0.005	10	90	0.05
0.001	2	98	0.05
0	0	100	0
No gelonin	0	100 (- toxin)	0

To investigate the effect of varying toxin concentration in the presence of a fixed polymer concentration on B16F10 cells, ISA 4 was dissolved in media to give concentrations of 0.005, 0.05, 0.3, 0.5, 1 and 1.5mg/mL. These specific ISA 4 concentrations were then used to dissolve RTA to give stock solutions of 10 and 0.1μg/mL respectively. These stock solutions were then diluted with media containing the appropriate concentration of ISA 4 to obtain RTA concentrations ranging from 0-10μg/mL as outlined in the table 2.3.

RTA/ISA 4 combinations (100μL) were then added to B16F10 cells and incubated for 67h before cell viability was assessed using the MTT assay as described above.

2.3.9 Synthesis, purification and characterisation of PAA-oregon green and gelonin-texas red conjugates for fluorescence microscopy

Conjugation of fluorescent dyes to PAAs and gelonin is a method for obtaining qualitative information on their subcellular distribution. Described below are the calibration, conjugation, purification and characterisation procedures for the fluorescent derivatives and their subsequent preparation for viewing after uptake into cells by fluorescence microscopy.

Derivatives of ISA 1 and ISA 23 containing a terminal amine to allow conjugation were synthesised (Malegsini et al, 2002). OG-SE (0.5mg in ISA 23 reaction and 1mg in ISA 1 reaction) was dissolved in DMSO (50μL) in an eppendorf tube. ISA 23-NH_2 (0.394g) and ISA 1-NH_2 (0.384g) were dissolved in $NaHCO_3$ (1mL of a 0.1M solution, pH 8.3) in round-bottomed flasks and stirred gently. Next, OG-SE (50μL) was added to each flask and both were then covered in foil to protect them from light. The flask containing the ISA 23-NH_2 and OG-SE reaction mixture was left to react for 2h at room temperature. As ISA 1-NH_2 contained two pendant hydroxyl groups which could potentially react with OG-SE, the flask containing this reaction mixture was placed at 4^0C for 24h to ensure preferential reaction of OG-SE with the pendant amine group and OG-SE (1mg) was used for the conjugation reaction.

TR-SE (0.5mg) was dissolved in DMSO (50μL) in an eppendorf tube. Gelonin (1mg) was dissolved in $NaHCO_3$ buffer (1mL of a 0.1M solution) in a round-bottomed flask and stirred gently. TR-SE (50μL) was then added to the flask which was then covered in foil. The mixture was then left to react for 2h at room temperature.

The void volume (V_0) of a PD10 G-25 sephadex column was determined by passing blue dextran through the column. The column was then calibrated using free

Table 2.3 RTA concentrations used in the cytotoxicity assay with a fixed concentration of polymer

RTA concentration (μg/mL)	Amount RTA (+ ISA 4) (μL)	Amount media (+ ISA 4) (μL)	RTA stock (mg/mL)
10	100	0	10
5	50	50	10
1	10	90	10
0.5	5	95	10
0.1	100	0	0.1
0.05	50	50	0.1
0.01	10	90	0.1
0.005	5	95	0.1
0.001	1	99	0.1
0	0	100	0

OG-SE and TR-SE to ensure that separation of unconjugated and conjugated compounds was possible. PD10 columns were drained of storage buffer and equilibrated in 5 x 5mL PBS (0.1M). Next, blue dextran (1mg/mL) in PBS was carefully placed onto the top of the PD10 column and eluted with 20 x 0.5mL PBS (0.1M). Fractions were collected in eppendorf tubes. A sample (100μL) was assessed spectrophotometrically in triplicate (280nm) using a microtitre plate reader. Data were plotted as a function of OD (280nm) vs. elution volume (mL) (results not shown, however V_0 is marked on all the elution profiles). OG-SE and TR-SE were made up in PBS (0.1M; 0.1mg/mL). These solutions were carefully placed onto the top of the PD10 columns and eluted with 20 x 0.5mL PBS (0.1M). Fractions were collected in eppendorf tubes and protected from light. Next, aliquots of each fraction (10μL) were transferred to a non-sterile 96-well flat-bottomed microtitre plate containing PBS (90μL). The fluorescence intensity of each fraction was then measured using a fluorescence spectrophotometer (ex 495; em 521 for OG-SE and ex 583; em 603 for TR-SE). Results were expressed as fluorescence units vs. elution volume (figure 2.4).

After calibration of PD10 columns using the dyes, these columns were used to separate unreacted OG-SE and N-hydroxysuccinimide from macromolecular ISA 1-OG or ISA 23-OG. Similarly they were used to separate unreacted TR-SE and N-hydroxysuccinimide from macromolecular gelonin-TR. PD10-columns were prepared as described above. Next ISA 1-OG, ISA 23-OG or gelonin-TR (0.5mL) were transferred on to the columns and eluted with 40 x 0.5mL PBS (0.1M) and fluorescence intensity measured as described above. The data were expressed as fluorescence units vs. elution volume.

Fractions in the macromolecular peak were then pooled and checked for purity by TLC analysis. A line was drawn with a pencil (the origin) about 0.5cm from the base end of an Alugram® SIL G/UV TLC plate. Pooled ISA 1-OG and ISA 23-OG fractions and OG-SE (0.1mg/mL; used as a reference control) were then spotted onto the origin. This was repeated for gelonin-TR fractions and TR-SE (0.1mg/mL used as a reference control). Next, the TLC plates were placed in a glass TLC beaker containing methanol (running phase) (5mL). Care was taken to ensure that solvent depth was below the level of the origin. When the level of the running phase had progressed to within 1cm of the top of the plate, the TLC plate was carefully removed air-dried. Plates containing OG samples were viewed using a short wavelength UV lamp. Plates containing TR samples were viewed using a long wavelength UV lamp. Movement of

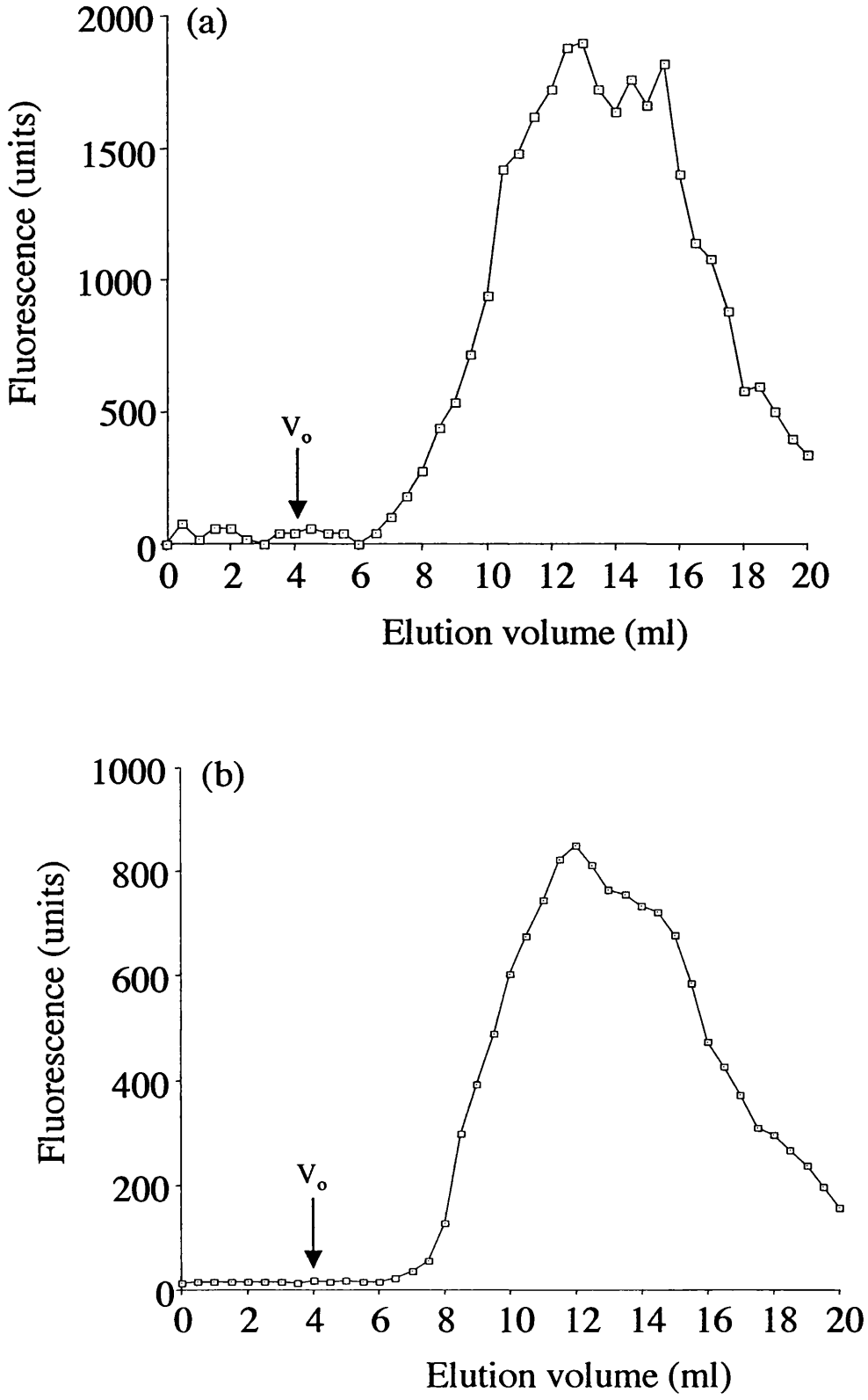

Figure 2.4 Elution profiles of fluorescent probes eluted on PD10 columns equilibrated in PBS. Panel (a) shows OG-SE; (b) TR-SE.

the compounds was expressed as an R_f value and compared to the free fluorophore standards. Once sample purity had been confirmed, gelonin-TR was stored at -4^{0}C and protected from light (sample quantity was too small for lyophilisation).

ISA 1-OG and ISA 23-OG were prepared for lyophilisation. PAA probes were poured into dialysis membranes 2000 (Mw cut-off) and dialysed against DDW for 2 days. Next, samples were poured into pre-weighed 50mL tubes and frozen in liquid nitrogen. Aluminium foil was then placed over the tubes and holes punched into the foil lid. Tubes were placed in a lyophiliser for 3 days and then weighed. Finally, the samples were stored at -20^{0}C and protected from light and water.

It was necessary to ensure that the prepared fluorescent conjugates contained the same excitation and emission spectra as free fluorescent dyes. TR-SE and OG-SE (0.01mg/mL) in PBS (2.5mL of a 0.1M solution) were each transferred to UV-grade spectrophotometric cuvettes and the emission and excitation spectra measured using a fluorescence spectrophotometer. Results were expressed as fluorescence units against wavelength. This procedure was repeated for ISA 1-OG, ISA 23-OG and gelonin-TR and the emission and excitation maxima for each compound compared with the free dye.

2.3.9.1 Construction of calibration curve of oregon green-succinimidyl ester concentration against fluorescence units

During the characterisation of PAA-OG conjugates, it was important to determine the degree of OG labelling to PAAs. In order to perform these calculations, a calibration curve of OG-SE concentration against fluorescence units was constructed. OG-SE (0.5mg) was made up to a stock concentration in DMSO (50µL; 10mg/mL). This was then diluted in PBS (0.1M), or $NaHCO_3$ (0.1M pH 8.3) to give stock solutions (0.001mg/mL). Serial dilutions of the stock solution were then performed in triplicate in a non-sterile 96-well flat-bottomed microtitre plate to yield OG-SE ranging from 0-0.001mg/mL. Fluorescence was then measured in a fluorescence spectrophotometer (ex 488; em 525) and results expressed as fluorescence units against OG-SE concentration.

2.3.9.2 Uptake studies of fluorescent-labelled PAAs and gelonin in B16F10 and HepG2 cells using fluorescence microscopy

Tissue-culture grade glass coverslips (0.1mm thickness), were sterilised in ethanol (100% (v/v)), dried in air and placed in each well of a sterile 6-well tissue-

culture plate. Each well was then washed (x2) in the appropriate media for the cell line used to ensure that no ethanol was remaining in the wells. Next, B16F10 of HepG2 cells were seeded to densities of 5 x 10^5 cells/mL (1mL vol) and incubated for 24h at 37^0C in an atmosphere of CO_2 (5% (v/v)). Test compounds (chapter 6) were then dissolved in corresponding media (1mL), filter sterilised, and added to wells after the media had been aspirated off. Next, the plate was covered in foil to protect it from light and incubated at 37^0C, in an atmosphere of CO_2 (5% (v/v)) for 5h or 24h.

To investigate whether the lysotracker dye (which localises to acidic intracellular vesicles) would colocalise with the PAA-OG probes, media was aspirated from each well after 4.5h or 23.5h incubation and lysotracker red (200nM) was added to wells in media (1mL) and incubated for 30min at 37^0C.

After incubation (with PAA-OG probes, lysotracker red dye, or both), media was aspirated from wells and ice-cold PBS (1mL of a 0.1M solution) was added to each well for 5min. After this time PBS was removed and a further 2 x 5min washes of ice-cold PBS (0.1M) was performed. Next, parafomaldehyde solution (1mL of 3% (w/v)) was transferred to each well and left for 30min. Fixative was then removed and 3 x 5min washes of PBS (0.1M) was performed. Cover-slips were then removed from wells using tweezers and dipped briefly in PBS (0.1M) followed by DDW. Next, cover-slips were placed cell-side down onto labelled microscope slides onto which a drop of cell mounting oil (Vectashield® with DAPI) had been placed. Excess mounting oil was then blotted off cover-slips which were then placed in the dark at 4°C before viewing using a Leica fluorescence microscope.

2.3.10 Techniques used to investigate PAA/IPEC formation

2.3.10.1 Evaluation of the stability of DNA to DNase II

PAA/DNA complex formation was assessed by measuring the ability of PAAs to protect DNA from degradation by the nuclease, DNase II. In order to determine if PAA complexation afforded any protection of DNA from degradation, DNA alone was first assessed for DNase II-mediated degradation over time. This method was adapted from the protocol of Richardson et al, (1999b).

Calf thymus DNA (1mg/mL) was dissolved in sodium acetate buffer (0.2M) pH 5.5 supplemented with potassium chloride (0.2M) and left for 24h at 4°C. The DNA solution was further diluted to 0.1mg/mL by the addition of sodium acetate buffer (0.2M) pH 5.5 supplemented with potassium chloride (0.2M) and heated to 37^0C. DNase II (300U/mL; 360μL) was added to the DNA solution (6mL total reaction

volume) in a 20mL centrifuge tube and the mixture was aspirated gently, before removal of 2 x aliquots (500μL) into sterile eppendorfs and the immediate addition of perchloric acid (500μL of a 10% (w/v) solution) to each aliquot to stop the reactions. This was denoted time 0min. The aliquots were then placed on ice for 20min prior to centrifugation at 1,200g x 20min to pellet undegraded DNA. Subsequent aliquots were removed from the mixture at 2, 5, 10, 15, 20, 30 and 60min. After centrifugation, supernatants were removed and placed in 1mL UV-grade cuvettes. The absorbency of each aliquot was read spectrophotometrically at 260nm in a UV-visible spectrophotometer, denoting the quantity of degraded DNA in the sample.

Experiments were then repeated with the addition of polymer to ascertain the ability of polymer to complex and protect DNA from degradation. All experiments were performed using polymer:DNA weight ratios ranging from 0.1:1 to 100:1. Polymer at the correct weight ratio was added to DNA in 20mL tubes and aspirated gently. Mixtures were left to stand for 30min to allow complex formation prior to addition of DNase II (300U/mL). Spectrophotometric data was expressed as DNA degradation as a percentage of degradation of a DNA control containing no polymer (mean ± S.D.) (n=3).

2.3.10.2 Evaluation of IPEC formation using a gel retardation assay

PAA/DNA IPEC formation was additionally assessed using a gel retardation assay. This method gives an indication of the condensation of DNA by the polymer from the degree of DNA retardation in the agarose gel.

Gels were made up using 1 x TAE buffer (100mL), (diluted from a 50x TAE stock: 242g Tris base, 57.1g glacial acetic acid, 100mL EDTA (0.5M) pH 8) and electrophoresis grade agarose (0.7g). The solution was boiled in order to dissolve the agarose, swirled to mix and then left to cool to 60°C before the addition of EtBr (0.25μg/mL) (Ausubel et al, 1994). The cooled gel was then poured into an electrophoresis tank with a 14-well gel comb and left to set. Electrophoresis buffer was made up from 1 x TAE buffer (1L) containing EtBr (0.25μg/mL). λ Hind III DNA (0.1mg/mL) was diluted in sterile saline (0.9% (w/v)). This was then mixed with polymers at defined polymer:DNA weight ratios ranging from 1:1 to 100:1 and left for 30min to allow complex formation. Once the gel had set, electrophoresis buffer was poured into the tank until it covered the gel by ~ 1mm. Samples and λ Hind III DNA alone were then mixed with 1x gel solution (3μL) and loaded onto the gel (maximum sample volume, 20μL). The lid was then placed over the electrophoresis tank and

connected to a power supply and run at 80V for 1h. After this time the gel was removed from the tank and DNA visualised under a UV transilluminator. Gels were photographed using a Polaroid gel documenting system.

2.3.10.3 Morphological analysis of IPECs using TEM

TEM was used to visualise the complexes formed between PAAs and DNA. IPECs were formed from pSV-β-galactosidase plasmid (1μg) at polymer:DNA weight ratios of 10:1 in sterile saline (0.9% (w/v)) and left for 30min to allow complex formation. Complexes were then added dropwise onto copper TEM grids and stained with a drop of uranyl acetate (1% (w/v)). After staining, grids were blotted onto filter paper and visualised using a Philips 201 TEM.

2.3.10.4 Evaluation of IPEC formation using an EtBr displacement assay

EtBr bound to DNA has a much higher fluorescence than the dye alone. EtBr itself absorbs UV light at 302 and 366nm. However, DNA, when complexed to the dye, absorbs UV light at 254nm and then transmits this to EtBr. All this energy is then re-emitted at 590nm in the red-orange part of the visible spectrum. Thus the amount of fluorescence is proportional to the amount of nucleic acid present. The degree of DNA complexation by polymers was measured using this assay.

Firstly, a 3mL-capacity fluorescence grade cuvette was filled with DDW (2mL) and EtBr (3μL; 1μg/μL stock) and the fluorescence output was then read in a fluorescence spectrophotometer (ex 516; em 590nm) and denoted F_0 (original fluorescence). Next, calf thymus DNA (15μL; 1μg/μL stock) was added to the cuvette which was swirled to mix the contents. Again the fluorescence intensity was measured after allowing the reading to stabilise and the reading was denoted F_{in} (initial fluorescence). Polymer solutions (1μg/μL), with the exception of PEI, were then made up in DDW and added incrementally to each cuvette at polymer:DNA weight ratios ranging from 0:1-100:1. Due its high charge density, PEI (1μg/μL) was added incrementally to cuvettes at polymer:DNA weight ratios ranging from 0.1:1-10:1. After each addition of polymer, cuvettes were swirled, and fluorescence measurements taken after the reading had stabilised. These readings were denoted F_{meas} (measured fluorescence).

After each incremental addition of polymer, fluorescent signals were corrected and expressed as a percentage of the signal attributed to that for DNA alone, denoted F_r

(relative fluorescence intensity) as described by the equation shown below (Rungsardthong et al, 2001):

$$F_r\ (\%) = (F_{meas}-F_o)/(F_{in}-F_o) \times 100$$

This data was expressed as (mean ± S.D.) (n=3).

2.3.10.5 Evaluation of IPEC stability to anionic challenge

As PAA/DNA complexes are being developed for i.v., it was important to study the stability of the IPECs in the presence of the anionic serum protein BSA. This was performed by adding aliquots of BSA to IPECs formed at defined polymer:DNA weight ratios and assessing for an increase in EtBr fluorescence intensity. This method was adapted from the protocol of Ramsay et al, (2000).

A polymer:DNA weight ratio of 40:1 was chosen, as substantial DNA condensation occurred at this ratio. Samples were made up in DDW as before and placed in a cuvette containing EtBr (3μL; 1μg/μL stock) and DDW (2mL). Fluorescence readings were taken and denoted. BSA was then added incrementally to samples (1μg/μL in DDW) at BSA:polymer weight ratios ranging from 0:1-20:1. After each addition of polymer, cuvettes were swirled, and fluorescence measurements taken after the reading had stabilised. Results were calculated according to the above equation and expressed as mean ± S.D. (n=3).

2.3.10.6 Zeta potential determination of IPECs

The zeta potential of PAA/pSV-β-galactosidase complexes was determined by microelectrophoresis using a Zetasizer. pSV-β-Galactosidase (20μg/ml) was mixed with filtered ISA 4 or ISA 23 at polymer:DNA weight ratios of 1:1, 5:1 and 10:1 respectively in degassed DDW (2.5mL volume) in a spectrophotometric cuvette. The mixtures were left for 30min to allow complex formation. Measurements were taken 3 times at 25^0C after instrument calibration using a 55mV standard.

2.3.11 Transfection assays using the plasmid vector pSV-β-galactosidase

2.3.11.1 Amplification, isolation and characterisation of pSV-β-galactosidase

The methods used in this section were adapted from Ausubel et al, (1994). Rapidly thawed *E. coli* DH5α cells (200μL) were transferred to a sterile pre-chilled eppendorf tube using a chilled sterile pipette tip. Next, pSV-β-galactosidase DNA (50ng) was diluted in sterile TE buffer (10μL; 10mM Tris pH 8, 1mM EDTA) and added to the eppendorf. The mixture was aspirated gently and then left on ice for

30min. *E. coli* DH5α cells were then heat-shocked to allow entry of plasmid into the cells. This was achieved by transferring the eppendorf tube to a waterbath heated to 42^0C for 90s. After this time, cells were incubated at 37^0C for 5min and then placed on ice for 2min. In order to encourage cell division of transformed *E. coli* DH5α cells, allowing amplification of the plasmid, sterile, LB broth (800μL), heated to 37^0C was added to the transformed cells in the eppendorf tube which was then incubated for 45min in a 37^0C waterbath. After this time, aliquots of transformed DH5α cells (200μL) were used to innoculate agar plates containing ampicillin (50μg/mL) to allow for selection of the plasmid which contained an ampicillin resistance gene. Inoculated plates were incubated overnight at 37^0C to allow growth of bacterial colonies.

A streak of colonies was scraped from the agar plate using a sterile pipette tip and placed in a sterile flask containing a starter culture media (10mL; LB media containing ampicillin (50μg/mL)), and incubated at 37^0C in an orbital shaker (200rpm). Every few hours an aliquot was removed and the optical density (growth) of the culture measured using a UV-visible spectrophotometer at 600nm. When the optical density reached 0.6, the starter culture was used to inoculate a baffled flask containing sterile LB broth (75mL). Following this the flask was incubated overnight at 37^0C in an orbital shaker (200rpm).

Cells grown in the baffled flask overnight were first subject to centrifugation (3,000g x 30min) at 4^0C to pellet bacterial cells. The supernatant was discarded and the cell pellet resuspended in 10mL STE buffer (0.1mM sodium chloride, 10mM Tris pH8, 1mM EDTA) and centrifuged as before. The pellet was then suspended (final volume 10mL) in a solution of cell lysis buffer (50mM glucose, 25mM Tris-HCl, pH 8, 10mM EDTA pH 8). To this suspension a lysozyme solution (2mL; 25mg/mL in 10mM Tris-HCL pH 8) was added followed by freshly prepared sodium hydroxide (0.2M) containing sodium dodecyl sulphate (20mL; 1%(w/v)). The cells were left to lyse for 10min at room temperature. Next, ice-cold preparation of solution A (15mL) (60mL; 5M potassium acetate, glacial acetic acid (11.5mL), DDW (28.5mL)) was added and the preparation placed on ice for 10min prior to centrifugation (20,000g x 15min) at 4^0C. The supernatant containing plasmid DNA was then decanted, filtered through a sterile cheesecloth, and isopropanol (0.6 vol) added to precipitate DNA. After a 10min incubation at room temperature, the sample was centrifuged (15,000g x 30min) at room temperature to pellet the precipitated nucleic acids. The supernatant was then decanted and disposed of and the pellet dissolved in TE buffer pH 8 (3mL).

To remove unwanted high molecular weight bacterial DNA, (1 vol) ice-cold lithium chloride (5M) was added to the preparation resulting in precipitation of high molecular weight DNA. The contaminating pellet was then removed by centrifugation (15,000g x 30min) at 4^0C. The supernatant was decanted into a fresh sterile tube, and DNA was again precipitated by the addition of isopropanol (0.6 vol) followed by centrifugation (15,000g x 30min) at 4^0C. Following this, the supernatant was discarded and the resulting pellet was resuspended in TE buffer pH 8 (500μL) containing RNase A (20μg/mL) for 30min at room temperature in a sterile eppendorf to remove unwanted RNA contaminating the sample.

Next, sodium chloride (1.6M) containing PEG 8,000 (13% (w/v)) (500μL) was added to the sample to precipitate plasmid DNA which was harvested by centrifugation (12,000g x 5min) at 4^0C. The supernatant was then discarded and the plasmid pellet dissolved in TE buffer pH 8 (400μL).

The solution was then subjected to phenol extraction to purify the plasmid DNA. This was carried out by firstly extracting DNA with an equal volume of equilibrated phenol:cholorform:isoamyl alcohol (25:24:1) and finally with an equal volume of chloroform. DNA in the aqueous phase was then transferred to a sterile eppendorf tube and precipitated with (0.1 vol) ammonium acetate (10M) and absolute ethanol (2.5 vol). DNA was left to precipitate for 1h at -20^0C before collection by centrifugation (1,200g x 15min) at 4^0C.

The purified plasmid DNA pellet was then resuspended in TE buffer pH 8 (500μL) and its concentration assessed by measuring its optical density at 260nm in a UV-visible spectrophotometer. The sample was then diluted (1mg/mL) with TE buffer pH 8. Purified plasmid (50μL aliquots) was transferred into sterile eppendorf tubes and stored at -20^0C until needed.

In order to ensure that the recovered plasmid was the same plasmid that was initially used to transform the *E. coli* DH5α cells, it was essential to perform a restriction analysis assay. In this assay, restriction enzymes are used to cleave double stranded DNA at specific base pair sequences. When these cleaved DNA fragments are run on an agarose gel, they should migrate the same distance as the cleaved DNA fragments from the original plasmid. The restriction enzymes used were Vsp 1 and Bam H1, as the original plasmid was known to contain these restriction sites within its DNA sequence. Firstly, isolated plasmid DNA (500ng), 1μL of the restriction enzyme Vsp 1 (10U) and react 2 buffer (5μL) were added to a sterile eppendorf and made to final volume of 50μL with TE buffer pH 8. Isolated plasmid DNA (500ng), restriction

enzyme Bam H1 (1μL; 10U) and react 3 buffer (5μL) were added to a second sterile eppendorf and made up to 50μL with TE buffer pH 8 as before. These restriction digests were repeated with the original plasmid to act as a control. Tubes were incubated at 37^0C for 1h before being subject to gel electrophoresis on an agarose gel (0.7% (w/v)) at 80V for 1h with a λ Hind III DNA ladder (1μg) and uncut plasmid (1μg) as controls. (For details of agarose gel electrophoresis see section 2.3.10.2). Gels were visualised using a UV transilluminator and photographed using a Polaroid gel documenting system.

2.3.11.2 Transfection assays

In order to investigate the endosomolytic capabilities of PAAs, the ability of PAAs to mediate transfection of pSV-β-galactosidase in comparison to other gene delivery vectors was performed.

HepG2 cells, seeded to a density of 1 x 10^6 cells/well in a 6-well tissue-culture plate were incubated for 24h at 37^0C. Next, pSV-β-galactosidase plasmid (1μg) was transferred to a sterile eppendorf in a class II laminar flow cabinet and sterile filtered polymers (1μg/μL) and a liposomal gene delivery vector LipofectACE™ (1μg/μL) made up in sterile PBS, were added to the DNA at a vector:DNA weight ratio of 5:1. The amount of plasmid was fixed (1μg) for all experiments. Tubes were mixed gently and left for 30min to allow complex formation. After this time, the vector/DNA complexes (50μL) were added to separate wells of pre-seeded 6-well plates and incubated for 48h at 37^0C. Next, the efficiency of the transfection was assayed using a commercially available kit (Promega E2000) which assayed for increases in β-galactosidase activity.

2.3.11.3 β-Galactosidase assay

After a 48h incubation, transfected cells in 6-well plates were removed from the incubator and the media removed with a pasteur pipette. Each well was gently washed twice with PBS (2mL) before addition of reporter lysis buffer (500μL) to each well. Next, using a pipette tip, the cell monolayer was scraped off the bottom of each well and cell lysis aided by passing cells through a 20-gauge needle attached to a syringe. Cuvettes (1mL capacity) were then filled with the cell lysate solutions (500μL) and assay buffer (500μL). Blank cuvettes were also prepared containing lysis buffer (500μL) and assay buffer (500μL). Samples of the cell lysates (50μL) from the

cuvettes were then removed into eppendorf tubes and stored at -20^{0}C for subsequent protein determination.

β-Galactosidase activity could be quantitated by measuring spectrophotometrically (420nm) for the release of O-nitrophenol from β-galactosidase after incubation with its substrate O-nitrophenyl-β-D-galactopyranoside (contained in assay buffer) over a 3h time course. Absorbance readings were taken every 30min, with samples incubated at 37^{0}C between readings. To standardise this assay, the velocity of O-nitrophenol release mediated by β-galactosidase standards (0.1-30mU) was measured and plotted against the amount of enzyme present (Man et al, 1999; Richardson, 1999b). The amount of β-galactosidase in an unknown sample could then be established by comparing the rate of O-nitrophenol release in the unknown sample with that of the standards. Finally a bicinchoninic protein (BCA) assay (section 2.3.12) was performed on thawed samples to assess protein content of transfected cells. Protein content also gave an indication of transfection associated toxicity. Results were expressed as units of β-galactosidase activity/mg protein (mean ± S.D.) (n=3)

2.3.12 Bicinchoninic (BCA) assay

This assay was used to determine the protein content of HepG2 cells (section 2.3.11.3), rat liver subcellular fractions (section 2.3.17), and toxin samples used in cytotoxicity assays (section 2.3.7). This colorimetric assay is based on the reduction of Cu (II) to Cu (I) by peptide bonds, and the amino acids cysteine, cystine, tyrosine and tryptophan in a concentration dependent manner, resulting in the formation of a stable purple coloured BCA-Cu (I) complex (Smith et al, 1985) (figure 2.5).

Firstly, reagent 1 was made by mixing $CuSO_4$ pentahydride (4%) with BCA reagent at a ratio of 1:50 respectively in a 20mL tube. Next, test samples (10μL) were added to the wells of a flat-bottomed non-sterile 96-well plate in triplicate and made up to a total volume (20μL) with PBS. To create a calibration curve, BSA (1μg/μL) was then made up in PBS and different volumes (0-20μL) were transferred to separate wells of the 96-well plate in triplicate and made up to a total volume (20μL) with PBS. PBS was used as a blank. Reagent 1 (200μL) was then added to all samples, (calibrants and blanks) and the plates left to incubate at 37^{0}C for 30min. After this time, plates were read spectrophotometrically at 550nm using a 96-well microtitre plate reader and the protein content of the unknown sample estimated using the BSA calibration curve. A typical BSA calibration curve can be seen in figure 2.6.

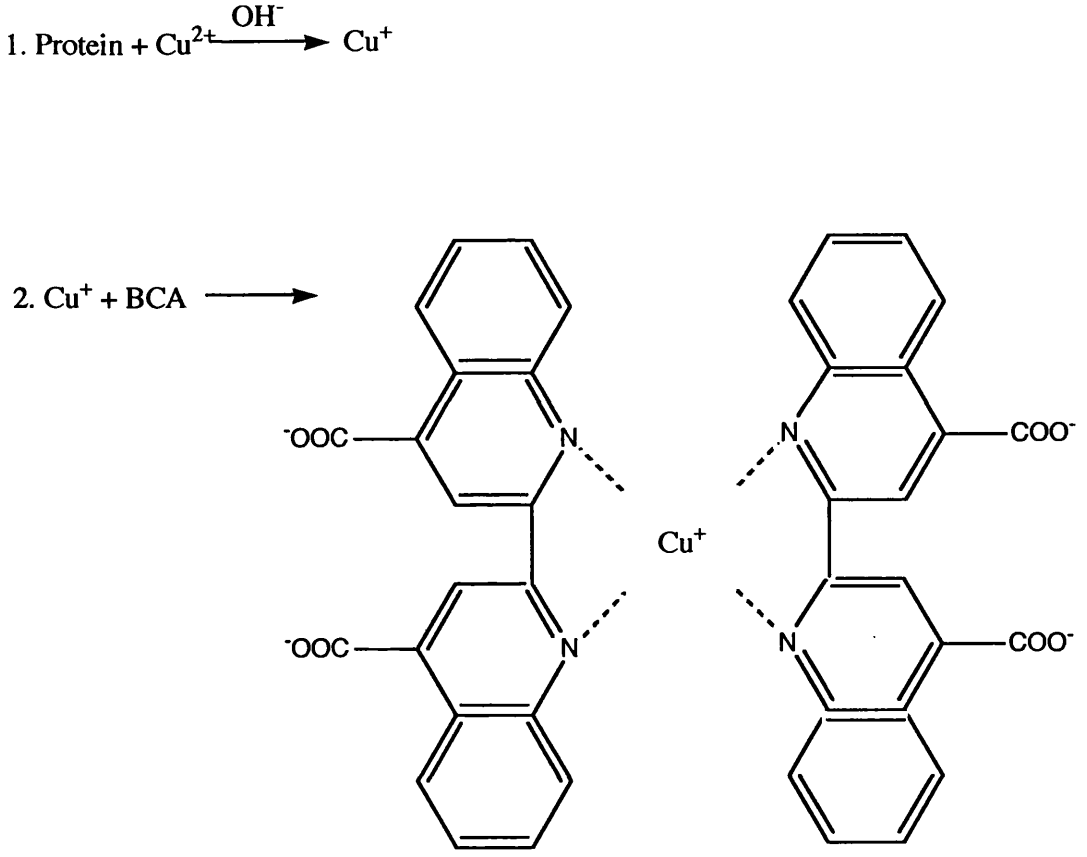

Figure 2.5 Reduction of Cu(II) to Cu(I) by proteins

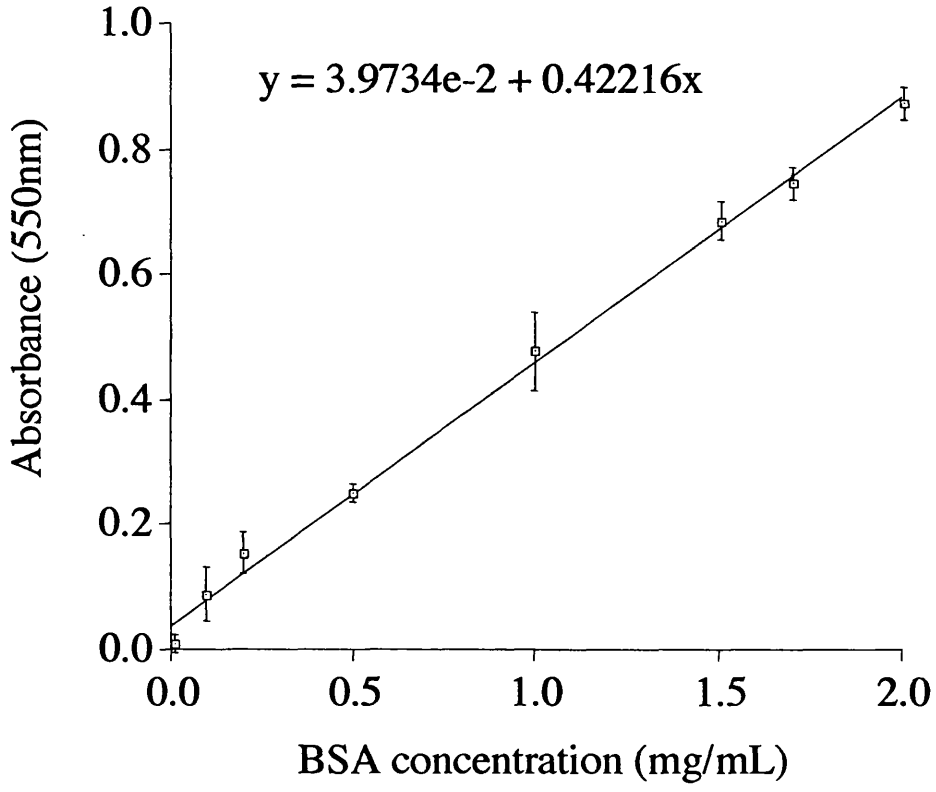

Figure 2.6 BSA calibration curve. Data represent mean ± S.D. (n=18).

2.3.13 N-acetyl-β-D-glucosaminidase (NAGase) assay

To quantitate the degree of lysosomal breakage, the lysosomal enzyme NAGase was measured. This enzyme can be measured by addition of the substrate 4-methylumbelliferyl-N-acetyl-β-D-glucosaminide. The action of NAGase causes cleavage of the substrate resulting in the release of the fluorescent compound 4-methylumbelliferone which can be assayed fluorometrically. The following method was adapted from the protocol of Barrett and Heath (1977).

Sodium-citrate buffer pH 5.0 (250μL; 0.2M) and sucrose-EDTA alone or containing triton X-100 (75μL; 250mM sucrose, 1mM EDTA; 0.1% (w/v) triton X-100) (to permeabilise lysosomal membranes) were transferred into a UV-grade spectrophotometric cuvette (3mL capacity) in triplicate and allowed to come to 37^0C by incubation for 10min in an incubator. Next, 4-methylumbelliferyl-N-acetyl-β-D-glucosaminidase (100μL; 10mM) at 37^0C, was added to each cuvette. Finally a fresh or thawed subcellular fraction (50μL) at 37^0C was added to the reaction mixture which was incubated for 1min at 37^0C. After this time the reaction was stopped by the addition of sodium bicarbonate solution (3mL; 1M) and 4-methylumbelliferone content was measured using a fluorescence spectrophotometer (ex. 360nm; em 448nm). Fractions incubated in the presence of triton X-100 (0.1% (w/v)) were used as a control to assess 100% NAGase release (total NAGase). NAGase release of fractions incubated without triton (free NAGase) was expressed as a percentage of total NAGase (mean ± S.D.) (n=3). To create a standard curve, 4-methylumbelliferone (30mg) was dissolved in methanol (5mL). This stock was diluted in methanol (total volume 50μL) and added to UV-grade spectrophotometric cuvettes (3mL capacity) containing sodium-citrate buffer pH 5.0 (250μL; 0.2M), sucrose-EDTA containing triton X-100 (75μL; 250mM; 0.1% (w/v) triton X-100) and sodium bicarbonate solution (3mL; 1M) to give appropriate 4-methylumbelliferone concentrations (0-3μM). These mixtures were transferred and allowed to come to 37^0C by incubation for 10min in an incubator. Absorbance was measured using a fluorescence spectrophotometer (ex. 360nm; em 448nm) and 4-methylumbelliferone content estimated using this curve. The 4-methylumbelliferone calibration curve can be seen in figure 2.7.

2.3.14 Use of the red blood cell (RBC) lysis assay to determine the pH-dependent lytic ability of PAAs

The ability of ISA 23 polymers of different Mw's (A, B and C) to disrupt RBCs in a pH-dependent manner was examined using a rat RBC lysis model. Firstly PBS

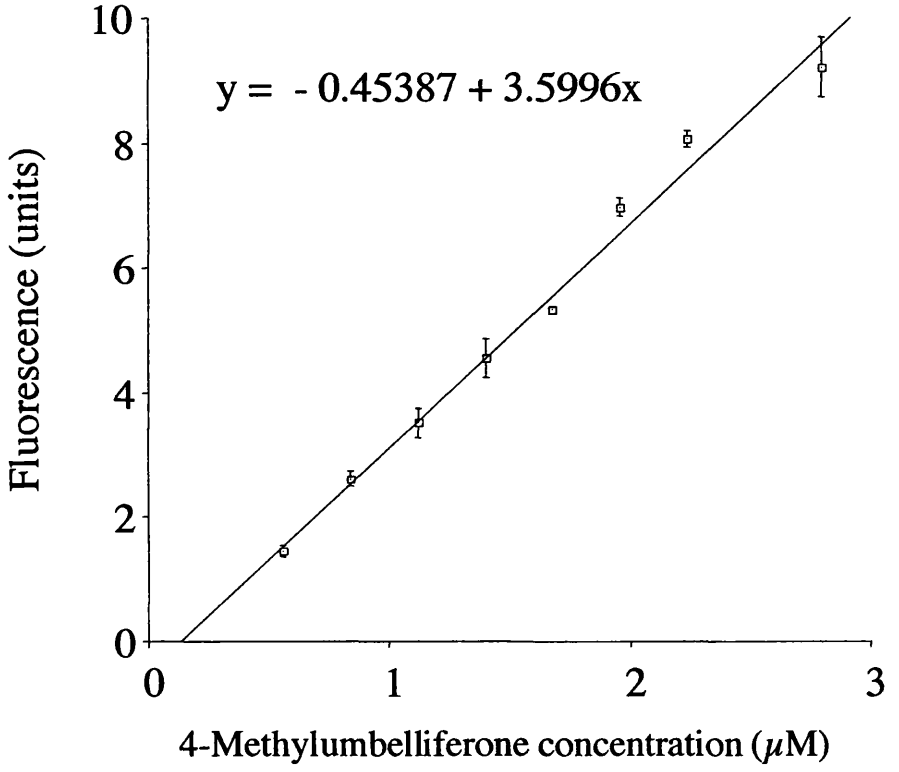

Figure 2.7 4-Methylumbelliferone calibration curve. Data represent mean ± S.D. (n=18).

(0.1M) was prepared at pH values of 5.5, 6.5 and 7.4 by the drop-wise addition of HCl (1M) and left on ice. Next, blood was obtained from male Wistar rats and collected in heparin blood tubes. RBCs were isolated by centrifugation at 1,000g x 10min at 4°C and the supernatant discarded using a pasteur pipette (Sgouras, 1990). PBS at the corresponding pH values was then added to the RBC suspension and mixed in a fresh pre-weighed centrifuge tube. Next, the RBCs were again pelleted by centrifugation and the supernatant discarded. PBS was again added to the RBC pellet at the corresponding pH value and the centrifugation process repeated once more. Following the final centrifugation, the supernatant was again removed and the tube weighed. As the weight of the RBC pellet was known, it was possible to resuspend the cells in a volume of PBS appropriate to the RBC suspension (2% (w/v)). Thus three suspensions of RBCs (2% (w/v)) were prepared at pH 5.5, 6.5 and 7.4.

Polymer solutions (100μL of a 2mg/mL solution) were then added to an equal volume of the RBC solution (2% (w/v)) in wells of a non-sterile 96-well flat-bottomed plate. Plates were then incubated at 37°C for the desired time (15min and 1h). At the end of the incubation period, the plates were centrifuged at 1,500g x 15min at room temperature to pellet intact RBCs. The supernatant was then removed (taking care not to disturb the pellet) and placed in fresh 96-well flat-bottomed microtitre plates. The absorbance of the supernatant was then measured at 550nm in a UV-visible spectrophotometer. PBS controls (without polymer) were used to provide the background haemolysis and a solution of triton-X-100 (1% (v/v)) was used to solubilise the RBC membranes and release 100% of the haemoglobin present. Haemolysis was expressed as a percentage of haemoglobin release in the presence of the triton X-100 control (mean ± S.D.) (n=3).

2.3.15 Scanning electron microscopy (SEM) of RBCs after incubation with PAAs at various pH values

RBCs incubated for 1h in the presence of PAAs A, B and C (1mg/mL) or triton-X-100 (1% (v/v)) were placed in centrifuge tubes (15mL total volume) and an equal volume of fixative solution (gluteraldehyde 2.5% (v/v) in cacodylate buffer (0.1M)) was added. Tubes were covered with parafilm and left to fix for 3min prior to centrifugation (300g x 2min) at room temperature. The supernatant was then removed and the same amount of fixative was again added to the pellet. Tubes were left to fix for 1h at 4°C. Following this, tubes were centrifuged (300g x 30s) and the supernatant removed. The pellet was then suspended in cacodylate buffer (0.1M) for 5min prior to centrifugation

(300g x 30s). This washing process was again repeated. Next, the supernatant was removed and osmium tetroxide solution (500μL of a 1% (w/w) solution) in cacodylate buffer (0.1M) was added and the solution left for 1h at 4°C.

After 1h, samples were centrifuged for (300g x 30s) and washed with cacodylate buffer (0.2M). Using a pipette, samples were carefully placed in holding chambers and the chambers placed on tissue-filled centrifuge tubes soaked in ethanol (70% (v/v)). The tubes were then covered in parafilm and centrifuged for (300g x 10s). Next, the holding chambers were placed onto a petri dish and sequentially dehydrated in a series of ethanol concentrations (50-100% (v/v)). After dehydration, chambers were dried in a critical point dryer (40°C, 1300psi) for up to 12h. Fixed samples were then mounted and gold plated prior to SEM analysis using a Philips SEM 208 scanning electron microscope.

2.3.16 Sodium dodecyl sulphate polyacrylamide gel electrophoreisis (SDS-PAGE) and visualisation of gelonin, RTA and RTA in combination with ISA 4

SDS-PAGE is used to investigate protein Mw and purity, as well as determination of the number and size of protein subunits. During sample preparation, polypeptides are denatured by reduction with β-mercaptoethanol, and saturated with SDS. As SDS is a negatively charged detergent, it coats the proteins and eliminates charge variability and thus confers onto them the same charge-to-mass ratio. The gel is then attached to a power supply, and the negatively charged proteins migrate to the cathode. As pore size decreases with higher acrylamide concentrations in the acyrlamide gel matrix, it is essential that the appropriate concentrations of acrylamide are used. Under these conditions, the mobility of proteins (R_f) is linearly proportional to the $\log_{10}$ of their mass.

The Laemmeli protocol (Laemmeli, 1970) for gel electrophoresis was used to analyse RTA and gelonin to assess their purity prior to analysis of their cytotoxicity (section 2.3.7). In this system, tris-HCl acrylamide gels are used in combination with broad molecular weight markers (6-200kDa) which acted as standards of known Mw.

The gel holding apparatus (Mini-PROTEAN II, Biorad, UK) was cleaned with decon and rinsed thoroughly. Next, the separating gel (12% (w/v)) acrylamide), comprising the mini-gel (8 x 10cm; 1.5mm thick), was prepared in a sterilin tube (bis-acrylamide (4mL of a 30% (w/v) solution); Tris-HCl pH 8.8 (2.5mL of a 3M solution); SDS (0.1mL of a 10% (w/v) solution); DDW (3.35mL)). The mixture was degassed by passing the solution through a syringe attached a filter (0.2μm) to exclude oxygen

which would inhibit the polymerisation process. Subsequently, APS (50μL of a 10% (w/v) solution) and TEMED (5μL) were added to the acrylamide mixture to initiate the polymerisation process. This solution was carefully pipetted into a glass plate sandwich within the gel holder apparatus until ~ 5cm from the top. DDW was then layered over the top of the gel to prevent dehydration leading the gel shrinkage. The mixture was then allowed to polymerise over a 45min time period.

During this time the stacking gel (4% (w/v)) acrylamide) was prepared (bis-acrylamide (1.33mL of a 30% (w/v) solution); Tris-HCl pH 6.8 (2.5mL of a 1.5M solution); SDS (0.1mL of a 10% (w/v) solution); DDW (6.1mL)). The purpose of the stacking gel was to ensure proper alignment of proteins before reaching the separating gel. The solution was degassed as before and freshly prepared APS (50μL of a 10% (w/v) solution) and TEMED (10μL) were added to the acrylamide solution. This solution was pipetted on top of the polymerised stacking gel in the glass sandwich after DDW had been poured off the stacking gel. A 10-well comb (7mm wide wells) was then positioned in between the glass sandwich in the stacking gel and polymerisation allowed to occur over a 45min time period. After this time the comb was removed from the stacking gel and the wells carefully rinsed with electrophoresis running buffer. The gel holding apparatus was then placed in an electrophoresis tank which contained 1 x electrophoresis running buffer (1L). This was prepared in DDW for a 5x concentration (Tris base (15g/L); Glycine (72g/L); SDS (5g/L)). Subsequently, 5x sample reducing buffer was prepared (DDW (3.8mL); Tris-HCl pH 6.8 (1mL of a 0.5M solution); glycerol (0.8mL); SDS (1.6mL of a 10% (w/v) solution); β-mercaptoethanol (0.4mL); bromophenol blue (0.4mL of a 1% (w/v) solution)).

Protein samples (1-5μg) were transferred to eppendorf tubes and mixed with sample reducing buffer at a 1:4 ratio respectively (30μL). For the RTA and ISA 4 combination, RTA (1μg and 3μg) were mixed with ISA 4 (1μg). These samples were then vortexed for 1min and placed in a boiling hot water bath for 5min. Next, they were centrifuged at 1000 rpm for 1min to ensure that all the sample could be loaded onto the gel. Samples were allowed to cool and loaded into the inner wells of the gel. The mixture of broad range Mw markers (8μL) were loaded onto the outer lane of the gel. Gels were run at 100V for 70min and then the gel holder was carefully removed from the electrophoresis tank. Next, the glass plate sandwich was pulled apart and the gel was carefully placed in a beaker in DDW for silver staining.

After soaking, gels were placed in a beaker containing fixative enhancer solution (methanol, 200mL; acetic acid, 40mL; fixative enhancer concentrate, 40mL;

DDW, 120mL) for 20min during which the gels were gently agitated. Next, the fixative enhancer solution was decanted and gels were rinsed in DDW (400mL) for 10min under gentle agitation. This rinsing was repeated 3 times using fresh DDW each time. After the rinsing step DDW (35mL) was placed into a large beaker and stirred gently. Next, silver complex solution (5mL), reduction moderator solution (5mL), image development reagent (5mL) and development accelerator solution (50mL) were added to the beaker in that order. The beaker was swirled gentle and the contents were added to the gel in the staining vessel. Gels were left to stain for 20min before the reaction was stopped in a solution of acetic acid (5% (v/v)) for 15min. After this time gels were rinsed in DDW for 5min. Finally, gels were soaked in glycerol (1%) and then dried overnight between cellulose sheets.

2.3.17 Isolation of rat liver subcellular fractions

Experiments were designed to quantitate the ability of PAAs to destabilise lysosomal membranes obtained by the subcellular fractionation of rat liver. In order to carry this out successfully it was considered important characterise the fractionation technique and ensure that the lysosomal enzyme NAGase was purified in each fractionation step. A schematic diagram of the subcellular fractionation procedure can be seen in figure 2.8. The method was adapted from De Duve et al, (1955) and Wedge, (1991).

A male Wistar rat weighing ~ 250g which had been fasted overnight was killed using CO_2 asphyxiation. The liver was removed, rinsed in pre-chilled (4^0C) sucrose (250mM), blotted dry and weighed. It was then cut into 3-5mm^3 cubes with pre-chilled scissors and forced through a wire mesh (1mm^3) into a weighing boat. The tissue was resuspended in 2.5mL/g of ice-cold sucrose-EDTA (250mM sucrose, 1mM EDTA) and homogenised using a Potter-Elvehjem homogeniser (0.019cm clearance, 3,000rpm) with 10 up-and-down strokes. The homogenate was then poured into a tared pre-chilled centrifuge tube (50mL capacity) and weighed, before removal of an aliquot (1mL) into an eppendorf tube. This aliquot (denoted the total homogenate fraction) was snap frozen by immersion into liquid nitrogen, and stored at -20^0C until further analysis (figure 2.8).

The remaining homogenate was then centrifuged (2,000g x 2min) at 4^0C, and the resulting supernatant decanted into a tared, chilled centrifuge tube and kept on ice. The pellet was resuspended in 5mL ice-cold sucrose-EDTA and re-homogenised using 10 up-and-down strokes in a Potter-Elvehjem homogeniser. This homogenate was then

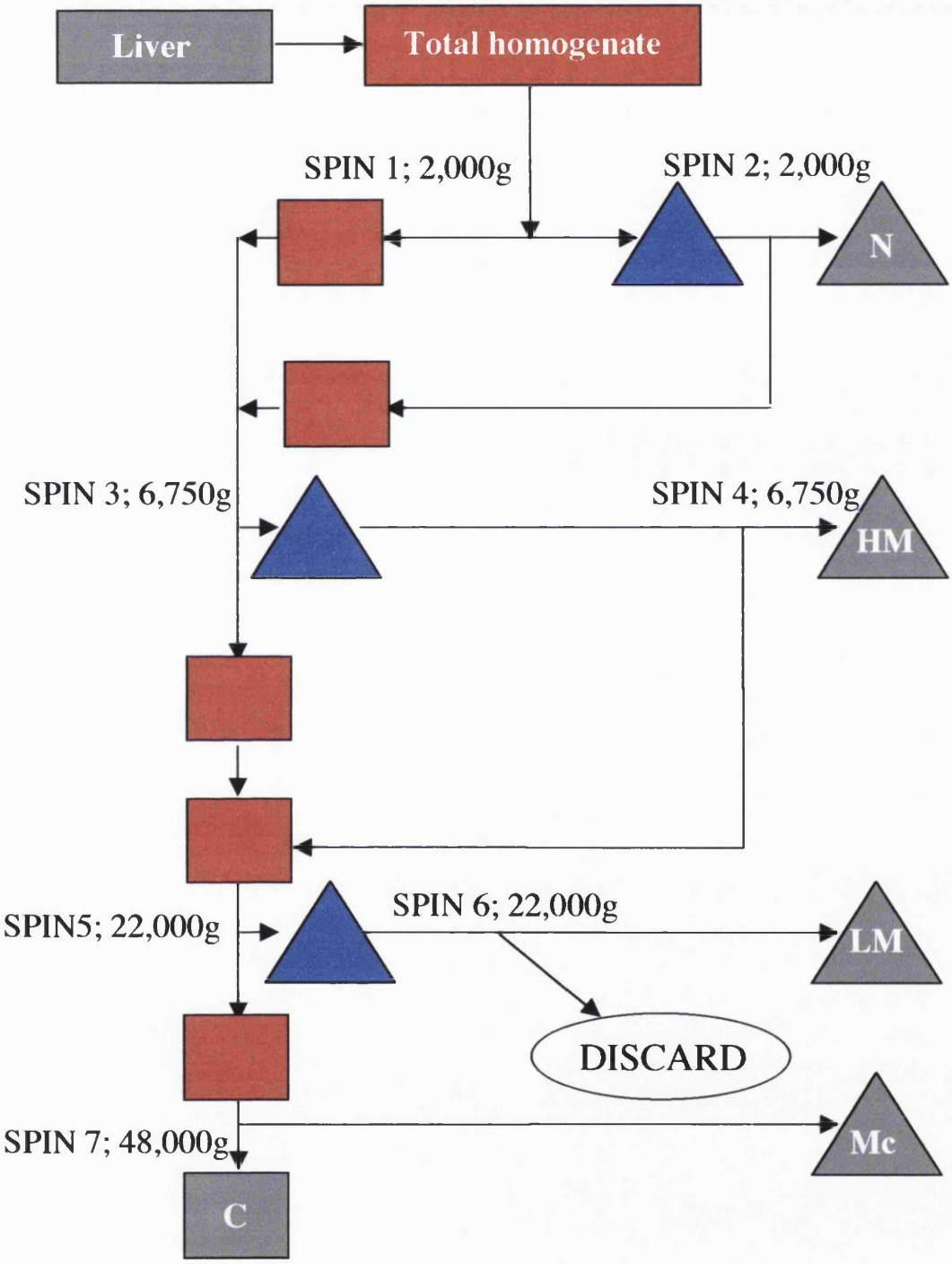

Figure 2.8 Procedure used for the differential centrifugation of rat liver. Key: WC = whole cell fraction; N = nuclear fraction; HM = heavy mitochondrial fraction; LM = light mitochondrial fraction; Mc microsomal; C = cytosolic fraction; supernatant □, pellet △. Samples taken for assay are indicated in grey.

re-centrifuged (2,000g x 2min), and the resulting supernatant removed and added to the supernatant from the previous centrifugation step. The remaining pellet was then resuspended in sucrose-EDTA (2mL), the tube weighed and an aliquot removed (1mL) and snap frozen and stored at -20^{0}C. This was denoted the nuclear fraction (figure 2.8).

The combined supernatants were then subject to centrifugation (6,750g x 4min) and the resulting supernatant decanted and kept as before in a tared centrifuge tube on ice. The pellet was resuspended as before and centrifuged (6,750g x 4min). The supernatant was decanted and added to the previous supernatant. The pellet was then resuspended and an aliquot removed and snap frozen for storage at -20^{0}C. This fraction was denoted the heavy mitochondrial fraction (figure 2.8).

The combined supernatants were centrifuged (22,000g x 9min) and the supernatant decanted and kept. The pellet was then resuspended in sucrose-EDTA (5mL) and again centrifuged (22,000g x 9min). The resulting supernatant was removed and discarded. The pellet was resuspended in sucrose-EDTA (2mL), weighed, and an aliquot removed and snap frozen and stored at -20^{0}C. This was denoted the light mitochondrial fraction (light mitochondrial fraction) (figure 2.8).

The supernatant was finally centrifuged (48,000g x 70min). Both the resulting pellet, (denoted the particulate fraction) which was resuspended in sucrose-EDTA, and the supernatant (denoted the cytosolic fraction) were weighed and aliquots snap frozen (figure 2.8).

The frozen aliquots of each fraction could later be thawed and assayed for protein content by the BCA protein assay as described in section 2.3.12 and for NAGase as described in section 2.3.13

The results obtained were interpreted as follows. Firstly, volumes of each fraction were calculated by dividing the weight of the fraction by 1.05 (estimated density of organelles in 250mM sucrose at 0^{0}C) (De Duve et al, 1955). Volumes were used to calculate the total NAGase and protein content in each fraction. The distribution of NAGase in each fraction was obtained by calculating the relative specific activity (RSA) of the enzyme in each fraction (i.e. the percentage of enzyme activity recovered in a fraction/the percentage of protein recovered in a fraction) (mean ± S.D) (n=3). The fraction with the highest RSA value for NAGase was used in subsequent PAA-mediated lysosomal breakage experiments.

2.3.18 Preparation of isolated light mitochondrial fractions containing ISA 1 for transmission electron microscopy (TEM)

Male Wistar rats (~ 250g) which had been fasted overnight were anaesthetised using an isofluorane (2% (v/v)) and O_2 (4% (v/v)) mixture. Next, ISA 1 (25mg/kg) dissolved in sterile saline (0.9%) was injected (100μL) i.v. via the caudal vein by syringe with a 20-gauge needle. The animals were then allowed to regain consciousness and left for 30min to allow endocytic internalisation and trafficking of injected samples to lysosomes. Animals were then killed by CO_2 asphyxiation. The liver was removed and subcellular fractionation was performed to obtain the light mitochondrial fraction exactly as described in section 2.3.17. For the positive control the light mitochondrial fraction was incubated for 30min in triton X-100 (0.2% (w/v)). Samples were immediately resuspended in cacodylate buffer (2ml; 0.05M) containing sucrose (250mM) and gluteraldehyde (1% (v/v)) and fixed for 45min at 4^0C. After this time aliquots (~2mL) of each sample were transferred to 15mL centrifuge tubes and an equal volume of cacodylate buffer (0.05M) was added. Tubes were centrifuged (500g x 1min), the supernatant removed and an equal volume of cacodylate buffer (0.05M) was again added to the tubes. The centrifugation was repeated, the supernatant was removed and osmium tetroxide (1% (w/v)) was added. After staining for 30min, the supernatant was removed (no centrifugation step) and DDW (4mL) was added to the samples which were then left for 10min. Samples were then centrifuged (500g x 1min), the supernatant removed and the washing process repeated twice more.

Uranyl acetate (0.5% (w/v)) was centrifuged (500g x 5min) to remove particles suspended in the solution and then 4mL of this solution was transferred to the samples and incubated for 30min at room temperature. After this time, the supernatant was removed (no centrifugation step) and samples were washed (1 x 10min) with DDW.

Next, ethanol (2mL of a 50% (v/v) solution) was added to the samples and left to incubate at room temperature for 10min. Samples were then centrifuged (500g x 1min) and the supernatant removed. Samples were then slowly dehydrated in a series of increasing concentrations of ethanol (70%, 85%, 90% (v/v)) for 10min at each concentration. Ethanol (100% (v/v)) was finally added to the samples for 3 x 10min incubations.

After the final centrifugation (500g x 1min), the ethanol supernatant was removed and propylene oxide (4mL) was added to the samples and mixed thoroughly. Samples were left for 10min, then the propylene oxide was removed using a pipette. Fresh propylene oxide (10mL) was added to an equal volume of freshly prepared

araldite resin mixture containing araldite CY212 (10g), BDMA (1.2g) and DDSA (10g). This mixture was added to samples and left for 2h to infiltrate the sample.

Next, clean dry BEEM® capsules were filled with embedding mixture to within 1-2mm from the top. Samples were then transferred to the capsule using a toothpick and left overnight at 60^0C in an incubator to allow polymerization. The resultant blocks were allowed to cool prior to sectioning using a microtome. The sections were placed on copper grids and counter-stained in uranyl acetate (0.5% (w/v)) and lead citrate (1% w/v)) for 10min before visualisation using a Philips TEM 201 transmission electron microscope.

2.3.19 Investigation of the ability of PAAs to destabilise isolated rat liver lysosomes

2.3.19.1 Evaluation of lysosomal breakage during incubation of polymers with isolated rat liver lysosomes (polymer outside the lysosome)

This method was adapted from Klemm et al, (1998). The pH of sucrose-EDTA (250mM sucrose, 1mM EDTA) solution was adjusted to 5, 6.5 or 7.4 by the addition of HCl (0.1M). The light mitochondrial fraction (containing isolated lysosomes) was isolated as described in section 2.3.17 and was suspended in sucrose-EDTA (2mL) at the different pH values. Next, polymers (0.5mg/ml in saline 0.9% (w/v)) were added to these lysosomal suspensions and incubated for 30min or 1h at 37^0C. To obtain 100% lysosomal lysis, triton X-100 (0.5mL of a 0.2% (w/v) solution) was added to lysosomal suspensions instead of polymers. After this time an aliquot (50μL) was removed and assayed for NAGase as described in section 2.3.13.

The ability of ISA 1 to destabilise rat liver lysosomal membranes in response to dose and time was further investigated. Isolated lysosomes were prepared as described above and ISA 1 (0-2mg/ml in saline 0.9% (w/v)), or triton X-100 (0.2% (w/v)) (0.5mL) were added to the lysosomal suspension and incubated for 45min or 2h at 37^0C. After this time an aliquot (50μL) was removed and assayed for NAGase as described in section 2.3.13.

Fractions incubated in the presence of triton X-100 (0.1% (w/v)) were used as a control to assess 100% NAGase release (total NAGase). NAGase release of fractions incubated without triton (free NAGase) was expressed as a percentage of total NAGase (mean ± S.D.) (n=3).

2.3.19.2 Investigation of the ability of ISA 1 to destabilise rat liver lysosomes (polymer inside the lysosomes)

Isolated rat liver lysosomes containing ISA 1 (10-50mg/kg) were prepared as described in section 2.3.17. Aliquots were removed (50μL) and assayed for NAGase as described in section 2.3.13. The remaining sample was placed in a 37^0C incubator and at time points (up to 120min) aliquots were removed and assayed for NAGase. Fractions incubated in the presence of triton X-100 (0.1% (w/v)) were used as a control to assess 100% NAGase release (total NAGase). NAGase release of fractions incubated without triton (free NAGase) was expressed as a percentage of total NAGase (mean ± S.D.) (n=3).

CHAPTER 3

EVALUATION OF THE ABILITY OF PAAS TO FORM INTERPOLYELECTROLYTE COMPLEXES AND TRANSFECT CELLS *IN VITRO*

3.1 Introduction

PAAs have many properties which make them attractive candidates for the delivery of genes to cells. Unlike many cationic lipids and cationic polymers, PAA structures have been identified which are non-toxic i.e. IC_{50} values > 2mg/mL (Ranucci et al, 1991; Richardson et al, 1999a) and structures can be prepared that avoid rapid liver clearance by the RES. It has been suggested that PAAs would display endosomolytic properties due to their ability to cause red blood cell lysis at low pH (Richardson et al, 1999a). Therefore, to investigate further whether PAAs might be able to promote cytosolic entry of macromolecules, it was decided to first assess PAA-mediated gene delivery. Although efficient transfection would only provide indirect evidence for the endosomolytic capability of PAAs, it was considered important to examine this also as a potential therapeutic application.

Gene therapy (outlined in chapter 1) was initially envisioned as a treatment for monogenic diseases such as cystic fibrosis. In this case replacement of the defective gene with a healthy copy should correct the deficiency (Johnson et al, 1992; Rosenfeld et al, 1992; reviewed in Wagner and Gardner, 1997). More recently, gene therapy for the treatment of cancer has been proposed. As this is a polygenic disorder, a number of genes could potentially be administered, such as tumour suppressor genes, genes encoding enzymes to activate a cytotoxic pro-drug within the cell, or genes encoding antigens designed to generate a protective immune response.

Many different vectors have been developed to mediate gene delivery (described in chapter 1), however the vast majority of clinical trials involve viral and liposomal formulations (81% and 13% respectively, reviewed in Mhashilkar et al, 2001). The cationic polymeric vectors such as PEI and poly-L-lysine, although yet to be tested in the clinic, are currently being extensively examined in the laboratory. The first polycation used for gene delivery was poly-L-lysine conjugated to the asialoorosomucoid ligand (Wu and Wu, 1987). Since then poly-L-lysine has been conjugated to numerous targeting ligands such as transferrin (Wagner et al, 1990), folate (Mislick et al, 1995) and fibroblast growth factor (Sosnowski et al, 1996). Targeting ligands have also been conjugated to the endosomolytic polymer PEI, (reviewed in Kircheis et al, 2001a) and complexes used for topical application to target mouse brain (Boussif et al, 1995) and intravenously to target mouse lung (Goula et al, 1998). However both these and other cationic compounds are limited in *in vivo* situations as a result of their hepatotropic nature and associated toxicity (Godbey and Mikos, 2001;

reviewed in Kircheis et al, 2001a) (chapter 1, table 1.4). Attempts to alleviate these properties by covalently conjugating polymers or polyplexes with PEG resulted in long circulating complexes, but their therapeutic potential is limited by diminished uptake and gene transfer *in vitro* (Choi et al, 2001a; Rungsardthong et al, 2001; Zuidam et al, 2000).

Despite the large number (571) of gene therapy clinical protocols ongoing in the world (reviewed in Merdan et al, 2002b), still no licensed gene medicines (both viral and non-viral) are currently available for the treatment of patients. Both types of vector are plagued with disadvantages. The drawbacks of viral gene delivery were discussed previously in chapter 1 but are chiefly concerned with safety issues (Verma and Somia, 1997; Marshall, 2000). Non-viral vectors, although considered safer, cheaper and easier to manufacture, are limited by lower transfection efficiencies compared to their viral counterparts (Kircheis et al, 2001a; Brown et al, 2001; Remy et al, 1998).

The basic requirements for mediating the multistep process necessary for efficient transfection are well known. They are listed below and shown in figure 3.1. It was therefore considered important to examine PAAs in terms of these fundamental requirements.

1) DNA condensation
2) protection of DNA from degradation
3) uptake into the cell
4) endosomal release
5) migration through the cytoplasm
6) nuclear uptake and expression of DNA

DNA condensation is said to occur when electrostatic bonds are formed between the nucleic acid and polymer chain to create a self-assembled complex in aqueous solution. This is sometimes referred to as an IPEC (Kabanov and Kabanov, 1998). Many methods have been used to characterise IPEC formation and their resultant physical properties, since a correlation between IPEC physico-chemical properties and gene transfection ability have been documented (Jones et al, 2000; Ramsay et al, 2000). Therefore in this study, these techniques were used to study the ability of PAAs to form IPECs and PAA/IPEC physico-chemical properties.

Agarose gel electrophoresis was one such method used to investigate PAA/IPEC formation. Electrophoresis describes the migration of molecules with a net charge

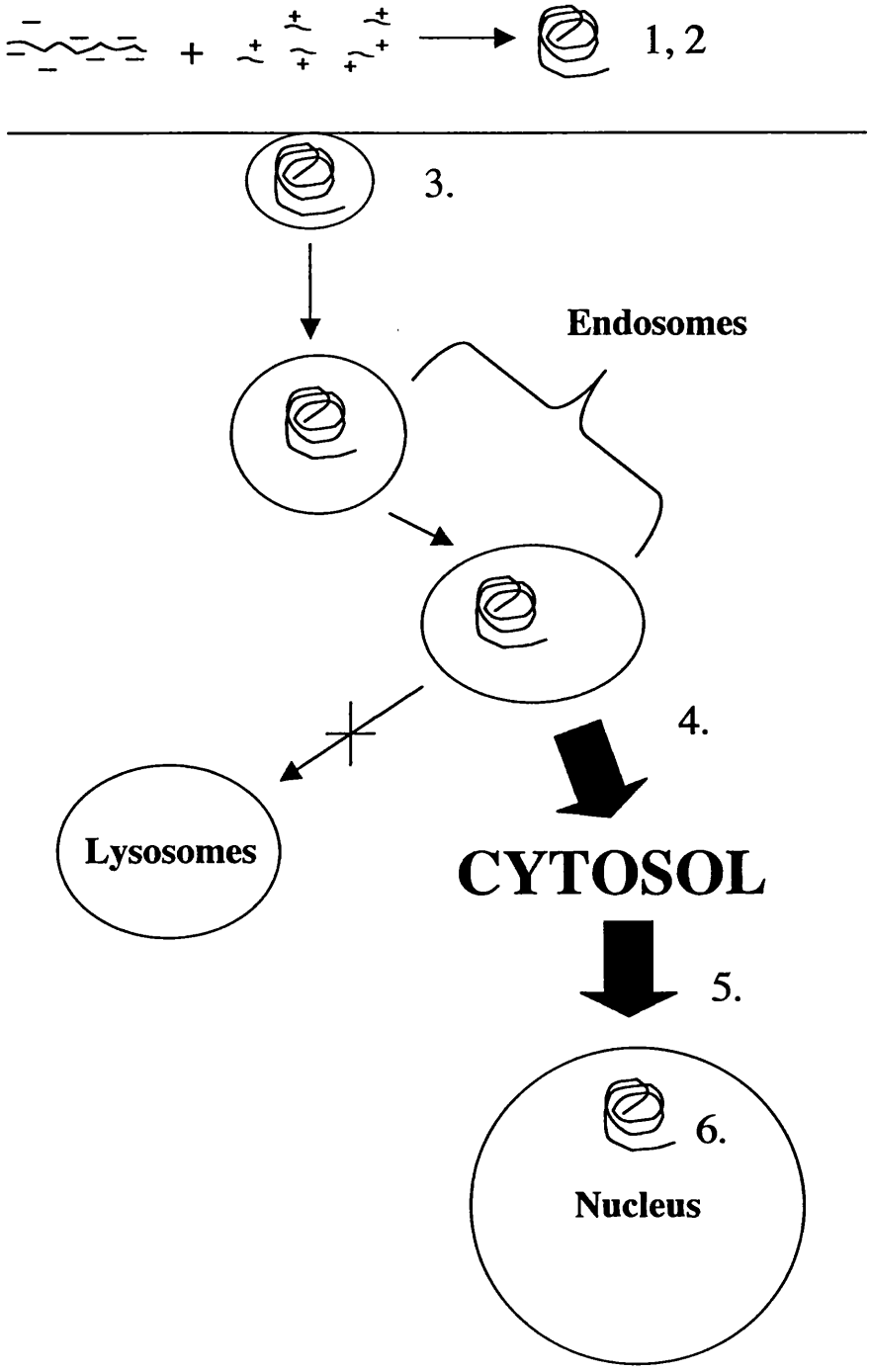

Figure 3.1 Schematic showing the multi-step process required for a non-viral delivery system.

towards the appropriate electrode. Nucleic acids are uniformly negatively charged, and thus move toward the cathode in an electrophoresis gel due to their net negative charge (Ausubel et al, 1994). IPEC gel retardation relies on partial or complete neutralisation of the non-bridging oxygen of the DNA backbone as a result of complexation with positively charged polymers. This reduces or abolishes the net negative charge associated with DNA, and a reduction in the migration of the DNA towards to the cathode occurs. (Wolfert et al, 1999). Therefore the degree of DNA retardation when complexed with PAAs gives an indication of the complexing and condensing properties of PAAs.

Another method used in this study to examine PAA/IPEC formation is the EtBr exclusion assay (Gershon et al, 1993). In this method, step-wise addition of PAAs to EtBr is performed and EtBr-DNA fluorescence is monitored. Complex formation is accompanied by a loss of EtBr fluorescence (Ramsay et al, 2000). As PAAs are being developed for i.v. administration, it was also important to assess the stability of PAA/IPECs in the presence of the serum protein BSA. As this protein is anionic, it could cause displacement of DNA from the IPEC by forming an ionic complex with PAAs. The EtBr exclusion assay was adapted to assess this by monitoring for a restoration in fluorescence intensity after step-wise addition of BSA to PAA/IPECs.

The microstructure of condensed DNA has been reported to vary significantly with parameters such as polymer Mw and structure (Laemmeli, 1975; Wolfert et al, 1996; Bloomfield, 1997). However commonly, condensed structures known as toroids are formed, which are amenable to uptake by endocytosis. As toroid formation can be used qualitatively to assess the condensation of DNA, the morphology of PAA/DNA complexes was examined using TEM.

The change in the tertiary structure of DNA caused by polymer condensation may in part, account for the inability of nucleases such as DNase II to reach or recognise the DNA as a substrate for catabolism (Moret et al, 2001). This protection of DNA from DNase II degradation is an advantageous attribute if the vector is to be developed for i.v., as many nucleases are present in the bloodstream. The ability of PAAs to protect DNA from degradation was therefore investigated using a DNase II degradation assay.

The surface charge of IPECs is considered to be one of the most critical parameters determining transfection efficacy (Jones et al, 2000). The electric potential at the surface of DNA-polymer complex particles will influence their colloidal stability and their interaction with blood components and the negatively charged surface of cells.

Therefore in this study it was also considered important to determine the zeta potential of PAA/IPECs at different polymer:DNA weight ratios to allow comparison of the effect of surface charge on transfection efficiency.

In addition to studying PAA/IPEC formation and their physico-chemical characteristics, the transfection capability of IPECs formed from PAAs and pSV-β-galactosidase plasmid was examined. The restriction map for the pSV-β-galactosidase plasmid (figure 3.2) shows that it contains an ampicillin resistance gene to allow selection for the plasmid during the amplification procedure, a strong viral SV40 promoter sequence to allow high levels of β-galactosidase expression, and the restriction sites Bam H1 and Vsp 1 to allow plasmid characterisation using restriction analysis. pSV-β-Galactosidase was chosen as a model because of the easy spectrophotometric quantitation of the gene product, β-galactosidase. In addition, published studies using this model had already been used to assess the optimum polymer DNA ratios (by weight) for transfection (figure 3.3) (Man et al, 1999; Richardson et al, 2001). These preliminary studies showed that the greatest level of β-galactosidase expression was mediated by ISA 23 at the 9:1 weight ratio. However analysis of protein concentration after transfection indicated that highest transfection levels were observed at the range at which reduced protein levels were evident, suggesting cellular toxicity. Interestingly, a similar trend was observed by Van de Wetering et al, (1997), whereby the maximum number of transfected cells (mediated by the polycation p(DMEAMA) was observed when cytotoxicity was 40-80%. Therefore in this study a 5:1 weight ratio of polymer/DNA was chosen to minimise cellular toxicity. As the transfection capability of ISA 22 and 23 had previously been investigated at this weight ratio, the PAAs ISA 1 and 4, and the control vectors PEI and LipofectIN™ were examined for their ability to transfect cells with pSV-β-galactosidase.

3.2 Methods

The PAAs used in these studies and their characteristics are shown in chapter 1, table 1.7. The techniques used to evaluate the ability of PAAs to form IPECs (agarsoe gel electrophoresis, EtBr exclusion, TEM analysis) and their physico-chemical properties (DNase II assays, zeta potential) are described in detail in chapter 2, section

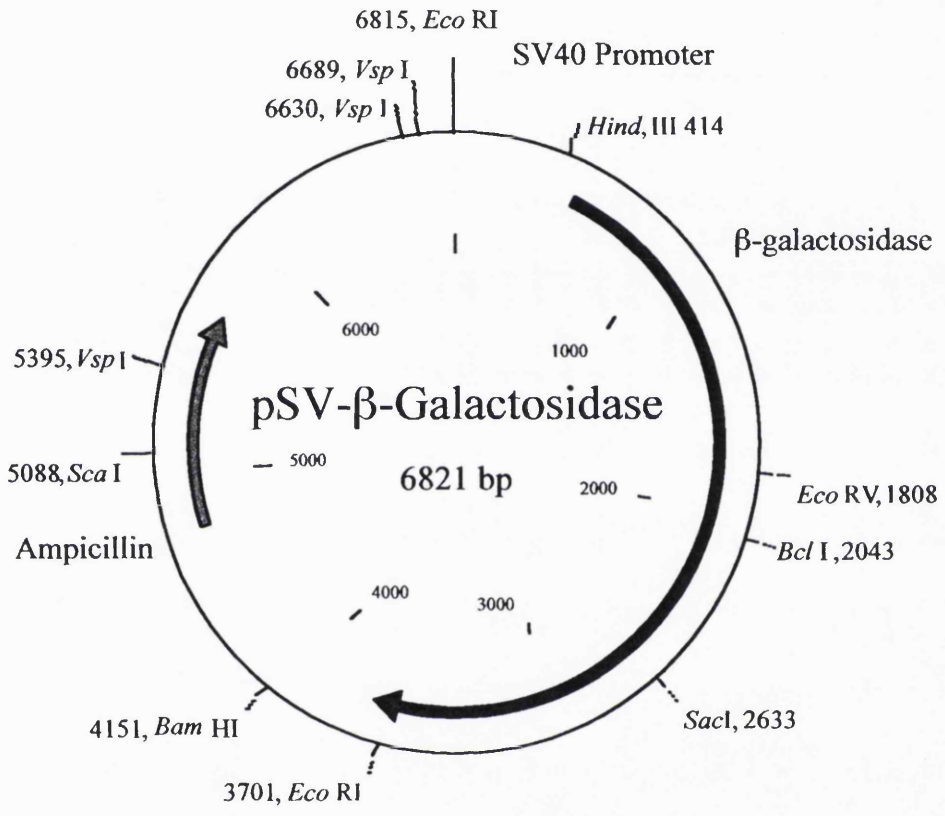

Figure 3.2 Restriction map of pSV-β-galactosidase from Promega.

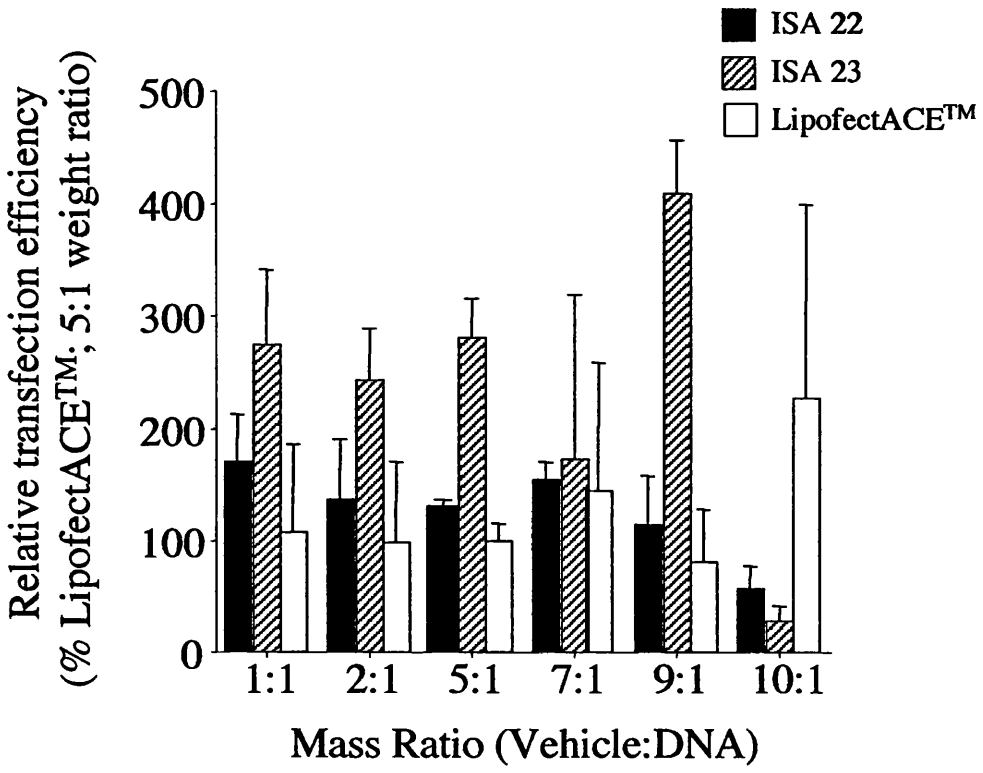

Figure 3.3 Effect of vehicle:DNA weight ratio on transfection of HepG2 cells. LipofectACE™ was used as a reference control. Data represent mean ± S.D. (n=3). (Man et al, 1999; Richardson, Pattrick et al, 2001).

2.3.10. Experiments outlining plasmid amplification and the ability of PAAs to mediate transfection of pSV-β-galactosidase are described in chapter 2, section 2.3.11.

To determine whether PAAs interfered with BCA reagent, the BCA assay (described in chapter 2, section 2.3.12) was performed with ISA 4 and ISA 23 as calibrants. The resulting calibration curves are shown in figure 3.4 and discussed later.

3.3 Results

3.3.1 Characterisation of pSV-β-galactosidase by restriction analysis

After amplification and isolation of pSV-β-galactosidase, its purity was evaluated using restriction analysis. Figure 3.5 shows the results of this agarose gel restriction assay. Following digestion with the restriction enzyme Vsp 1 (lane 1), two fragments were visible, indicating that the plasmid was cut in two places. From the restriction map of pSV-β-galactosidase (figure 3.2), it is clear that the plasmid contains three Vsp 1 sites. However, one of the fragments generated is only 59 base pairs which is too small to be resolved on the 0.7% agarose gel, thus two fragments were seen. There is one Bam H1 site associated with pSV-β-galactosidase (lane 2), and the resultant restriction digest resulted in a linear plasmid of size ~ 6.8kbp when compared with the λ Hind III DNA ladder (lane 4). This band also migrated the same distance as the linear form of the original pSV-β-galactosidase plasmid from Promega (lane 3). The covalently closed circular (CCC) form of the plasmid is also visible on the gel. The CCC form migrated further than the linear form due to its compact conformation. As the plasmid obtained by amplification in bacteria demonstrated all the characteristics of pSV-β-galactosidase used in the original transformation, it indicates that the amplified plasmid was identical to the purchased Promega plasmid. This amplified plasmid was then used to study the morphological properties of IPECs by transmission electron microscopy and in the subsequent transfection assays described below.

3.3.2 Ability of PAAs to form IPECs assessed by electrophoresis

The migration of λ Hind III DNA after addition of various polymers (ISA 23, ISA 22, ISA 4, ISA 1, PEI and dextran) in an agarose gel is shown in figure 3.6a and b. Gel lanes where DNA migration was prevented or where EtBr fluorescence was reduced are labelled with white arrows. ISA 1 and 4 were able to completely prevent migration of DNA at polymer:DNA weight ratios of 100:1 and 10:1, and caused almost a complete reduction in EtBr fluorescence. At a polymer:DNA weight ratio of 1:1, ISA 1

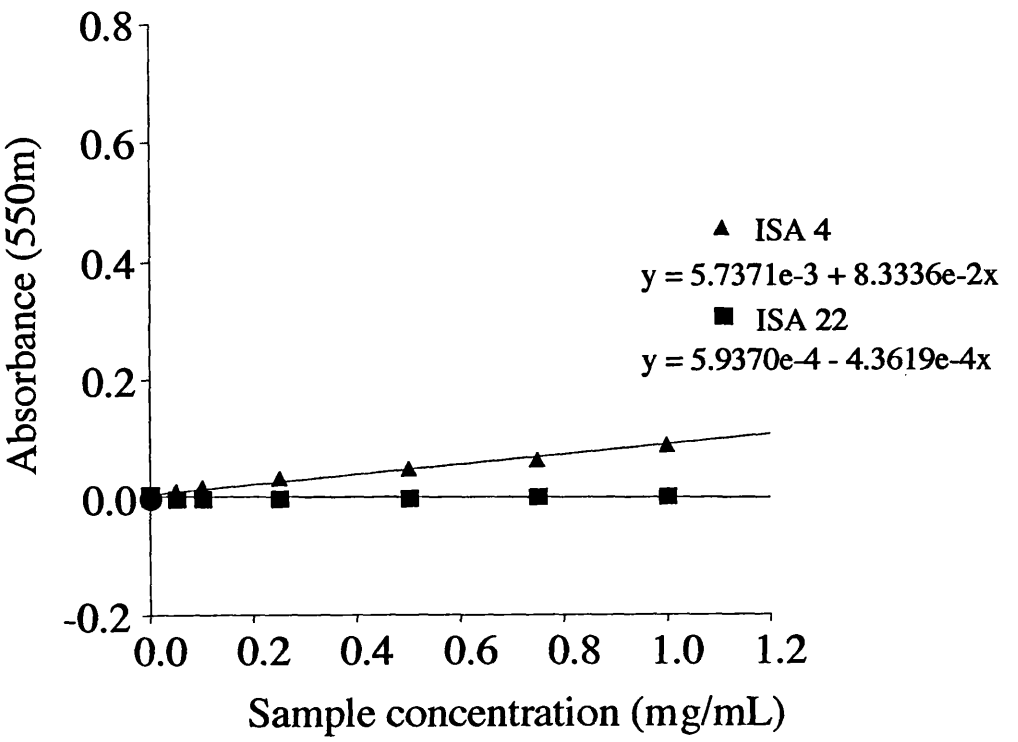

Figure 3.4 BCA assay using ISA 4 and ISA 23 as calibrants. Data represent mean± S.D. (n=18).

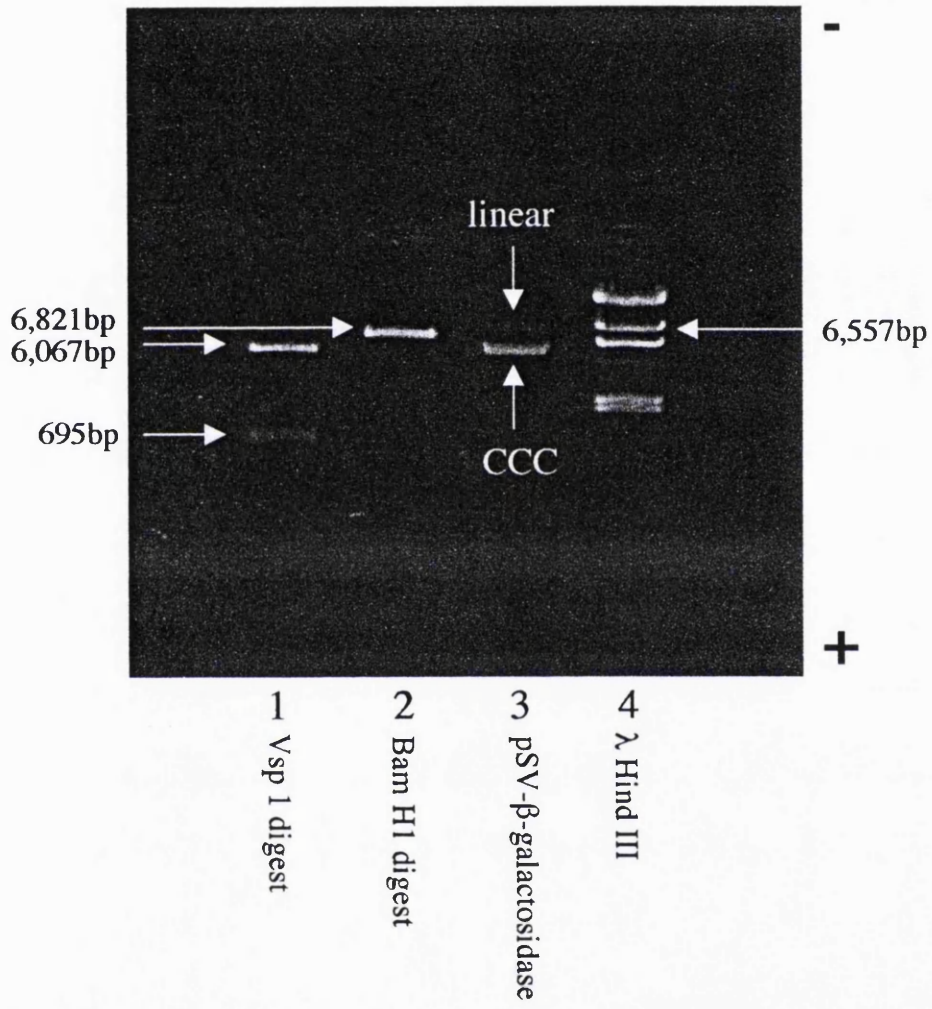

Figure 3.5 Restriction analysis of recovered pSV-β-galactosidase.

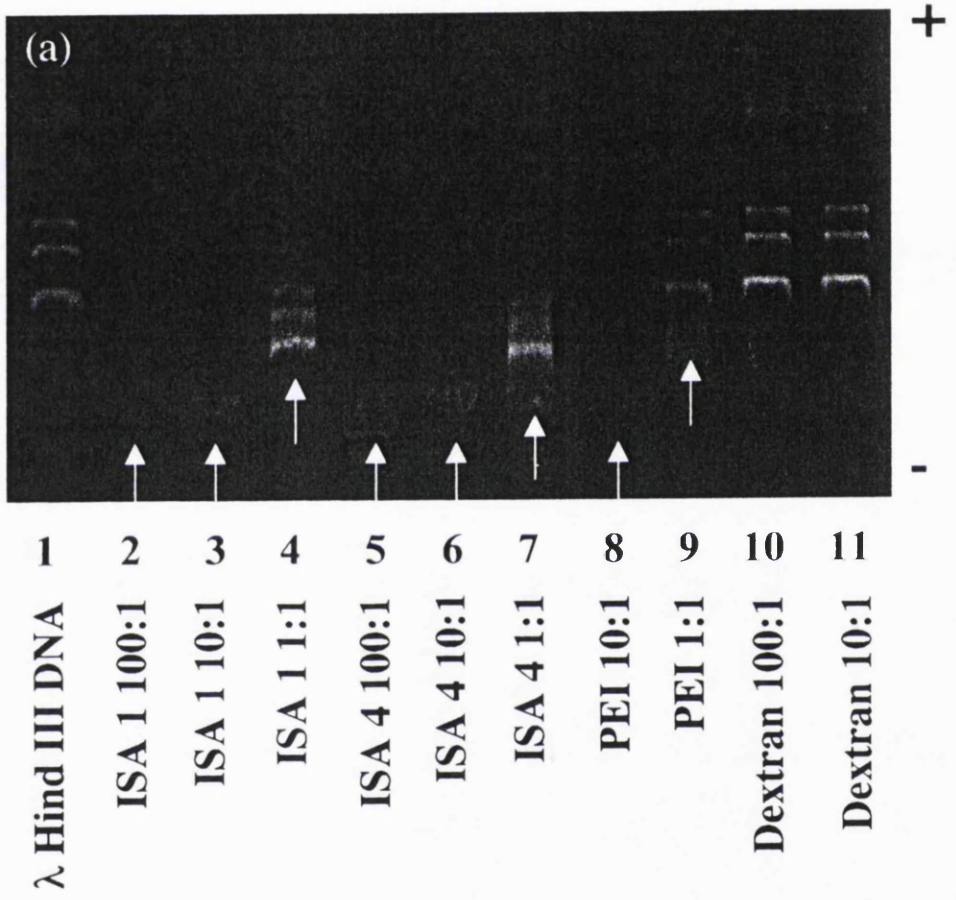

Figure 3.6 DNA retardation during agarose gel electrophoresis of polymer complexes. The gels were loaded with 1μg of λ Hind III DNA/well. Panel (a) shows ISA 1, 4 and the controls PEI and dextran; (b) ISA 22 and 23 (Richardson, Pattrick et al, 2001).

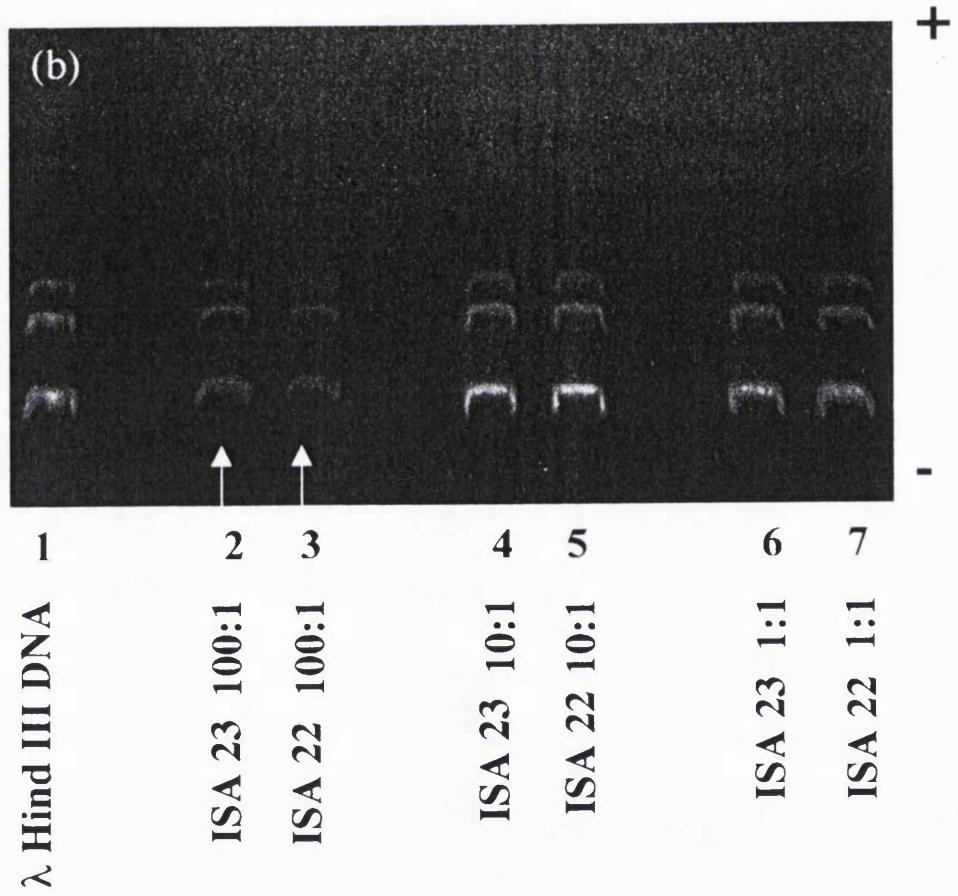

Figure 3.6 Cont.

and ISA 4 prevented DNA migration to a greater extent than PEI at the same weight ratio. Dextran was unable prevent migration of DNA at both polymer:DNA weight ratios tested (100:1; 10:1) (figure 3.6a).

ISA 22 and ISA 23 (figure 3.6b) were unable to prevent migration of DNA at all the polymer:DNA weight ratios tested (100:1; 10:1; 1:1) however, a decrease in EtBr fluorescence was observed for both polymers at a polymer:DNA weight ratio of 100:1.

3.3.3 Ability of PAAs to form IPECs assessed by an EtBr displacement assay

Addition of all polymers (ISA 23, ISA 22, ISA 4, PEI and dextran) to DNA/EtBr complexes caused displacement of EtBr (figure 3.7a). Maximum reduction in fluorescence was observed following the addition of PEI at a polymer:DNA weight ratio of 1.1:1 (fluorescence intensity: 4.95 ± 1.12%). ISA 4 caused maximum fluorescence reduction at a polymer:DNA weight ratio of 60:1 (fluorescence intensity 0.70 ± 1.39%) whereas this occurred for ISA 22 and 23 at a polymer:DNA weight ratio of 100:1 (fluorescence intensities 2.23 ± 1.94% and 2.65 ± 1.19% respectively). At the maximum polymer:DNA weight ratio tested (100:1), dextran was only able to reduce EtBr fluorescence to 47.23 ± 3.24%.

To allow quick comparison of the extent of EtBr exclusion afforded by the various polymers, the term Fr_{50} was designated. Fr_{50} is the polymer:DNA weight ratio that caused 50% EtBr exclusion. These values are shown in table 3.1. From these values, it is possible to determine the rank order of the polymers tested in respect of their ability to exclude EtBr. This order is PEI > ISA 4 > ISA 23 > ISA 22 > dextran.

The stability of PAA/IPECs in the presence of the serum protein BSA was also assessed. The fluorescence of DNA solutions in water was calibrated to 100% and PAAs were added until a polymer:DNA weight ratio of 40:1 was reached. BSA was then added in a stepwise manner and fluorescence intensity monitored (figure 3.7b). At the weight ratios studied no increase in fluorescence intensity was observed for all PAA/IPECs tested.

3.3.4 TEM analysis of IPEC morphology

Micrographs of IPECs formed during the addition of pSV-β-galactosidase plasmid DNA to PAAs are depicted in figure 3.8a-e. IPECs formed from poly-L-lysine appear as discrete toroids of size 60-100nm. IPECs formed by ISA 4 and 22 were also toroids within the size range 40-150nm diameter (figure 3.8b-d). The morphology of IPECs formed from LipofectACE™ appeared as disordered globular masses,

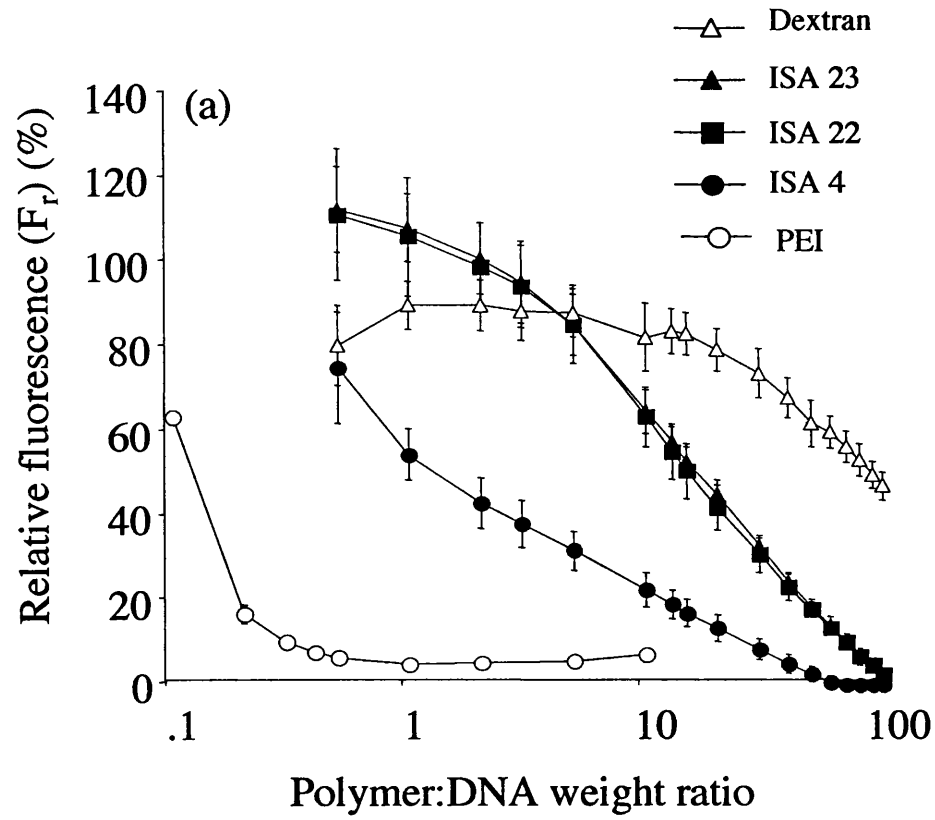

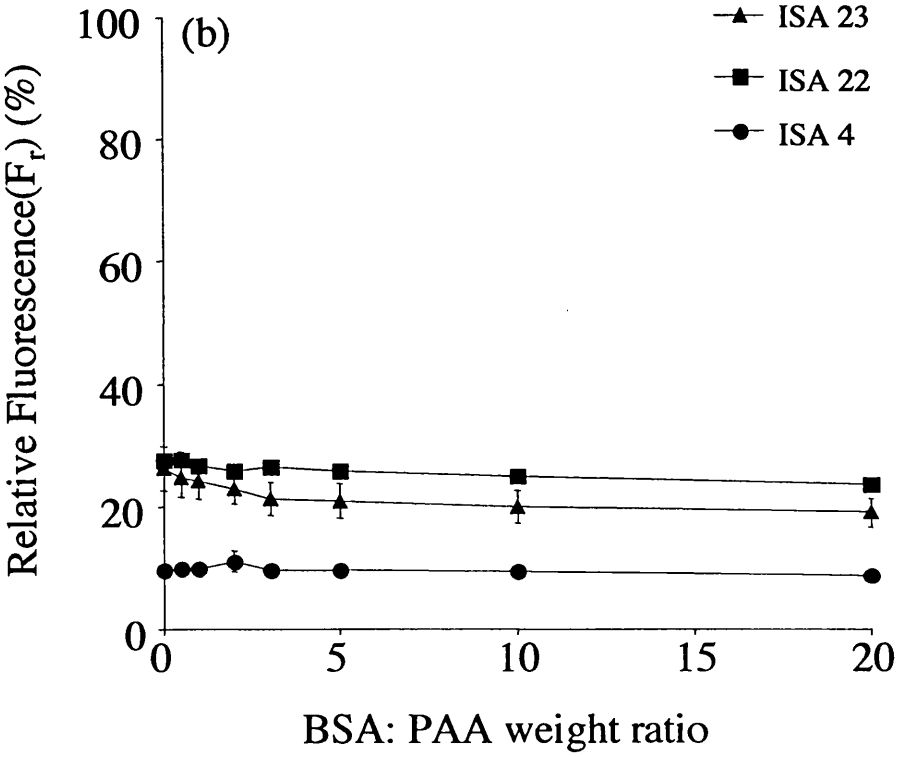

Figure 3.7 EtBr exclusion assay. Panel (a) shows EtBr displacement from DNA by the addition of various polymers. In panel (b) the effect of adding BSA to IPECs formed from various polymers on EtBr fluorescence is shown. (PAA:DNA weight ratio of 40:1 established prior to addition of BSA). Data represent mean ± S.D. (n=3).

Table 3.1 Summary of the ability of polymers to exclude EtBr from DNA

Polymer	$^{\dagger}Fr_{50}$
Dextran	90.0:1
ISA 23	15.6:1
ISA 22	17.0:1
ISA 4	2.7:1
PEI	0.2:1

$^{\dagger}Fr_{50}$ denotes the polymer:DNA weight ratio that caused 50% EtBr exclusion.

Data represent mean ± S.D. (n=3).

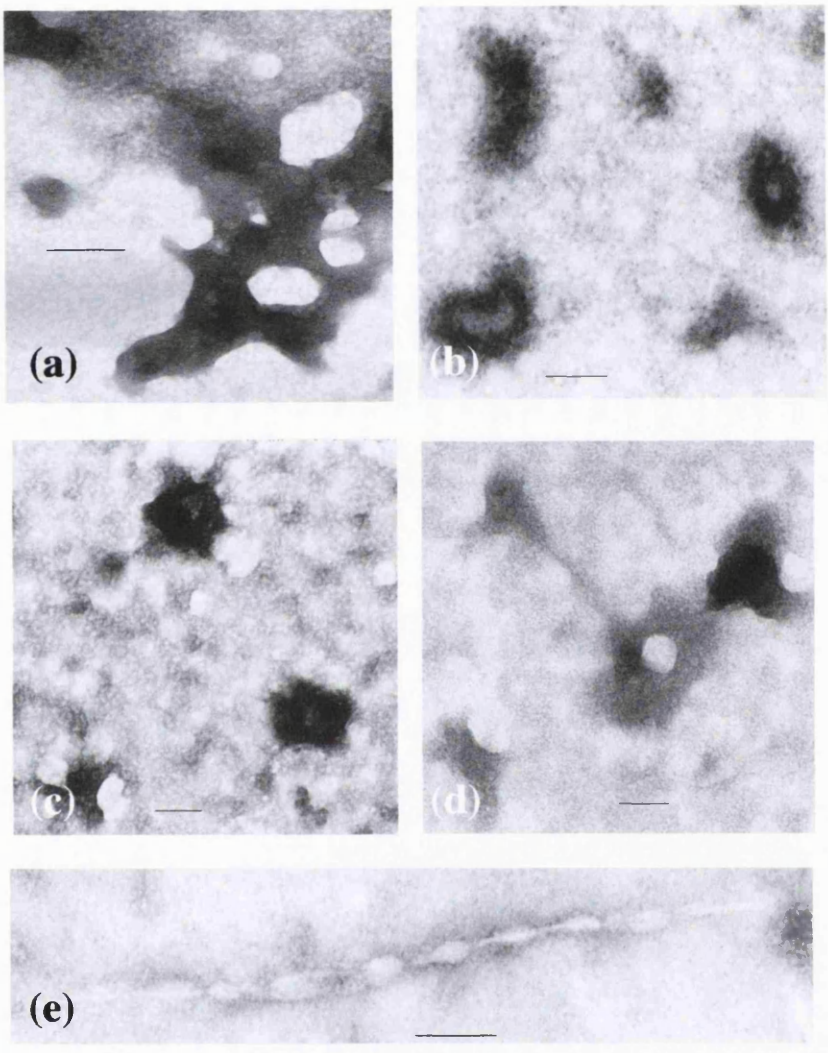

Figure 3.8 TEMs showing morphology of IPECs. In each case IPECs were formed at a 10:1 polymer:DNA weight ratio. Panel (a) shows LipofectACE™ (size bar 67nm); (b) poly-L-lysine (size bar 67nm); (c) ISA 22 (size bar 45.4nm); (d) ISA 4 (size bar 140nm); (e) plasmid (size bar 67nm). (Richardson, Pattri ck et al, 2001).

most likely due to heterogeneous structures of DNA coated with lipid (Mönkkönen and Urtti, 1998).

3.3.5 Evaluation of IPEC stability to DNase II

When incubated with DNase II, all PAA/IPECs were able to protect DNA from degradation (figures 3.9a-d, table 3.2). ISA 1 and 4 showed greater protection at a 1:1 polymer:DNA weight ratio than ISA 22 and 23, with percentage inhibition values of 86.5 ± 1.9% and 87.2 ± 3.3% for ISA 1 and ISA 4 compared to 12.7 ± 2.7% and 34.5 ± 0.7% for ISA 22 and 23 respectively.

At a 1:1 polymer:DNA weight ratio, PEI was able to completely protect DNA from degradation (figure 3.9e). Dextran caused slight protection of DNA at 100:1 and 1:1 polymer:DNA weight ratios (percentage inhibition values of 12.7 ± 6.6% and 17.5 ± 2% respectively) (figure 3.9f). Thus a comparison of the extent of protection afforded by the various polymers at a polymer:DNA weight ratio of 10:1 gave a rank order of PEI > ISA 4 > ISA 1 > ISA 22 > ISA 23 > dextran.

3.3.6 Measurement of the zeta potential of IPECs

The charge of IPECs formed from pSV-β-galactosidase and the PAAs ISA 23 and ISA 4 is shown in table 3.3 below. Zeta potential measurements indicated that as the ratio of PAA to DNA increased, the overall charge of the complexes became more cationic.

3.3.7 Transfection of HepG2 cells by IPECs formed from pSV-β-galactosidase and various vectors

The relative transfection efficiencies of various vectors in HepG2 cells are shown in figure 3.10. All PAAs tested were able to transfect cells to a greater extent than plasmid alone. ISA 23, PEI and the liposomal formulation LipofectIN™ showed the highest transfection levels and were all equi-effective at transfecting cells. ISA 1, 4 and LipofectACE™ were equi-effective at transfecting cells however these levels were ~ 2-fold lower than observed for ISA 23.

The level of protein in HepG2 cells after transfection was measured to allow expression of values in mU β-galactosidase/mg protein and also to crudely assess cell viability. Protein levels in HepG2 cells after transfection with ISA 1 and 4 were similar to that achieved with ISA 23 (~ 10mg/mL). This level was slightly lower than background suggesting slight cellular toxicity. To ensure that the amount of protein

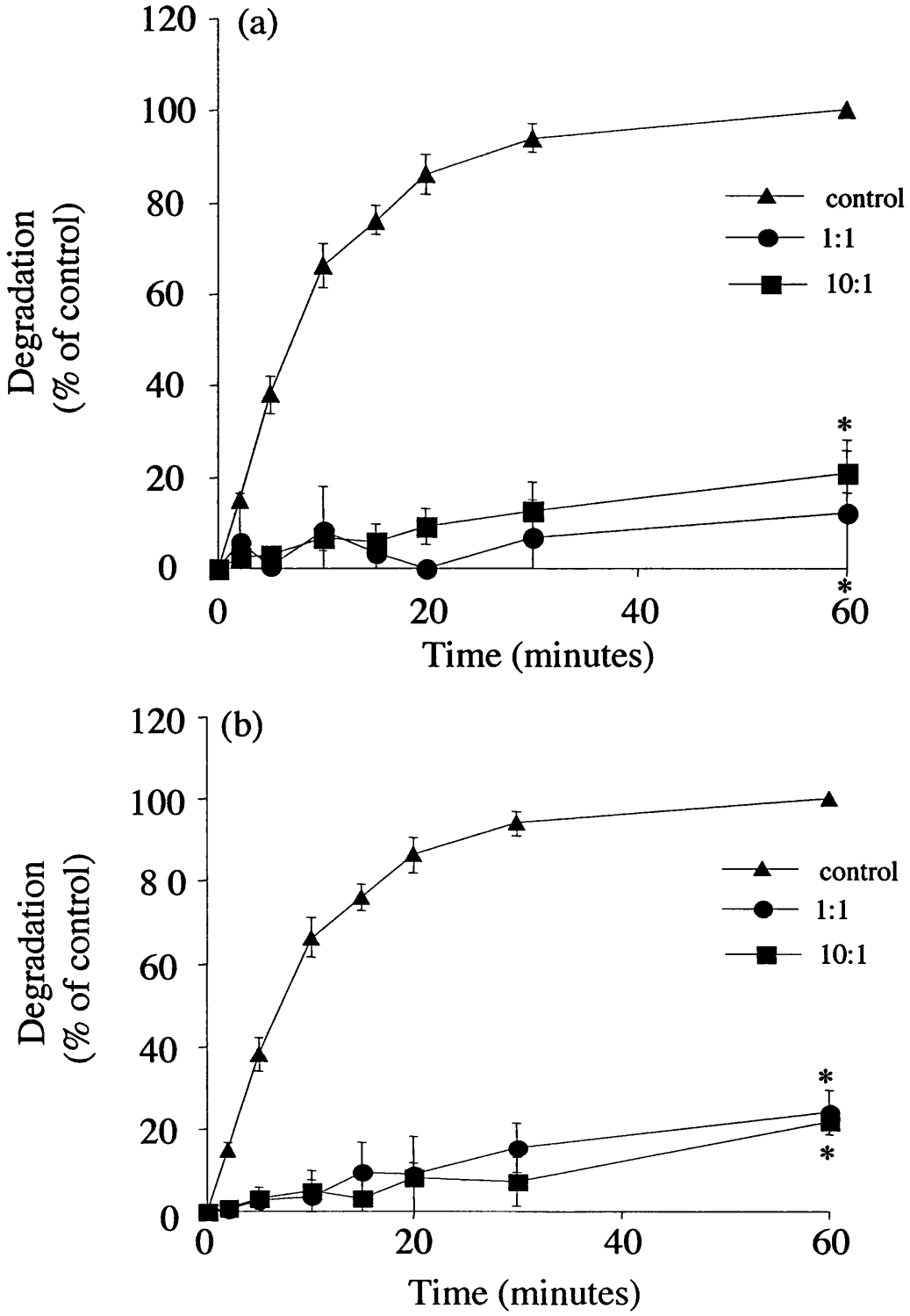

Figure 3.9 Protection of DNA from degradation by various polymers. Panel (a) shows ISA 4; (b) ISA 1; (c) ISA 22; (d) ISA 23 (e) PEI; (f) dextran. Data represent mean ± S.D. (n=3). A student's two-tailed t-test was performed on the DNA degradation in the presence of polymer versus control DNA degradation without polymer to assess the level of statistical significance. P values were designated as follows: NS p= > 0.05; * p < 0.01 (Richardson, Pattrick et al, 2001).

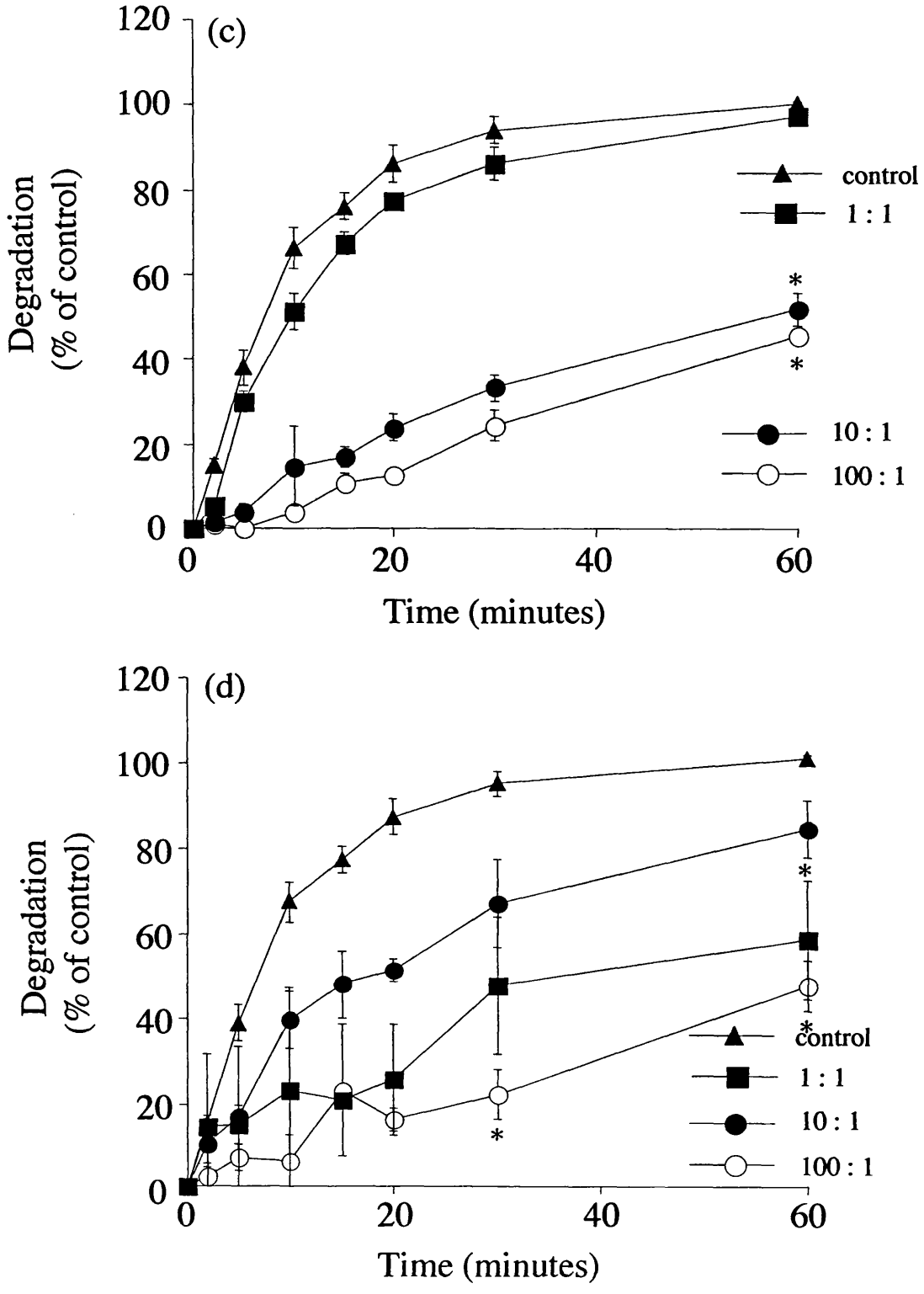

Figure 3.9 Cont.

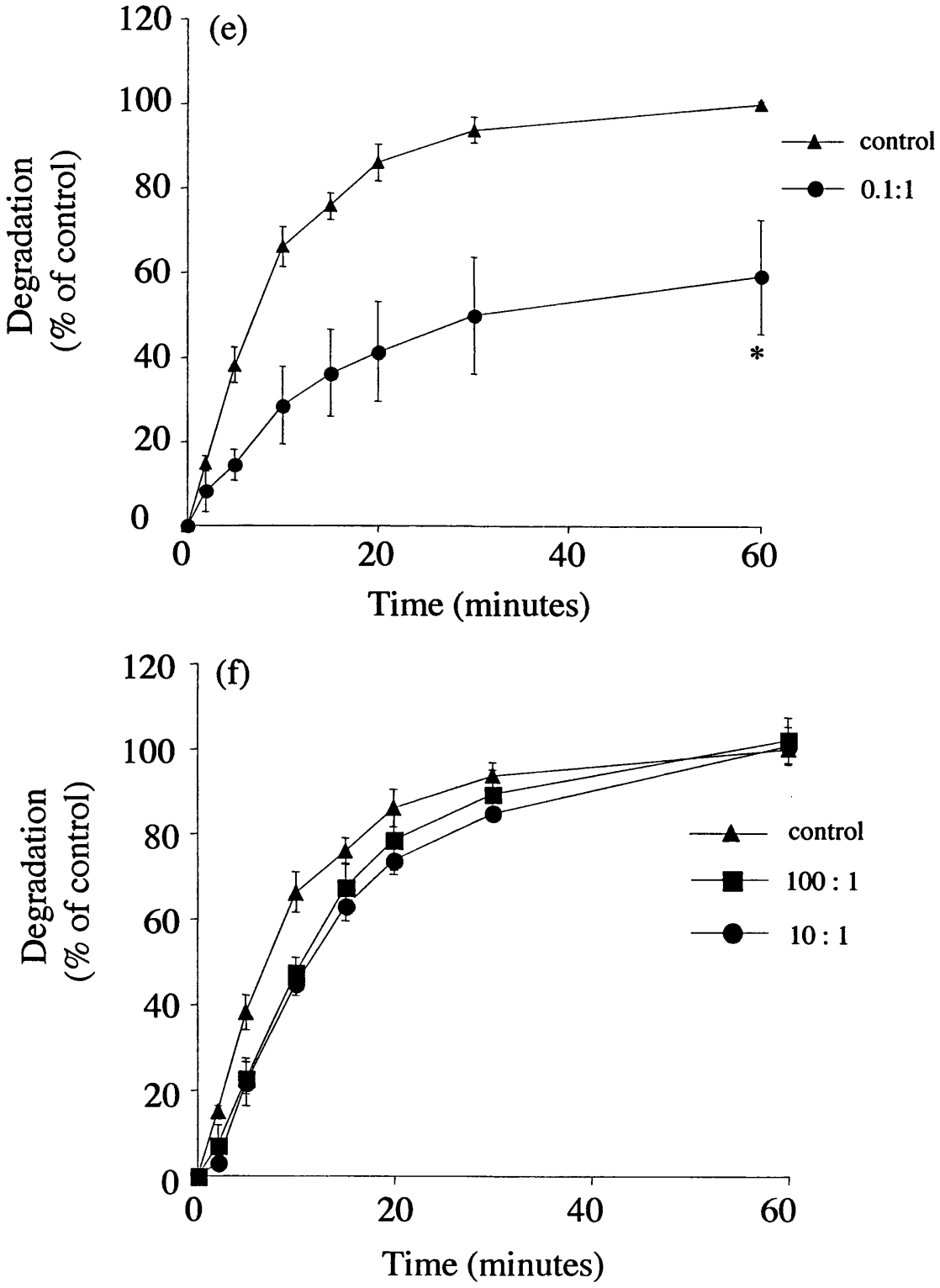

Figure 3.9 Cont.

Table 3.2 Summary of the effect of IPEC formation on DNA degradation caused by DNase II

	Weight polymer: weight DNA ratios[†]			
Polymer	100:1	10:1	1:1	0.1:1
ISA 1	ND	89.6 ± 6.1	86.5 ± 1.9	ND
ISA 4	ND	92.2 ± 11.2	87.2 ± 3.3	ND
ISA 22	79.5 ± 0.3	69.4 ± 3.7	12.7 ± 2.7	ND
ISA 23	74.5 ± 7.3	58.0 ± 10.0	34.5 ± 0.7	ND
PEI	ND	100.0	100.0	49.9 ± 13.6
Dextran	12.7 ± 6.6	17.5 ± 2.0	ND	ND

[†]Results are expressed as DNase II inhibition (%) relative to a control containing no polymer. This was done by expressing the area under the curve (calculated by trapezoid approximation and extrapolation to zero) of the polymer containing experiment as a percentage of the area under the curve of a control and subtracting the result from 100%. Data represent mean ± S.D. (n=3). ND: not determined. (Richardson et al, 2001).

Table 3.3 Zeta potential of IPECs formed from ISA 23 or ISA 4 at various weight ratios

Polymer	Weight polymer:weight DNA ratio	Zeta potential (mV)
ISA 23	1:1	-52.3 ± 10.5
ISA 23	5:1	-5.5 ± 0.3
ISA 23	10:1	-8.7 ± 1.2
ISA 4	1:1	-25.1 ± 0.3
ISA 4	5:1	+26.2 ± 1.7
ISA 4	10:1	+31.5 ± 0.6

Data represent mean ± S.D. (n=3)

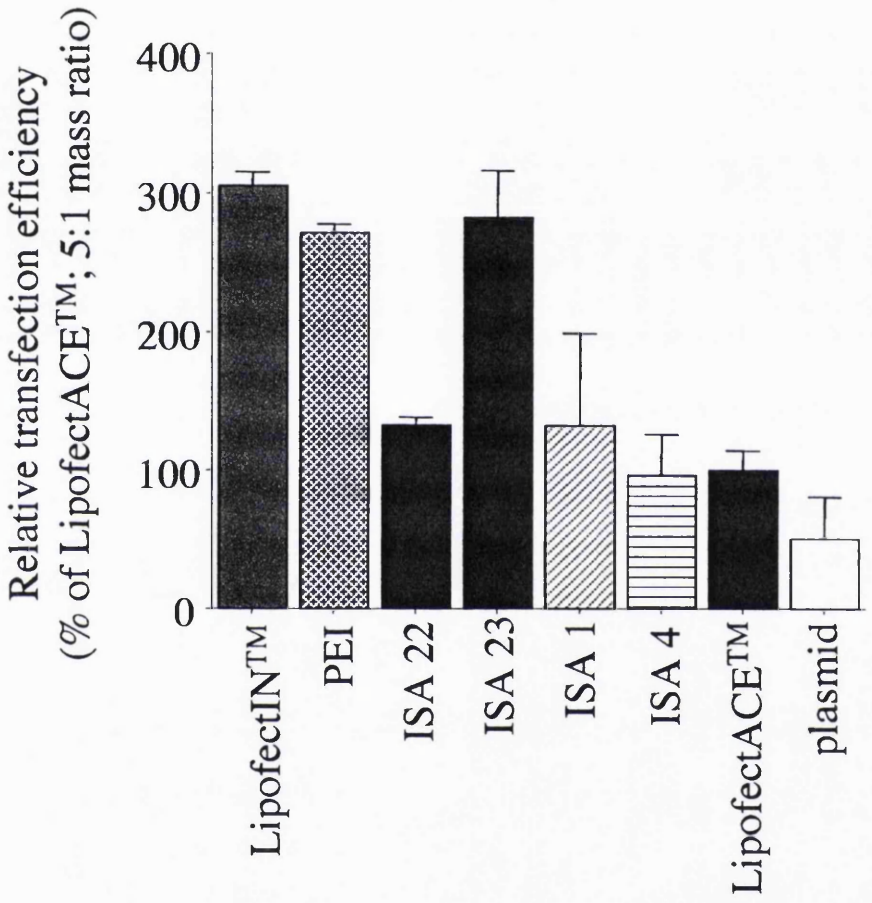

Figure 3.10 Transfection of HepG2 cells by IPECs formed from pSV-β-galactosidase and various vectors at a vehicle:DNA weight ratio of 5:1. Data represent mean ± S.D. (n=3) (Richardson, Pattrick et al, 2001).

measured was due to cellular proteins and not due to interaction of PAAs with the BCA reagent, a BCA assay was performed using a series of ISA 23 and ISA 4 standards (figure 3.4). ISA 23 did not cause an increase in absorbance after addition of BCA reagent. ISA 4 caused a slight increase in absorbance however this effect was negligible compared to that obtained with BSA standards (chapter 2 figure 2.7).

3.4 Discussion

Thermodynamically it is believed that DNA condensation typically occurs when 90% of the DNA charge is neutralised by counterions (reviewed in Bloomfield, 1997). DNA condensation mediated by polymers can result in discreet particles small enough to be endocytosed (80-150nm diameter) and reduces DNA degradation by nucleases due to cleavage site inaccessibility after compaction (Ferrari et al, 1999; Moret et al, 2001).

In order to assess the ability of PAAs to condense DNA and form stable IPECs, agarose gel electrophoresis, EtBr exclusion assays and morphological analysis of PAA/DNA, PEI/DNA and poly-L-lysine DNA samples was performed. Unlike PAAs, the pK_a value for PEI has remained elusive because of the requirement to obtain an ionisation constant for every amine group (which can easily exceed 1000) (Suh et al, 1994). With each PEI nitrogen having its own local environment influencing its protonability, the overall buffering capacity over a range of pH's is perhaps more important than the pK_a value (Godbey et al, 1999a). The overall protonation level of PEI increases from 20-45% between pH values of 7 and 5 (Remy et al, 1998). It was therefore surprising that the IPECs formed from ISA 1 and ISA 4 showed a greater gel retardation at a 1:1 polymer:DNA weight ratio than PEI (figure 3.6a) considering PEI has the highest charge density per monomer than any of the PAAs. This could however, be due a difference in the solution behaviour characteristics between PEI and PAAs. For example, some PAA structures have been shown to display unusually high polymer chain stiffness (Ferruti et al, 2000).

Both ISA 22 and ISA 23 were unable to retard the electrophoretic mobility of DNA in the agarose gel (figure 3.6b), although some evidence for DNA condensation was indicated by a decrease in EtBr fluorescence of samples in gel lanes. As ISA 22 and 23 are amphoteric, some DNA condensation may have occurred but the excess negative charges within the IPEC probably hindered DNA retardation in the gel.

Further evidence for IPEC formation was observed morphologically from TEM analysis (figures 3.7a-e) and from the ability of PAAs to cause exclusion of EtBr from EtBr/DNA complexes (figure 3.7a). When viewed using TEM, DNA condensed by

polymers is seen as toroids. These are compact, highly ordered structures having a well-defined central hole surrounded by double helical strands (Tang and Szoka, 1997). Toroids formed from ISA 4 and 22 were in a similar size range to toroids formed from polyamine/DNA complexes (50-150nm diameter) (Marx and Ruben, 1983). The size of poly-L-lysine/DNA complexes in this study (Mw poly-L-lysine 54,000) was also similar to AFM diameters of poly-L-lysine/DNA complexes of equivalent Mw (80nm) (Wolfert and Seymour, 1996). Although PEI/DNA complexes were not examined using EM analysis in this study, toroidal PEI/DNA complexes have been reported to be in the size range 40-80nm depending on the Mw of PEI used and PEI structure (Tang and Szoka, 1997; Ogris et al, 1998).

Fr_{50} values showed that PEI caused the maximum amount of EtBr displacement, followed by ISA 4, ISA 22 and ISA 23 (table 3.1). When observing the pK_a values of the PAAs tested (chapter 1, table 1.7), at pH ranges 5-7.4, ISA 1 and 4 have an excess of positive charge over ISA 22 and ISA 23. Therefore ISA 1 and ISA 4 were able to form tighter complexes with DNA at an equivalent charge ratio. Dextran surprisingly showed a slight propensity to displace EtBr. As this polymer is uncharged, DNA interaction was probably be due to small non-ionic interactions with DNA at the higher polymer:DNA weight ratios causing DNA phase separation (reviewed in Lasic et al, 1998).

Previous work by Richardson, (1999b) demonstrated that ^{125}-I labelled ISA 4/DNA complexes were cleared rapidly from systemic circulation. However ^{125}-I labelled ISA 22/DNA complexes displayed a longer plasma residence time similar to the parent polymer. These studies however, did not directly address the stability of IPECs in the systemic circulation. Serum albumin has been implicated as the major protein to associate with poly-L-lysine/DNA complexes in serum by competing with DNA for polymer binding. As a result of surface opsonisation of poly-L-lysine by BSA, DNA may be displaced from the IPEC and the poly-L-lysine/BSA complex cleared from the blood by the RES (reviewed in Dash et al, 1999; reviewed in Lasic and Templeton, 1996; Goula et al, 1998; Verbaan et al, 2001; Godbey and Mikos, 2001). To establish whether PAA/IPECs were subject to DNA displacement by BSA, complex stability was assessed in the presence of BSA. BSA was unable to displace DNA from PAA/IPECs after its addition (figure 3.7b), however the amount of BSA added may not have been high enough to represent physiological levels in serum. Clearance of ISA 4/DNA complexes from the systemic circulation was probably due to the overall

positive charge of the complexes (table 3.3) allowing BSA to associate with the IPEC to form a BSA/PAA/DNA complex. As the overall charge of ISA 23 IPECs was slightly negative at all the weight ratios tested (table 3.3), it is likely that BSA may not have been able to associate as strongly with these IPECs and therefore these complexes displayed a longer plasma residence time.

The pharmacokinetics of an IPEC is not the only parameter governed by IPEC surface charge. The overall charge of IPECs can also affect transfection efficiency (reviewed in Kircheis et al, 2001a). There is considerable controversy surrounding this topic. It has been stated that *in vitro*, a net polyplex positive charge is essential for transfection. This is required to aid cell binding by electrostatic interaction with the negatively charged cell membrane (reviewed in Kircheis et al, 2001a). However, negatively charged particles have been shown to be optimal for *in vivo* transfection experiments (Prokop et al, 2001). When comparing the zeta potential of PAAs at a 5:1 weight ratio with transfection efficiency, it is clear that the highest transfection levels were achieved with negatively charged complexes. This is in contrast to the documented positive charge needed for *in vitro* transfection. As the transfection and zeta potential measurements in this study were preliminary experiments, it is put into question whether a correlation between the two to be made.

Although transfection efficiency is governed by many factors in addition to endosomal escape (shown in table 1.3, chapter 1), it can give an indication of the endosomolytic ability of a vector and thus is a useful tool for screening potential candidates. It is encouraging that the PAAs tested were able to achieve comparable transfection efficiency to the liposomal formulations (figure 3.10). Cationic lipids are documented to have high transfection efficiencies as a result of lipid fusion with the endosomal membrane (Zelphati et al, 1996). This indicates that endosomal escape is not a rate-limiting step for PAAs and provides indirect evidence for their endosomolytic ability. The ability of PAAs to be membrane lytic at pH 6.5 (chapter 1, figure 1.13 and Richardson et al, 1999a) is consistent with their observed transfection capability. This is particularly demonstrated with ISA 23, which was more membrane lytic at pH 6.5 that the other PAAs tested. From this model system, the endosomolytic ability of the PAAs is given in the rank order ISA 23 > ISA 22 > ISA 1 = ISA 4.

Comparison of the results obtained here with the data obtained using other vector/β-galactosidase complexes is difficult because of variations in the transfection protocol, promoter used and cell-line (Sosnowski et al, 1996). For example,

transfection levels observed for ISA 23 were 5000-fold less than that achieved when chitosan/IPECs at a 3:1 polymer:DNA weight ratio were used to transfect 293T cells (Lee et al, 2001). However, when IPECs formed from poly-L-lysine conjugated to basic fibroblast growth factor were used were used to transfect COS cells, similar levels of transfection to that of ISA 23 were obtained (Sosnowski et al, 1996). Remy and colleagues investigated in detail the effect of cell line on transfection efficiency. It was shown that large variations in transfection (70-90% transfection in 3T3 cells compared with 0.5-1% transfection in IMR32 cells) could be achieved depending on the cell type used (Remy et al, 1998). In order to investigate whether PAA transfection was dependent on cell-type, preliminary transfection experiments were performed in B16F10 cells (results not shown). As negligible PAA-mediated transfection was observed in this cell-line at a 5:1 PAA:DNA weight ratio, this system is indeed cell-type dependent.

Protein levels were assessed in this study to give an indication of cellular toxicity and to calculate transfection levels in mU/β-galactosidase/mg protein. It has been documented that PAA concentration can be determined using the Bradford assay for protein determination (Jones et al, 2000). Therefore there was a concern that protein content was not accurate due to the contribution of PAAs to the absorbance measured during the protein assay. Although BCA, not Bradford reagent was used for protein determination, it was still considered important to investigate any possible effect of PAAs on the resultant absorbance. Standard curves demonstrated that at the PAA concentrations used in the experiments (5μg/well) the contribution of PAA to the overall absorbance was negligible (figure 3.4). The PAA structures used by Jones et al, (2000) are more cationic than the structures used in this study, therefore it is possible that detection by the Bradford assay is dependent on the number of protonated amine groups along the polymer backbone.

If β-galactosidase is to be considered as a vector for further transfection experiments, it is important to clarify that transfection is due to plasmid β-galactosidase expression and not the up-regulation of endogenous β-galactosidase. Many groups use other non-endogenous commercially available marker genes such as luciferase encoding plasmids (Midoux and Monsigny, 1999; Remy et al, 1998; Boussif et al, 1995; Kircheis et al, 2001a). However, these marker genes and the detection systems required are considerably more expensive than conventional the β-galactosidase system. In addition,

PAA/DNA weight ratios were already optimised for the β-galactosidase system (Man et al, 1999; Richardson et al, 2001).

3.5 Conclusions

In summary of the results obtained in these studies, it has been shown that PAAs are able to form stable IPECs with DNA. ISA 1 and 4 formed stronger complexes with DNA than ISA 22 and 23 due to their cationic nature. Unlike ISA 22 and 23, ISA 1 and 4/IPECs were able to retard the electrophoretic mobility of DNA. All PAAs however, formed toroids in the size range 40-150nm diameter, protected DNA from degradation by DNase II and caused a reduction in EtBr/DNA fluorescence. In this preliminary study, PAAs were also shown to mediate transfection of β-galactosidase in HepG2 cells (Richardson et al, 2001). This model provided indirect evidence for their endosomolytic ability. ISA 23 was able to demonstrate a higher level of transfection compared to the other PAAs tested. Additionally this polymer and IPECs formed from it display a long plasma residence time after i.v. administration. This evidence suggests that ISA 23 would be a good candidate for future transfection experiments. However it is important to note that it is impossible to examine all the cellular barriers that a vector must overcome using transfection experiments. To design gene delivery vectors for commercial use, all these requirements will have to be addressed, which is likely to involve the synthesis of a multi-component system. Bearing this in mind, it was decided to reduce the number of cellular barriers normally required for a gene delivery vehicle, and examine the potential of PAAs to deliver the therapeutic macromolecules RTA and gelonin to the cytosol, as described in chapter 4.

CHAPTER 4

EVALUATION OF THE ABILITY OF PAAS TO MEDIATE INTRACYTOPLASMIC DELIVERY OF RTA AND GELONIN TOXINS

4.1 Introduction

Transfection efficiency is governed by many factors in addition to endosomal escape (chapter 1, table 1.3). In particular, liberation of DNA from the IPEC, trafficking of DNA to the nucleus (reviewed in Pouton, 1998), followed by stable gene expression. These additional requirements were not taken into account in the transfection experiments outlined in chapter 3. It was therefore decided to develop an alternative model to investigate the endosomolytic properties of PAAs, which eliminated the need for nuclear trafficking. In this novel system, the therapeutically active plant toxins RTA and gelonin (detailed in chapter 1, section 1.5.1 and figure 4.1) were chosen for PAA-mediated cytosolic delivery.

Ricin, derived from *Ricinus communis* beans is a highly cytotoxic protein when present in the native dimeric form (maximum tolerated dose in humans 23μg/m^2; Fodstad et al, 1984). This protein is a type II ribosome-inactivating protein, as it contains two polypeptide chains, the catalytic ribosome-inactivating A-chain (RTA) and the cell binding and internalisation B-chain (RTB) (Lord et al, 1994). Once ricin is endocytosed, RTA is translocated to the cytosol by utilising the ERAD pathway (Argent et al, 2000). Pharmacological activity occurs when the N-glycosidic bond of an adenosine nucleotide of the 60S ribosomal subunit is cleaved (Endo et al, 1987; Simpson et al, 1999) (figure 4.2a). RTA alone does show some inherent toxicity towards cells but this is a very inefficient process. This effect is greatly reduced compared to the toxicity of the holotoxin (Simpson et al, 1999).

Gelonin, derived from the seeds of *Gelonium multiflorum*, is a type I ribosome-inactivating protein, as it lacks a cell-binding subunit. As a result it is non-toxic to intact cells (Stirpe et al, 1980), as it is assumed to be trapped in endo/lysosomal compartments after cellular uptake (Selbo et al, 2000; Frankel et al, 2000) (figure 4.2b).

The cellular impermeability, but potent toxicity of RTA, gelonin and other plant toxins, has been utilised to develop a new class of anticancer therapeutic, the immunotoxins. Immunotoxins are comprised of a protein toxin connected to a binding ligand such as an antibody or growth factor. These molecules bind to cell surface antigens which are internalised and kill cells by catalytic inhibition of protein synthesis within the cell cytosol (reviewed in Krietman, 1999; reviewed in Frankel et al, 2000). A number of clinical trials have been conducted with immunotoxins over the last 16 years and produced promising results. The immunotoxin ONTAK, composed of the catalytic and transmembrane domains of diptheria toxin fused to human interleukin II, was the first immunotoxin to receive Food and Drug Administration approval for sale

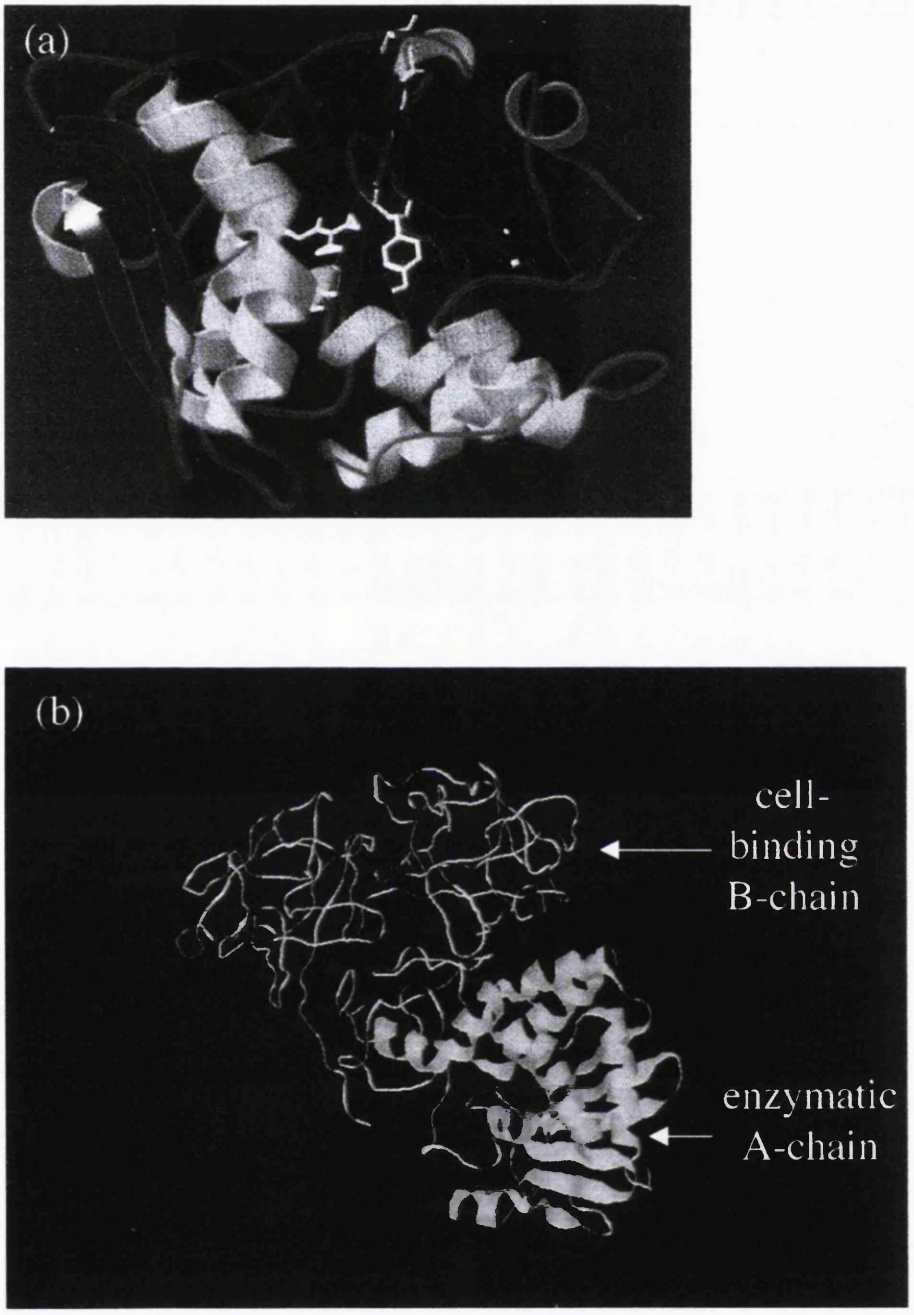

Figure 4.1 Ribbon diagrams of toxins. Panel (a) shows gelonin (Hosur et al, 1995); (b) ricin (Rutenber et al, 1991).

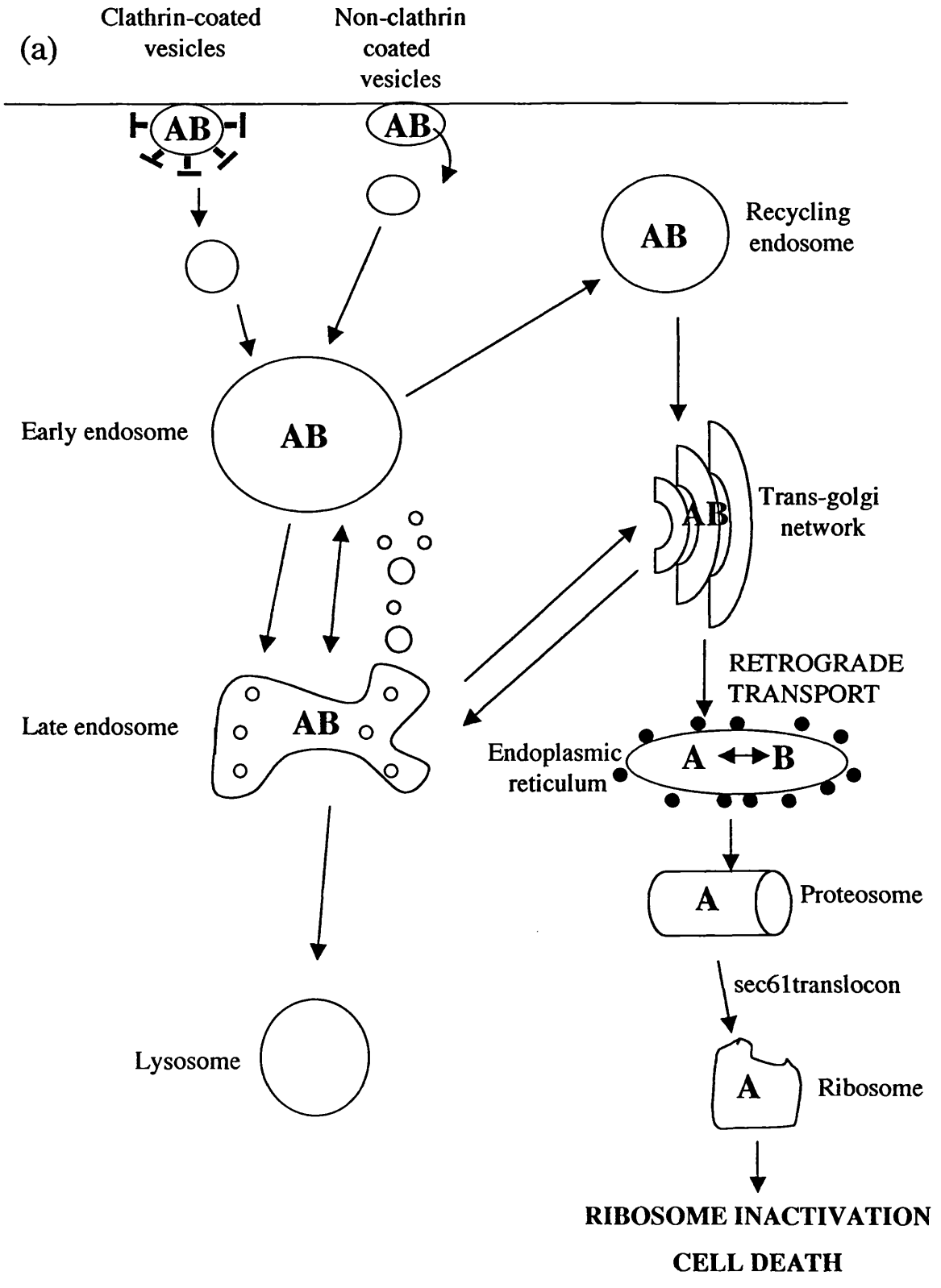

Figure 4.2 Proposed intracellular trafficking of toxins after endocytic uptake. Panel (a) shows ricin holotoxin (denoted AB); (b) RTA and gelonin (denoted A).

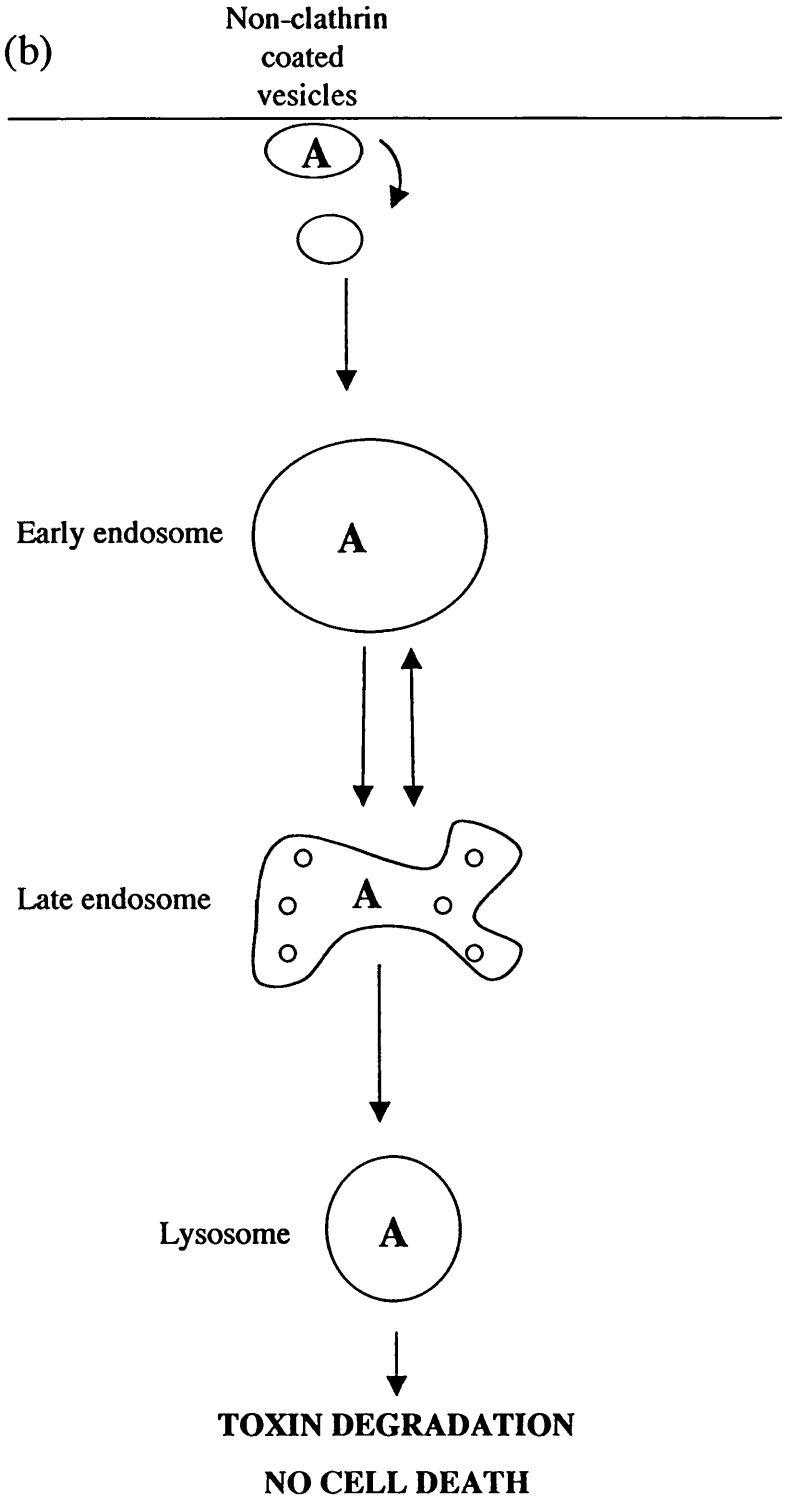

Figure 4.2 Cont.

for the treatment of cutaneous T-cell lymphoma (CTCL) (Olsen et al, 2001; reviewed in Frankel et al, 2000). There are at least three other targeted toxins (LMB-2; HN66000; BL22) currently undergoing clinical trials showing ≥ 30% complete and partial remission rates for the treatment of different types of cancers (Kreitman et al, 2000; Laske et al, 1997; Kreitman et al, 2001).

Despite the successes of these immunotoxins in clinical trials, there are still major challenges to be overcome if their potential for cancer therapy is to be realised. One such barrier is immunotoxin-related immunogenicity. This is particularly evident in patients with solid tumours who become immunised much more readily than those with haematologic tumours (reviewed in Kreitman, 1999). VLS is another major drawback to immunotoxin therapy. This is often responsible for the dose-limiting toxicities of many of the most successful immunotoxins. It is attributed to non-specific uptake of immunotoxins by normal human tissues, resulting in damage to vascular endothelial cells (Baluna et al, 2000). Another limitation, particularly concerning immunotoxins prepared from type I ribosome-inactivating proteins, is their relatively low efficacy due to trafficking of the conjugate to lysosomes (Press et al, 1998; reviewed in Rhíová, 1998).

In order to improve translocation efficiency of toxins to the cytosol, some studies have been performed using endosomolytic agents to deliver these toxins to cells (table 4.1). However, many of these systems are of limited use clinically, due to their unsuitability for i.v. administration (described in chapter 1, section 1.7). In contrast, PAA structures, in addition to their transfection capability, have been shown to be non-toxic and display a long plasma residence time after i.v. administration. Therefore it was considered important to assess their ability to deliver RTA and gelonin toxins to the cell cytosol. Although this model would only provide indirect evidence for PAA-mediated endosomal rupture, it was important to use a second model system (in addition to transfection, discussed in chapter 3) for measuring endosomolytic ability. Secondly, it was important to investigate this model with a view to developing PAA-toxin constructs as an alternative anti-cancer therapeutic to immunotoxins.

4.2 Methods

The PAAs used in these studies and their characteristics are shown in chapter 1, table 1.7. It was important that the same polymers were used for toxin delivery assays as the transfection experiments described in chapter 3 to allow comparison of endosomolytic ability between the two models. The techniques used to evaluate the

Table 4.1 Intracytoplasmic delivery systems used to deliver toxins

Intracytoplasmic delivery system	Toxin	Cell line	IC_{50} (μg/mL)	Minimum cell viability achieved	Reference
PPAAc	RTA	Ramos	-	-	Lackey et al, 1999a
Aluminium phthalocyanine	gelonin	NHIK	3	30% (as measured by ^{3}Hleucine incorporation	Selbo et al, 2000a
Listeriolysin O encapsulated in liposomes	gelonin	B16F10	$1x10^{-4}$	40% (as measured by formazan salt absorbance)	Stier et al, 2002
Fusogenic peptides derived from influenza virus hemagglutinin	Anti-HIV antibody conjugated to RTA	H9/NL4-3	700	12% (as measured by ^{35}Smethionine incorporation)	Tolstikov et al, 1997

toxicity of polymers and toxins towards B16F10 and HepG2 cells are described in detail in chapter 2, sections 2.3.6-2.3.7. Evaluation of cytotoxicity of toxin/polymer combinations towards B16F10 and HepG2 cells is described in chapter 2, section 2.3.8. SDS-PAGE experiments to allow visualisation of gelonin, RTA and RTA in combination with ISA 4 are described in chapter 2, section 2.3.16.

4.3 Results

4.3.1 SDS-PAGE analysis of RTA, gelonin and RTA/ISA 4 combinations

SDS-PAGE was used for two studies. First, to determine the purity of RTA and gelonin before starting the cytotoxicity experiments. Second, to investigate whether PAA/toxin complexes could be formed.

Application of RTA on the SDS-PAGE gel gave four bands and most material had a Mw between 29,000-32,000Da consistent with the RTA Mw of 29,500Da (Lord et al, 1994) (figure 4.3). The appearance of multiple bands in this region may have been RTA isoforms. The lower band corresponding to a Mw of ~ 12,000 was probably a contaminating protein or an RTA degradation product. Application of gelonin produced one distinct band at a Mw of ~ 29,000-31,000Da consistent with the Mw of gelonin of 30,500 (Stirpe et al, 1980). Two other bands corresponding to Mws of ~ 34,000 and 48,000 were probably contaminating proteins. Although RTA and gelonin toxins were not pure, the level of contamination was considered to be minimal. To obtain pure toxin preparations, recombinant toxins should be considered.

SDS-PAGE analysis of the ISA 4/RTA mixture was performed to see if any direct evidence for complex formation could be observed. If present, interaction would act to increase the Mw of RTA, causing a reduction in its migration through the gel. However gel lanes containing the RTA/ISA 4 combination did not show any alteration in RTA mobility compared to RTA alone (figure 4.4), suggesting that using this method there was no complex formation.

4.3.2 Cytotoxicity of toxins, polymers and toxin/polymer combinations towards B16F10 and HepG2 cells

The concentration-dependent cytotoxicity of ricin, RTA and gelonin towards B16F10 cells and gelonin towards HepG2 cells was evaluated (figure 4.5). Ricin and RTA displayed IC_{50} values of 0.3 and 1.4μg/mL respectively towards B16F10 cells. Gelonin was non-toxic over the range studied when incubated in B16F10 cells. Gelonin displayed an IC_{50} value of 4μg/mL towards HepG2 cells. In all further experiments,

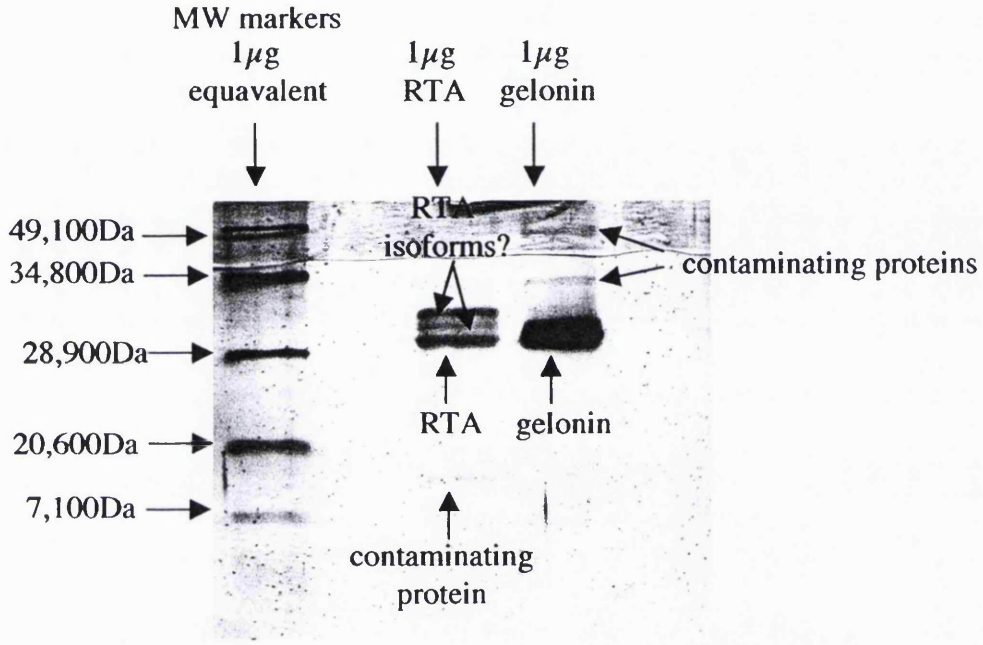

Figure 4.3 SDS-PAGE of RTA and gelonin. The protein bands were visualised by silver staining and Mw markers were applied as a reference.

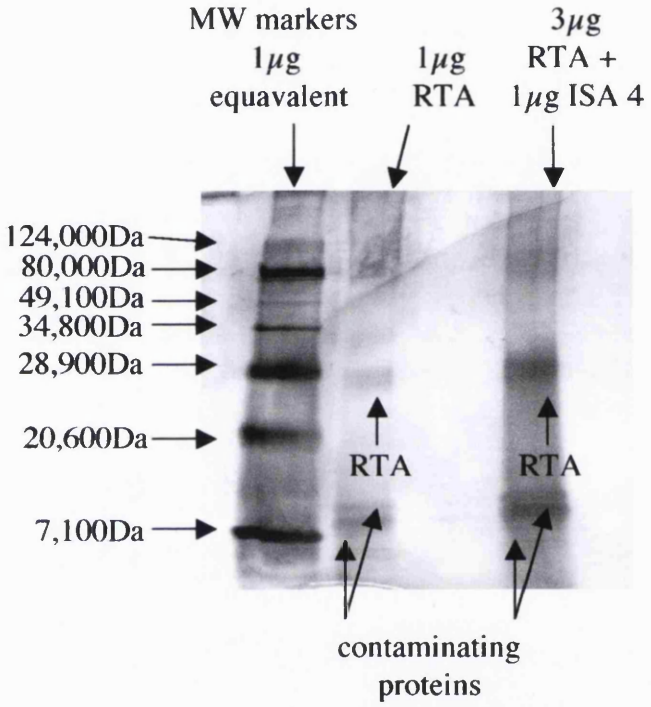

Figure 4.4 Investigation of ISA 4/RTA interaction using SDS-PAGE. The protein bands were visualised by silver staining and Mw markers were applied as a reference.

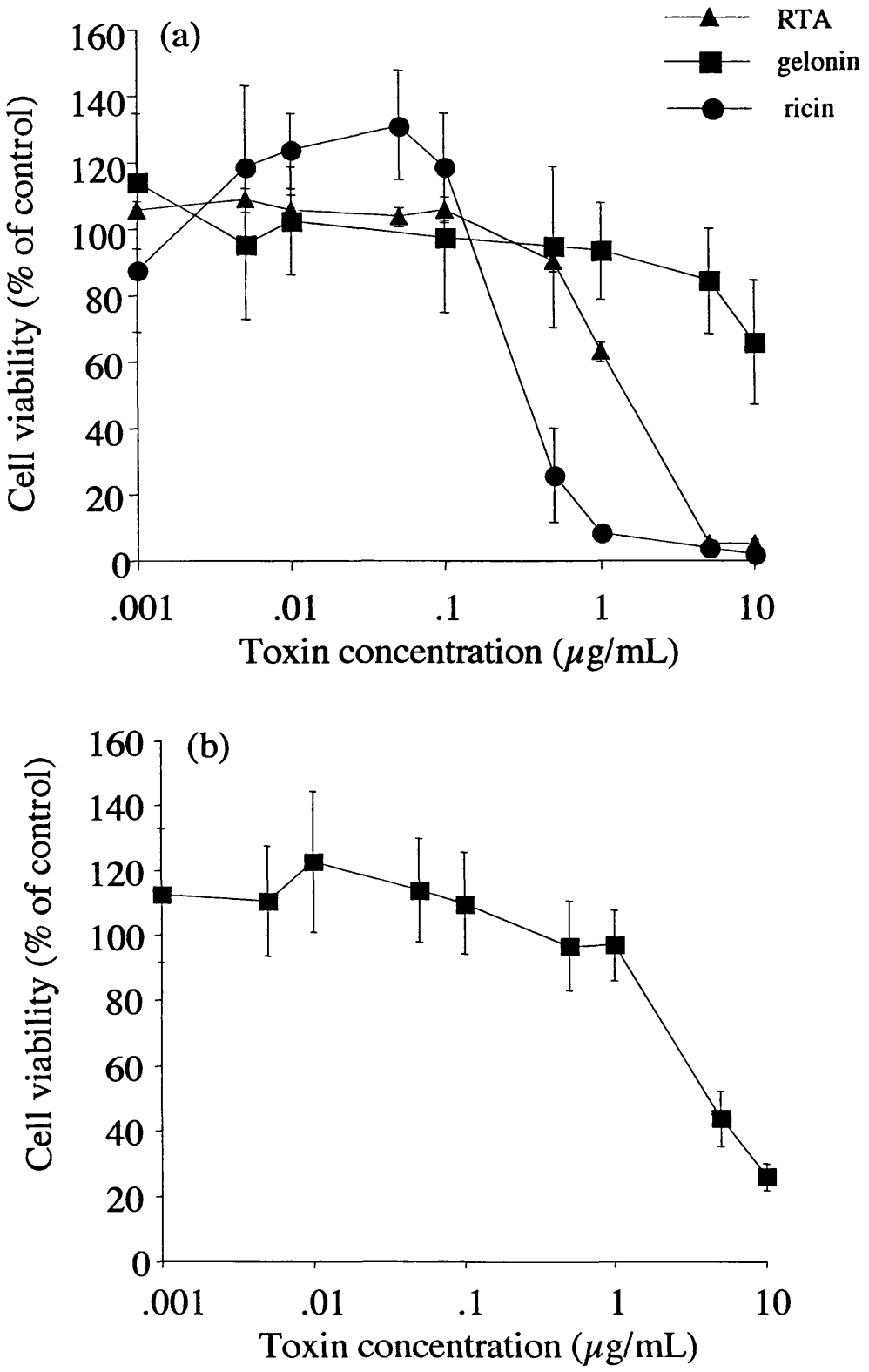

Figure 4.5 Cytotoxicity of RTA, ricin holotoxin and gelonin. Panel (a) shows cytotoxicity towards B16F10 cells; (b) shows cytotoxicity towards HepG2 cells. Cells were incubated with toxin for 67h and viability assessed using the MTT assay. Data represent mean ± S.D. (n=18).

(unless otherwise stated) non-toxic concentrations of RTA (250ng/mL) and gelonin (1.4μg/mL) were selected for further experiments with B16F10 cells. A non-toxic concentration of gelonin (0.1μg/mL) was used in subsequent experiments with HepG2 cells.

The cytotoxicity of the PAAs used in subsequent studies (PEI and dextran used as reference controls) towards B16F10 and HepG2 is summarised in table 4.2. For statistical purposes, dose-response curves for these polymers alone are plotted on the same graphs as cytotoxicity assays for the polymer and toxin combinations (figures 4.6-4.8).

Cytotoxicity of RTA/polymer combinations against B16F10 cells

When ISA 1 was combined with 250ng/mL RTA, the observed IC_{50} value decreased from > 2mg/mL to 0.65 ± 0.05mg/mL in B16F10 cells. Similarly when a combination of ISA 4 and RTA was used, the IC_{50} value fell from > 1.8mg/mL to 0.57 ± 0.03mg/mL (figure 4.6a). Cytotoxicity for the ISA 1/RTA combination was statistically greater than ISA 1 alone between ISA 1 concentrations of 1-2mg/mL. The cytotoxicity caused by the ISA 4/RTA combination was also statistically greater than ISA 4 alone between ISA 4 concentrations of 0.5-2mg/mL. However when ISA 22 was added in combination with RTA, no increase in cytotoxicity was observed (figure 4.6b). Incubation of B16F10 cells with dextran and an RTA combination resulted in no increase in cytotoxicity. PEI alone was toxic to B16F10 cells. When co-incubated with RTA, a further small increase in cytotoxicity was observed, with the IC_{50} value dropping from 0.02mg/mL to 8.0 ± 1.0μg/mL. However at PEI concentrations above 0.05mg/mL, toxicity of the polymer alone was significantly greater than the PEI/RTA combination up to the maximum PEI concentration tested of 1mg/mL (figure 4.6c).

Cytotoxicity of gelonin/polymer combinations against B16F10 cells

When ISA 1 or ISA 4 were incubated with gelonin, its toxicity towards B16F10 cells increased. In this case, the IC_{50} values observed were 0.55 ± 0.12mg/mL and 0.43 ± 0.26mg/mL respectively (figure 4.7a). The cytotoxicity caused by the ISA 1/gelonin and ISA 4/gelonin combinations were both statistically greater than ISA 1 and ISA 4 alone between PAA concentrations of 0.5-2mg/mL. No increased gelonin cytotoxicity was seen when ISA 22 was combined with gelonin (figure 4.7b).

As with RTA, dextran was unable to promote the cytotoxicity of gelonin. However, the combination of gelonin with PEI did cause an increase in cytotoxicity.

Table 4.2 Cytotoxicity of polymers against B16F10 and HepG2 cells

Polymer	Cell line	
	B16F10	HepG2
	IC_{50} (mg/mL)	IC_{50} (mg/mL)
ISA 22	> 2.00	> 2.00
ISA 4	1.80	> 2.00
ISA 1	> 2.00	> 2.00
Dextran	> 2.00	> 2.00
PEI	0.02	0.01

Polymers were incubated with cells for 67h and viability assessed using the MTT assay. Data represent mean ± S.D. (n=18).

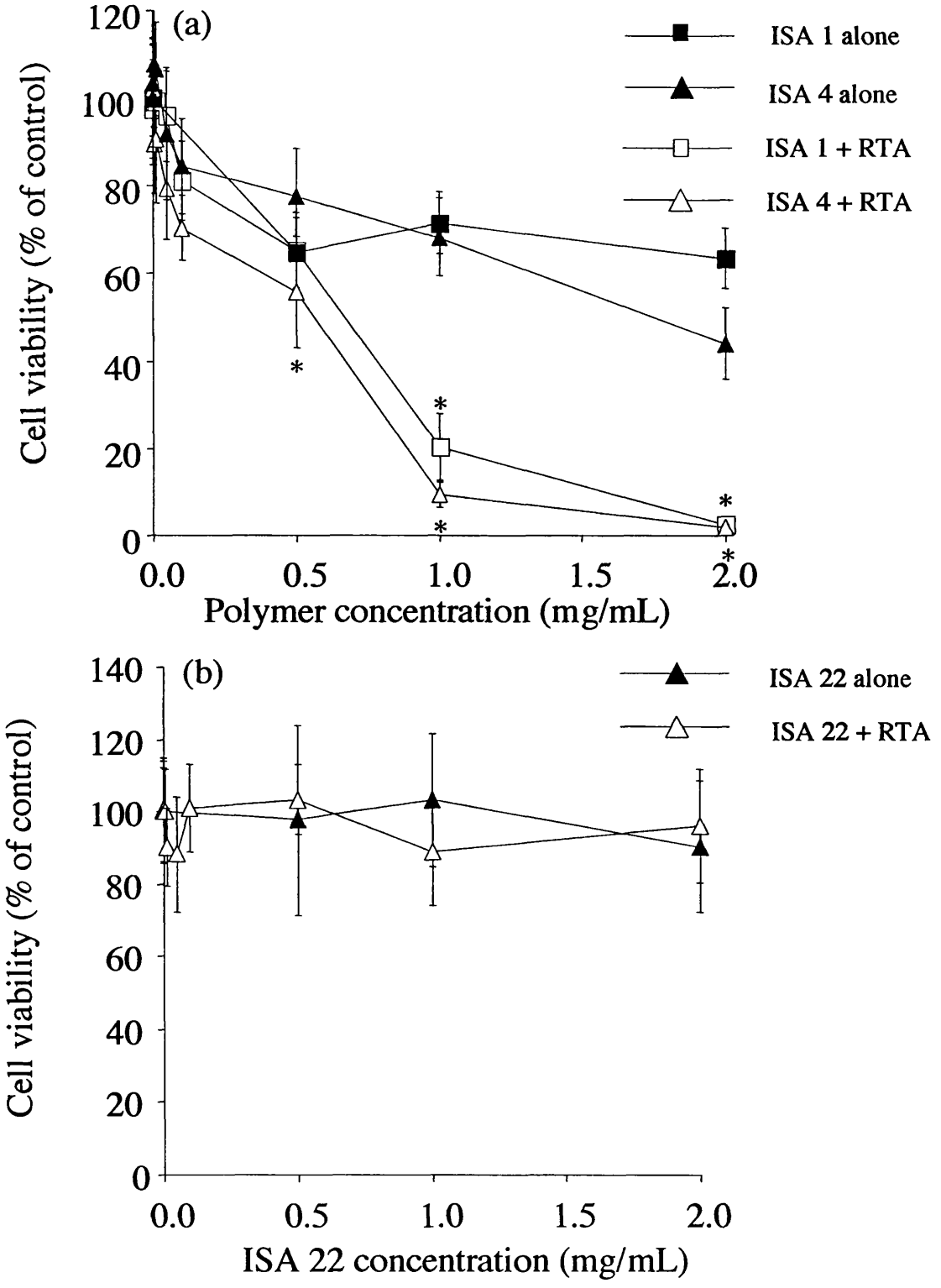

Figure 4.6 Cytotoxicity of polymers and polymer/RTA combinations against B16F10 cells. Panel (a) shows ISA 1, 4; (b) ISA 22; (c) PEI, dextran. Cells were incubated with polymers and/or toxins for 67h and viability assessed using the MTT assay. Data represent mean ± S.D. (n=18). A student's two-tailed t-test was performed on the cytotoxicity of PAA/toxin combinations versus cytotoxicity of PAA alone to assess the level of statistical significance. P values were designated as follows: NS p= > 0.05; * p < 0.01 (adapted from Pattrick et al, 2001).

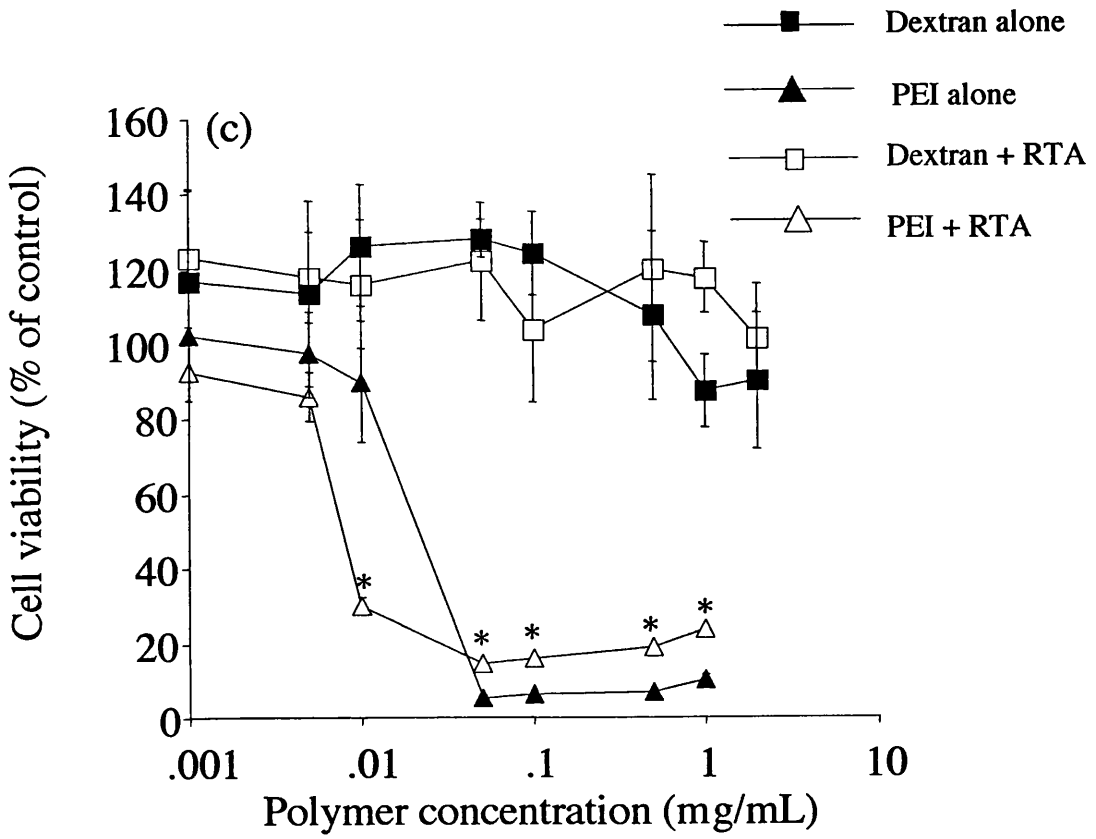

Figure 4.6 cont.

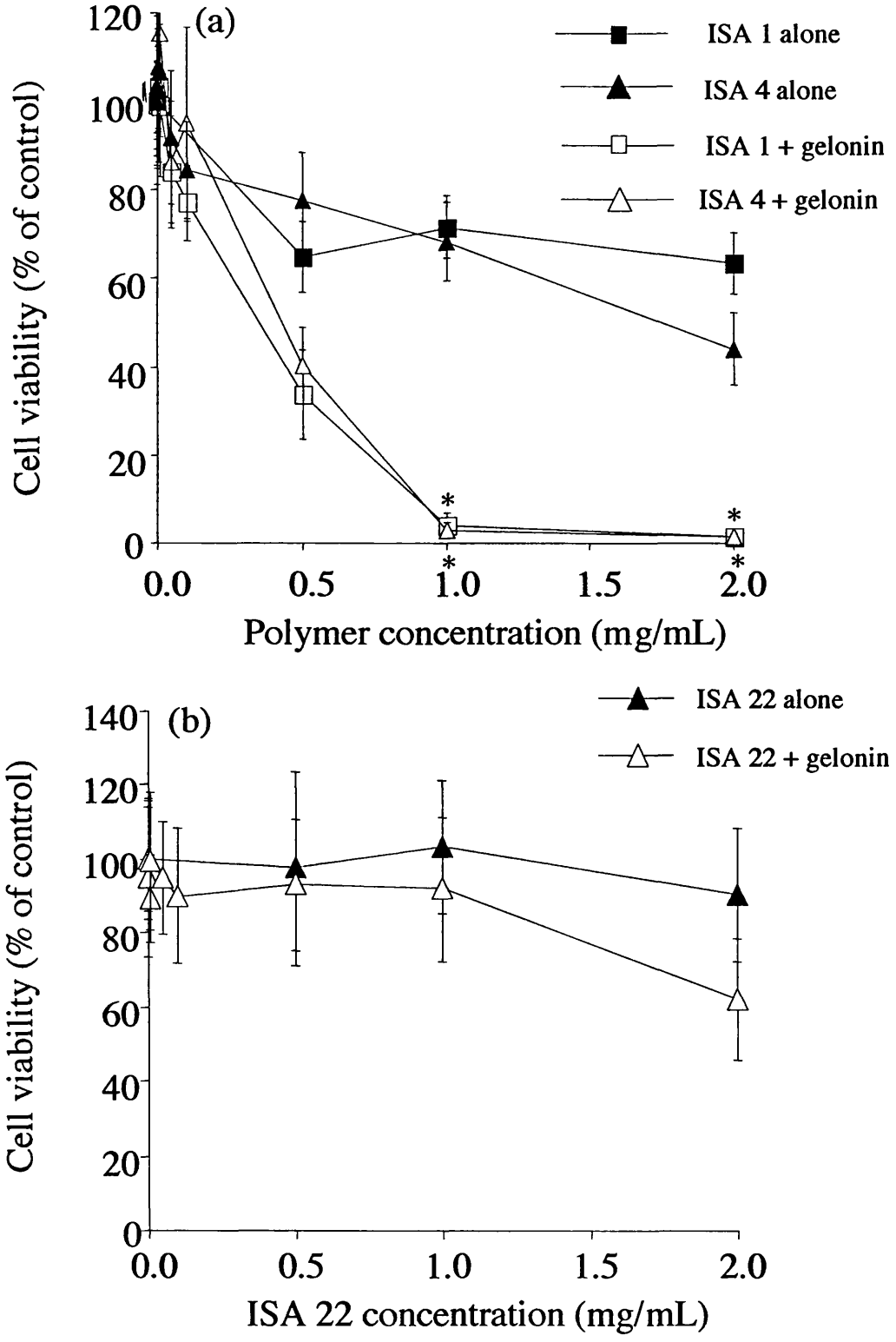

Figure 4.7 Cytotoxicity of polymers and polymer/gelonin combinations against B16F10 cells. Panel (a) shows ISA 1, 4; (b) ISA 22; (c) PEI, dextran. Cells were incubated with polymers and/or toxins for 67h and viability assessed using the MTT assay. Data represent mean ± S.D. (n=18). A student's two-tailed t-test was performed on the cytotoxicity of PAA/toxin combinations versus cytotoxicity of PAA alone to assess the level of statistical significance. P values were designated as follows: NS p= > 0.05; * p < 0.01 (adapted from Pattrick et al, 2001).

The IC_{50} value of the combination was 8.0 ± 1.0μg/mL. At PEI concentrations of 0.05mg/mL and above, toxicity of PEI alone was statistically greater than the PEI/gelonin combination (figure 4.7c).

Cytotoxicity of gelonin/polymer combinations against HepG2 cells

The combination of ISA 1 with gelonin resulted in a significant increase in cytotoxicity. At an ISA 1 concentration of 1mg/mL, HepG2 viability was 91% and this fell to 69.2% when cells were incubated with the ISA 1 and gelonin combination. Similarly, at an ISA 4 concentration of 1mg/mL, HepG2 viability was 98%, but this decreased to 58.7% after incubation with the gelonin and ISA 4 combination. The IC_{50} values for PAA and PAA/toxin combinations could not however be determined because cell viability did not fall below 50% at the concentrations tested (figure 4.8a). ISA 22 appeared to stimulate cell viability at ISA 22 concentrations > 0.5mg/mL. This may have been caused by inaccuracies when measuring formazan salt absorbance. The ISA 22 and gelonin combination caused a reduction in cell viability but it was not great enough to allow definition of an IC_{50} value (figure 4.8b).

Combination of dextran with gelonin caused no increase in cytotoxicity. However when the PEI/gelonin combination was added to HepG2 cells, the IC_{50} value decreased from > 2mg/mL to 3.5 ± 2.0μg/mL (figure 4.8c). This increased cytotoxicity of the PEI/gelonin combination was significant at PEI concentrations of 0.05-0.01mg/mL. At higher concentrations, cytotoxicity towards HepG2 cells was identical for PEI alone and the PEI/gelonin combination.

Cytotoxicity of RTA/ISA 4 combinations using a fixed concentration of polymer against B16F10 cells

To ascertain the efficiency of ISA 4 at promoting cytotoxicity of RTA in comparison to the activity of ricin holotoxin, cytotoxicity assays were performed where B16F10 cells were incubated with a fixed concentration of ISA 4, but in this case with increasing concentrations of RTA (0-10μg/mL) (figure 4.9). Molar ratios of ISA 4:RTA were then calculated. Greatest cytotoxicity was achieved when 1.5mg/mL ISA 4 was co-incubated with RTA (IC_{50} value of 0.05μg/mL). Under these conditions, the ISA 4/RTA mixture produced an IC_{50} value that was lower than seen for ricin holotoxin (IC_{50} = 0.39μg/mL). This ricin holotoxin IC_{50} value was approximately equal to that observed when 1mg/mL ISA 4 was combined with RTA (0.4μg/mL).

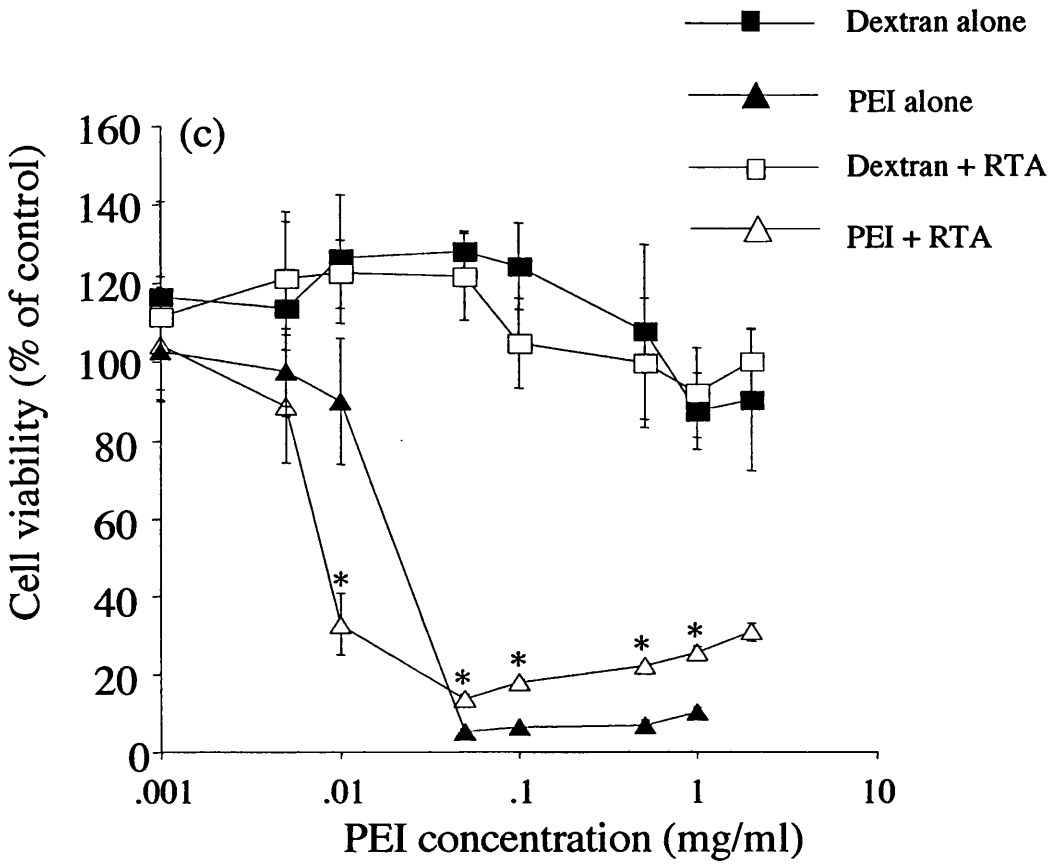

Figure 4.7 cont.

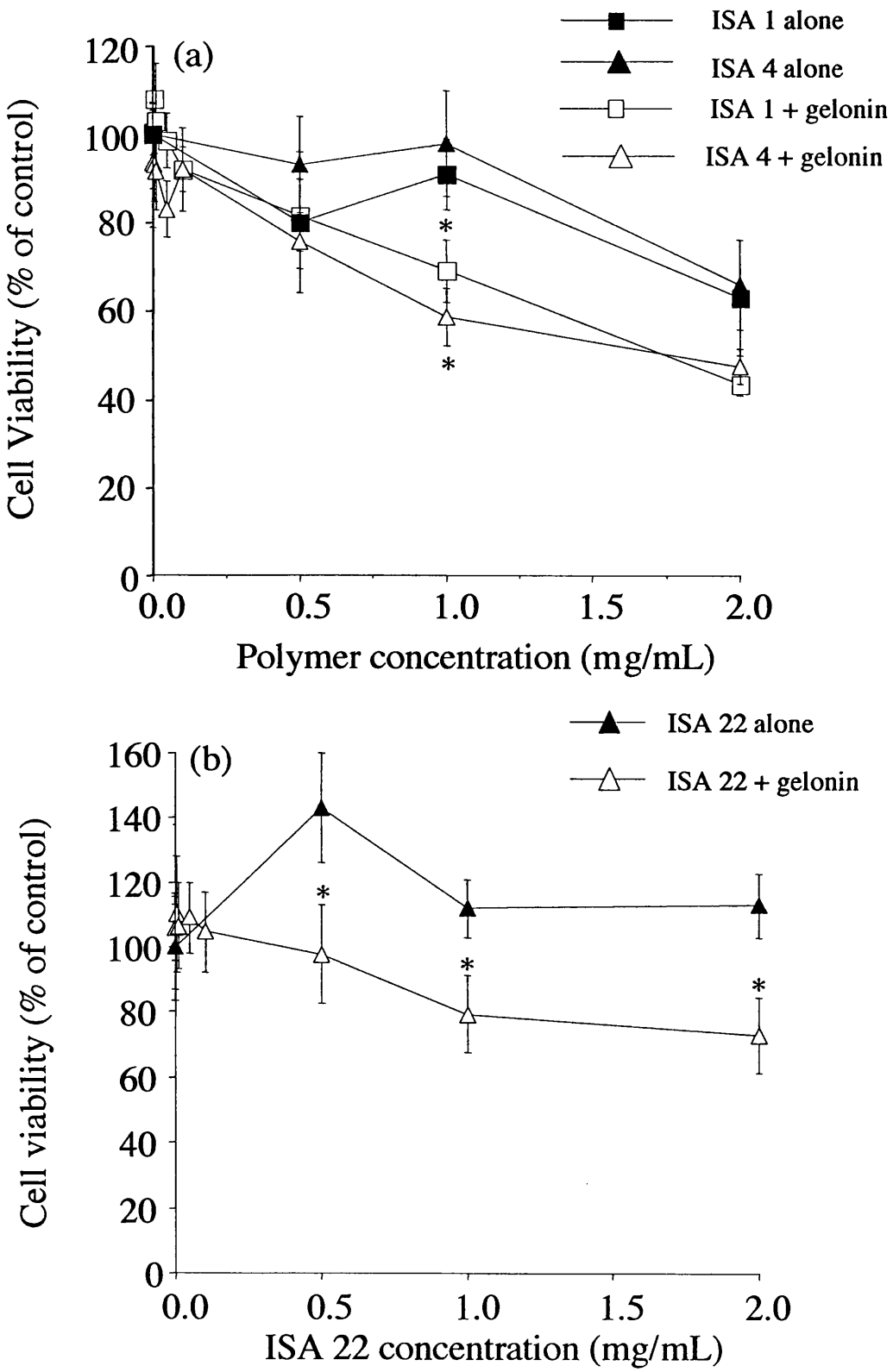

Figure 4.8 Cytotoxicity of polymers and polymer/gelonin combinations against HepG2 cells. Panel (a) shows ISA 1, 4; (b) ISA 22; (c) PEI, dextran. Cells were incubated with polymers and/or toxins for 67h and viability assessed using the MTT assay. Data represent mean ± S.D. (n=18). A student's two-tailed t-test was performed on the cytotoxicity of PAA/toxin combinations versus cytotoxicity of PAA alone to assess the level of statistical significance. P values were designated as follows: NS p= > 0.05; * p < 0.01

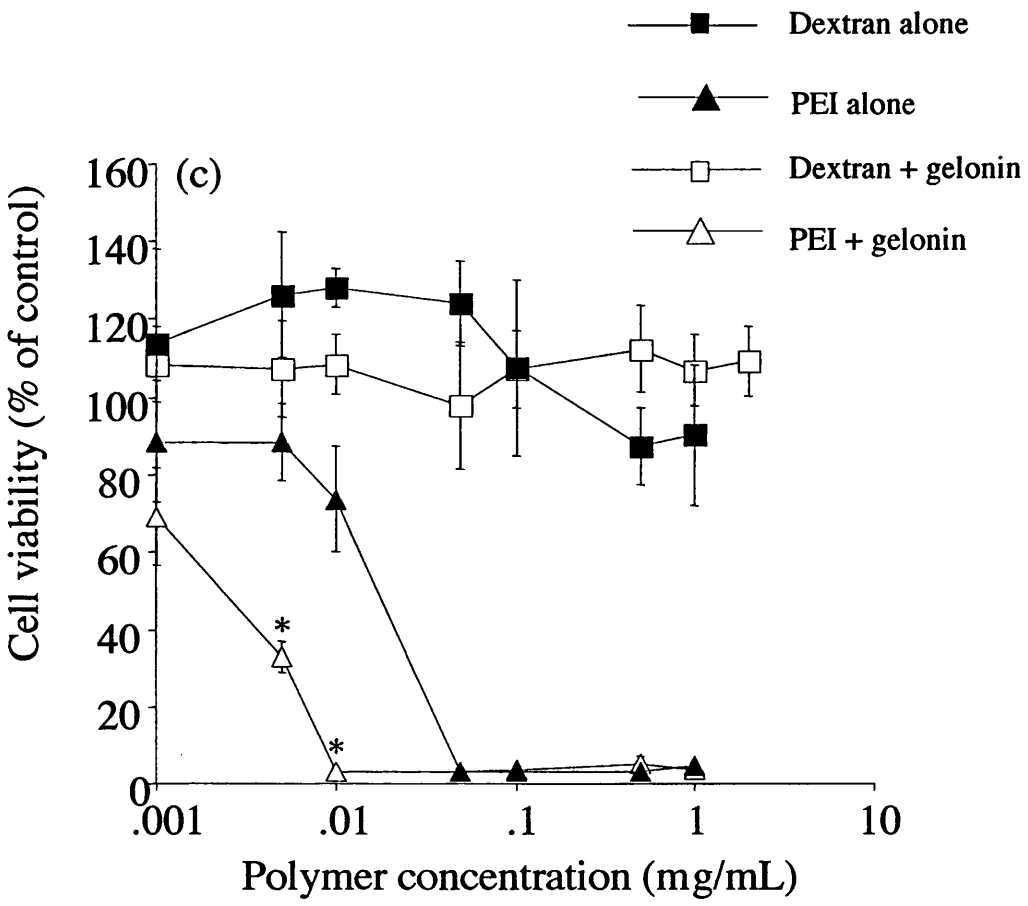

Figure 4.8 cont.

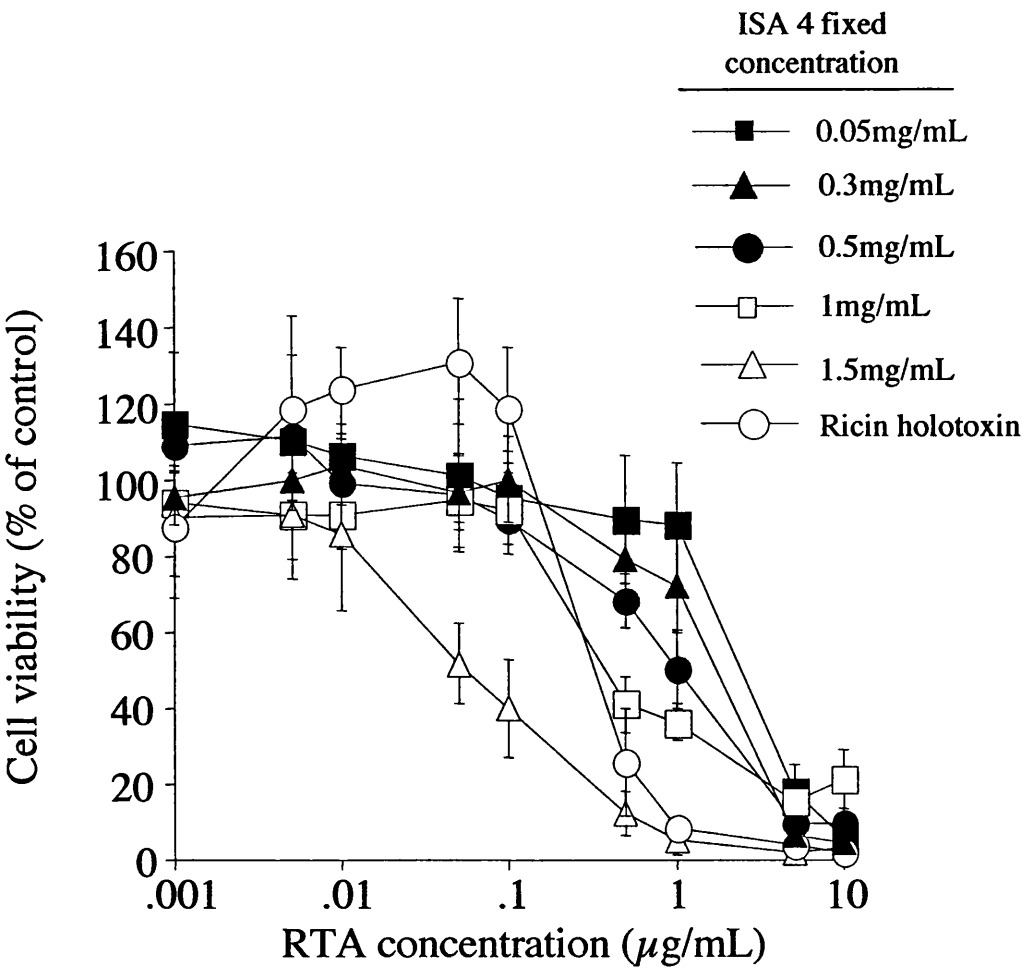

Figure 4.9 Cytotoxicity of increasing concentrations of RTA when incubated with B16F10 cells in the presence of a fixed concentration of ISA 4. Fixed ISA 4 concentrations are described in the key above. Cells were incubated with toxin for 67h and viability assessed using the MTT assay. Data represent mean ± S.D. (n=18) (Pattrick et al, 2001).

4.4 Discussion

A new method was set up to assess the endosomolytic ability of PAAs. In this system the ability of PAAs to deliver toxins to the cytosol of B16F10 cells was investigated. This cell line was chosen for study as it is a particularly aggressive cell line and an *in vivo* tumour model using this cell line has already been established. Cytotoxicity assays demonstrated that the PAAs ISA 1 and 4 were able to promote cytotoxicity of RTA and gelonin (used at non-toxic concentrations in this assay) towards B16F10 cells (figures 4.6a and 4.7a). As neither RTA nor gelonin penetrate the cell efficiently, the increase in cytotoxicity suggests PAA-mediated endosomal membrane rupture thus allowing toxin delivery to the cytosol, and subsequent ribosomal inactivation. Alternatively, the increased cytotoxicity could have resulted from increased toxin uptake into the cell.

Only a few molecules of RTA are required to inactivate thousands of ribosomes (Walsh et al, 1991) and cause cell death. Therefore it was considered important to quantify the efficiency of ISA 4-mediated RTA cytosolic delivery in order to allow comparison of cytosolic transfer with the highly potent ricin holotoxin. From the theoretical estimates made, it would seem that approximately 7,023 ISA 4 molecules are required to cause the same level of cytotoxicity as one molecule of ricin holotoxin (table 4.3). Although this suggests that cytosolic delivery of RTA by ISA 4 is much less efficient than seen for ricin holotoxin, it must be noted that unlike ricin holotoxin, ISA 4 and RTA were added to cells as a mixture and not as a covalent conjugate. In addition, uptake of ISA 1 and ISA 4 is presumably less efficient than the receptor-mediated uptake of ricin caused by RTB.

It was surprising that ISA 22 was unable to mediate the cytosolic delivery of both toxins to B16F10 cells (figures 4.6b and 4.7b), as this polymer was previously shown to be more haemolytic at pH 6.5 (endosomal pH) (Richardson et al, 1999a) and was also shown to be a better transfection agent than both ISA 1 and ISA 4 (chapter 3). For these reasons the inability of ISA 22 to promote toxin delivery as seen for ISA 1 and 4 was considered unlikely to be due to lack of ISA 22 endosomolytic ability. One possible explanation for this difference could be due to the different pathways of PAA intracellular trafficking (e.g. CCV pathway; caveolae-mediated or by other routes). As PAA-mediated intracellular delivery is reliant on the polymer and toxin being present in the same endosomal compartment at a particular moment in time, it is possible that ISA 1 and ISA 4 are (at least to some extent) taking the same endocytic pathway through the cell as the toxins. Thus when endosomal breakage occurs, a toxin molecule(s) is

Table 4.3 Molar ratio of ISA 4:RTA responsible for the IC_{50} values seen figure 4.9[†]

Compound	Fixed concentration of ISA 4 (mg/mL)	Observed IC_{50} value (μg/mL)	Molar ratio ISA 4:RTA
ISA 4 + RTA	0.005	4.00	3:1
ISA 4 + RTA	0.050	2.50	56:1
ISA 4 + RTA	0.300	1.80	468:1
ISA 4 + RTA	0.500	1.00	1404:1
ISA 4 + RTA	1.000	0.40	7,023:1
ISA 4 + RTA	1.500	0.05	84,285:1
Ricin holotoxin	-	0.39	-

[†]RTA/ISA 4 combinations were then added to B16F10 cells and incubated for 67h before cell viability was assessed using the MTT assay. Molar ratios were calculated from the resultant IC_{50} values and ISA 4 concentrations assuming the Mn of ISA 4 was 10.5kDa and the Mw of RTA was 29.5kDa.

available for cytosolic delivery. In addition, ISA 1 and ISA 4 could be entering cells efficiently by absorptive endocytosis (due to their cationic charge at physiological pH) as well as the fluid-phase mechanisms of endocytosis, thus increasing the local concentration of polymer in the endosome to allow toxin delivery to the cytosol. ISA 22 however, may be entering the cell by a different endocytic pathway than the toxins or indeed less efficiently (fluid-phase endocytosis) as it is unlikely to bind to the membrane electrostatically due to its negative charge (Ferruti et al, 2000).

The cationic charge of ISA 1 and 4 may also facilitate electrostatic interactions with the negatively charged toxin molecules. Subsequent endocytosis and trafficking of the complex to the same endosomal compartment would then occur, leading to delivery of toxin to the cytosol. If PAA/toxin complexes are formed, the question is raised as to whether the whole complex is transferred to the cytosol, and if so, whether the rate of ribosomal inactivation by the toxins is altered when complexed to PAAs. Although SDS-PAGE analysis of ISA 4/RTA combinations did not prove that any complexation occurred (figure 4.4), the harsh conditions of SDS-PAGE could have caused dissociation of the complexes. Alternative methods that could have been used to assess interaction include native-PAGE, column chromatography and fluorescence microscopy. In this thesis, fluorescence microscopy was used to further investigate if PAA/toxin interaction occurs, as this method allowed visualisation of the intracellular trafficking of labelled PAA and toxin probes in B16F10 and HepG2 cells (chapter 6).

PEI has been proposed to cause endosomal membrane damage by the proton-sponge effect (Godbey et al, 1999a). Its ability to promote cytotoxicity of both RTA and gelonin toxins could however also be related to its cationic nature as hypothesised for ISA 1 and 4 (figures 4.6c, 4.7c) or as a result of PEI-mediated damage to the cell membrane due to its low IC_{50} values towards both cell lines. It was surprising that greater cytotoxicity was observed for PEI alone compared to the PEI/toxin combinations at concentrations of 0.05mg/mL and above. However this could have been due to an interaction of the PEI/toxin combination with the MTT used for assessing cell viability.

Comparing the efficacy of PAA-mediated toxin delivery with other endosomolytic systems is difficult because so few studies documenting toxin delivery have been reported (table 4.1). Lysosomotropic amines such as choroquine and ammonium chloride have been shown to enhance the effect of immunotoxins containing RTA (Casellas et al, 1984; Raso and Lawrence, 1984), but were unable to enhance

toxicity of immunotoxins based on type I ribosome-inactivating proteins (Selbo et al, 2000b). An IC_{50} value of 1 x 10^{-4}μg/mL has been documented using a liposome encapsulating a pore-forming haemolysin/gelonin combination (Stier et al, 2002). Although this value is considerably lower than the IC_{50} value achieved with the PAA/toxin combinations, it must be noted that the minimum cell viability achieved during this assay was 40%. Similarly, when the photosensitive agent aluminium phthalocyanine was combined with gelonin, cell viability only dropped to 30% (Selbo et al, 2000a). In contrast, viability of cells incubated with PAA/toxin combinations was < 3%. Therefore, it is unlikely that the levels of cytotoxicity observed for other systems are high enough to cause a significant therapeutic effect. Additionally, unlike PAAs, these systems are limited due to toxicity, immunogenicity and their unsuitability for i.v. administration (Provoda and Lee, 2000; Zelphati et al, 1996; Moret et al, 2001).

To assess the potential of using PAA/toxin combinations as a therapeutic, it was important to investigate the ability of PAAs to mediate delivery in other cell lines. As PAA-mediated transfection was demonstrated in HepG2 cells, this cell line was chosen to allow comparisons between the two models to be made. However, unlike experiments performed using B16F10 cells, all PAA/gelonin combinations tested were unable to display a high level of cytotoxicity in HepG2 cells (figure 4.8a and b). It is interesting to note that this diversity of cytotoxic response between cell lines has also been reported when photochemical agents were used to deliver a gelonin-containing immunotoxin (Selbo et al, 2000b) and was observed in transfection experiments (chapter 3) where PAA-mediated DNA delivery was demonstrated in HepG2 cells but not B16F10 cells. One explanation for this difference could be due to differential trafficking of PAAs and gelonin in HepG2 cells such that gelonin molecules do not converge in the same intracellular compartment as PAAs. Transfection experiments also demonstrated that ISA 22 was able to promote transfection to a greater extent than ISA 1 and 4, whereas in toxin delivery assays only ISA 1 and 4 were able to promote cytosolic delivery of toxins. Both DNA and toxins have very different physico-chemical characteristics, and it is likely that their interaction with PAAs and the resultant alteration in physico-chemical characteristics could affect subsequent cellular uptake and intracellular trafficking. However it is clear that in order to investigate these issues, further experiments need to be designed.

4.5 Conclusions

The experiments reported in this study demonstrate the potential of the PAAs ISA 1 and 4 as enhancers of intracellular delivery in B16F10 cells. However, the results of these experiments have raised certain questions which need to be addressed if a successful anti-cancer conjugate is to be developed. Firstly, it is crucial to understand the reasons for the inability of ISA 22 but the ability of ISA 1 and 4 to deliver toxins to the cytosol, and the cell-type dependence of toxin delivery. Both ISA 1 and 4 are cationic, and thus unlike ISA 22, they display liver tropism after i.v. administration. If ISA 22 can be synthesised to deliver toxins, it affords the possibility of designing an ISA 22-toxin conjugate that can target tumours by the EPR effect. To investigate this issue further, PAA and toxin intracellular trafficking and complex formation was evaluated in B16F10 and HepG2 cells using fluorescence microscopy (chapter 6). It was also considered necessary to see if a covalent conjugate of PAA and toxin would have the same properties as the PAA/toxin mixtures. Therefore the effect of conjugation of gelonin to ISA 1 on PAA-mediated toxin delivery was investigated (chapter 7).

Although the data here suggest again endosomolytic ability, the toxin could theoretically be introduced via an alternative route (e.g. plasma membrane) or cytotoxicity could result from an alternative pathway. To understand better the full potential of PAAs for intracytoplasmic delivery it was decided to seek direct evidence of their mechanisms of action. The following chapter reports experiments that sought direct evidence for PAA-mediated intracellular vesicle damage.

CHAPTER 5

DIRECT EVIDENCE FOR PAA-INDUCED LYSOSOMAL MEMBRANE RUPTURE

5.1 Introduction

The techniques used in the previous studies provided indirect evidence of the endosomolytic ability of PAAs (chapter 3 and chapter 4). However it was considered important to seek direct evidence for PAA-mediated endosomal disruption. Previously, the rat RBC lysis model was used to study the pH-dependence of PAA-mediated membrane breakage (Richardson et al, 1999a). Although this method is useful, there is a vast difference between the structures of the RBC membrane and intracellular vesicle membranes. RBC membranes are composed of 49% protein, 43% lipid and 8% carbohydrate by weight (Becker et al, 2000). The composition of protein in RBC cell membranes is much less than found in most other cell membranes, and is due to the simple metabolism of this cell type (Mathews and Van Holde, 1990). The major proteins in the RBC membrane are α-spectrin, β-spectrin, ankyrin, actin, and glycophorin A, B and C. These proteins form a specialised network which allow cells to temporarily deform when passing through narrow capillaries and then to return to a robust erythrocyte shape (reviewed in Discher and Carl, 2000). Much less is known about the composition of the lysosomal membrane due to the difficulty in preparing a pure lysosomal fraction. However, lysosomes do contain higher quantities of membrane proteins, which include substrate specific porters (Lloyd, 2000), the glycoproteins LAMP-1 and LAMP-2 (Chen et al, 1985) and the V-type H^+-ATPase which maintains the acidic pH of the lysosome (Becker et al, 2000).

To accurately demonstrate the effect of PAAs on intracellular membranes (endosomes/lysosomes), an isolated lysosome model was chosen. An isolated lysosomal fraction can be obtained by differential centrifugation. Differential centrifugation, developed by De Duve et al, (1955) is a mode of centrifugation in which the sample is separated into two phases: a pellet consisting of sedimented material and a supernatant. It is based on the differences in sedimentation rate of particles of different size and density. The tissue homogenate is centrifugally divided into a number of fractions by increasing (stepwise) the applied centrifugal field. The centrifugal field is chosen so that a particular type of organelle will be sedimented as a pellet, and the supernatant will be centrifuged at a higher centrifugal field for further fractionation. Differential centrifugation is probably the simplest method for the isolation of organelles from homogenized tissue. However, a limitation of the method is that a pure organelle fraction is theoretically not achievable (Dean, 1977). Hence, a marker enzyme of the desired organelle (in this case, lysosomes) must be quantitiated to follow organelle enrichment throughout the centrifugation procedure.

Over 60 hydrolytic enzymes have been discovered within the lysosomal lumen (reviewed in Barrett and Heath, 1977; reviewed in De Duve and Wattiaux, 1966), however the most common marker enzymes are NAGase (Klemm et al, 1998; Decharneux et al, 1992), acid phosphatase (De Duve, 1955), arylsulphatase (Duncan et al, 1986; Laurent et al, 1999) and β-galactosidase (Wattiaux et al, 1997). As lysosomes display structure linked latency, total enzyme activity present in a lysosomal fraction is commonly measured in the presence of the membrane disrupting detergent, triton X-100. The level of purification of a marker enzyme is usually expressed in terms of relative specific activity (RSA). This is commonly calculated by dividing the percentage distribution of NAGase by the percentage distribution of protein in each fraction (reviewed in Dean, 1977; Lopez-Saura et al, 1978; Wedge, 1991). RSA values of 4.8 (Wedge, 1991) and 9.3 (Hari et al, 1996) have been documented for the lysosomal marker enzyme NAGase obtained from the light mitochondrial fraction of rat liver.

Entry of compounds into the lysosome has been documented to occur by several mechanisms. Small molecules such as hexoses, nucleosides and several classes of amino acid can enter and leave the lysosome via specific porters in the lysosome membrane. Some substances (depending on their notional hydrogen bonding capacity) can also enter the lysosome via passive-diffusion through the lysosomal membrane (reviewed in Lloyd, 2000). The influx of certain compounds into the lysosome by either of these mechanisms can cause lysosomal disruption. Lysosomal membrane destabilisation can be quantitated because the activity of lysosomal marker enzymes towards their substrates increases if the lysosomal membrane is compromised (Wattiaux et al, 1997). This is known as free activity of the enzyme. When molecules such as α-L-amino acid esters (Goldman and Kaplan, 1973) and dipeptides (Bird and Lloyd, 1995) are incubated with an isolated lysosomal fraction, lysosomal membrane disruption was reported to occur as a result of an osmotic imbalance created by a faster influx of these molecules via porters then the efflux of their degradation products (Bird and Lloyd, 1995). Free radicals, such as those generated by the xanathine-xanathine oxidase system have also been shown to disrupt lysosomal membranes (Decharneux et al, 1992). This mechanism is thought to occur due to hydroxyl radicals inducing peroxidation of the lysosomal membranes resulting in dissipation of the proton-gradient and leakage of their enzyme contents (Mak et al, 1983).

Recently, lysosomal membrane destabilisation has been used to demonstrate the endosomolytic ability of cationic lipids (Wattiaux et al, 1997) and cationic polymers (Klemm et al, 1998). Wattiaux showed that incubation of low concentrations of DOTAP (0.005% (w/v)) with an isolated lysosomal fraction at pH 7.4 caused an increase in the free activity of the lysosomal enzyme β-galactosidase towards its substrate, methylumberlliferyl-β-galactopyranoside. Higher concentrations of DOTAP (> 0.015% (w/v)) were required to observe a significant release of β-galactosidase into the medium in unsedimentable form. This suggested that interaction of DOTAP with the lysosomal membrane at low concentration caused an increase in lysosomal membrane permeability, allowing access of the substrate into the lysosome but not permitting the enzyme to exit the lysosome. At higher lipid concentrations, disruption of the lysosomal membrane occurred allowing enzymes to escape from the lysosome. Lysosomal membrane damage was proposed to occur as a direct result of electrostatic interaction between the lipid and the lysosomal membrane, allowing fusion between lipid bilayers (Xu and Szoka, 1996; Wattiaux et al, 1997) (chapter 1, section 1.7.1.2). When DOTAP was incubated with lysosomal fractions at different pH values, free β-galactosidase activity was greater at pH 6 and 7.4 compared to free activity induced at pH 5 (Wattiaux et al, 1997).

Incubation of the cationic polymer PEI (Mw 50,000), at a concentration of 90μg/mL with isolated lysosomal fractions at pH values of 5-8 caused ~ 50% increase in the free activity of the lysosomal enzyme NAGase after 30min. In this case, the free activity caused by PEI was similar at all pH values tested (Klemm et al, 1998).

To allow a comparison of the lysosomolytic ability of PAAs with other lysosomal disruption agents (table 5.1), in this study PAAs were incubated with an isolated rat liver lysosomal fraction at pH values of 5-7 and the free activity of NAGase was measured. This lysosome disprution model measures enzyme release after interaction of substances with the outer lysosomal membrane. To assess the effect of PAAs on the inner lysosomal membrane, a second lysosome disruption model was designed. In this model, the hepatotropic PAA ISA 1 was injected intravenously into rats. Following endocytic uptake and subsequent trafficking of ISA 1 to endolysosomes, (30min), the liver was removed and an isolated lysosomal fraction obtained by differential centrifugation. Free activity of NAGase was then measured over time. In parallel, morphological studies of isolated lysosomal fractions containing PAAs was also performed using TEM. Lysosome integrity was compared to a control isolated lysosomal fraction and to a fraction incubated in the presence of triton X-100.

Table 5.1 Lysosomal membrane disrupting agents

Lysosome disrupting agent	Concentration (mg/mL)	Incubation time (min)	Free activity of lysosomal enzyme (% of total activity)	Reference
PEI	0.09	30	49	Klemm et al, 1998
DOTAP	0.04	20	78	Wattiaux et al, 1997
glucose	0.25	30	90	Decharneux et al, 1992
L-Ala-L-Ala	0.01	30	46	Bird and Lloyd, 1995
L-alanine methyl ester	0.002	10	54	Goldman and Kaplan, 1973

5.2 Methods

The PAAs used in these studies and their characteristics are shown in chapter 1, table 1.7. The protocol for the differential subcellular fractionation of rat liver is described in chapter 2 section 2.3.17. The NAGase and BCA assays are both detailed in chapter 2, sections 2.3.12-2.3.13. The assay measuring lysosomal breakage during incubation of polymers with isolated rat liver lysosomes (polymer outside lysosomes) is detailed in chapter 2 section 2.3.19.1. The assay to assess the ability of ISA 1 to destabilise rat liver lysosomes (polymer inside lysosomes) is described in chapter 2 section 2.3.19.2. The protocol for preparing ISA 1-treated lysosomes for TEM is detailed in chapter 1 section 2.3.18.1.

5.3 Results

5.3.1 Isolation of rat liver lysosomes

Following subcellular fractionation, the recovery of protein and NAGase was determined for each fraction (table 5.2). The percentage recovery of protein and NAGase (when compared to the homogenate) was found to be 99.1 and 57.0% respectively. Standard curves used to calculate these recoveries are shown in chapter 2. The total recovery of NAGase was lower than expected and was likely to be due to inhibition of the enzyme as a result of protease degradation. For the purpose of these experiments, the loss in activity was not considered to be a major limitation, but if it was essential to minimise the loss, protease inhibitors such as PMSF could be included in the homogenisation medium.

If these recoveries are assumed to approximate to 100%, any losses incurred between each fractionation step can be ignored. This allows the enrichment of lysosomes to be determined with respect to the relative specific activity of NAGase for each fraction (percentage of enzyme activity in each fraction/percentage of protein in each fraction) (Lopez-Saura et al, 1978; Wedge, 1991). Percentage distribution profiles for NAGase and protein used to calculate RSA values are shown in figure 5.1. The RSA for NAGase was subsequently plotted in the form of a histogram (figure 5.2). The light mitochondrial fraction was most enriched in the lysosomal marker NAGase having an RSA = 4.4 (table 5.3). This value agrees closely to the RSA value for NAGase documented by Wedge, (1991) of 4.8. Both these values are lower than the RSA value documented by Hari et al, (1996) of 9.3. This could be due to differences in liver homogenisation equipment and the strain of rat used.

Table 5.2 Recovery of protein and NAGase activity in rat liver fractions

Rat liver fractions	Protein (mg)	NAGase activity (μM substrate converted/min)
Nuclear	45.5	4.1
Heavy mitochondrial	6.1	4.5
Light mitochondrial	4.7	6.8
Particulate	38.4	7.3
Cytosolic	6.2	2.6
Total in Sum	100.9	25.3
Liver homogenate	101.8	44.4
Recovery (%)	99.1 ± 0.15	57.0 ± 6.58

Data represent mean ± S.D. (n=3).

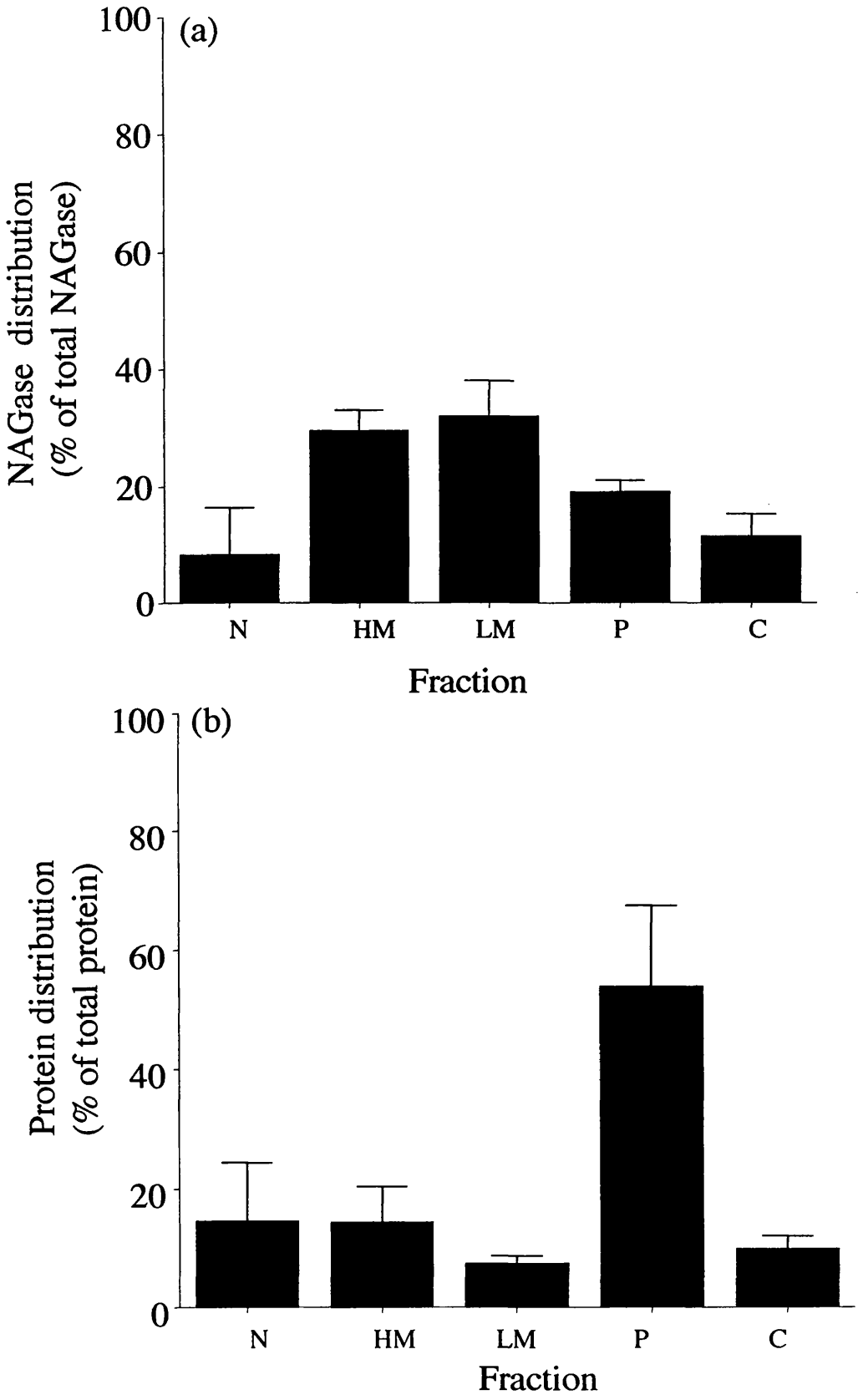

Figure 5.1 Enzyme and protein distributions of rat liver subcellular fractions. Panel (a) shows NAGase; (b) protein. Key: N = nuclear; HM = heavy mitochondrial; LM = light mitochondrial; P = particulate; C = cytosolic. Data represent mean ± S.D. (n=3)

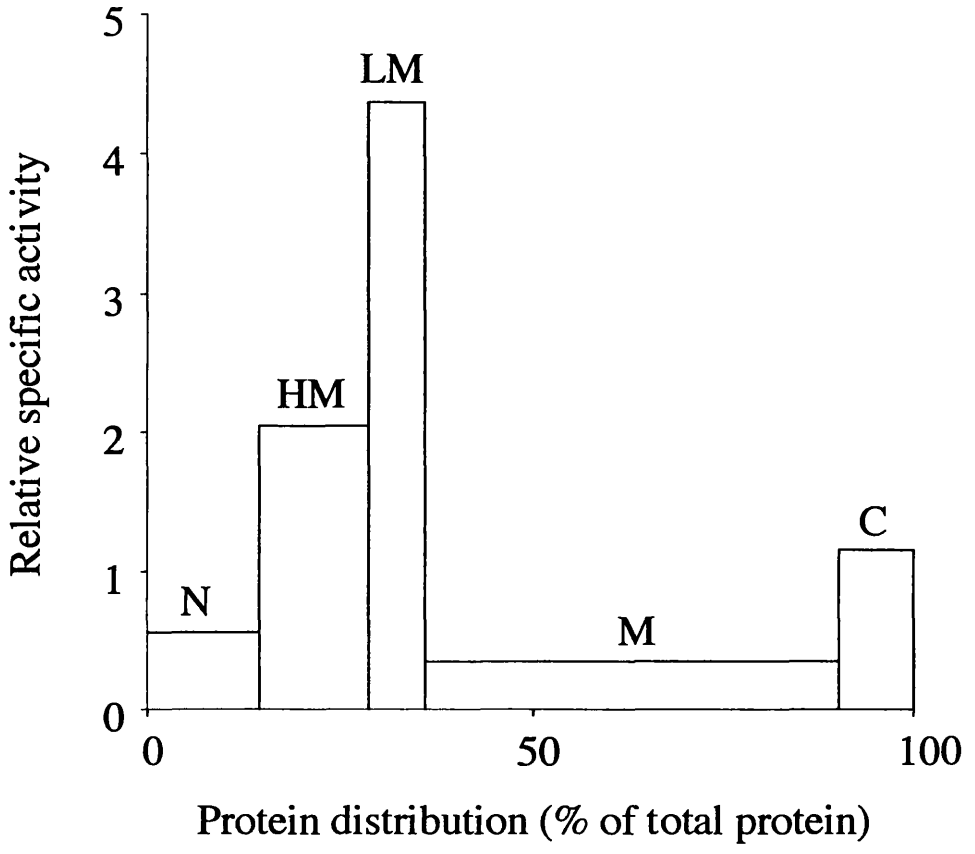

Figure 5.2 Subcellular distribution of NAGase in rat liver subcellular fractions. Fractions are represented by blocks. The lengths of the blocks is proportional to the protein content of the fractions; their height is the RSA. RSA values were calculated by dividing the percentage distribution of NAGase by the percentage distribution of protein in each fraction. (Wedge, 1991 Lopez-Saura et al, 1978). Key: N = nulear; HM = heavy mitochondrial; LM = light mitochondrial; P = particulate; C = cytosolic.

Table 5.3 The RSA of NAGase in rat liver fractions[†]

Rat liver fractions	RSA
Liver homogenate	1.0
Nuclear	0.6
Heavy mitochondrial	2.1
Light mitochondrial	4.4
Particulate	0.4
Cytosolic	1.2

[†]The RSA of NAGase in each fraction was calculated by dividing the fractional percentage distribution of NAGase by the fractional percentage distribution of protein in each fraction. Data represent mean ± S.D. (n=3).

The cytosolic fraction had the third greatest RSA value (1.2), which was almost certainly due to lysosomal breakage that occurred during the subcellular fractionation procedure, which led to premature NAGase release in to the medium.

5.3.2 Evaluation of the pH-, time- and concentration dependence of lysosomal rupture caused by polymers incubated with isolated rat liver lysosomes (polymer outside the lysosome)

Neither ISA 1 nor ISA 23 caused significant release of NAGase compared to the saline control when incubated with isolated lysosomes in 250mM sucrose at both 30min and 1h at all pH values tested (figure 5.3a and b). PEI did accelerate NAGase release in a time- and pH-dependent manner (figure 5.3c). After 30min, NAGase release at pH 5 and 6.5 was approximately 2.5-fold greater than seen in the control. At pH 7.4 however, only a 1.5-fold greater NAGase release was seen compared to the control. This pH-dependent effect was more pronounced after 1h. In this case, PEI-mediated NAGase release was 3-fold greater at pH 5 and 6.5 compared to the control.

To see whether higher concentrations of ISA 1 would increase NAGase release, the isolated lysosomes were incubated with ISA 1 over the concentration range 0-2mg/mL. Even under these conditions NAGase release was not significantly different from that observed for the controls ($\leq$ 20% release) (figure 5.4).

5.3.3 Evaluation of lysosomal stability after internalisation of ISA 1: Time- and dose-dependency (polymer inside the lysosomes)

After i.v. injection of ISA 1 it targets to the liver (Richardson et al, 1999a) and during the 30min following injection it is endocytosed and localises in the liver lysosomes. When these lysosomes (containing ISA 1) were isolated and incubated in 250mM sucrose, NAGase release was measured. ISA 1 caused a time- and dose-dependent increase in NAGase liberation at doses of 25-50mg/kg (figure 5.5). At the highest dose nearly a 3-fold increase in NAGase release (30%) was observed after 120min compared to the control.

5.3.4 TEM of lysosomes containing ISA 1

Lysosomes isolated in the light mitochondrial fraction were typically dark, densely staining vesicles of diameter ~ 0.8-1.2μm (figure 5.6a and c) consistent with the documented lysosomal size range of between 0.5-2μm diameter (Pratten et al, 1980). In

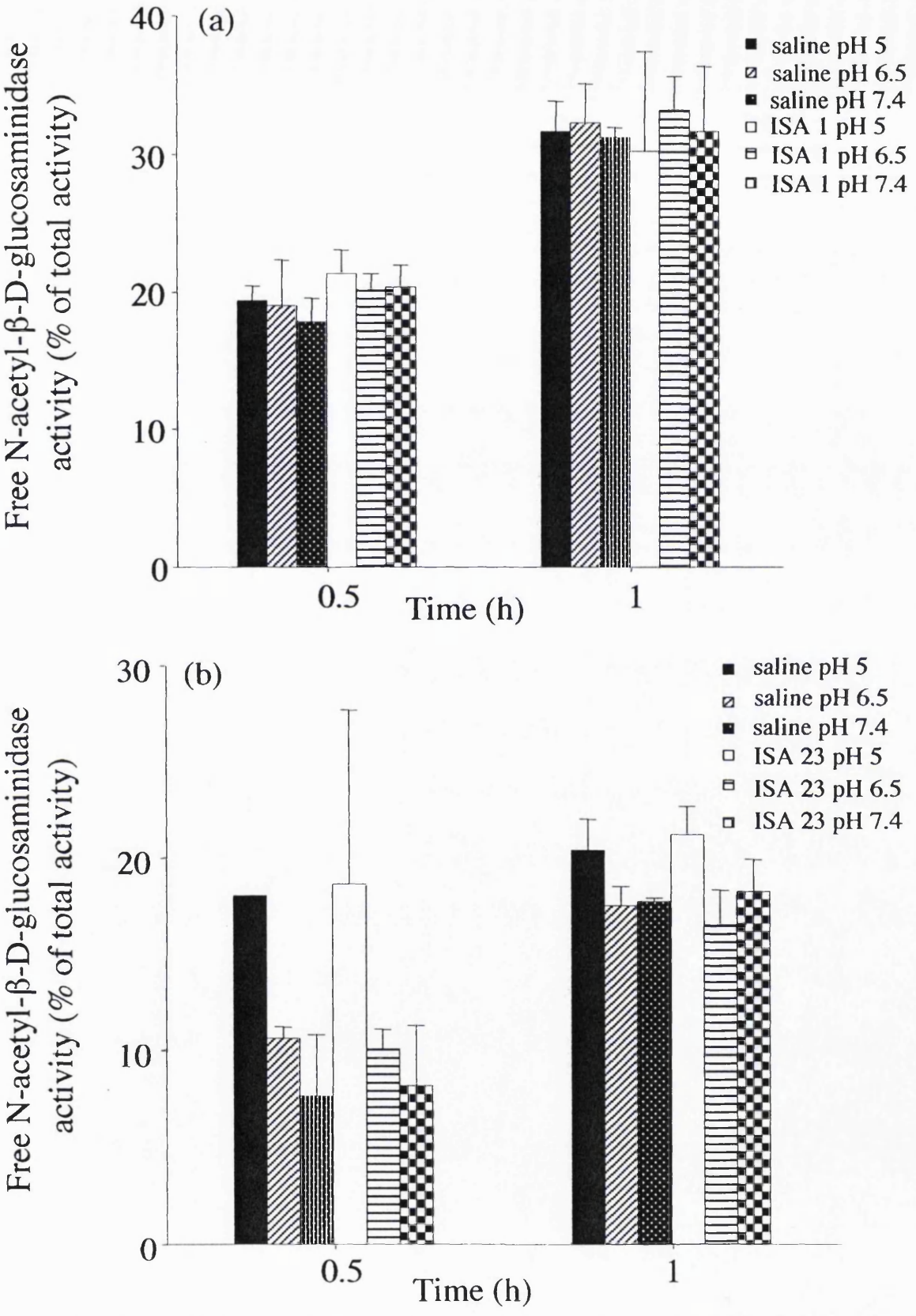

Figure 5.3 Release of NAGase from isolated rat liver lysosomes at 0.5 and 1h incubated in 0.25M sucrose with various polymers (0.5mg/mL). The effect of incubation at pH 5, 6.5 and 7.4 is also shown. Panel (a) shows ISA 1; (b) ISA 23; (c) PEI. Enzyme activities are expressed in arbitrary fluorescence units. Data represent mean ± S.D. (n=3)

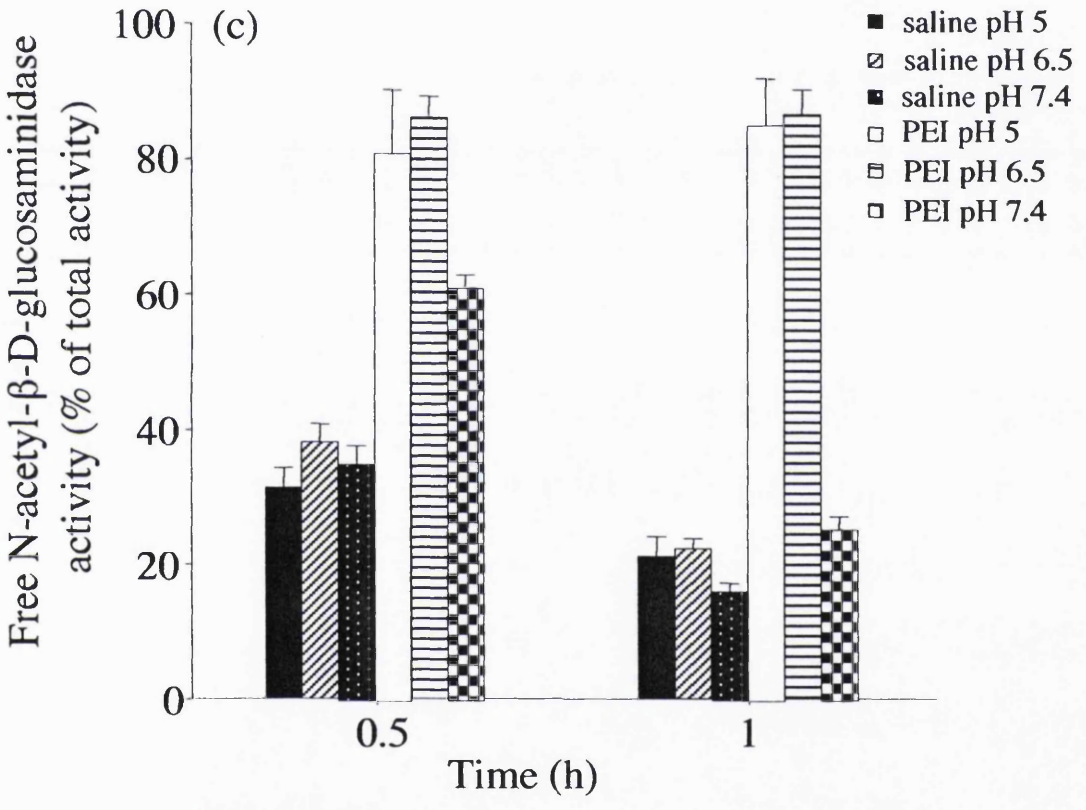

Figure 5.3 Cont.

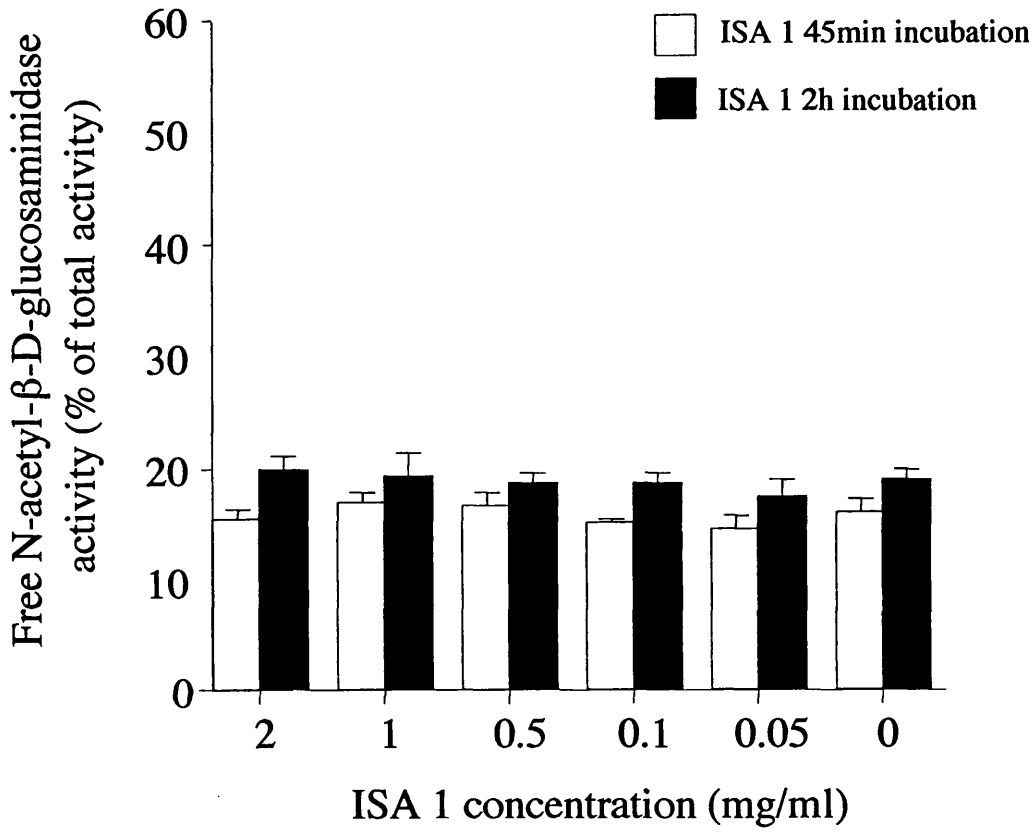

Figure 5.4 Effect of ISA 1 concentration on the release of NAGase from isolated rat liver lysosomes at pH 5. Polymer was incubated with lysosomes for either 45min or 2h. Enzyme activities are expressed in arbitrary fluorescence units. Data represent mean ± S.D. (n=3)

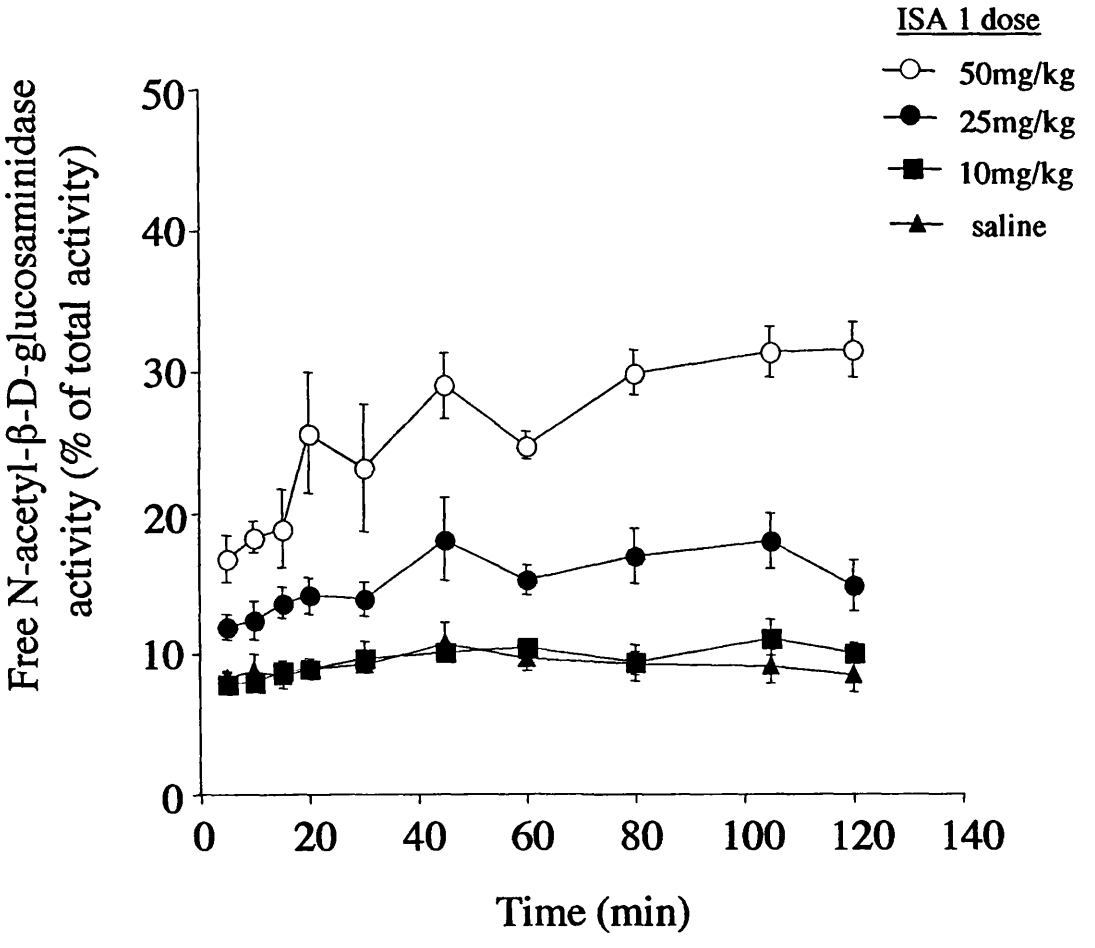

Figure 5.5 Effect of endocytically internalised ISA 1 on the release of NAGase from isolated rat liver lysosomes. ISA 1 (at the doses shown) was administered i.v. and the liver removed after 30min and subject to subcellular fractionation. Release of NAGase from the lysosomes in the light mitochondrial fraction was then measured over time. Enzyme activities are expressed in arbitrary fluorescence units. Data represent mean ± S.D. (n=3)

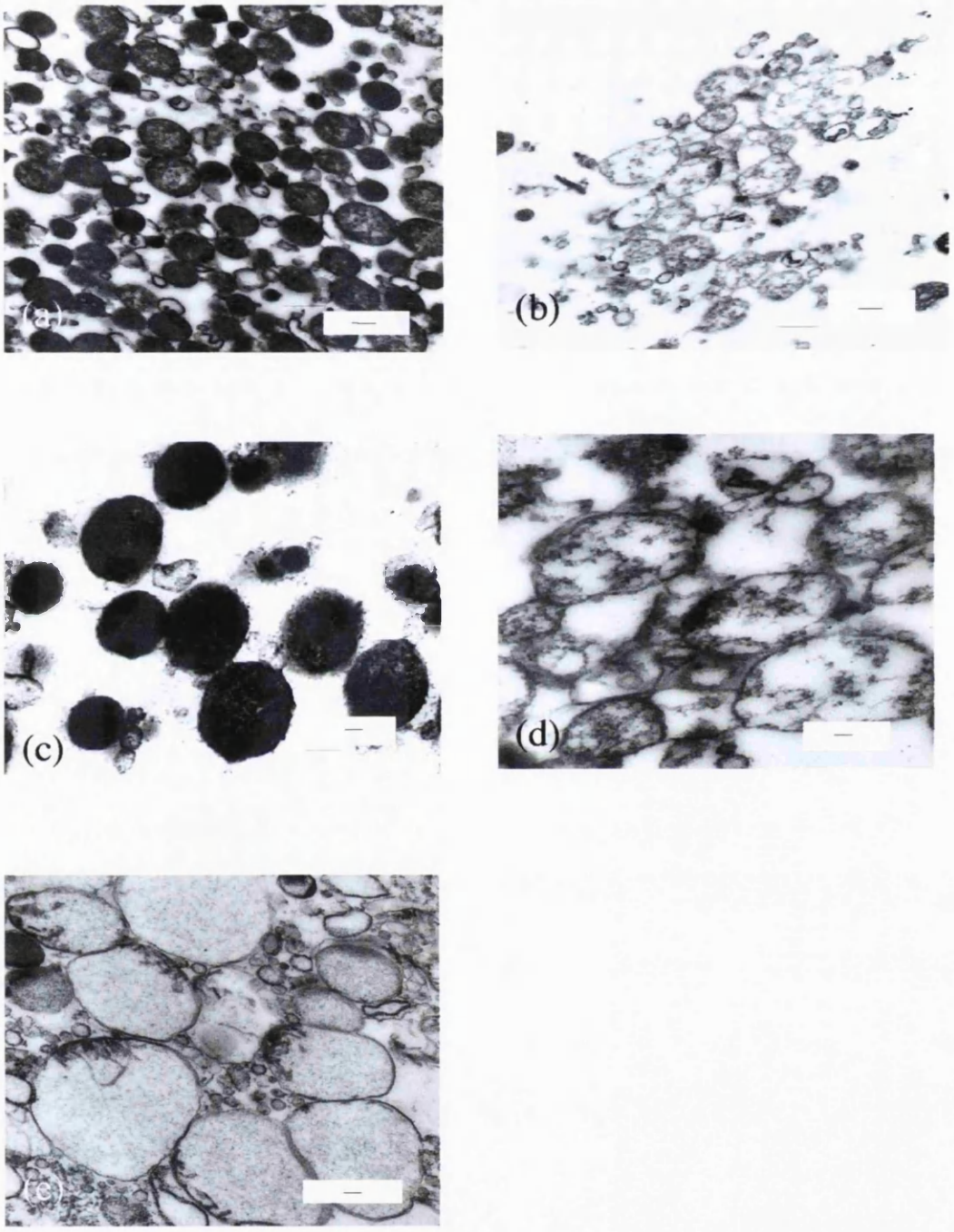

Figure 5.6 TEM of isolated lysosomes with and without ISA 1 in their interior. Panel (a) saline (size bar 1μm); (b) 25mg/kg ISA 1 (size bar 1μm); (c) saline (size bar 300nm); (d) 25mg/kg ISA 1 (size bar 300nm). (e) Lysosomes isolated and incubated in 0.1% triton X-100 (w/v) in 250mM sucrose for 1h (size bar 300nm). (Pattrick et al, 2002).

contrast, the vesicular fraction obtained after i.v. administration of 25mg/kg ISA 1 had a different morphology. They were no longer densely staining (figure 5.6b and d), and in some cases their lumen looked completely empty. For the positive control, isolated lysosomes were incubated in the presence of triton X-100 (0.2% (w/v)) in order to destabilise their membranes. ISA 1-containing lysosomes had a similar appearance to the triton X-100 treated lysosomes (figure 5.6e) and to lysosomes treated with a free radical generating system that is documented to disrupt lysosomes (Decharneux et al, 1992), (figure 5.7).

5.4 Discussion

A lysosome-rich fraction from rat liver normally exhibits latency with respect to enzyme activity in the range 10-20% of the total activity in that fraction (Goldman and Kaplan, 1973). However when saline controls were incubated with the light mitochondrial fraction, NAGase release was variable and in some cases > 20% was detected (figures 5.3a-c). These variable levels may have resulted from lysosome instability after their addition to 250mM sucrose at different pH values and due to premature lysosomal breakage incurred during the fractionation procedure.

NAGase release caused by PEI (0.5mg/mL) at pH values of 5.0 and 6.5 (when incubated on the outside of lysosomal membranes) showed substantial NAGase release ($\geq$ 80%) after 30min and 1h. In contrast NAGase release caused by ISA 22 (0.5mg/ml) (figure 5.3b) and ISA 1 (0-2mg/mL) (figure 5.4) (when incubated on the outside of lysosomal membranes) at pH values 5.0-7.4 was not significantly different to the controls. The ability of PEI to cause lysosomal membrane breakage in a pH-dependent manner was surprising since experiments performed by Klemm et al, (1998) (described in the introduction to this chapter) demonstrated that although PEI caused lysosomal membrane perturbation, this did not occur in a pH-dependent manner. Although the concentration of PEI used by Klemm (90μg/mL) was much lower than the concentration of PEI used in this study (0.5mg/mL), a correlation between both sets of results was still expected. The protonation level of PEI increases from 20-45% between pH values of 7 and 5 (Remy et al, 1998). Therefore the increased membrane breakage at pH values of 5 and 6 could be due to the increased cationic nature of PEI. A second possibility for the increased free activity of NAGase when incubated with PEI at low pH values is due to the increased activity of NAGase at low pH values. As this enzyme is lysosomal, its pH optimum has been reported to be in the pH range 4.5-6.0 (Barrett and Heath, 1977).

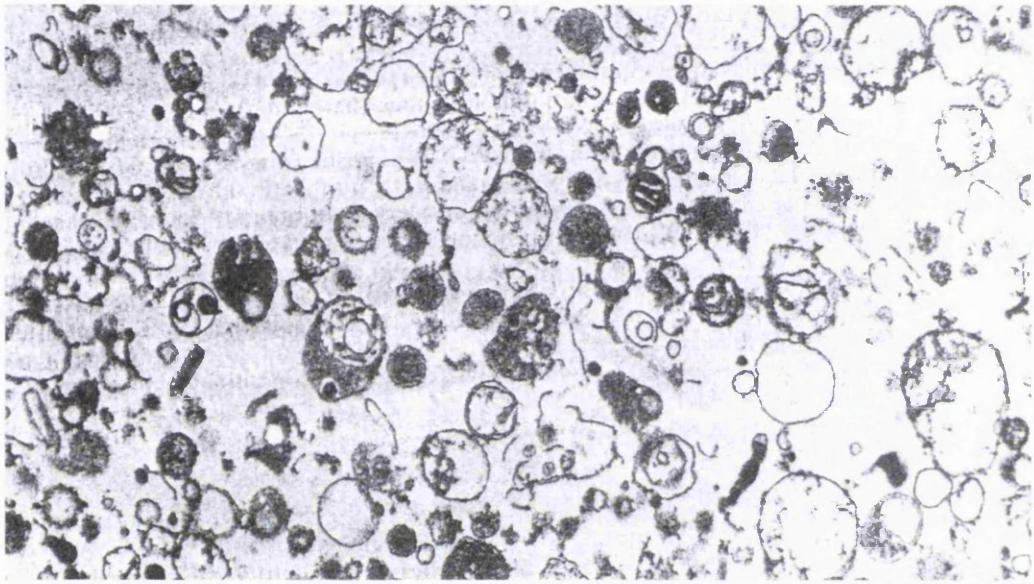

Figure 5.7 Morphology of lysosomes after incubation in the presence of the free radical generating system (xanathine-xanathine oxidase) (from Decharneux et al, 1992).

No correlation was found between the RBC lysis model for membrane disruption and the lysosomal membrane disruption model (polymer on outside) demonstrated in this study. When PEI (1mg/mL) was incubated with isolated RBCs at pH values of 5.5, 6.5 and 7.4, lysis of RBCs was not pH-dependent (Wan et al, 2002). However ISA 23, which was previously shown to lyse RBCs at pH 5.5 and 6.5 but not at pH 7.4 (Richardson et al, 1999a), was unable to cause NAGase release in a pH-dependent manner. A specific reason for this was not determined, however, as lysosomal membranes have a very different morphology to RBCs (discussed in the introduction to this chapter), polymer interaction with the outer lysosomal membrane could be very different to their interaction with a RBC membrane.

This model describes polymer interaction with the outer lysosomal membrane, which is effectively the wrong face of the membrane. The physiological model assesses the effect of incubating polymers with the inner lysosomal bilayer, after their endocytic uptake and subsequent trafficking to lysosomes. As NAGase release was shown quantitatively to occur using this method (figure 5.5), it is possible that PAAs preferentially interact with the inner lysosomal bilayer compared to the cytoplasmic-facing lysosomal membrane. Lysosomal membrane perturbation may also have been observed with this model due to a higher concentration of ISA 1 inside the lysosome than the model describing polymer interaction with the outer lysosomal membrane. Endocytosis of ISA 1 causes its continuous delivery to the lysosomal compartment, thus it will be increasingly concentrated on this internal surface. This theory has also been proposed by Klemm et al, (1998) to explain the differences in PEI concentration required to cause efficient lysosomal membrane destabilisation and gene transfection. Transfection efficiency was reported to be maximal at PEI concentrations of 2.5μg/mL. In these transfection experiments PEI was endocytosed, and therefore would be concentrated in intracellular compartments. However, when PEI was incubated with the outer lysosomal membrane, PEI concentrations ~ 20 times greater were required to cause significant NAGase release (Klemm et al, 1998).

A marked change in the morphology of lysosomes containing ISA 1 compared to control lysosomes was observed from TEM studies (figure 5.6). This also suggested that the inner lysosomal bilayer was compromised by ISA 1 to allow release of the densely staining lysosomal contents out of the lysosome. Further evidence for the ability of PAAs to disrupt lysosomes after their endocytic uptake was demonstrated when 10mg/kg ^{125}I-labelled ISA 4 was administered i.v. to rats. At different times post-injection differential subcellular fractionation was performed on the removed liver.

60min post-injection, ~ 20% radioactivity was found in the cytosolic fraction, compared to < 10% 30min post-injection. The appearance of the polymer in the cytosolic fraction was also accompanied by an increase in NAGase in this fraction (~ 15%). These experiments suggested that endocytosed ISA 4 was able to destabilise lysosomal membranes leading to release of ISA 4 and NAGase into the surrounding medium (Richardson, 1999c; Pattrick et al, 2002).

After endocytic uptake of ISA 1 (25mg/kg), vesicles were observed by TEM without densely staining lumen. This again suggested their membranes were destabilised by ISA 1.

It is essential that any non-viral vector developed for i.v. administration should not cause toxicity to normal cell membranes or cause breakage of the lysosomal membrane following endocytic uptake. Excess lysosomal damage leads to cell death due to the degradative action of lysosomal enzymes released into the cell cytosol (Ichihara et al, 1991). Indeed, substantial polymer-mediated cytotoxicity was observed when PEI (Mw 25,000) was incubated *in vitro* with 293T cells after 2h (IC_{50} 7μg/mL) (Lee et al, 2001). PAAs, however, are relatively non-toxic to cells *in vitro* (IC_{50} > 2mg/mL, Ranucci et al, 1991), and doses up to 100mg/kg ISA 4 administered *in vivo* have shown no toxicity. Therefore, taken together with the indirect evidence for PAA-mediated endosomolytic ability discussed in chapters 3 and 4, it is likely that PAAs are mediating both endosomal- and lysosomal- membrane perturbation.

5.5 Conclusions

Although the PAAs ISA 1 and 23 did not to cause lysosomal rupture when incubated on the cytoplasmic face of the lysosomal membrane, these experiments indicated PAA-mediated lysosomal membrane perturbation after internalisation into rat liver lysosomes following administration of doses > 10mg/kg. The mechanism(s) responsible for polymer-mediated lysosomal membrane and endosomal membrane destabilisation must be characterised. The endosomal and lysosomal membranes have common origins although they are different in composition. Therefore to continue these studies further it is necessary to isolate endosomes and determine how PAAs interact with them.

In order to move the development of PAA-toxin conjugates into clinical development, it was important to further investigate the intracellular trafficking of PAAs alone and in combination with the plant toxin gelonin. In the next chapter the

synthesis and visualisation of fluorescent-labelled PAAs and gelonin after endocytic uptake is described.

CHAPTER 6

SYNTHESIS AND CHARACTERISATION OF FLUORESCENT-LABELLED PAA AND GELONIN CONJUGATES AND VISUALISATION OF THEIR ENDOCYTIC CAPTURE

6.1 Introduction

In chapter 4 it was shown that ISA 1 and 4 promote RTA and gelonin delivery into the cytosol of B16F10 cells causing cytotoxicity (Pattrick et al, 2001). However these experiments also raised certain questions. Why were ISA 22 and ISA 23 unable to mediate toxin delivery in B16F10 cells when these PAAs promoted transfection (Richardson et al, 2001)? Also, why did all the PAAs fail to promote toxin delivery in HepG2 cells? To investigate these questions further and to study the endocytosis of PAAs and toxins in different cell types, it was decided to prepare fluorescent derivatives of these compounds for fluorescence microscopy.

Fluorescence microscopy has been widely used to study intracellular trafficking and the approach is advantageous as different fluorophores can be used to label the carrier and its payload (table 6.1). For example, in a recent study by Merdan et al, (2002a), PEI and its macromolecular payload, a 37-mer ribozyme, were labelled with the fluorescent dyes oregon green 488 (OG) (green) and rhodamine (red) respectively. Colocalisation (localisation of both carrier and payload in the same spatial compartment) of PEI (2.2μg) and ribozymes (2μg) was observed in vesicles of SW13 cells (as indicated by a yellow fluorescence). In some instances, (> 20min incubation), vesicles were shown to swell and burst, leading to release of PEI-OG throughout the cell. These experiments provided evidence for the proton-sponge mechanism of PEI-mediated membrane rupture. However it was not known at which stage of the endocytic pathway the vesicles were bursting (Merdan et al, 2002a).

In another study, the cellular uptake of OG-labelled PAMAM dendrimer (20μg/mL)/TAMRA-labelled oligonucleotide (0.25M) complexes was investigated in HeLa cells. Accumulation of PAMAM-oligonucleotide complexes was detected in cell nuclei post-internalisation (1h), although a substantial amount of material also remained bound at other sites in the cell, presumably the plasma membrane and endomembrane compartments (Yoo and Juliano, 2000).

To allow visualisation of the intracellular trafficking of PAAs, a fluorescent dye had to be chosen for conjugation. The choice of fluorescent probe is important. Fluorescence output of the typically used probes are affected by many factors including local pH, conjugation to molecules and prolonged exposure to visible light (Haugland, 1999). For example, the green dye FITC (ex 494nm; em 519nm) displays an excellent fluorescence quantum yield and good water solubility, but it has disadvantages of a relatively high rate of photobleaching and quenching after conjugation to proteins. This limits the use of FITC in certain applications. As many optical filter sets have been

Table 6.1 Studies which have used fluorescent-labelled endosomolytic carriers (and/or their macromolecular payload) to study intracellular trafficking

Endosomolytic delivery system	Macromolecular payload	Cell line	Reference
PEI-oregon green	DNA-rhodamine	EA.hy 926	Godbey et al, 1999b
pH-sensitive liposomes	Albumin-FITC	Rat peritoneal macrophages	Tachibana et al, 1998
Generation 5 PAMAM dendrimer-oregon green	DNA-TAMRA	HeLa	Yoo and Juliano, 2000
PEI-FITC	DNA-YOYO-1	L929	Rémy-Kristensen et al, 2001
p(DMAEMA)	DNA-Ethd-1	OVCAR-3	Zuidam et al, 2000
PEI-oregon green	Ribozyme-rhodamine	SW13	Merdan et al, 2002a

optimised to efficiently excite and detect the fluorescence of FITC, alternative fluorophores have been designed to replicate its fluorescence spectrum. One such compound, OG, was chosen as the probe for attachment to PAAs in these studies. OG was selected as it has nearly an identical absorption and emission spectra with FITC (ex. 495nm; em. 521nm), is more photostable, and displays reduced conjugation-dependent quenching (Haugland, 1999).

OG is available in N-hydroxysuccinimide ester (OG-SE) form, to allow simple conjugation to molecules containing a terminal amine group (figure 6.1). To allow conjugation of OG-SE to PAAs, PAA-NH_2 polymers were previously synthesised (Malgesini et al, 2002). ISA 23-NH_2 and ISA 1-NH_2 were obtained by polyaddition of N-trimethyl-mono-substituted 1,2-diaminoethane to 2,2-bis-acrylamido-acetic acid or 1,4-bis-acryloyl-piperazine respectively. The reaction mixture was maintained for 3 days at r.t. under a nitrogen atmosphere. The resulting viscous solution was then diluted with water to give a white precipitate after filtration. Subsequent removal of the protecting triphenylmethyl group was performed by treating the polymers with aqueous HCl (39% (v/v)). The product was finally isolated by ultrafiltration through a membrane with a nominal cut-off of 10,000Da, and recovering by lyophilisation the portion retained by the membrane. PAA-NH_2 polymers were characterised by ^{1}H-NMR and ^{13}C-spectroscopy, intrinsic viscosity measurements and GPC. The conjugation reaction of OG-SE to ISA 23-NH_2 and ISA 1-NH_2 is shown in figures 6.2a and b. This chemistry forms a stable amide bond which is important as the fluorescent dye should not then be liberated into the cell (Hermanson, 1996).

To see if PAA-OG probes were internalised by endocytosis and transferred to acidic intracellular vesicles in B16F10 and HepG2 cells, PAA-OG uptake experiments were conducted in combination with a marker of acidic vesicles, lysotracker red (ex 577nm; em 590nm) (figure 6.3). The two dyes could be followed simultaneously since the red fluorescence of lysotracker red had very little spectral overlap with the green fluorescence of OG. Lysotracker red comprises a weakly basic amine, partially protonated at neutral pH, linked to a fluorescent probe which freely diffuses through cell membranes and selectively accumulates in endosomes and lysosomes. Its mechanism of retention has not been firmly established but is likely to involve protonation at acidic pH and retention in the organelles' membranes (Haugland, 1999).

In order to visualise the intracellular fate of gelonin in combination with PAA probes, it was also necessary to conjugate a fluorescent dye to gelonin. As with lysotracker red, it was important that the dye chosen had minimal spectral overlap with

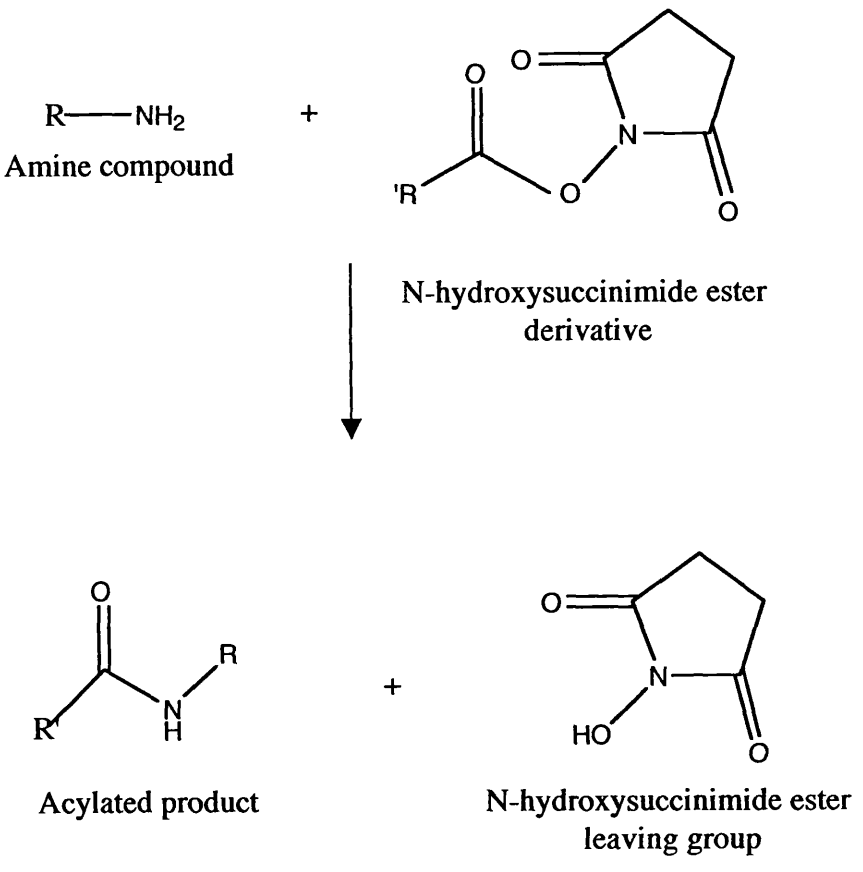

Figure 6.1 Reaction of N-hydroxysuccinimide esters with nucleophiles.

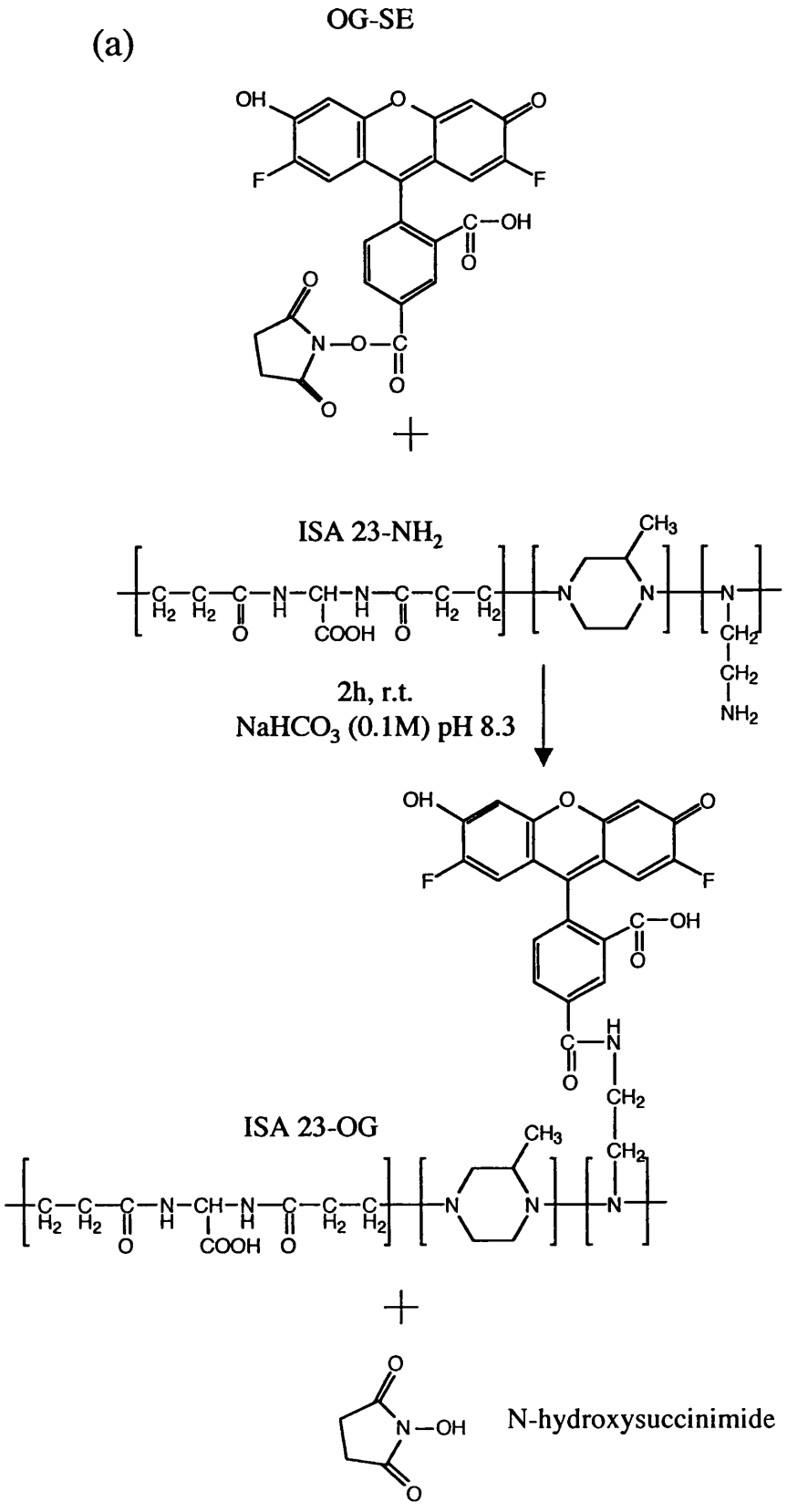

Figure 6.2 Typical reaction of OG-SE with PAAs containing a terminal NH_2 group. Panel (a) shows ISA 23-NH_2 (Mw 22,700; Mn 11,500); (b) ISA 1-NH_2 (Mw 16,700; Mn 9,800).

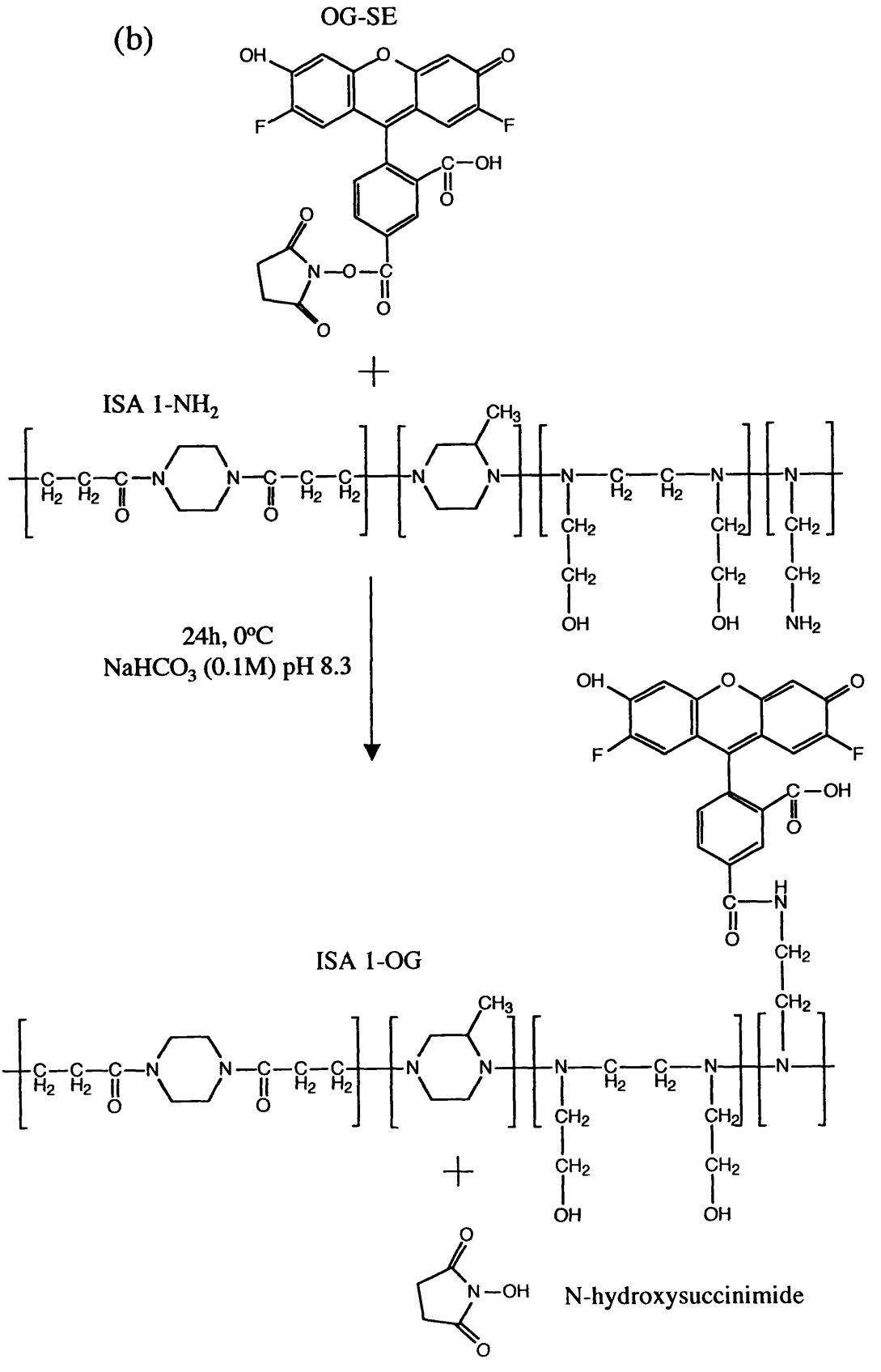

Figure 6.2 Cont.

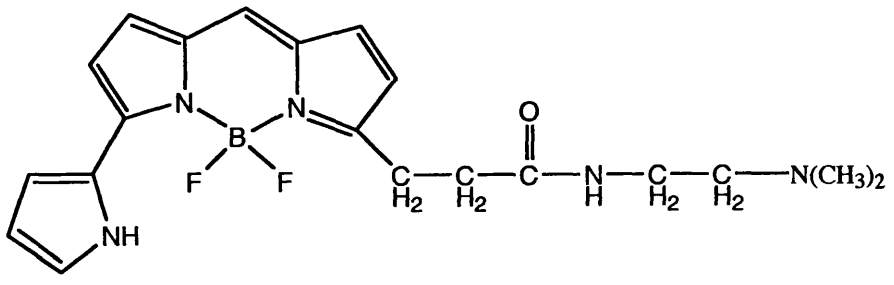

Figure 6.3 Structure of lysotracker red

OG to allow both PAA-OG conjugates and the fluorecent-labelled gelonin to be co-incubated with cells and visualised. The dye chosen for conjugation to gelonin was texas red (TR). This is a longer wavelength dye (ex 583nm; em 603nm), which is amongst the most photostable fluorescent labelling agents, is not affected by changes in pH between 4 and 10 and its conjugates are brighter giving a lower background than other commonly used fluorescent dyes (Haugland, 1999). TR is available in succinimidyl ester form (Mw 816.94) and therefore it can be conjugated to gelonin (figure 6.4).

6.2 Methods

PAA-NH_2 polymers used in these studies and their characteristics are shown in figure 6.2a and b.

PAA-OG probes and gelonin-TR were synthesised and the fluorescent-labelled conjugates were then purified on a PD10 G-25 sephadex column. The purity of PAA-OG and gelonin-TR fractions eluted from the PD10 column was then checked using TLC analysis. Once free OG-SE could no longer be detected, PAA-OG probes were lyophilised. In order to characterise the fluorescent-labelled conjugates, excitation and emission spectra were measured and compared to the free dyes OG-SE and TR-SE respectively. These techniques are all described in chapter 2, section 2.3.9. A calibration curve of OG-SE concentration against fluorescence units was then constructed to determine the labelling efficiency of OG to PAAs. This is described in chapter 2, section 2.3.9.1. In order to visualise the uptake of PAA-OG conjugates with lysotracker red or gelonin-TR, cell uptake experiments were performed in B16F10 or HepG2 cells after 5h or 24h. Cells were then fixed and processed for fluorescence microscopy. These experiments are detailed in chapter 2, section 2.3.9.2.

6.3 Results

6.3.1 Purification and characterisation of fluorescent-labelled conjugates

To evaluate the amount of OG conjugated to ISA 1-NH_2 and ISA 23-NH_2, it was first necessary to construct a calibration curve for OG-SE concentration against fluorescence intensity (figure 6.5a and b). This was performed in the solvent buffer ($NaHCO_3$), to determine OG concentration in the crude reaction mixture, and in PBS to determine OG concentration after elution of the crude reaction mixture on a PD10 column. In order to use these curves to determine OG-labelling efficiency, it was assumed that the OG fluorescence spectrum did not change after conjugation. It should

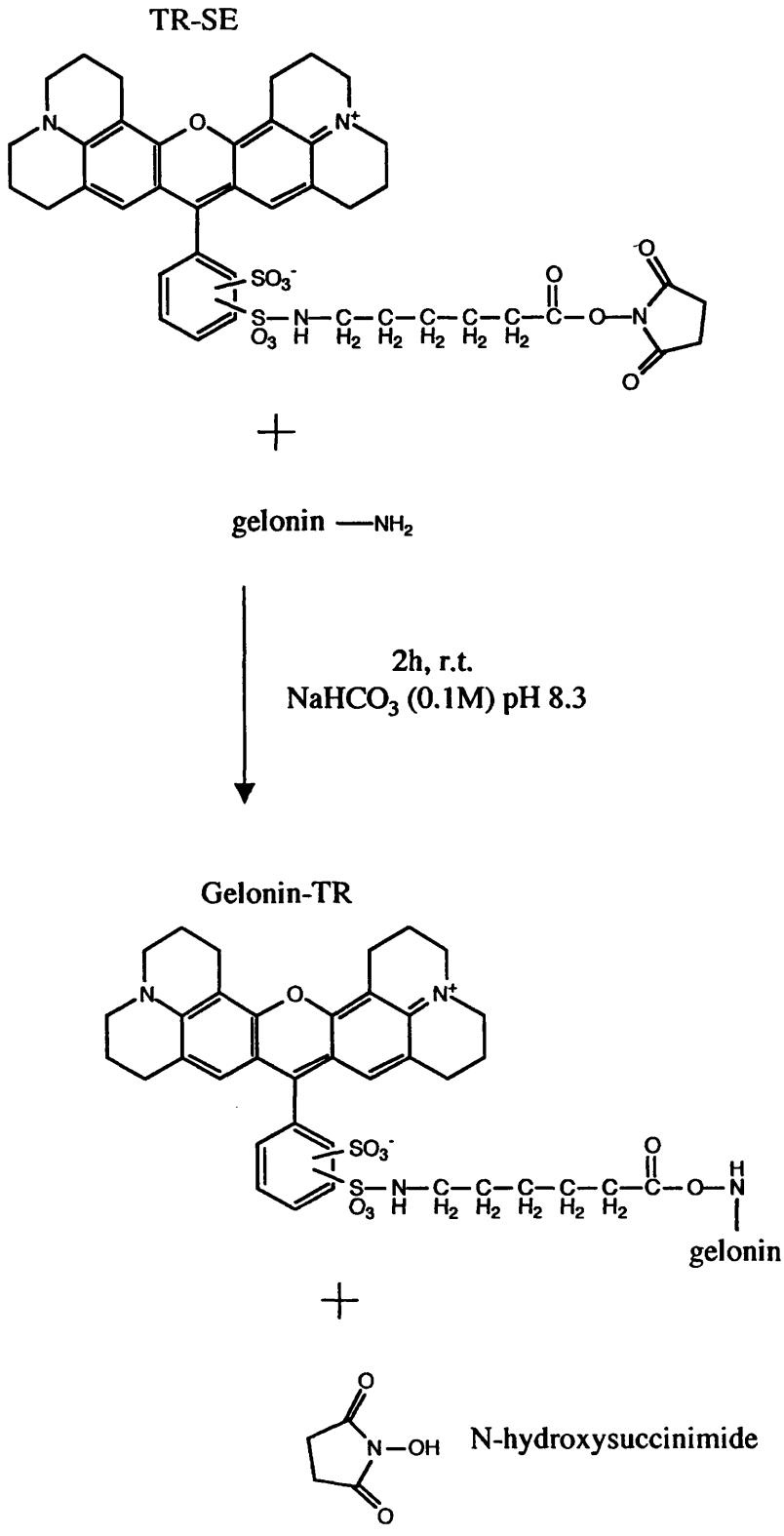

Figure 6.4 Conjugation reaction of TR-SE with gelonin

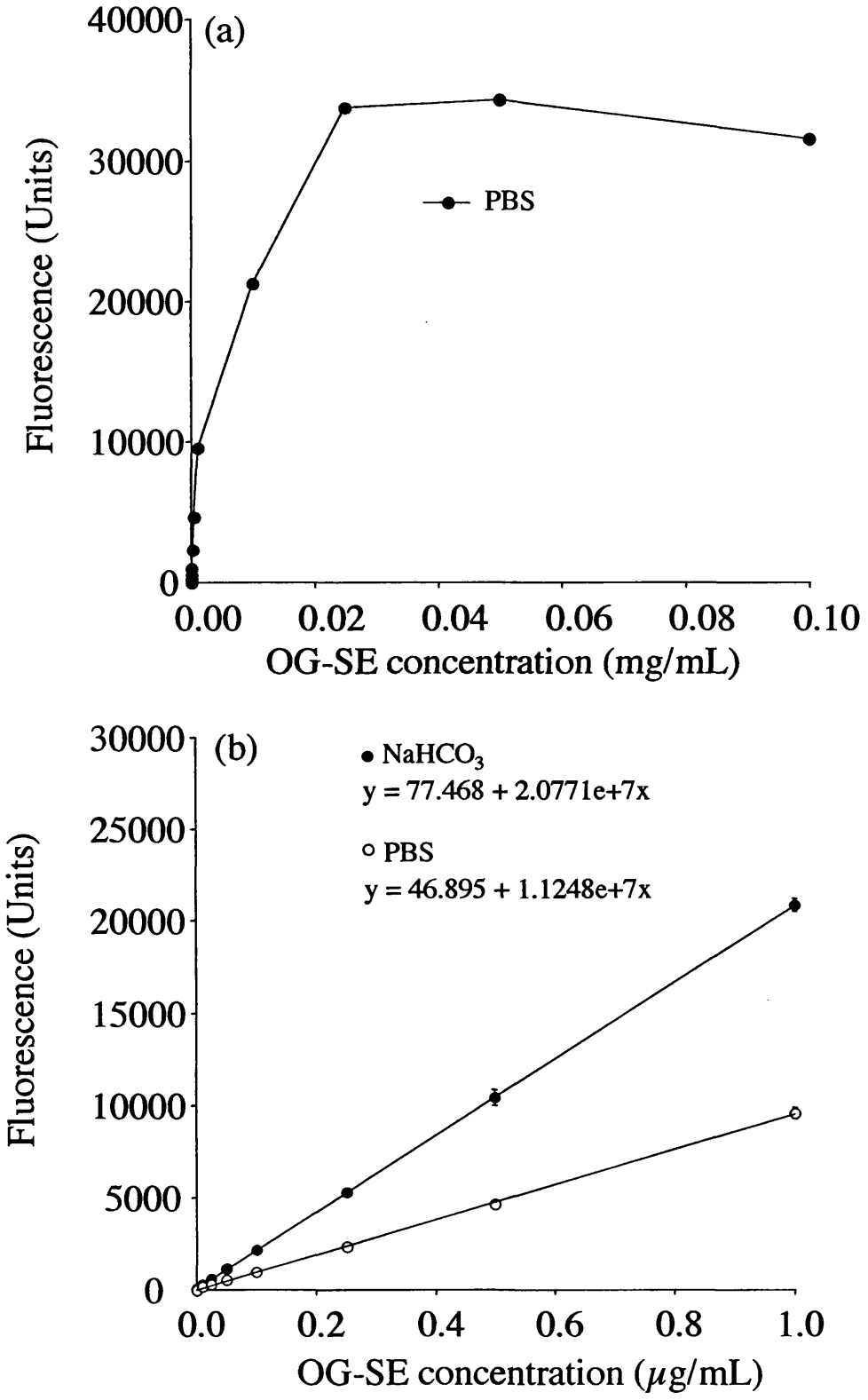

Figure 6.5 Calibration curves showing the effect of OG-SE concentration on fluorescence intensity. Panel (a) shows the fluorescence of OG solutions (0-0.1mg/mL) made up in PBS; (b) fluorescence of OG solutions (0-1μg/mL) made up in $NaHCO_3$ buffer pH 8.3, or PBS. Data represent mean ± S.D. (n=3).

be noted that quenching of OG-SE fluorescence occurred at dye concentrations > 5μg/mL (figure 6.5a). Within the linear portion of the graph (0-1.0μg/mL), fluorescence intensity observed at specific OG-SE concentrations was higher with $NaHCO_3$ buffer (pH 8.3), than PBS (pH 7.4) (figure 6.5b).

A 1:1 molar ratio of OG fluorophore:ISA 23 and ISA 1-pendant amine group was used in the conjugation reactions. A 1:1 molar ratio of TR fluorophore:gelonin would have required 18.1mg gelonin. However only 1mg of gelonin was subsequently used for the conjugation reaction due to the expense of gelonin and therefore the quantity of TR used was in great excess. Separation of macromolecular fluorescent-labelled conjugates (ISA 23-OG, ISA 1-OG, gelonin-TR) and unlabelled compounds (ISA 23, ISA 1, gelonin) from the reaction product N-hydroxsuccinimide and unreacted free dyes (OG-SE and TR-SE) was performed using GPC with PD10 G-25 sephadex columns. This system contains two phases: one stationary and one mobile. The stationary phase consists of dextran that has been polymerised with epichlorohydrin to form porous beads (size 50-150μm). The mobile phase consists of a buffer. The separation depends on the ability of molecules to enter the pores. Smaller molecules can diffuse into the beads and move more slowly down the column. Molecules are therefore eluted in order of decreasing molecular size. By varying the degree of cross-linking the gels are optimised for different molecular weight ranges. G-25 sephadex columns are optimised to separate molecules of 1,000-5,000Mw (Meloan, 1999).

In order to calibrate the PD10 column, the void volume (V_o) was determined by passing high Mw blue dextran through the column after its equilibration in PBS. OG-SE and TR-SE were then passed through the columns to determine the elution volume of the free dye (chapter 2, figure 2.5). After the PD10 columns were calibrated, the crude mixtures resulting from the conjugation reactions were passed through the columns. A distinct peak eluted between fractions 6-12 was observed from the elution profile of the ISA 23-NH_2 and OG-SE reaction (figure 6.6a). As this peak occurred at the same elution volume as V_o, it corresponded to macromolecular ISA 23-OG. Free OG-SE was determined to be 7%. The labelling efficiency of ISA 23-OG was thus determined to be 93%.

The elution profile resulting from the ISA 1-NH_2 and OG-SE conjugation reaction displayed two unresolved peaks. The first peak which eluted at V_o corresponded to ISA 1-OG (fractions 4-15), and the second peak eluted at the elution volume of free OG-SE (fractions 16-35) (figure 6.6b). Free OG-SE from this peak was

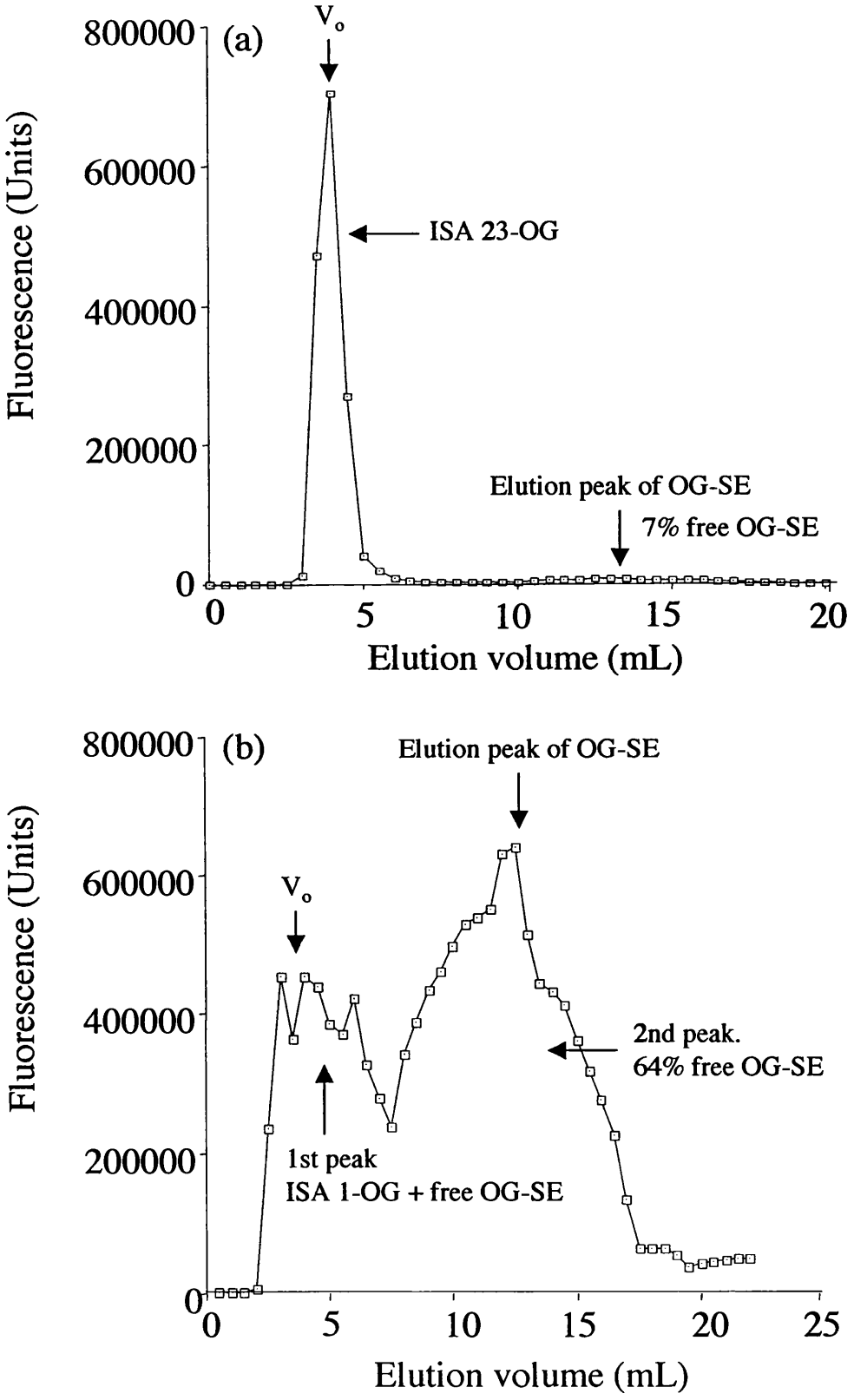

Figure 6.6 PD10 elution profiles for fluorescent conjugates. Panel (a) shows ISA 23-OG; (b) ISA 1-OG; (c) TR-gelonin. Arrows are shown to represent the elution peak for free OG-SE (shown in chapter 2, figure2.5a) and the void volume (V_o) determined by passing blue dextran through the column.

~ 64.3%. As the first peak was unresolved, the labelling efficiency could not be determined.

When the crude mixture resulting from the gelonin and TR-SE conjugation reaction was passed through the PD10 column, a peak was observed which eluted at V_0 (figure 6.6c). This peak therefore corresponded to macromolecular gelonin-TR. The calculated labelling efficiency for gelonin-TR was 94%.

Thin layer chromatography (TLC) is a type of chromatography which uses a thin layer (0.25mm) of a special finely ground matrix coated onto a glass plate or incorporated onto a plastic film as the stationary phase. Solutions of the mixtures and reference compounds to be analysed are spotted near one edge and the edge of the plate is then dipped in solvent. The solvent travels up the matrix by capillarity, moving the components of the samples at various rates because of their different degrees of attachment to the matrix and solubility in the developing solvent. The components, visible as separated spots, are identified by comparing the distances they have travelled up the matrix with those of the known reference controls (Meloan, 1999).

TLC analysis of pooled fractions 6-12 obtained from the PD10 column from the ISA 23-NH_2 and OG-SE conjugation reaction revealed a distinct spot which did not migrate from the baseline ($R_f = 0$). The OG-SE reference control migrated near to the solvent front ($R_f = 0.86$). This therefore indicated that fractions 6-12 only contained a macromolecular constituent (ISA 23-OG) (figure 6.7a).

Analysis of pooled fractions 4-15 from the ISA 1-NH_2 and OG-SE conjugation (first peak from PD10 elution profile) reaction revealed two spots. The first spot did not migrate from the baseline ($R_f = 0$). The second spot migrated almost the same distance as the OG-SE reference control (figure 6.7a) ($R_f = 0.83$). This confirmed that the first peak contained both ISA 1-OG and free OG-SE. TLC analysis of fractions 16-35 (second peak from PD10 elution profile) revealed one spot which migrated almost the same distance as free OG-SE ($R_f = 8.1$), and therefore these fractions contained only free OG-SE. As removal of free OG-SE from ISA 1-OG was not sufficient using a PD10 column, fractions 4-15 of the ISA 1-NH_2 and OG-SE reaction mixture were subjected to ethyl acetate extraction. Mixing of these fractions with ethyl acetate yielded an aqueous phase and an organic phase. Purification of ISA 1-OG from OG-SE could be performed as free OG-SE dissolves more readily in organic solvents being hydrophobic. The aqueous phase containing ISA 1-OG was therefore poured off and an aliquot of this was analysed by TLC analysis. One spot was visible on the matrix which

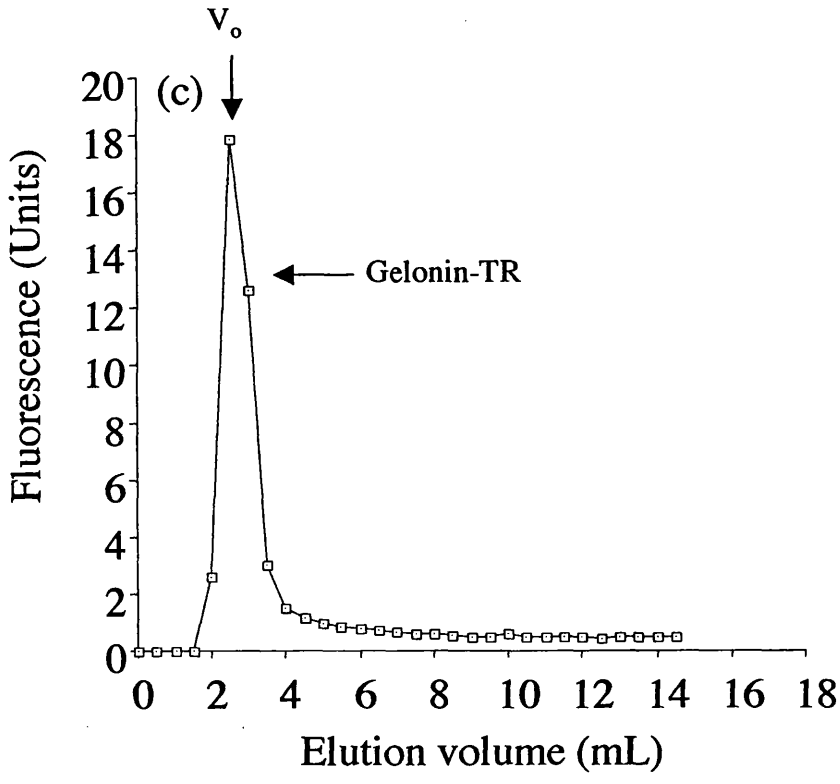

Figure 6.6 Cont.

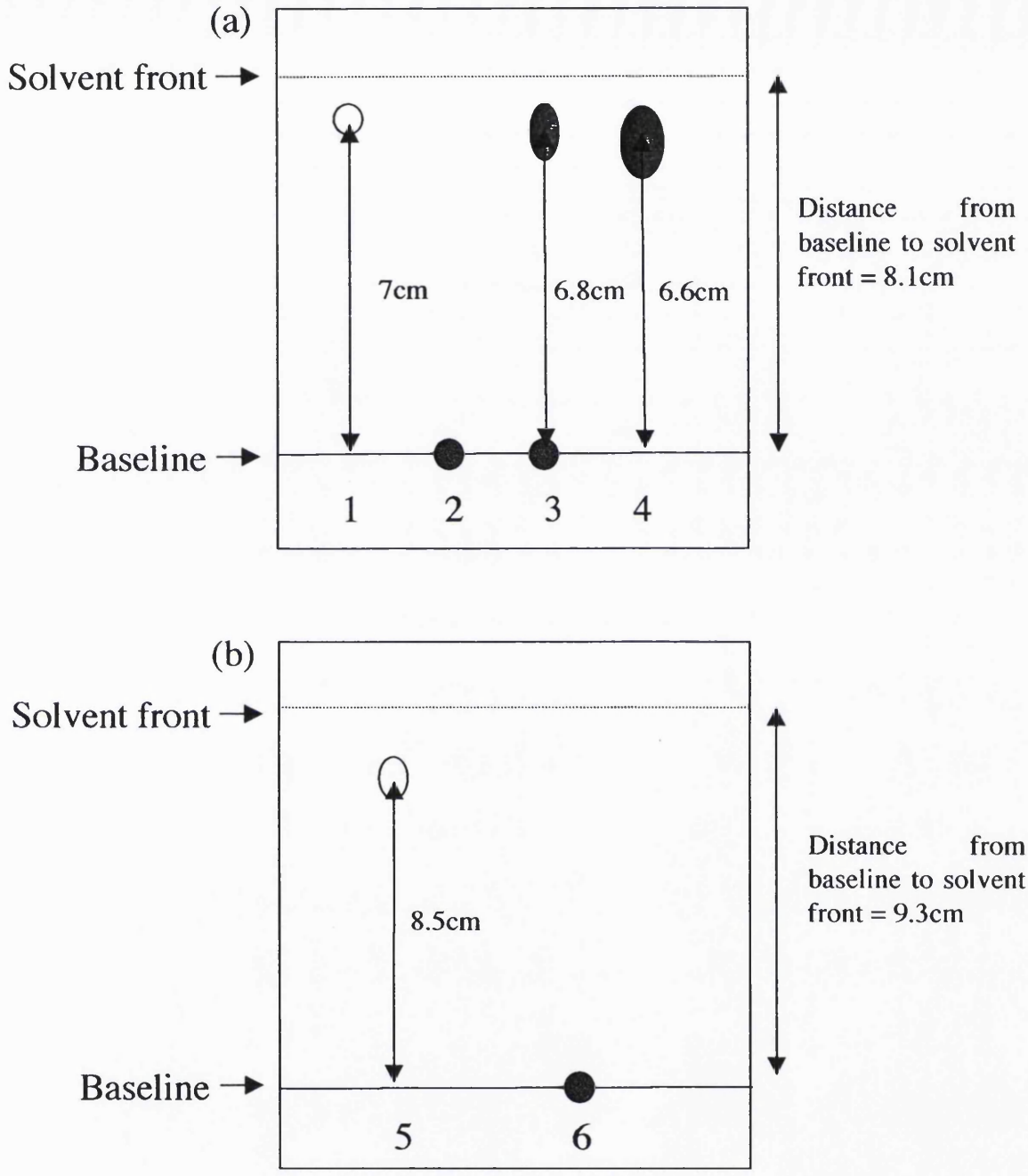

Figure 6.7 Schematic showing TLC analysis of fluorescent probes after purification on a PD10 G-25 sephadex column using Alugram® SIL G/UV TLC plates and methanol solvent. Panel (a) shows OG-containing samples; (b) TR-containing samples. Key: Spot 1 = OG-SE reference control (R_f 7/8.1 = 0.86); spot 2 = pooled fractions 6-12 from ISA 23-NH_2 and OG-SE conjugation reaction (R_f = 0/8.1 = 0); spot 3 = pooled fractions 4-15 from ISA 1-NH_2 and OG-SE conjugation reaction (R_f = 6.8/8.1 = 0.83); spot 4 = pooled fractions 16-34 from ISA 1-NH_2 and OG-SE conjugation reaction (R_f = 6.6/8.1 = 0.81); spot 5 = TR-SE reference control (R_f = 8.5/9.3 = 0.91; spot 6 = pooled fractions 4-12 from gelonin and TR-SE conjugation reaction (R_f = 0/9.3 = 0).

did not migrate from the baseline ($R_f = 0.84$) (results not shown). This confirmed that fractions 4-15 contained only ISA 1-OG. The labelling efficiency of ISA 1-OG was determined to be 8.7%.

Analysis of fractions 4-12 from the gelonin and TR-SE reaction by TLC revealed one spot which did not migrate from the application spot ($R_f = 0$). The TR-SE reference control migrated near to the solvent front ($R_f = 0.91$). This therefore indicated that fractions 4-12 only contained a macromolecular constituent (gelonin-TR) (figure 6.7b). The purified ISA 23-OG fractions 6-12 and ISA 1-OG fractions 4-15 were dialysed against DDW for 2 days and then lyophilised. The yield of ISA 23-OG and ISA 1-OG recovered was 19% and 19.5% respectively. The content of OG conjugated to ISA 23 and ISA 1 was 0.85mol% and 0.59mol% respectively. The quantity of pooled gelonin-TR (fractions 4-12) was too small to lysophilise and therefore it was stored at -4°C. The amount of TR conjugated to gelonin was calculated by measuring the absorbance of gelonin-TR at 280nm and of the dye at its absorbance maximum (595nm). The Beer-Lambert Law was then used to calculate the approximate number of dye molecules conjugated per gelonin molecule. From this calculation ~2.7 texas red molecules were conjugated per molecule of gelonin.

To determine whether the fluorescent-labelled conjugates retained the same excitation and emission spectra as the free OG-SE and TR-SE dyes, these were determined for the conjugates. Excitation and emission maxima for OG-SE occurred at ~495nm and ~521nm respectively. ISA 23-OG and ISA 1-OG conjugates showed identical emission and excitation maxima (figure 6.8a and b). The emission spectrum for PAA-OG conjugates also showed an additional peak (indicated with arrows) and this was probably a result of PAA conjugation to OG-SE. Excitation and emission maxima for TR-SE occurred at 583nm and 603nm respectively. Although the excitation spectrum for gelonin-TR revealed a small shoulder (indicated with an arrow) not visible for the TR-SE excitation spectrum, the excitation and emission maxima were identical to TR-SE (figure 6.8c).

6.3.2 Fluorescence microscopy

In order to determine the intracellular localisation of fluorescent-labelled conjugates, cell uptake experiments were performed in B16F10 and HepG2 cells and fixed cells were then visualised using fluorescence microscopy. First it was necessary to determine the autofluorescence of the cells used, by viewing B16F10 and HepG2

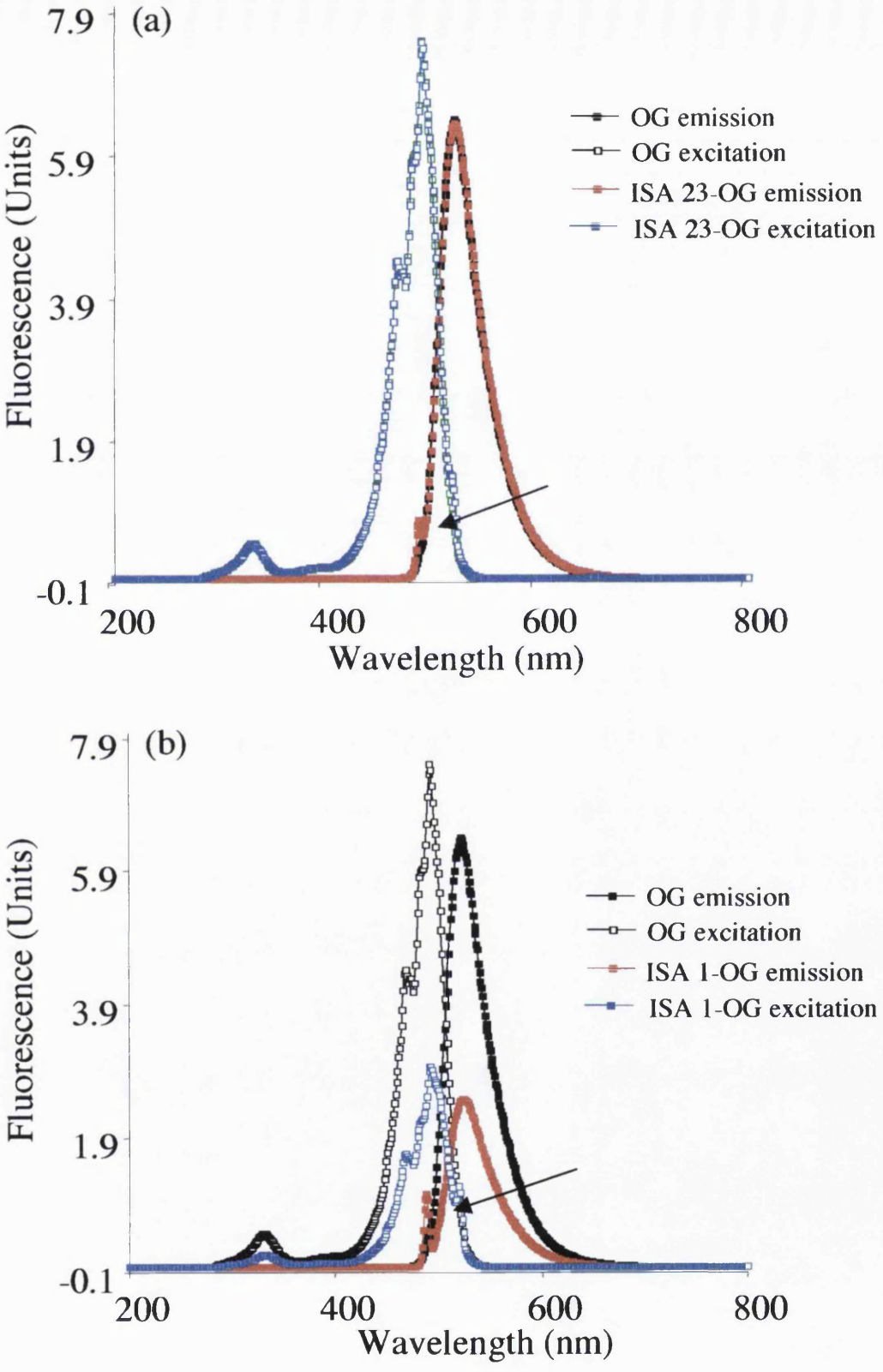

Figure 6.8 Emission and excitation spectra of fluorescent conjugates. Panel (a) shows OG-SE and ISA 23-OG; (b) OG-SE and ISA 1 -OG; (c) TR-SE and gelonin-TR. Additional peaks are indicated with arrows.

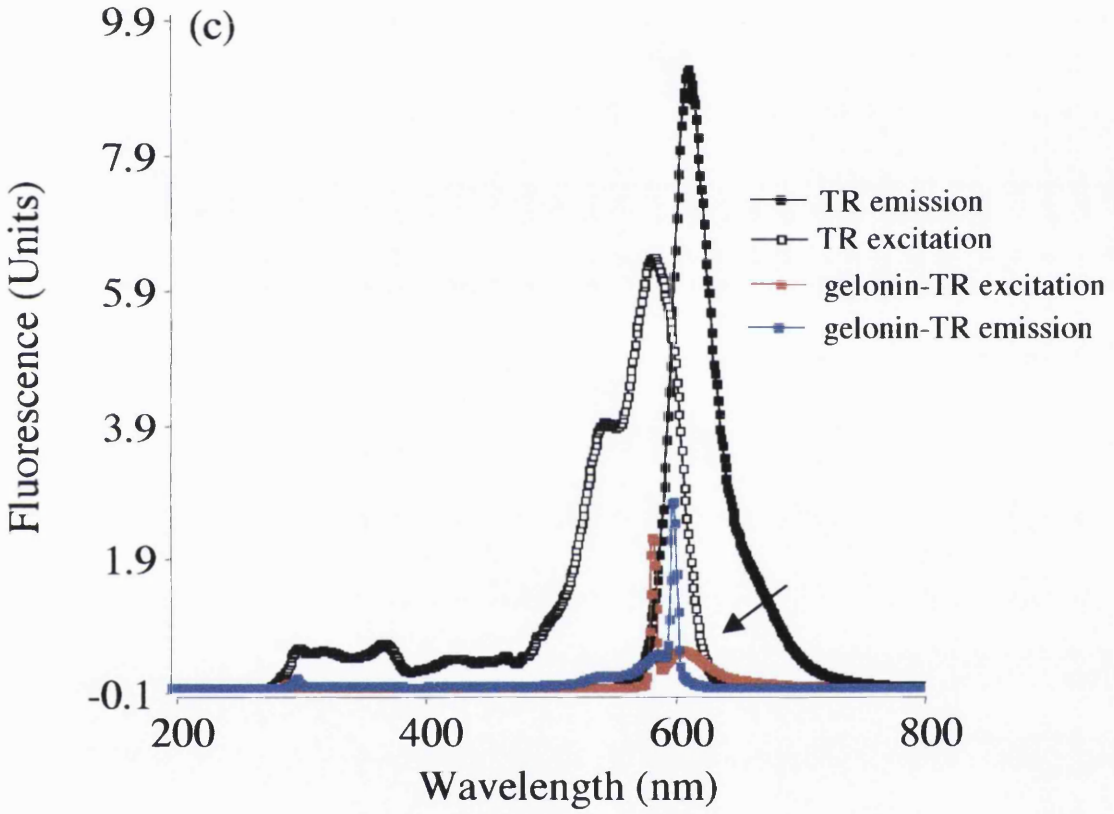

Figure 6.8 Cont.

cells through the FITC (green) and TRITC (red) optical filter sets of the fluorescence microscope. B16F10 cell nuclei produced a slight autofluorescence with the FITC filter (figure 6.9a). This made it difficult to distinguish between vesicles containing OG-conjugates in the perinuclear region. B16F10 cells showed virtually no autofluorescence with the TRITC filter (figure 6.9b). No autofluorescence was seen for HepG2 cells with either filter sets (figure 6.9a and b).

The quantity of PAA-OG conjugates used in B16F10 and HepG2 cell uptake experiments was 1mg/mL. At this concentration sufficient OG fluorescence could be detected using fluorescence microscopy. Gelonin was shown to be non-toxic to B16F10 cells at a concentration of 10μg/mL (chapter 4, Pattrick et al, 2001) and therefore this concentration of gelonin-TR was used in cell uptake studies in B16F10 cells. However, this concentration of gelonin-TR could not be used with HepG2 cells, as at this concentration gelonin was toxic (IC_{50} ~ 4μg/mL after 67h incubation) (chapter 4). As the fluorescence of gelonin-TR at concentrations < 4μg/mL was too low to be detected using fluorescence microscopy, the gelonin-TR concentration used in cell uptake experiments with HepG2 cells was 5μg/mL. At this concentration, cytotoxicity caused by gelonin was minimal at the maximum cell incubation time of 24h.

6.3.2.1 Uptake of ISA 23-OG and ISA 1-OG with lysotracker red in B16F10 cells

To confirm that ISA 23-OG and ISA 1-OG were entering the cells by endocytosis and entering vesicles of acidic pH, each PAA conjugate was incubated with B16F10 cells together with lysotracker red. The numerous yellow vesicles seen at 24h indicated colocalisation of ISA 1-OG and lysotracker red (figure 6.10). Some cells showed a lot of colocalisation around the cell periphery and a high degree of cytoplasmic fluorescence. In contrast the pattern of fluorescence seen after incubation of B16F10 cells with ISA 23-OG and lysotracker red indicated partial colocalisation, with yellow vesicles observed throughout the cell cytoplasm (figure 6.11). Uptake of both polymers and lysotracker red also resulted in distinct green and red vesicles. Green vesicles corresponding to ISA 23-OG were also observed in the nuclear region (indicated by arrows)

6.3.2.2 Uptake of gelonin-TR alone or in combination with ISA 1-OG and ISA 23-OG with B16F10 cells

Experiments were performed to investigate the pattern of uptake of fluorescent-labelled PAAs and gelonin. After addition of gelonin-TR alone, virtually no red

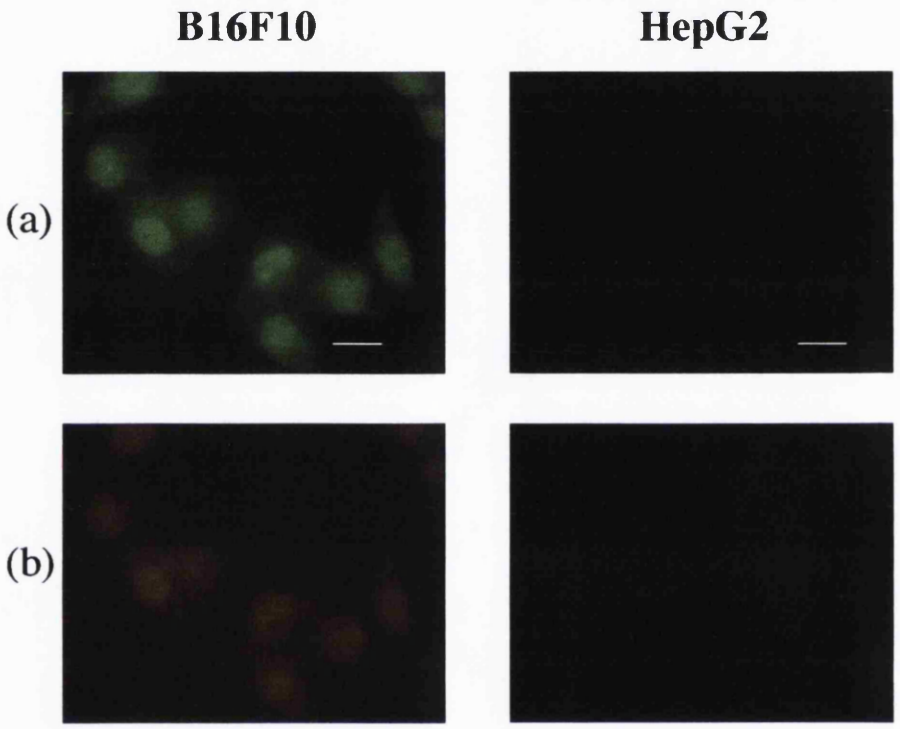

Figure 6.9 Fluorescence micrographs of untreated cells. B16F10 or HepG2 cells grown on coverslips were fixed in 3% paraformaldehyde and processed for fluorescence microscopy. Panel (a) shows B16F10 and HepG2 cells through green (FITC) channel; (b) B16F10 and HepG2 cells through red (TRITC) channel. Size bar 10μm.

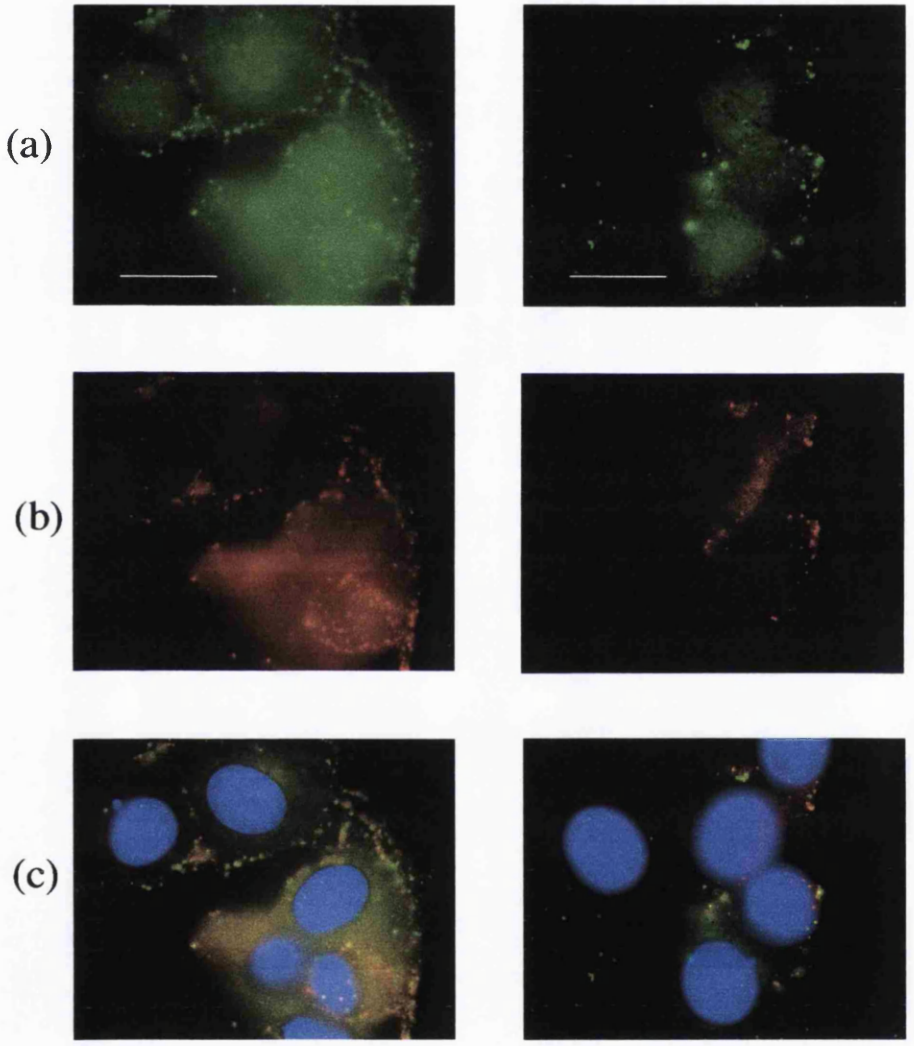

Figure 6.10 Cellular distribution of ISA 1-OG (1mg/mL) and lysotracker red (200nM) after incubation in B16F10 cells for 24h. After treatment B16F10 cells were fixed in 3% paraformaldehyde and processed for fluorescence microscopy. Panel (a) shows ISA 1-OG through green (FITC) channel; (b) lysotracker red through red (TRITC) channel; (c) superimposition of a) and b) (nuclei are stained blue). Size bar 10μm.

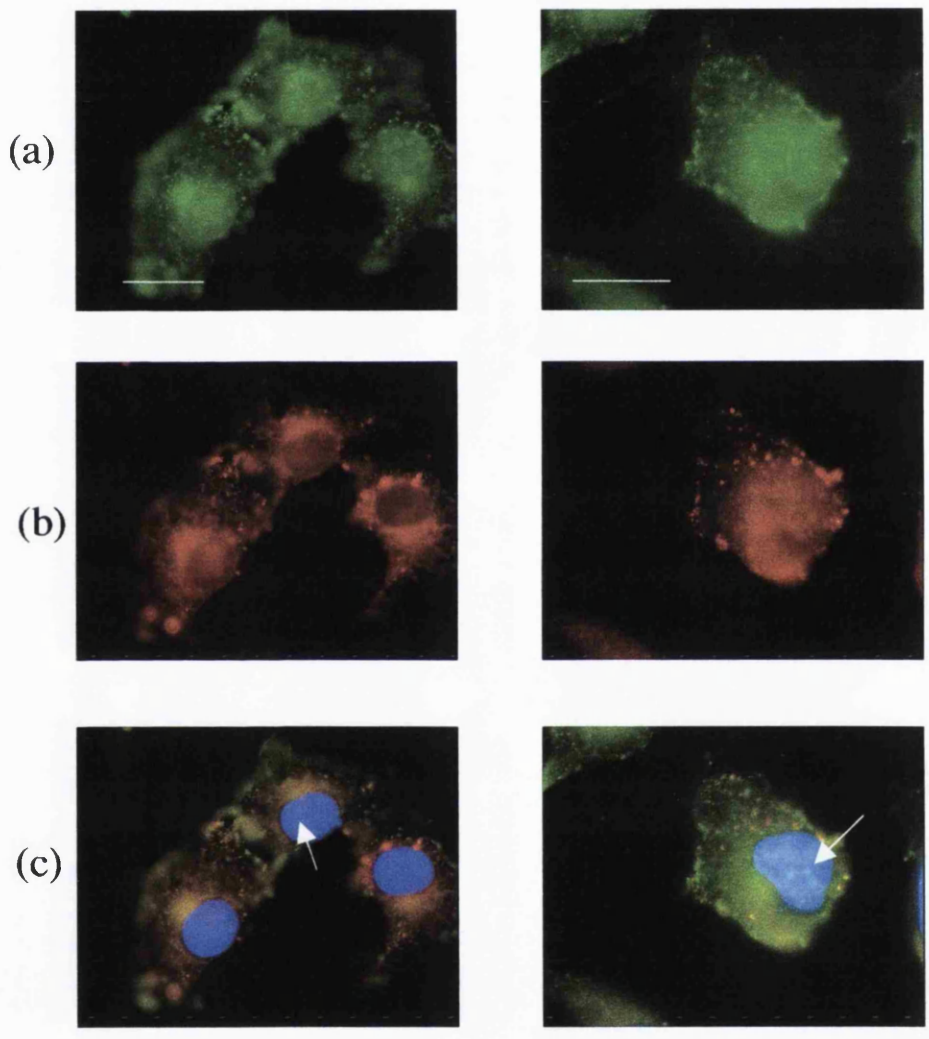

Figure 6.11 Cellular distribution of ISA 23-OG (1mg/mL) and lysotracker red (200nM) after incubation in B16F10 cells for 24h. After treatment B16F10 cells were fixed in 3% paraformaldehyde and processed for fluorescence microscopy. Panel (a) shows ISA 23-OG through green (FITC) channel; (b) lysotracker red through red (TRITC) channel; (c) superimposition of (a) and (b) (nuclei are stained blue). Green vesicles that appear to be in the nucleus are indicated by an arrow. Size bar 10μm.

fluorescence was observed in cells after 24h (figure 6.12). This pattern of fluorescence seen in B16F10 cells was dramatically different to that observed when gelonin-TR and ISA 1-OG were incubated in B16F10 cells for 24h (figure 6.13). Many red vesicles were observed throughout cells which almost completely colocalised with green ISA 1-OG vesicles (as indicated by arrows) (figure 6.13). Colocalisation of ISA 1-OG and gelonin-TR was also apparent after a 5h incubation, although the yellow spots assumed a large and irregularly shaped appearance (indicated by arrows) (figure 6.14). In contrast, the uptake of gelonin-TR by B16F10 cells after 5h or 24h was not altered when added together with ISA 23-OG. In this case few red vesicles were seen (as indicated by arrows), and there was no colocalisation with ISA 23-OG containing vesicles (figure 6.15 and 6.16).

6.3.3.3 Uptake of ISA 23-OG and ISA 1-OG with lysotracker red in HepG2 cells

As with B16F10 cells, it was first necessary to examine whether fluorescent-labelled PAAs were endocytosed and trafficked to acidic vesicles in HepG2 cells. Incubation of ISA 1-OG with lysotracker red after 24h showed some yellow vesicles, but distinct red and green vesicles were also observed (figure 6.17). Similarly, partial colocalisation of ISA 23-OG and lysotracker red was seen after their incubation in HepG2 cells for 24h (figure 6.18).

6.3.3.4 Uptake of gelonin-TR alone or in combination with ISA 1-OG and ISA 23-OG in HepG2 cells

When observing cells after the addition of gelonin-TR (5μg/mL), uptake appeared minimal, with few red vesicles observed (figure 6.19). Gelonin-TR uptake increased when it was added to cells in combination with ISA 1-OG after 24h and 5h. Partial colocalisation with ISA 1-OG occurred in large irregularly shaped vesicles (as indicated by arrows) (figure 6.20 and 6.21). However gelonin-TR uptake was not altered when added in combination with ISA 23-OG after 24h or 5h (figure 6.22 and 6.23).

6.4 Discussion

Conjugation of fluorescent probes to proteins and polymers has been widely used to study their intracellular localisation using fluorescence microscopy. This study documents for the first time the synthesis of fluorescent-labelled PAAs to allow insight

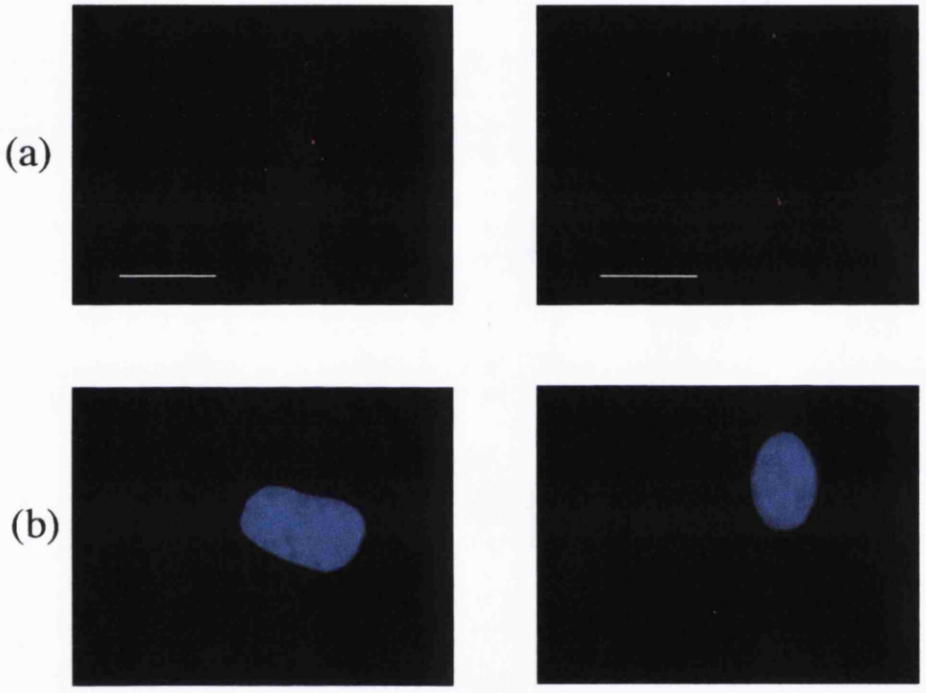

Figure 6.12 Cellular distribution of gelonin-TR (10μg/mL) after incubation in B16F10 cells for 24h. After treatment B16F10 cells were fixed in 3% paraformaldehyde and processed for fluorescence microscopy. Panel (a) shows gelonin-TR through red (TRITC) channel; (b) superimposition of (a) with blue (DAPI) stained nuclei. Size bar 10μm.

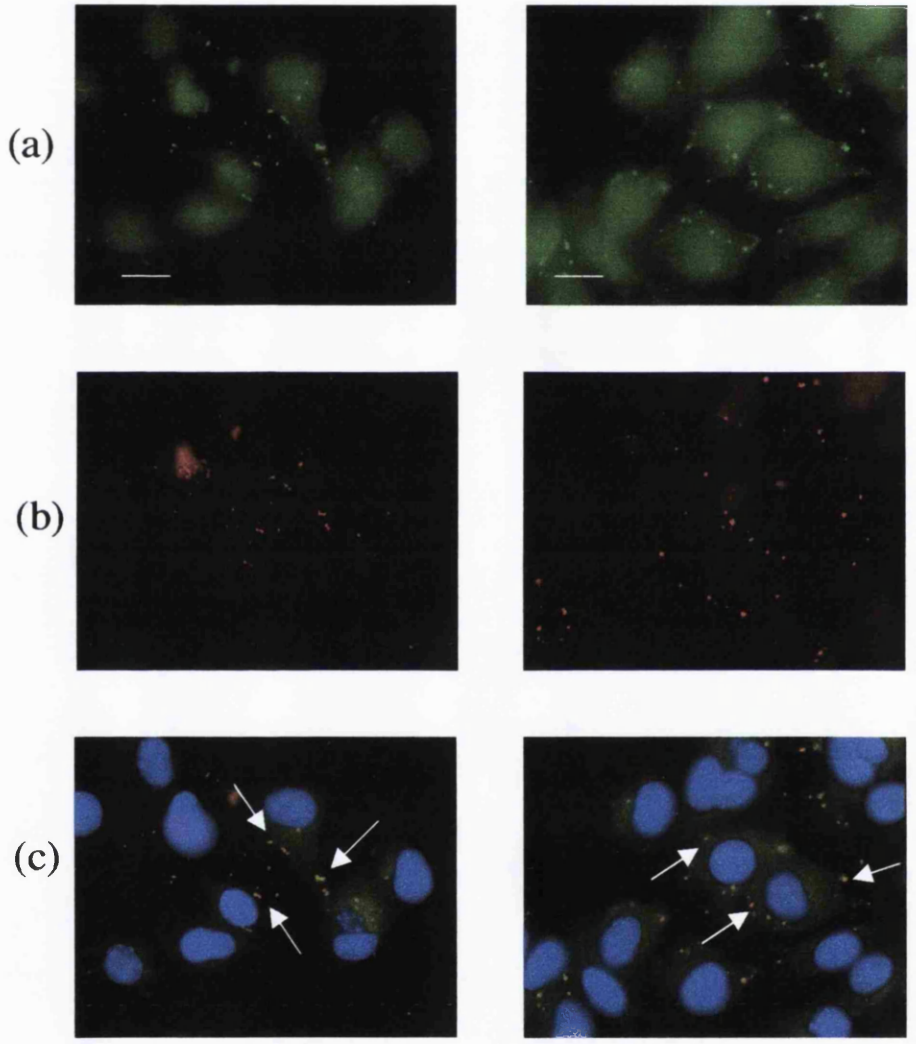

Figure 6.13 Cellular distribution of ISA 1-OG (1mg/mL) and gelonin-TR (10μg/mL) after incubation in B16F10 cells for 24h. After treatment B16F10 cells were fixed in 3% paraformaldehyde and processed for fluorescence microscopy. Panel (a) shows ISA 1-OG through green (FITC) channel; (b) gelonin-TR through red (TRITC) channel; (c) superimposition of (a) and (b) (nuclei are stained blue). Some yellow vesicles are indicated by arrows. Size bar 10μm.

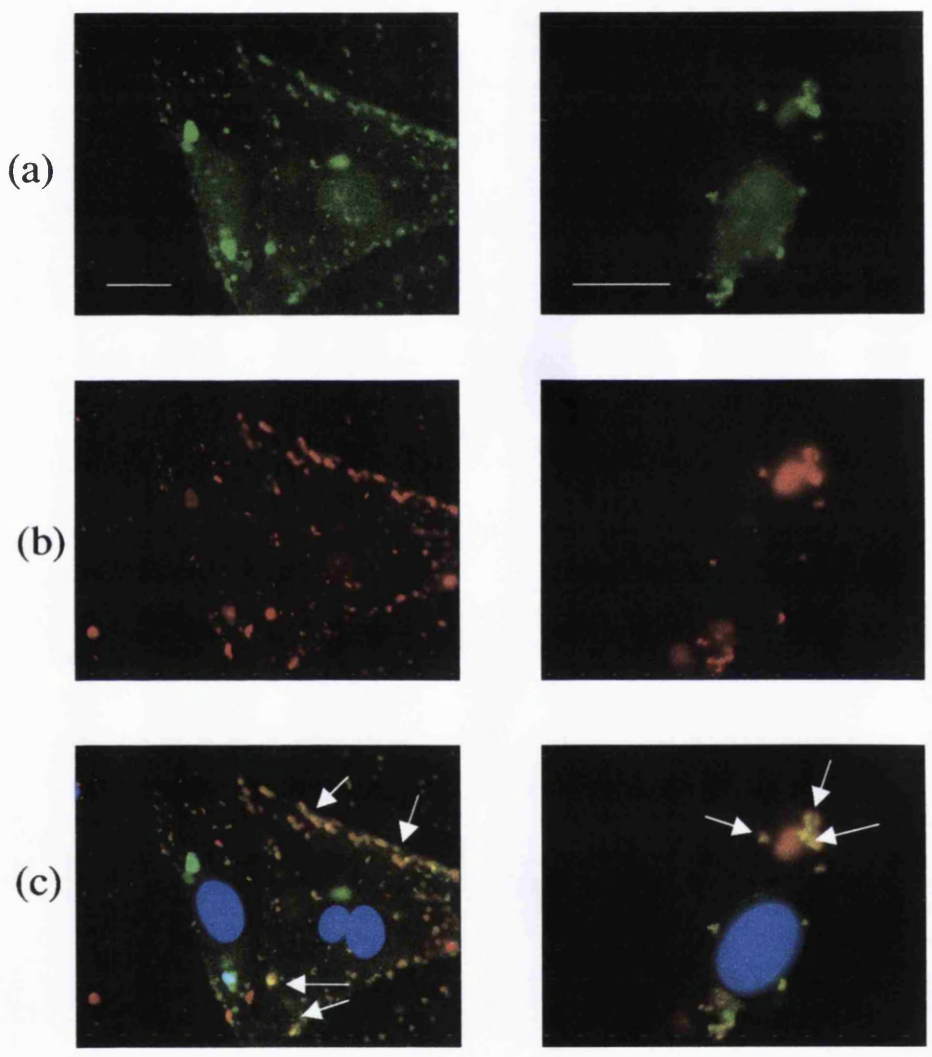

Figure 6.14 Cellular distribution of ISA 1-OG (1mg/mL) and gelonin-TR (10μg/mL) after incubation in B16F10 cells for 5h. After treatment B16F10 cells were fixed in 3% paraformaldehyde and processed for fluorescence microscopy. Panel (a) shows ISA 1-OG through green (FITC) channel; (b) gelonin-TR through red (TRITC) channel; (c) superimposition of (a) and (b) (nuclei are stained blue). Large yellow vesicles are indicated by an arrow. Size bar 10μm.

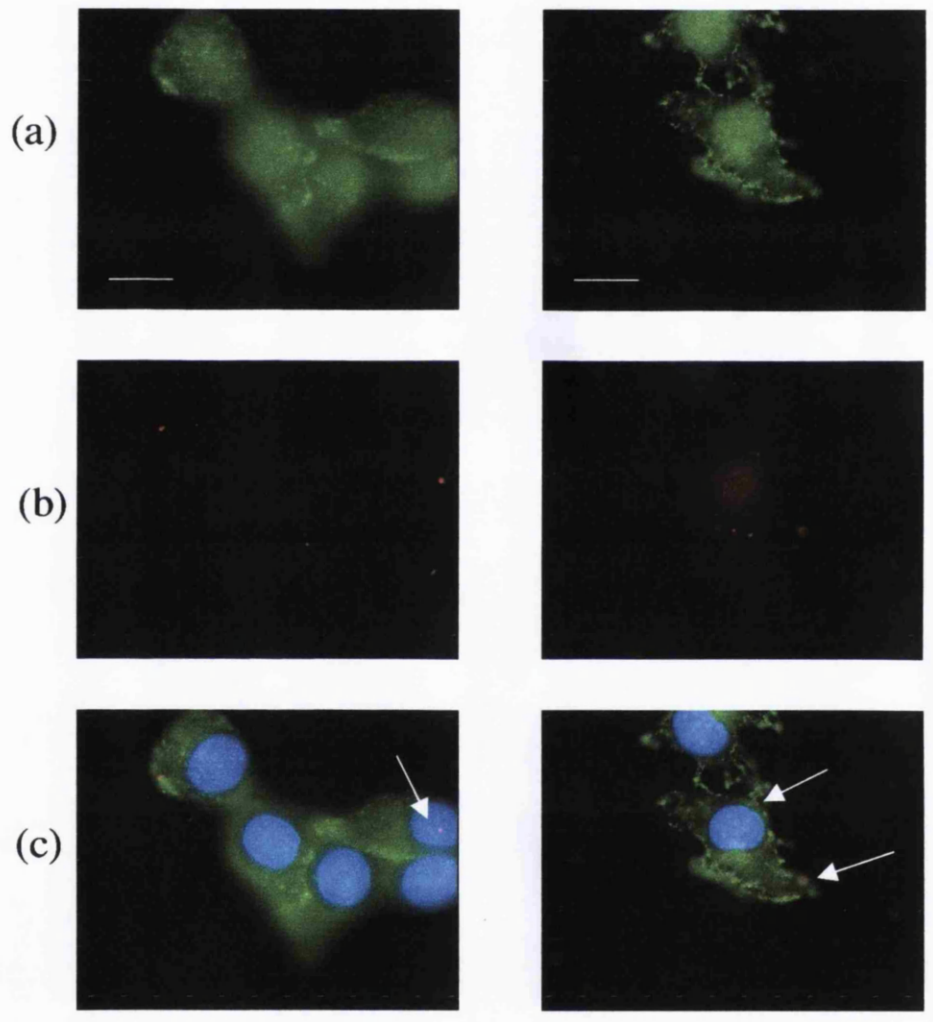

Figure 6.15 Cellular distribution of ISA 23-OG (1mg/mL) and gelonin-TR (10μg/mL) after incubation in B16F10 cells for 24h. After treatment B16F10 cells were fixed in 3% paraformaldehyde and processed for fluorescence microscopy. Panel (a) shows ISA 23-OG through green (FITC) channel; (b) gelonin-TR through red (TRITC) channel; (c) superimposition of (a) and (b) (nuclei are stained blue). Red vesicles are indicated by an arrow. Size bar 10μm.

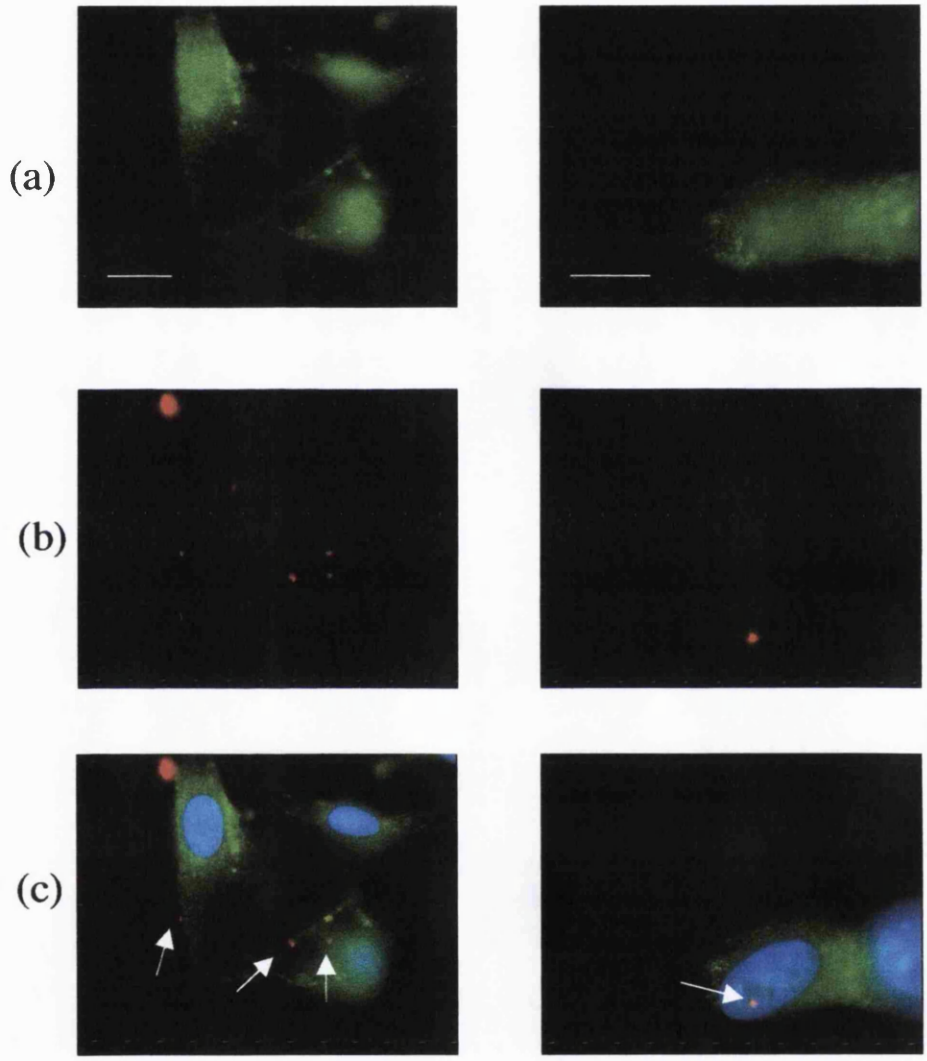

Figure 6.16 Cellular distribution of ISA 23-OG (1mg/mL) and gelonin-TR (10μg/mL) after incubation in B16F10 cells for 5h. After treatment B16F10 cells were fixed in 3% paraformaldehyde and processed for fluorescence microscopy. Panel (a) shows ISA 23-OG through green (FITC) channel; (b) gelonin-TR through red (TRITC) channel; (c) superimposition of (a) and (b) (nuclei are stained blue). Red vesicles are indicated by arrows. Size bar 10μm.

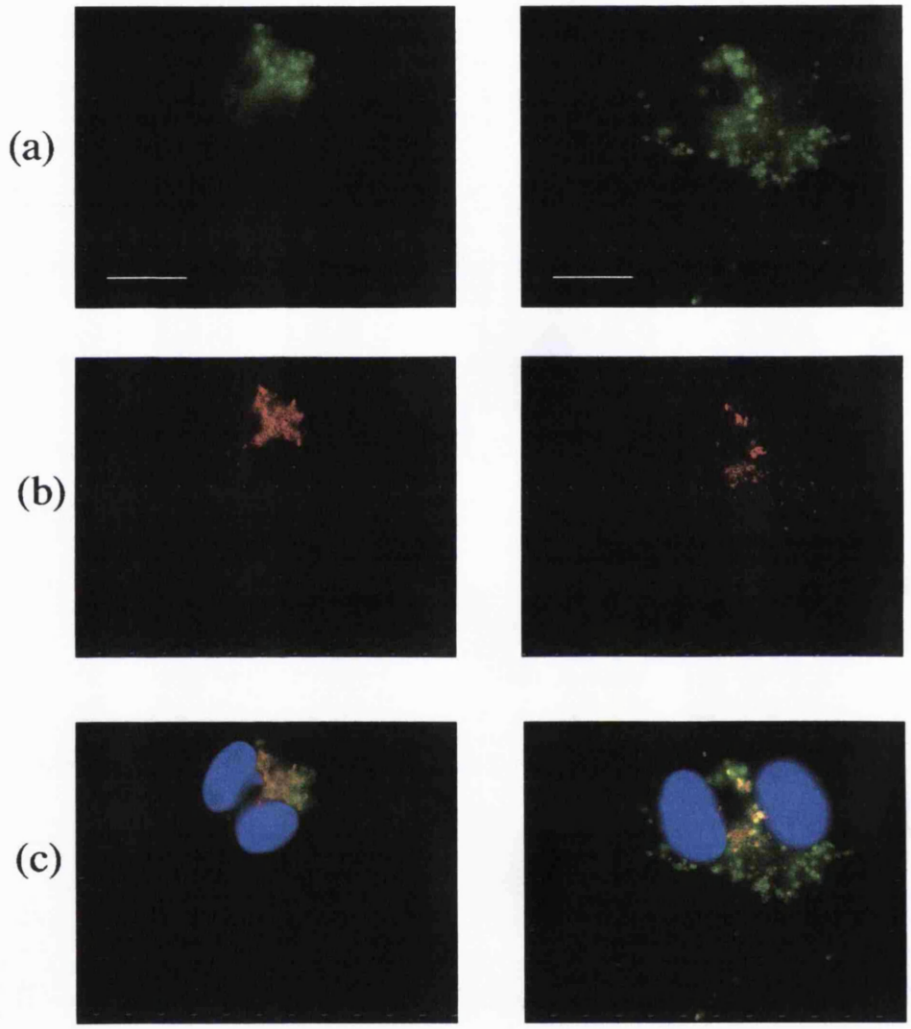

Figure 6.17 Cellular distribution of ISA 1-OG (1mg/mL) and lysotracker red (200nM) after incubation in HepG2 cells for 24h. After treatment HepG2 cells were fixed in 3% paraformaldehyde and processed for fluorescence microscopy. Panel (a) shows ISA 1-OG through green (FITC) channel; (b) lysotracker red through red (TRITC) channel; (c) superimposition of (a) and (b) (nuclei are stained blue). Size bar 10μm.

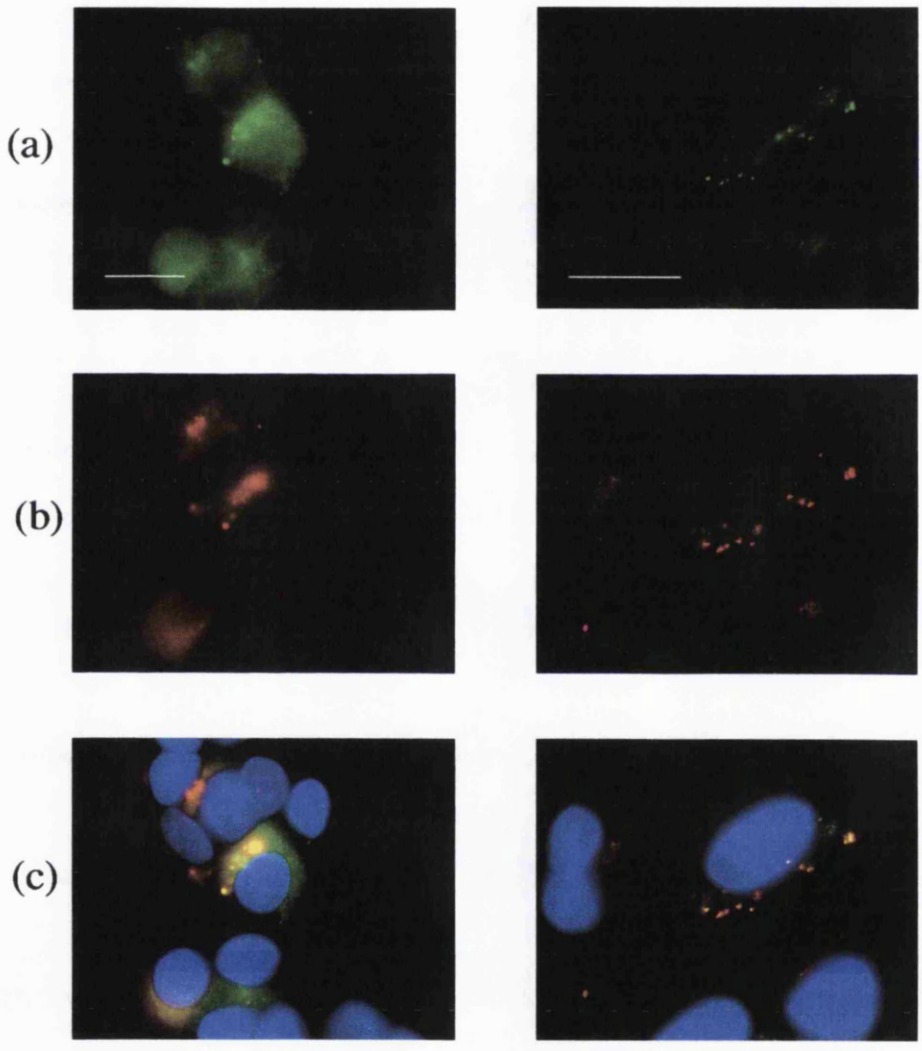

Figure 6.18 Cellular distribution of ISA 23-OG (1mg/mL) and lysotracker red (200nM) after incubation in HepG2 cells for 24h. After treatment HepG2 cells were fixed in 3% paraformaldehyde and processed for fluorescence microscopy. Panel (a) shows ISA 23-OG through green (FITC) channel; (b) lysotracker red through red (TRITC) channel; (c) superimposition of (a) and (b) (nuclei are stained blue). Size bar 10μm.

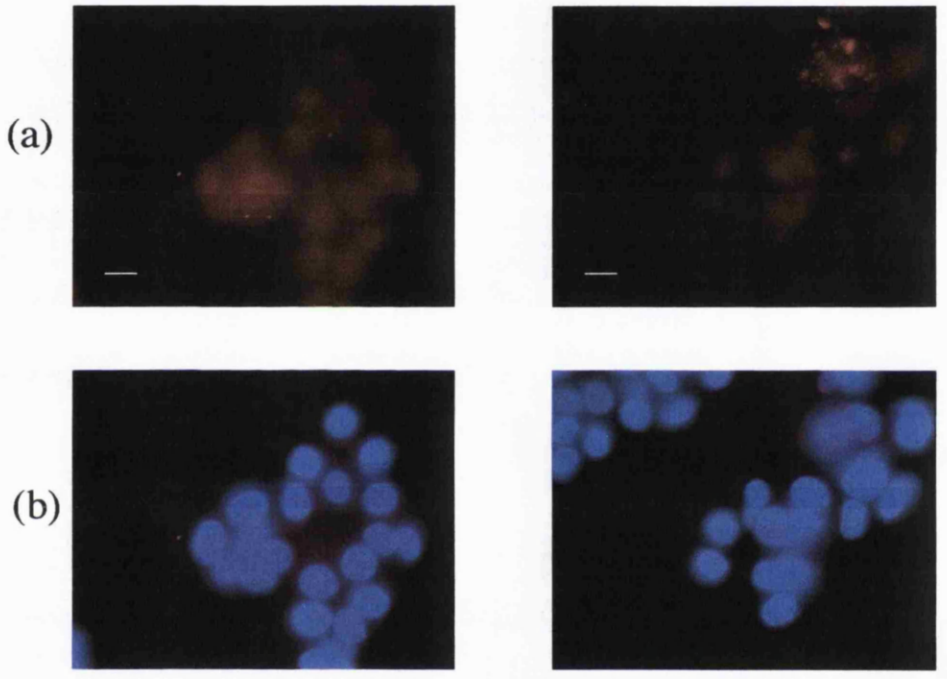

Figure 6.19 Cellular distribution of gelonin-TR (5μg/mL) after incubation in HepG2 cells for 24h. After treatment HepG2 cells were fixed in 3% paraformaldehyde and processed for fluorescence microscopy. Panel (a) shows gelonin-TR through red (TRITC) channel; (b) superimposition of (a) with blue (DAPI) stained nuclei. Size bar 10μm.

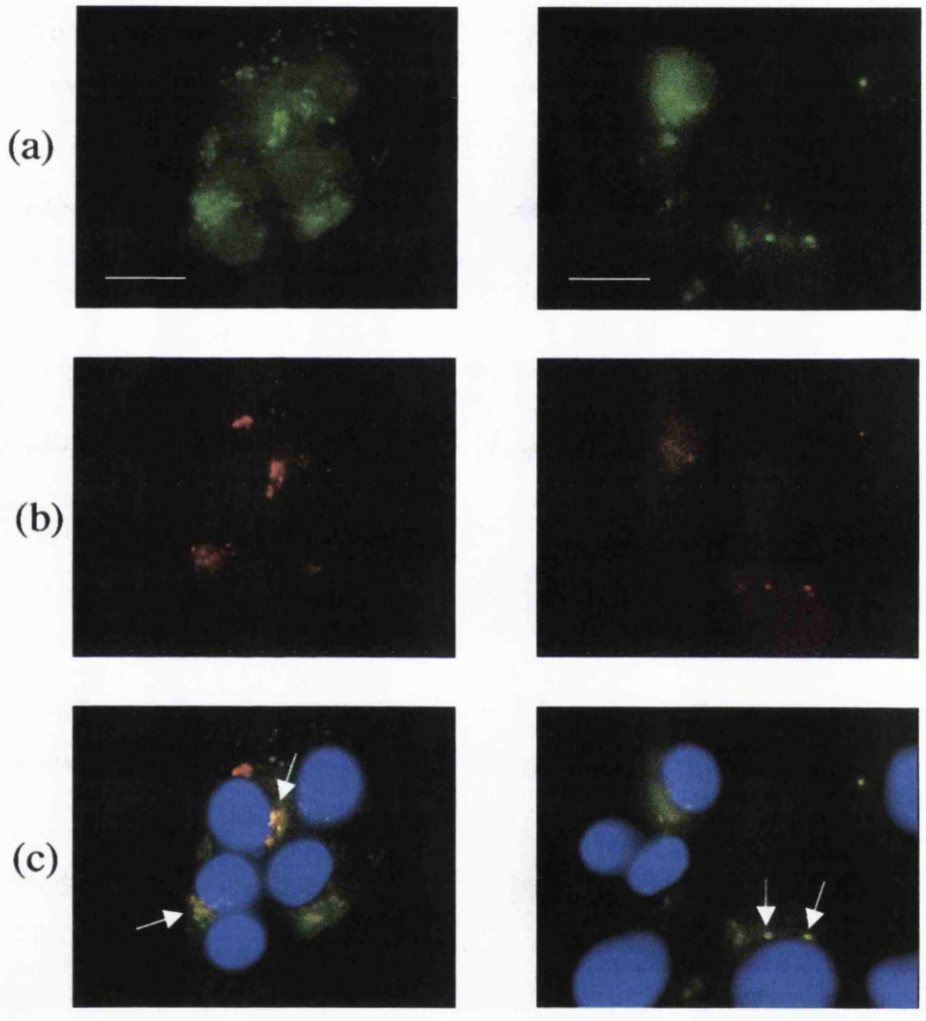

Figure 6.20 Cellular distribution of ISA 1-OG (1mg/mL) and gelonin (5μg/mL) after incubation in HepG2 cells for 24h. After treatment HepG2 cells were fixed in 3% paraformaldehyde and processed for fluorescence microscopy. Panel (a) shows ISA 1-OG through green (FITC) channel; (b) gelonin-TR through red (TRITC) channel; (c) superimposition of (a) and (b) (nuclei are stained blue). Yellow vesicles are indicated by arrows. Size bar 10μm.

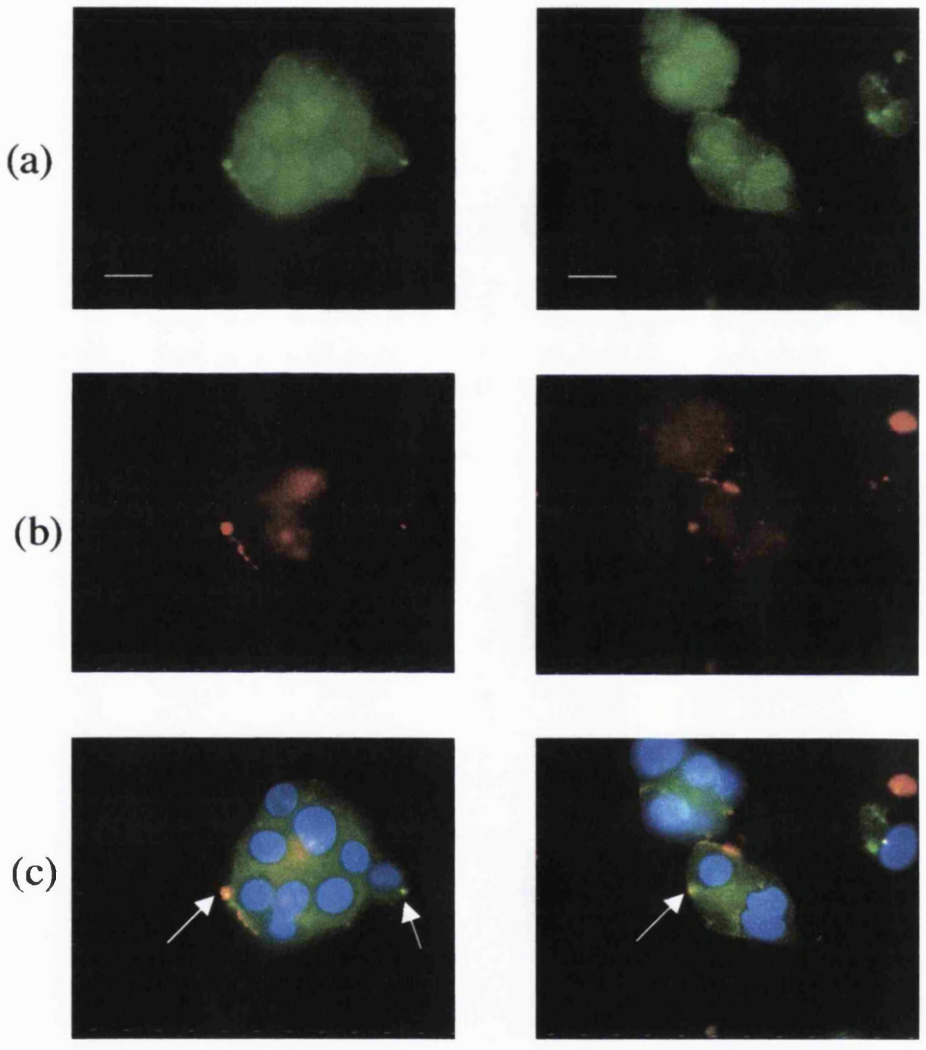

Figure 6.21 Cellular distribution of ISA 1-OG (1mg/mL) and gelonin (5μg/mL) after incubation in HepG2 cells for 5h. After treatment HepG2 cells were fixed in 3% paraformaldehyde and processed for fluorescence microscopy. Panel (a) shows ISA 1-OG through green (FITC) channel; (b) gelonin-TR through red (TRITC) channel; (c) superimposition of (a) and (b) (nuclei are stained blue). Yellow vesicles are indicated by arrows. Size bar 10μm.

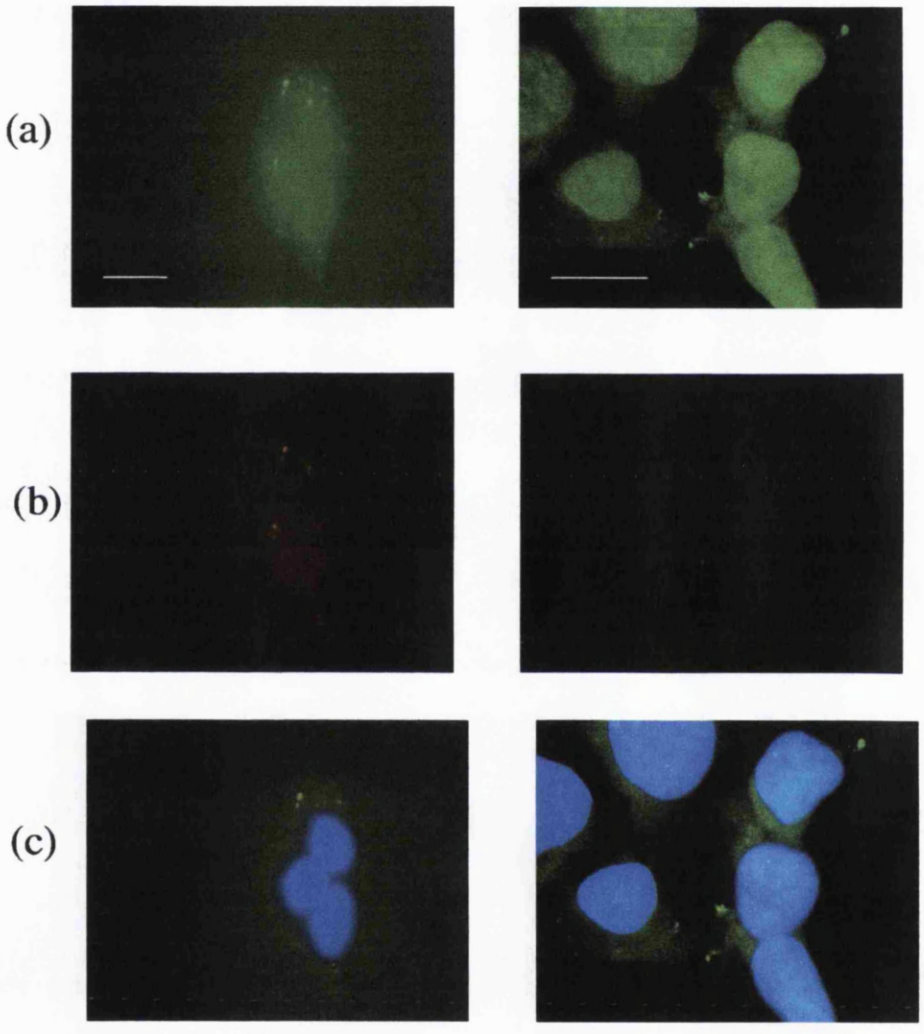

Figure 6.22 Cellular distribution of ISA 23-OG (1mg/mL) and gelonin (5μg/mL) after incubation in HepG2 cells for 24h. After treatment HepG2 cells were fixed in 3% paraformaldehyde and processed for fluorescence microscopy. Panel (a) shows ISA 23-OG through green (FITC) channel; (b) gelonin-TR through red (TRITC) channel; (c) superimposition of (a) and (b) (nuclei are stained blue). Size bar 10μm.

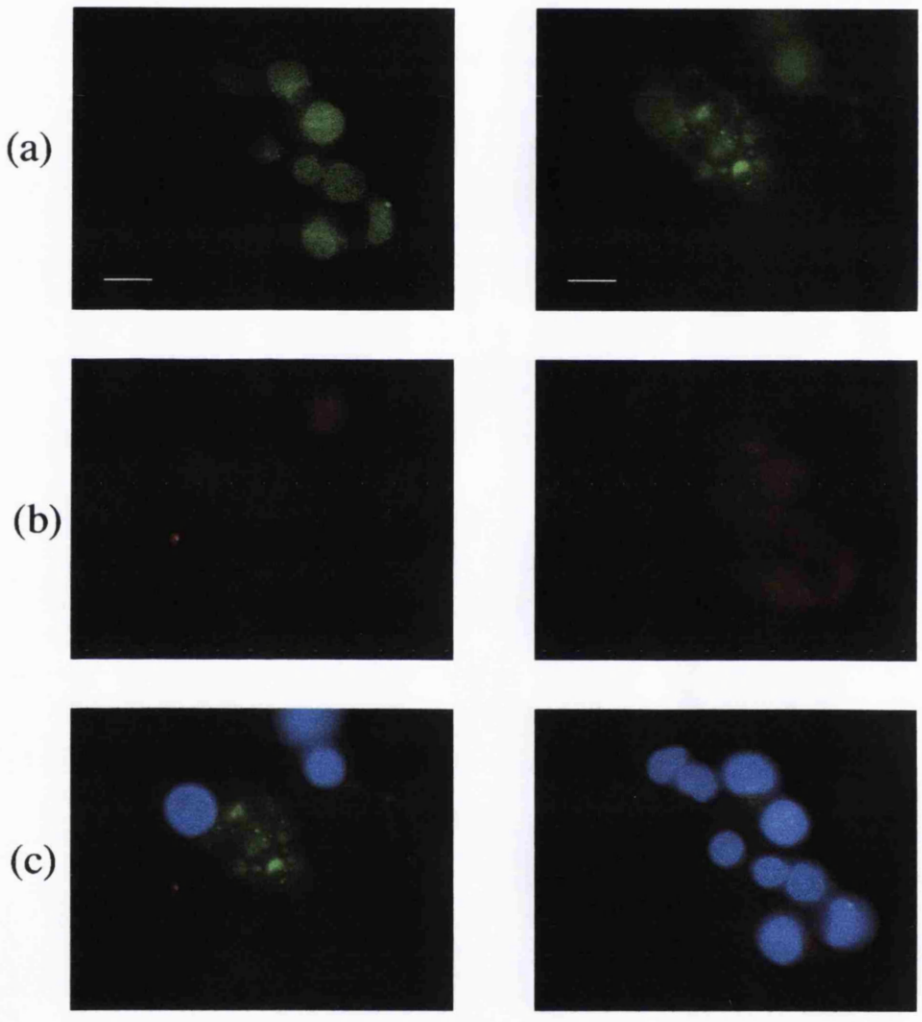

Figure 6.23 Cellular distribution of ISA 23-OG (1mg/mL) and gelonin (5μg/mL) after incubation in HepG2 cells for 5h. After treatment HepG2 cells were fixed in 3% paraformaldehyde and processed for fluorescence microscopy. Panel (a) shows ISA 23-OG through green (FITC) channel; (b) gelonin-TR through red (TRITC) channel; (c) superimposition of (a) and (b) (nuclei are stained blue). Size bar 10μm.

into their intracellular trafficking when added alone or in combination with fluorescent-labelled gelonin in B16F10 or HepG2 cells.

Synthesis of fluorescent conjugates was performed by reacting the amine-reactive fluorophore OG-SE to ISA 23-NH_2 and ISA 1-NH_2 polymers respectively. A second amine-reactive fluorophore, TR-SE was conjugated to gelonin. Synthesis of ISA 23-OG and ISA 1-OG resulted in labelling efficiencies of 93% and 8.7% respectively. Recent literature has documented the efficiency of OG labelling to an HPMA-copolymer to be ~ 82% (Jensen et al, 2001) and therefore the efficiency of ISA 23-OG labelling is comparable. The low labelling efficiency for ISA 1-OG was most likely due to slow conjugation reaction kinetics. This reaction was carried out at 4^0C to prevent side-reaction of OG-SE with the two hydroxyl groups of ISA 1 (figure 6.2b). Although the reaction time was extended to 24h, this low temperature probably still limited the overall efficiency of conjugation and resulted in a large excess of free OG-SE present after conjugation. It may be possible to improve conjugation efficiency to ISA 1 by blocking the potentially reactive hydroxyl groups of this PAA before performing the conjugation reaction.

The content of OG in ISA 23-OG and ISA 1-OG conjugates was 0.85mol% and 0.59mol% respectively. These values were somewhat lower than the 1.6mol% OG content documented for an HPMA-gly-gly-OG conjugate (Jensen et al, 2001). However the PAA-NH_2 polymers contained only 0.05mol% -NH_2 groups to react with OG-SE compared to 4.7mol% reactive groups for the HPMA-copolymer. Due to the expense of gelonin, only 1mg was used for conjugation with TR-SE. The resultant conjugation efficiency was low (15%) probably because at least 2mg/mL is recommended for optimal conjugation (Haugland, 1999).

It is important to note that there was no definitive proof that conjugates were synthesised. Conjugation of OG-SE to PAAs and TR-SE to gelonin was assumed after macromolecular fluorescent-labelled compounds were detected using TLC analysis. However, detection of macromolecular compounds may also have arisen from a non-covalent interaction of the dyes with PAAs and gelonin. In practise, for detection of an amide bond ^{13}CNMR analysis would be the best method to confirm conjugation. However this was not performed in this study due to the small amounts of gelonin and PAAs recovered after the conjugation reactions.

It was assumed for the purpose of this study that conjugates were synthesised and subsequently used for uptake studies in B16F10 and HepG2 cells. As endocytosis is a dynamic process, the internalisation of polymers cannot be definitively confirmed

using fixed cell microscopy. However the appearance of punctate green vesicles containing PAA-OG conjugates at the plasma membrane and in the cytosol, and their colocalisation with the lysotracker red dye after 24h suggested endocytic uptake and trafficking to endo/lysosomes (figure 6.10; 6.11; 6.17; 6.18). The fluorescence pattern of ISA 1-OG when added in combination with lysotracker red in B16F10 cells showed yellow spots which accumulated around the peri-nuclear region (figure 6.20). This fluorescence pattern was similar to that seen for PEI-FITC conjugates after their incubation with L929cells after 24h (Rémy-Kristensen et al, 2001). In contrast, ISA 23-OG showed less colocalisation with lysotracker red and vesicles were seen throughout the cytoplasm of B16F10 cells after 24h (figure 6.11). Some green vesicles corresponding to ISA 23-OG were also observed in the nucleus (indicated by arrows). (It must be noted that firm evidence for this nuclear localisation could not be demonstrated due to the green autofluorescense of B16F10 cell nuclei and the use of a fluorescence microscope which was unable to take confocal sections (z-sections)). Nuclear localisation of PEI-OG was also observed by Godbey et al, (1999b) 4.5 hours after its addition to EA.hy 926 cells.

The fluorescence pattern of PAA-OG uptake in HepG2 cells was different to uptake in B16F10 cells. Uptake of both lysotracker red and PAA-OG conjugates appeared to be less than in B16F10 cells. Larger vesicles were observed with colocalisation occurring mainly in the peri-nuclear region (figure 6.17 and 6.18). Different cell-types have been shown to affect the uptake of fluorescent-labelled PEI conjugates (Godbey et al, 1999b; Rémy-Kristensen et al, 2001; Merdan et al, 2002a). In addition the ability of polymers to mediate transfection (Richardson et al, 2001; Remy et al, 1998) and deliver toxins (chapter 4) has also been shown to be cell-type dependent. This was probably due to differential trafficking pathways between different cell types.

For both conjugates and in both cell lines, only partial colocalisation was observed with lysotracker red after 24h. Distinct green spots corresponding to PAA-OG conjugates were also visualised. A similar distribution pattern was documented by Merdan et al, (2002a), where separate green vesicles corresponding to PEI-OG/DNA complexes were observed in SW13 cells after co-incubation with lysotracker blue for 1h. To explain this phenomenon it was proposed that either PEI molecules were residing in nonacidic prelysosomal compartments, or that these vesicles were lysosome remnants that had been burst by the membrane destabilising effect of PEI. It is possible that PAAs were mediating both these events. Evidence for the ability of PAAs to alter

the buoyant density of lysosomes, and therefore delay vesicle transfer from endosomes to lysosomes has been shown (Richardson, 1999c; Pattrick et al, 2002). In addition, evidence for PAA-mediated endosomolytic ability presented in this thesis could also explain that this similar distribution pattern represented vesicle bursting by PAAs.

In order to examine whether interaction between free TR and OG occurred in cells, unreactive derivatives of these dyes were synthesised (TR-COOH and OG-COOH). Control experiments were then carried out where the free dyes were added together or in combination with conjugates to B16F10 or HepG2 cells. As only partial colocalisation was observed (results not shown), it was attributed to random trafficking of the compounds to the same subcellular compartment and not interaction between the dyes. This finding was important, as it allowed dual labelling studies of PAAs and gelonin to be performed. Initial uptake experiments with gelonin-TR showed conjugate uptake to be minimal in both cell lines (figure 6.12 and 6.19). Gelonin lacks the cell-binding moiety of ricin (Stirpe et al, 1980), and therefore its inefficient uptake into cells was not surprising. In a similar study, gelonin labelled with the green fluorophor Alexa 488 showed a higher degree of uptake into THX cells, and showed endosomal and lysosomal localisation (Selbo et al, 2000a). However this fluorescence pattern can be attributed to the higher concentration of gelonin used (30μg/ml), and the different cell-line used for uptake studies.

First direct evidence for complex formation between ISA 1 and gelonin was shown when gelonin-TR uptake was dramatically increased when added in combination with ISA 1-OG after 24h. Almost complete colocalisation of gelonin-TR with ISA 1-OG was observed in both cell lines (figure 6.13 and 6.20). To ascertain if this process occurred at an earlier stage of uptake, cells were also analysed 5h post-incubation. At this time point colocalised spots were seen which did not have a punctate vesicular appearance (figure 6.14 and 6.21). It is unknown whether this was due to gelonin/ISA 1 interaction within vesicles causing a change in vesicle morphology, or whether structures observed had burst vesicles and were located in the cell cytosol. As this interaction was observed for the ISA 1/gelonin combination but not the ISA 23/gelonin combination (figure 6.15; 6.16; 6.22; 6.23), it is likely that complex formation was responsible for the observed cytotoxicity of gelonin in B16F10 cells, by increasing gelonin uptake into cells (discussed in chapter 4).

The close association of gelonin-TR and ISA 1-OG suggested that gelonin-ISA 1-OG complexes were able to enter the cytosol and gelonin was still able to inactivate ribosomes when complexed to ISA 1. Similarly, OG-labelled PAMAM dendrimer

TAMRA-labelled oligonucleotide complexes remain in close proximity after endocytosis, and the oligonucleotide within the complex was able to mediate transfection (Yoo and Juliano, 2000). In contrast, when PEI-OG/rhodamine-labelled ribozyme complexes were added in combination to SW13 cells, some dissociation of PEI and ribozymes was observed after vesicle bursting. A predominately green fluorescence was observed throughout the whole cell, whilst the remnants of the burst vesicles were red and therefore seemed to contain ribozymes (Merdan et al, 2002a). A similar fluorescence pattern was observed when a gelonin-Alexa 488 conjugate was added in combination with the photosensitizing agent, AlPcS2a. After exposure to light, fluorescence of the gelonin-Alexa complex was broadly distributed throughout the whole cell, whilst diffuse perinuclear fluorescence from the photosensitizer was detected (Selbo et al, 2000a). These results suggest that it may not be necessary for a drug to dissociate from an endosomolytic system in order to cause a therapeutic effect. In some cases, dissociation may be caused by interactions of the polymer/payload with components of the membrane or specific proteins.

The question that remained unanswered from these studies was why ISA 1 was unable to deliver gelonin in HepG2 cells when interaction of gelonin and ISA 1 was observed in both cell lines. One possibility could be that HepG2 cells displayed a lower level of endocytosis. Less gelonin-TR and ISA 1-OG fluorescence was seen associated with HepG2 cells than B16F10 cells. As a result of this, even in combination with ISA 1, a high enough concentration of gelonin may not have been present in cells to cause efficient ISA 1-mediated cytosolic delivery. A variety of different techniques could be used to allow better quantitation of the subcellular localisation and trafficking pathways of these compounds in the different cell types. Endocytosis rates can be measured by analysing the uptake of the marker of membrane endocytosis, FM4-64 in cells over time, and comparing this rate with that of fluorescent-labelled PAAs. A study by Rémy-Kristensen et al, (2001) showed that vesicles containing PEI/DNA complexes labelled with the fluorescent dye YOYO-1 colocalised with FM4-64, suggesting these complexes were internalised by fluid-phase endocytosis. The subcellular localisation of PAAs and gelonin could also be determined using both radiolabelled and/or fluorescent-labelled conjugates. After addition of labelled-molecules to cells, subcellular fractionation is performed and their colocalisation with a specific organelle marker indicates their localisation in that subcellular compartment. Yoo and Juliano, (2002) isolated nuclei from cells dosed with PAMAM-OG/TAMRA-oligonucleotide

complexes. Recovered nuclei contained ~ 5.3% of the total dendrimer and ~ 4.8% of oligonucleotides, respectively.

The use of radiolabelled PAAs and gelonin to quantitiate rates of uptake and their subcellular localisation would also help to confirm whether the addition of the hydrophobic fluorescent dyes to compounds affected their native subcellular trafficking. At present, this question remains unanswered. Jensen et al, (2002) found no significant difference in the subcellular trafficking of HPMA when three different fluorophores (FITC, OG, Lissamine Rhodamine B) were conjugated to it. However Yoo and Juliano, (2000) demonstrated that a PAMAM-OG conjugate was a much better gene delivery agent than its unlabelled counterpart.

6.5 Conclusions

Further evidence for the endosomolytic mechanism of PAAs was demonstrated by their accumulation in nonacidic, as well as acidic vesicles, suggesting endo/lysosomal rupture. In addition, evidence for the mechanism of ISA 1-mediated gelonin cytosolic delivery in B16F10 cells was demonstrated as a result of complex formation between ISA 1-OG and gelonin-TR leading to enhanced gelonin uptake. As ISA 1 was unable to promote toxicity of gelonin in HepG2 cells but complex formation was observed, it was proposed that endocytic uptake of complexes was not high enough to cause sufficient gelonin entry and transfer to the cytosol in this cell line.

It was proposed in chapter 4 that PAA-gelonin conjugates may have potential as anticancer agents. To further the development of these conjugates, in the next chapter, the effect of ISA 1 conjugation to gelonin on the ability of the polymer to the deliver the toxin was examined. As ISA 22/23 were unable to mediate toxin delivery, the effect of Mw on ISA 23-mediated endosomolytic ability was also investigated with a view to synthesising lead PAA structures with enhanced membrane-destabilising properties.

CHAPTER 7

PRELIMIANRY SCREENING OF PAA STRUCTURES WITH A VIEW TO IMPROVING ENDOSOMOLYTIC ABILITY

7.1 Introduction

The emergence of polymer-protein and polymer-drug conjugates onto the market and clinical trials suggests that these new entities represent an important new class of anticancer therapeutics (reviewed in Nucci et al, 1991; reviewed in Duncan et al, 1996). This has provided an opportunity to design second-generation polymer-based drugs such as PAAs, which are being developed for the intracytoplasmic delivery of macromolecules. As experiments outlined in chapter 4 demonstrated the ability of certain PAA structures to mediate the cytosolic delivery of toxins, there is potential for the further development of PAA-toxin constructs as anticancer agents for clinical testing. However, in order to optimise the biological properties of these polymers for clinical applications, it was important to initially understand the polymer physico-chemical criteria required to achieve optimum PAA-mediated endosomolysis, before evaluating the activity of PAA-toxin constructs.

Polymer physico-chemical characteristics such as charge (Van de Wetering et al, 1999) hydrophobicity (Murthy et al, 1999) and counter-ion (Wan et al, 2002) are all reported to affect the endosomolytic properties of a polymer. However, the effect of polymer Mw on endosomolytic ability has been the most widely studied characteristic, commonly quantitated using a transfection assay (Jeong et al, 2001; Remy et al, 1998; Godbey et al, 1999a; van de Wettering et al, 1997). Godbey and colleagues investigated the Mw dependence of PEI and determined that as the Mw increased, so did transfection efficiency (Godbey et al, 1999a). However some reports have detailed an increase in gene transfection with a decrease in PEI Mw (Fischer et al, 1999). In contrast, when the transfection efficiency of DMAEMA polymers in the Mw range 4-817kDa was examined, polymers > 300kDa were shown to better transfection agents than their low Mw counterparts (Van de Wettering et al, 1997). Considering these conflicting results, it was decided to examine the effect of Mw on endosomolytic ability with a view to synthesising lead PAA structures with enhanced membrane-destabilising properties. This was performed by examining the endosomolytic ability of ISA 23 polymers of different Mw.

ISA 23 polymers of different Mw were denoted A, B and C. ISA 23 was synthesised as described previously (Richardson et al, 1999a). Polymer A was isolated by ultrafiltration of the product through a membrane with a nominal cut-off of 25,000Da. The portion retained by the membrane was lyophilised. The filtrate was retained and subsequently ultrafiltered through a membrane with a nominal cut-off of

15,000Da. The portion retained by the membrane was denoted B and lyophilised. The filtrate was retained and ultrafiltered through a membrane with a nominal cut-off of 5,000Da. The portion retained by the membrane was denoted C and lysophilised. All polymers were characterised by GPC, NMR and viscometric measurements. The structure of ISA 23 and the characteristics of A, B and C ISA 23 polymers are shown in figure 7.1.

Commonly, efficiency of transfection is used to assess the degree of endosomal destabilisation. However it is important to note that transfection efficiency is also governed by the size and charge of the resulting polyplexes, which in turn is dependent on the experimental protocol of complex formation. Also, factors such as nuclear trafficking of the polyplex, gene expression and cell type (discussed in chapter 3) can also influence efficiency. Therefore, here pH-dependent RBC lysis, SEM and toxin cytosolic delivery were chosen as model systems to examine the endosomolytic ability of these new PAAs.

The long-term aim of this project was to develop therapeutically active PAA-constructs, therefore it was also considered important to examine the biological properties of PAA-toxin conjugates. As discussed in chapter 1, conjugation of polymers to protein drugs offers many advantages, including reduced immunogenicity, increased protein stability and prolonged circulating half-life (Ulbrich et al, 2000; Seymour et al, 1991; Duncan, 2000; reviewed in Harris et al, 2001). Although ISA 1 is cationic, and therefore would be unsuitable for i.v. administration due to a hepatotropic pharmacokinetic profile (Richardson et al, 1999a), it was shown to enhance the cytotoxicity of gelonin (chapter 4). Therefore it was thought useful to initially assess whether an ISA 1-gelonin conjugate would retain cytotoxicity *in vitro* activity against B16F10 cells.

An ISA 1-gelonin conjugate was synthesised by Professor P. Ferruti. Gelonin was dissolved in DDW and 1,4 bisacryoylpiperazine was added. The mixture was left to react for 5h before addition of 2-methylpiperazine. The reaction mixture was maintained for 3 days at r.t. under a nitrogen atmosphere. After this time 1,4 bisacryoylpiperazine and 1, 2-bis(2-hydroxyethylamino)ethane were added to the reaction mixture, which was left to react for 24h. Morpholine was then added to act as a chain terminator, in order to saturate all of the residual double bonds that are present. The conjugate was then treated with HCl (39% (v/v)) and ultrafiltered through a

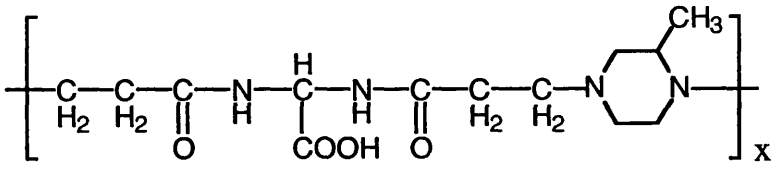

Figure 7.1 Structure of ISA 23. Polymers of different Mw were denoted A (Mw 33,100, Mn 20,300); B (Mw 23,800, Mn 18,200) and C (Mw 12,000, Mn 9,000).

membrane with nominal cut-off 30,000Da. After lyophilisation, the conjugate was characterised using GPC analysis. Its structure is shown in figure 7.2.

7.2 Methods

The structure of ISA 23 and the characteristics of the A, B and C polymers are shown in figure 7.1. The ISA 1-gelonin construct and its chemical characteristics are shown in figure 7.2. The PAAs A, B and C were tested for their ability to deliver toxins to B16F10 cells. This PAA/toxin cytotoxicity experiment is described in detail in chapter 2, section 2.3.8. PAAs A, B and C were also tested for their ability to lyse RBCs in a pH-dependent manner. This experimental protocol is detailed in chapter 2, section 2.3.14. After incubation with A, B and C, RBCs were subject to SEM analysis and this protocol is described in chapter 2, section 2.3.15. The cytotoxicity of the ISA 1-gelonin conjugate towards B16F10 cells is described in chapter 2, section 2.3.6.

7.3 Results

7.3.1 Investigation of the effect of ISA 23 Mw on pH-dependent haemolysis

The PAAs A, B and C (1mg/mL) were incubated with RBCs at pH values of 5.5, 6.5 and 7.4 to assess the effect of PAA Mw on their haemolytic ability. A 15min incubation with A, B and C caused 56%, 51% and 62% lysis respectively at the representative endosomal pH of 6.5 (figure 7.3a). After a 1h incubation with RBCs at pH 6.5, A, B and C caused 59%, 59% and 58% haemolysis respectively (figure 7.3b). Lysis caused by A, B and C at pH 5.5 was less than at pH 6.5 and haemolysis values < 50% was observed at both time points. At pH 7.4, lysis caused by A, B and C was minimal (< 6%). Haemolysis caused by PBS buffer and dextran controls was indicative of membrane stability at pH values between 5.5-7.4.

7.3.2 SEM of RBCs after incubation of ISA 23 of different Mw

RBCs were incubated with PAAs (1mg/mL) for 1h. RBC morphology was normal after exposure of A, B and C at pH 7.4 (figure 7.4a-c). After incubation of polymers A, B and C, at pH 6.5 and 5.5 however, RBC morphology changed significantly. RBCs adopted an amorphous membrane mass or crystalline appearance at both pH values which indicated a high degree of membrane fusion (figure 7.4a-c). In all cases disruption of RBC morphology looked significantly worse at pH 5.5 than 6.5.

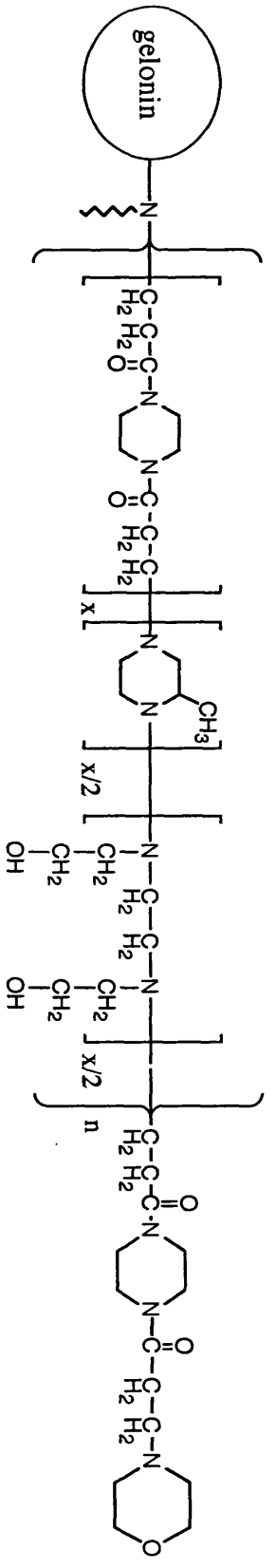

Figure 7.2 Structure of ISA 1-gelonin (Mw 37, 405)

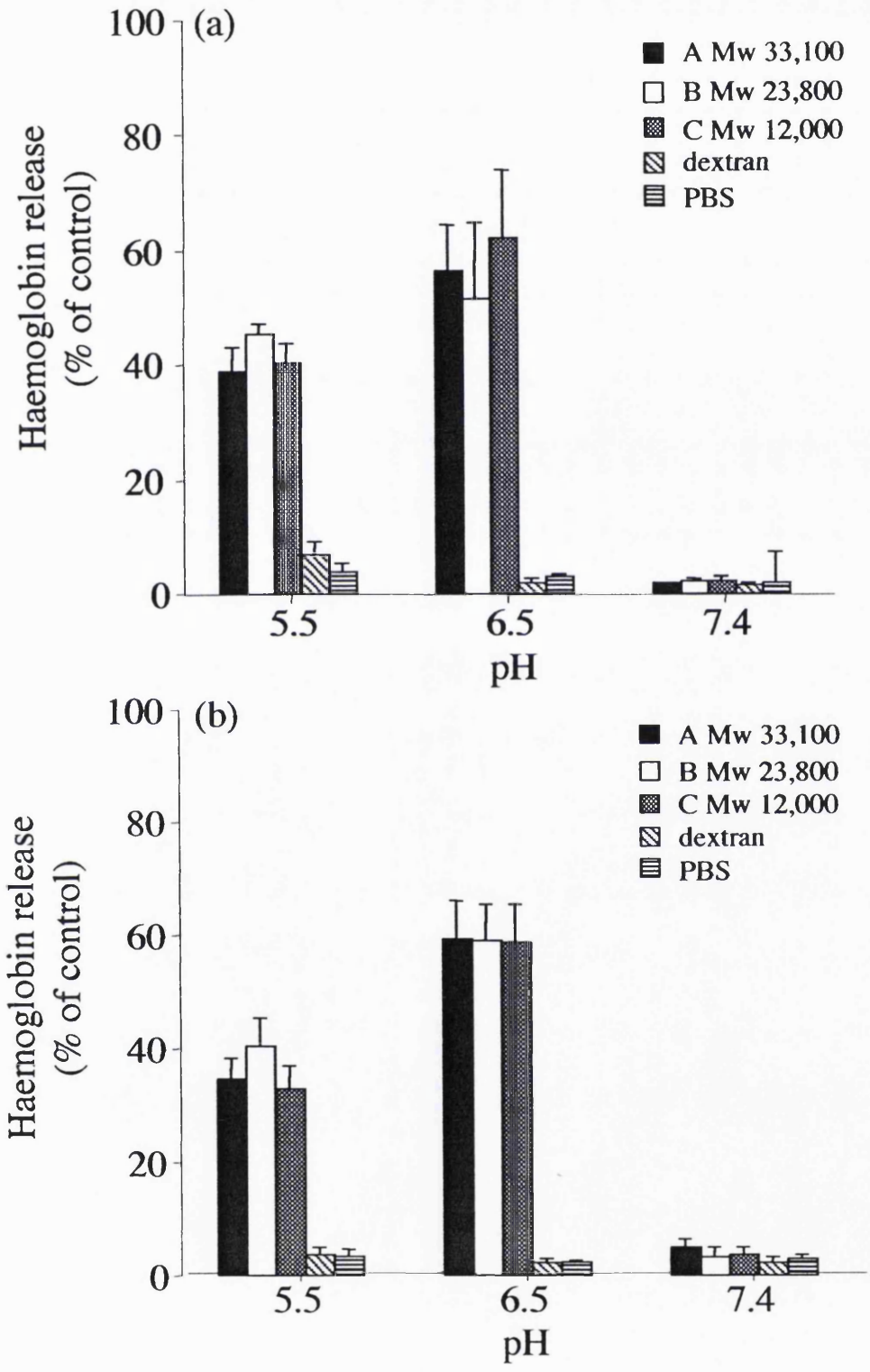

Figure 7.3 Haemolysis of rat RBC's after incubation with polymers (1mg/mL). Dextran and PBS were used as controls. Panel (a) shows haemoglobin release after 15min; (b) 1h. Data represents mean ± S.D. (n=3).

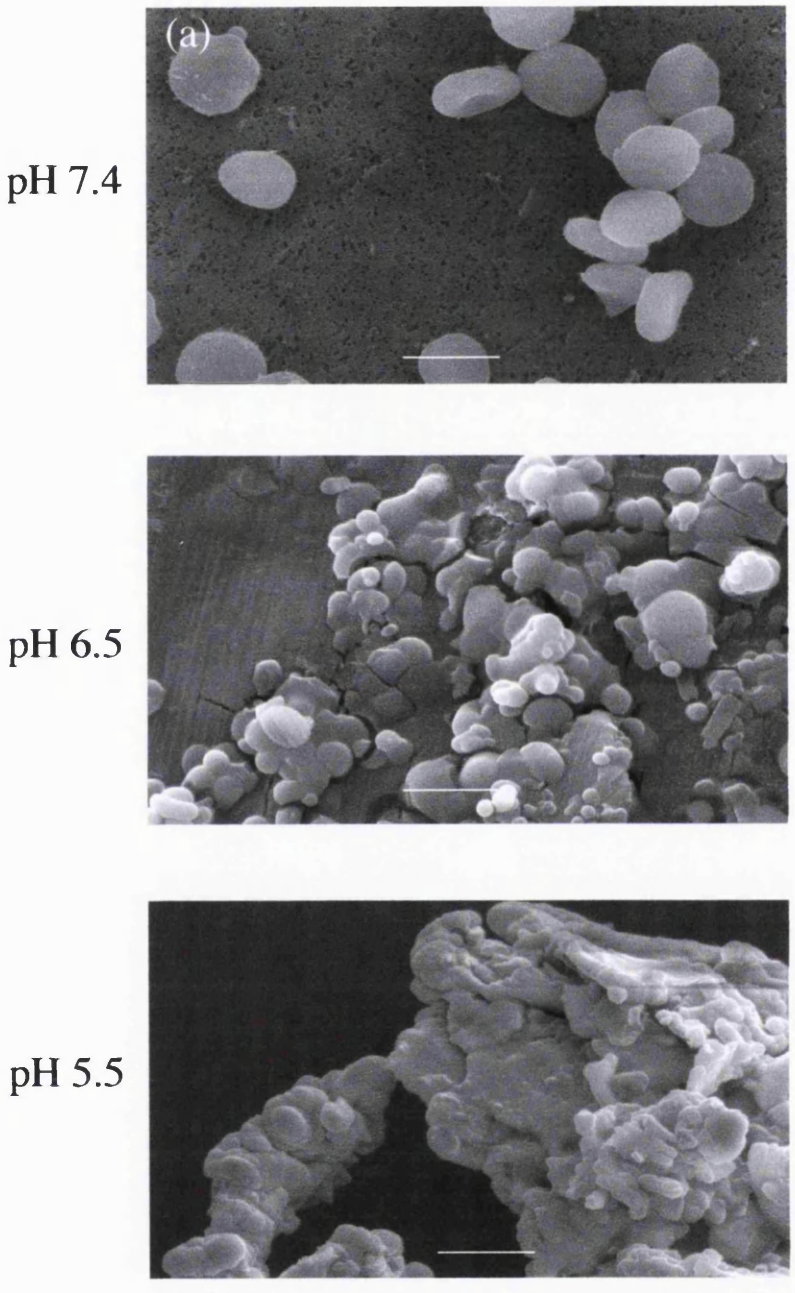

Figure 7.4 Effect of pH on RBC morhology after incubation with PAAs (1mg/mL) for 1h. Panel (a) A (size bar 5μm); (b) B (size bar 5μm); (c) C (size bar 5μm).

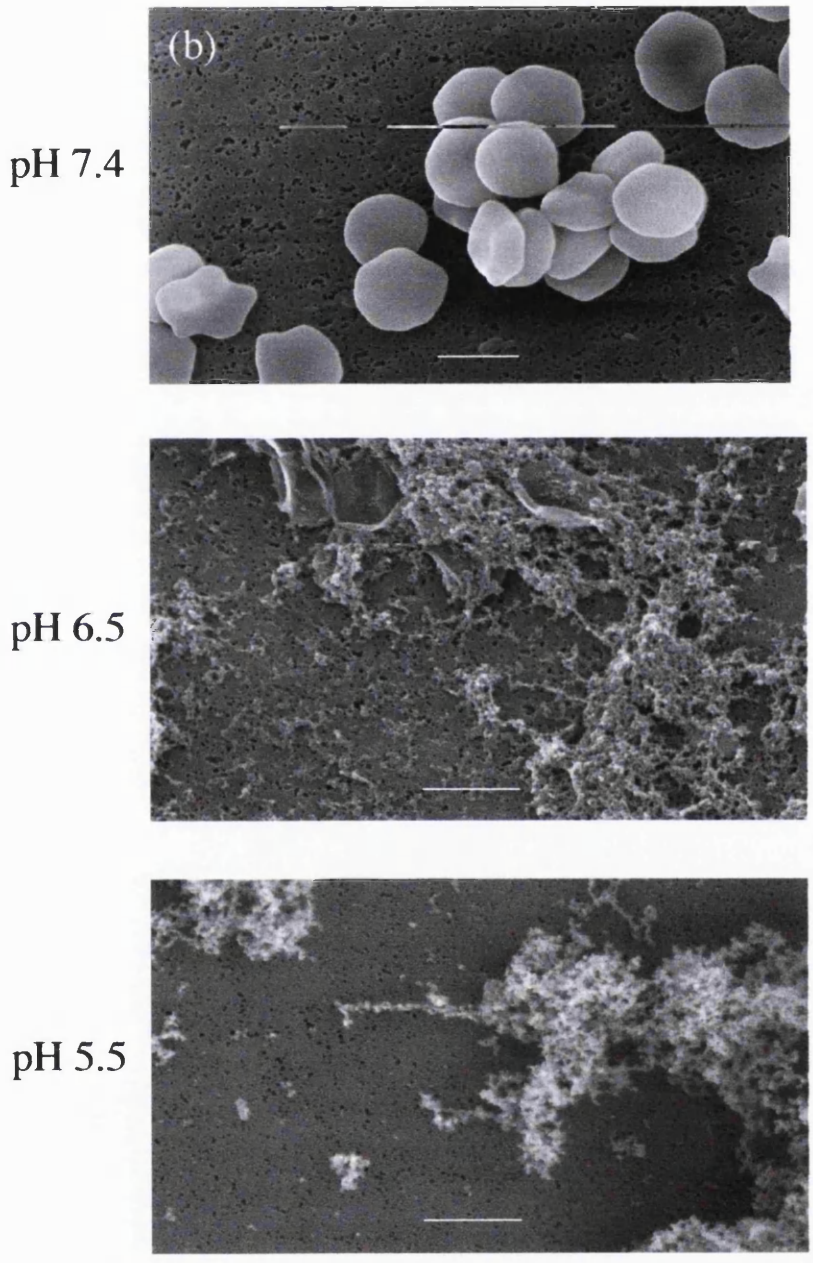

Figure 7.4 Cont.

pH 7.4

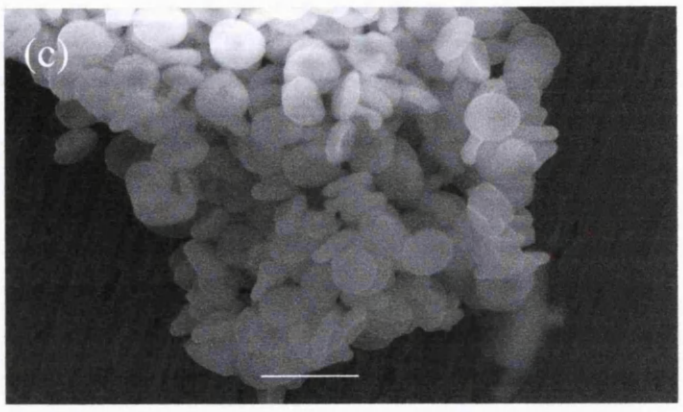

pH 6.5

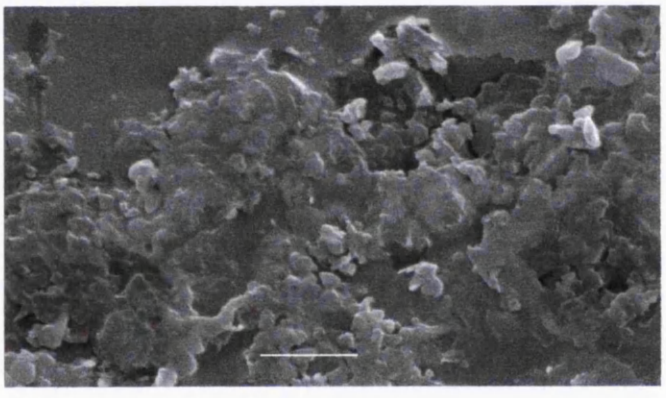

pH 5.5

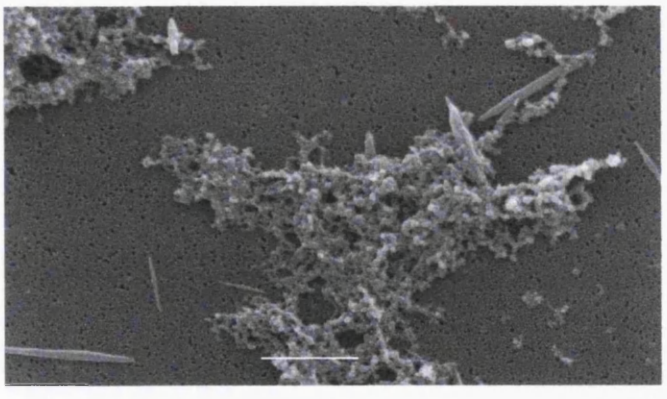

Figure 7.4 Cont.

7.3.3 Investigation of the effect of ISA 23 Mw on their cytotoxicity alone and in combination with gelonin towards B16F10 cells

The PAAs ISA 23, A, B and C were all non-toxic, displaying IC_{50} values >2mg/mL (figure 7.5a). When these PAAs were added in combination with a non-toxic concentration of gelonin, no increase in cytotoxicity was observed (figure 7.5b).

7.3.4 Investigation of the cytotoxicity of an ISA 1-gelonin conjugate towards B16F10 cells

The cytotoxicity of ISA 1 alone and added in combination with 1.4μg/mL gelonin towards B16F10 cells was > 2mg/mL and 0.55 ± 0.12mg/mL respectively (Pattrick et al, 2001; chapter 4). The amount of gelonin conjugated to ISA 1 was not evaluated due to the small amount of conjugate recovered (~ 5mg). However from GPC analysis the sample contained ~ 1:1 gelonin:ISA 1 loading, however free PAA was also present in the sample. Incubation of the ISA 1-gelonin conjugate with B16F10 cells resulted in a slight decrease in cytotoxicity compared to ISA 1 alone, with the IC_{50} value dropping to 1.12 ± 0.21mg/mL (figure 7.6).

7.4 Discussion

A major goal in developing an effective polymer-based intracytoplasmic delivery system lies in increasing polymer-endosomal membrane interaction and disruption, allowing efficient release of the endocytosed therapeutic agent from the endosome into the cytoplasm. pH-Dependent haemolysis was initially used to investigate the effect of ISA 23 Mw on their membrane activity. In addition it was used to assess the potential of these PAAs to disrupt endosomes as it has been shown previously that there is a correlation between haemolytic activity at pH 6.5 and endosomal disruption (Plank et al, 1994; Plank et al, 1998). It was surprising that the haemolytic ability of the PAAs A, B and C were similar at each pH value. This suggests that in the Mw range tested, PAA-membrane interaction is not dependent on Mw and other parameters are responsible. Morphological analysis of RBCs showed a loss of RBC morphology at pH 6.5 and 5.5. However the loss in RBC morphology appeared significantly worse at pH 5.5 than 6.5. This disagrees with haemolysis assays which showed a greater degree of haemoglobin release at pH 6.5 than at 5.5. This suggests that RBC morphology does not necessarily reflect the amount of haemoglobin release.

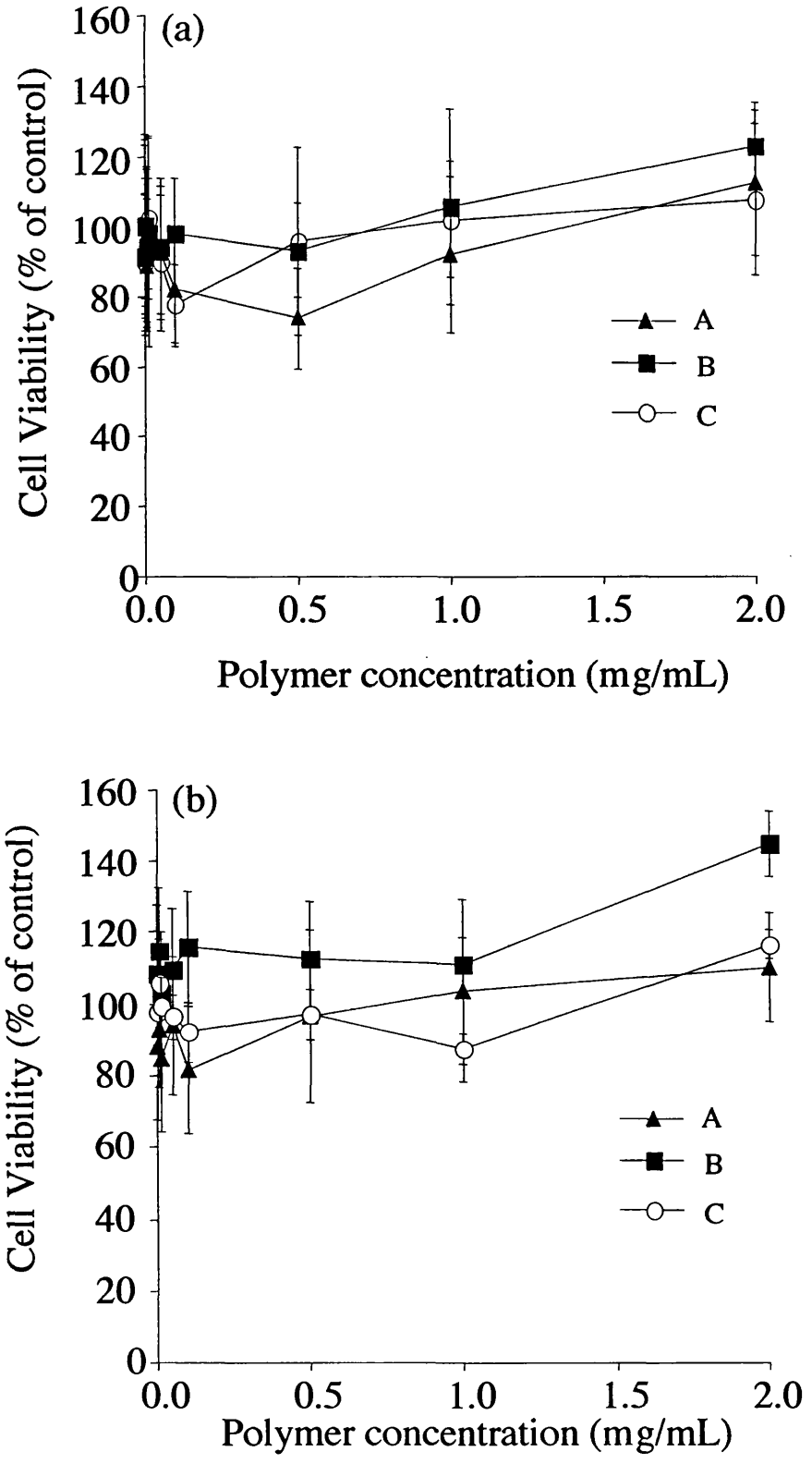

Figure 7.5 Cytotoxicity of ISA 23 of different Mw towards B16F10 cells. Panel (a) shows cytotoxicity of A, B and C alone; (b) cytotoxicity of A, B and C co-incubated with 1.4μg/mL gelonin. Data represents mean ± S.D. (n=18).

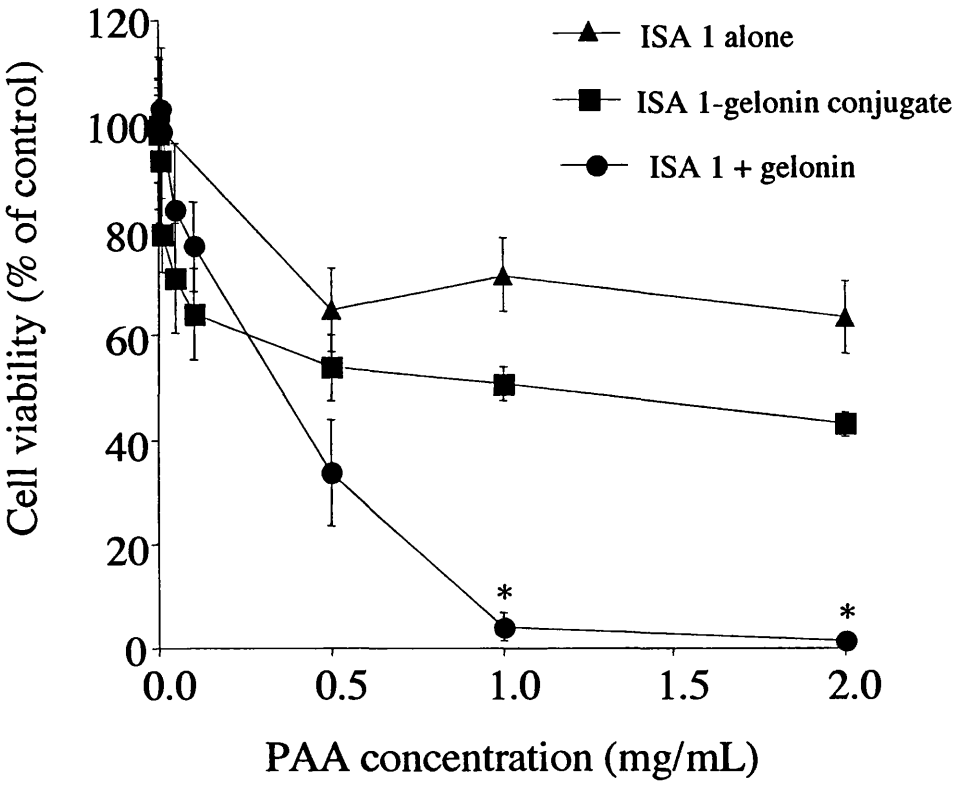

Figure 7.6 Cytotoxicity of ISA 1, ISA 1-gelonin and ISA 1 co-incubated with 1.4μg/mL gelonin towards B16F10 cells. Cells were incubated with toxin for 67h and viability assessed using the MTT assay. Data represent mean ± S.D. (n=18). A student's two-tailed t-test was performed on the cytotoxicity of PAA/toxin combinations versus cytotoxicity of PAA alone to assess the level of statistical significance. P values were designated as follows: NS p= > 0.05; * p < 0.01

The membrane lytic activity of A, B and C at pH 6.5 was not reflected in toxin delivery assays, as all PAAs were unable to cause cytotoxicity when added in combination with gelonin. A possibility for the lack of correlation between pH-specific erythrocyte disruption and gelonin delivery could be due to differential trafficking pathways of toxin and PAA leading to PAA and gelonin residing in different intracellular compartments (discussed in chapter 4). It was theorised in chapter 4 that increasing the local concentration of PAA and gelonin by conjugation would increase the efficacy of toxin cytosolic delivery and prevent differential trafficking of the PAA and toxin (if this indeed occurs). However the activity of the ISA 1-gelonin conjugate towards B16F10 cells was almost completely abolished compared to the activity of the mixture. There are a few possible reasons for the inactivity of ISA 1-gelonin. For example, conjugation of gelonin to ISA 1 may sterically block the active site of gelonin or sterically hinder the ability of ISA 1 to change conformation at acidic pH. In addition, conjugation may reduce the cellular association of ISA 1.

Although none of these theories have been validated, evidence from other studies suggests that all these factors may be responsible. Conjugation of a tumour-specific antibody (B72.3) to an HPMA copolymer resulted in a loss of tumour targeting by the antibody, due to masking of the antigen-recognition site of the antibody by polymer chains (Seymour et al, 1991). PEG conjugation to the endosmolytic polymers PEI and DMEAMA was shown to result in a total loss of polymer-mediated transfection. This was probably due to a reduction in cellular uptake due to neutralisation of polyplex charge, and a restriction in polymer conformation (Choi et al, 2001a; Rungsardthong et al, 2001; Zuidam et al, 2000; Erbacher et al, 1999a). A total loss in endosomolytic ability was also observed for ISA 23-PEG conjugates (PEG Mw 2,000; Mw 4,000) (figure 7.7). Constructs were unable to mediate lysis of RBCs within the pH range of 5.5-7.4, and were unable to promote cytosolic delivery of gelonin (Khaled, 2000). Large molecules conjugated to PAAs have thus far have been incorporated directly within the PAA backbone. As the conformation of the PAA backbone is essential for its inherent endosomolytic ability, it is not surprising that the activity of PAA-conjugates was reduced. It may be advantageous to bind gelonin to PAAs via streptavidin-biotin binding. Both the endosomolytic polymer PPAAc and an anti-CD3 antibody were biotinylated and a complex was formed by mixing the two conjugates with streptavidin. The antibody was able to direct the complex to CD3-expressing Jurkat T-cells and PPAAc retained its endosomolytic ability causing release of the complex into the cytosol (Lackey et al, 2002). Another method of

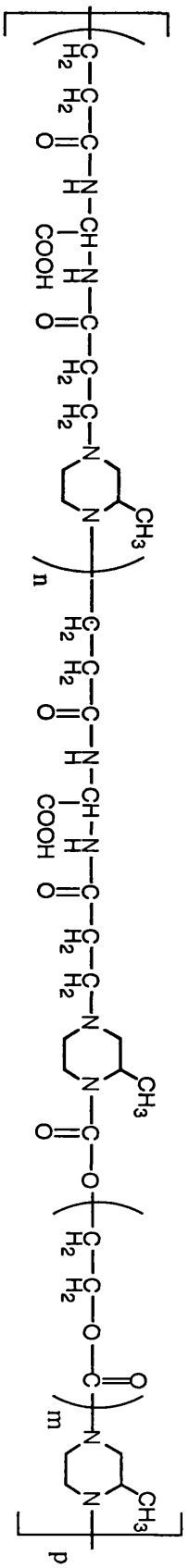

Figure 7.7 Structure of ISA 23-PEG. ISA 23-PEG 2000 n=7; m=45; p=10. ISA 23-PEG 4000 n=14; m=90; p=5

macromolecule incorporation is conjugation to PAAs via a spacer group. Many of the polymer-conjugates in clinical evaluation today include a spacer group that not only allows the active material to be released in a specific pharmacological location, but acts to separate the active drug from the polymeric backbone so that the latter does not interfere with the biological activity of the bound material (Duncan 1992; Ringsdorf, 1975). The addition of a spacer moiety between a PAA molecule and gelonin may reduce steric hinderance of the polymer coil and reduce any masking of the gelonin active site to restore endosomolytic ability.

7.5 Conclusions

The factors governing enhanced polymer-mediated membrane interaction and destabilisation have still to be elucidated, as Mw in this instance has proved not to have a significant effect. However the Mw variation of the PAAs tested may not have been distinct enough to make an accurate comparison. Many groups have found that enhancing polymer or peptide hydrophobicity significantly improved membrane interaction (Murthy et al, 1999; Suda et al, 1992; Van Kan et al, 2001) thus altering PAA structure in this way may increase PAA-mediated endomembrane lysis.

Conjugation of gelonin to ISA 1 resulted in loss of endosomolytic ability. This effect may have been due to steric hinderance caused by the gelonin molecule. In future other methods to bind gelonin to PAAs should be investigated, such as conjugation via a spacer moiety or construction of a biotin-streptavidin complex.

CHAPTER 8

GENERAL DISCUSSION

General discussion

The emergence of novel macromolecular drugs such as genes, ribozymes and toxins that require cytosolic access means that the pressure to identify intracytoplasmic carriers has never been greater (Kircheis et al, 2001a). Although the majority of research to date has focused on the use of viral vectors to mediate intracytoplasmic delivery of these drugs, safety issues (Kielian et al, 1999; reviewed in Verma and Somia, 1997) have led to increased interest in non-viral delivery systems such as cationic lipids and polymers. Although many non-viral transfection agents have been identified (reviewed in Garnett, 1999), they commonly display lower transfection efficiencies compared to their viral counterparts (Graham and van der Eb, 1973; Cheung et al, 2001), and therefore recent research has focused on improving their efficacy. To achieve this, transfection agents have been combined with membrane destabilising compounds such as fusogenic peptides and cholesterol to improve their ability to lyse intracellular membranes (Choi et al, 2001b; Crook et al, 1998, Mahato et al, 1999; Lee et al, 2001), or conjugated to receptors to increase endocytic uptake (reviewed in Kircheis et al, 2001a; reviewed in Wu and Wu, 1998). Much attention has also been directed towards evaluating the biophysical parameters of carriers and their complexes (reviewed in Godbey et al, 1999a; Midoux et al, 1999; Wolfert et al, 1999). In addition, fluorescence microscopy has also proved a useful technique to evaluate the subcellular trafficking of non-viral carriers and their payloads (Schaffer et al, 1999; Yoo and Juliano 2000).

Synthetic, pH-sensitive polymers that can mimic the function of fusogenic peptides such as PEI and PEAAc have also been investigated (Godbey et al, 1999a; Midoux and Monsigny, 1999; Kyriakides et al, 2002). The specificity of these polymers for endomembrane lysis means that there is no additional requirement for membrane destabilising agents to achieve efficient transfection. However, these vectors are still limited by toxicity (Godbey et al, 1999a; Van de Wetering et al, 1997) and non-specific interactions with serum proteins and the RES after i.v. administration (Lecocq et al, 2000; Verbaan et al, 2001). Therefore the main challenges are to decrease these non-specific interactions (reviewed in Zuber et al, 1999) and to increase tissue-specific targeting (Kircheis et al, 2001b). In addition, efforts have focused towards providing evidence for their endosomolytic ability. As well as using indirect methods such as transfection, research has moved towards directly demonstrating intracellular membrane

perturbation, using techniques such as subcellular fractionation and fluorescence microscopy (Klemm et al, 1998; Merdan et al, 2002a).

The vast majority of both cationic and endosomolytic polymers are being developed for cancer therapy. This is by far the most important proposed application of gene and antisense therapy and many clinical trials are underway (figure 8.1). More than two-thirds of gene therapy trials employ viral vectors, only 13% use lipid vectors and ~ 10% use naked DNA. As of yet, polymeric vectors have not advanced into clinical trials due to problems of vector toxicity (Merdan et al, 2002b).

Why investigate PAAs?

PAAs were initially identified as potential drug carriers due to their water-solubility, degradation profile (Ranucci et al, 1991) and the ability of drug conjugates to display activity against a mouse tumour model (Ferruti et al, 2002). However, demonstration of a pH-dependent conformational change within the PAA backbone (Duncan et al, 1994) provided the opportunity to design pH-responsive PAAs which selectively lysed intracellular membranes (Richardson et al, 1999a). First evidence for potential endosomolytic ability was demonstrated by PAA-mediated RBC lysis at pH 6.5 and 5.5 but not at pH 7.4 (Richardson et al, 1999a). In addition, structures were shown to display little toxicity against a variety of immortal cell lines (> 2mg/mL), display a reduced liver uptake after intravenous administration to rats (< 10% after 5h), and passively target tumours by the EPR effect (Richardson et al, 1999a). The potential of PAAs to act as endosomolytic agents was further demonstrated by their ability to transfect cells *in vitro* using a β-galactosiadse marker gene (Richardson et al, 1999b; Man et al, 1999), and *in vivo* after detection of both ISA 4 and NAGase in the cytosolic fraction of rat liver (Richardson et al, 1999c).

These preliminary experiments outlined the potential of PAAs as intracytoplasmic carriers for macromolecular drugs. Therefore it was considered important that studies should seek further indirect and direct evidence for the endosomolytic activity of PAAs. These experiments are described in this thesis.

Further evidence for PAA-mediated endosomolytic ability

One possible use of PAAs is to act as potential gene delivery agents, and therefore the physico-chemical properties of PAA-DNA complexes was investigated (chapter 3). Experiments reported here demonstrated for the first time PAA IPEC

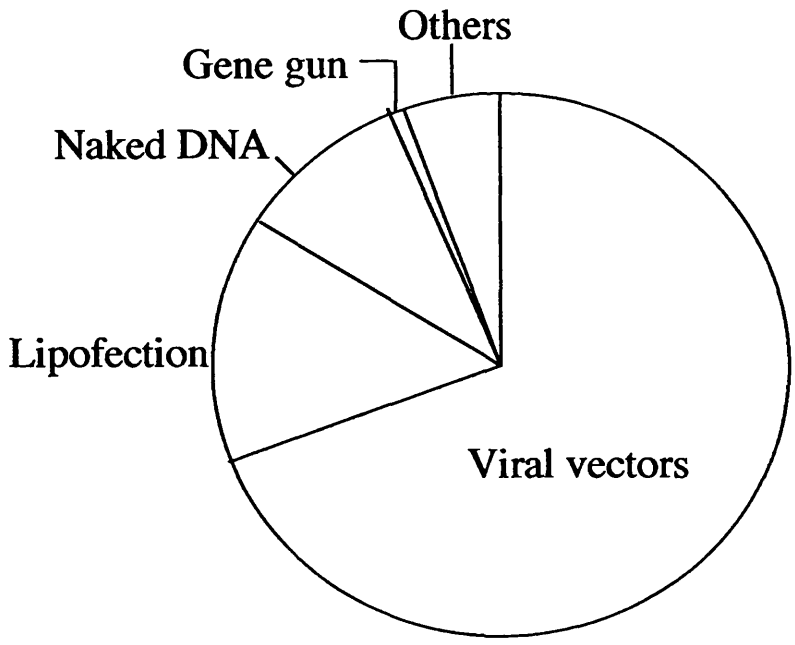

Viral vectors	
Retrovirus	35.8% (n=212)
Adenovirus	27.7% (n=164)
Pox virus	6.2% (n=37)
Adeno-associated virus	2.2% (n=13)
Herpes simplex virus	0.5% (n=3)
Non viral vectors	
Lipofection	13% (n=77)
Naked DNA	9.3% (n=55)
Gene gun	0.9% (n=5)
RNA transfer	0.8% (n=5)

Figure 8.1 Gene therapy vectors used in clinical trials (data from http://www.wiley.co.uk/gene therapy/clinical/).

formation as well as the ability of these IPECs to protect DNA from degradation. Indirect evidence for PAA-mediated endosomolytic activity was also provided by their ability to transfect HepG2 cells with a β-galactosidase marker gene *in vitro* (Richardson et al, 2001). Transfection efficiency is however dependent on many factors in addition to endosomal escape, and therefore it was decided to develop a more accurate model for quantitating endosomolysis. In this new model, RTA and gelonin toxins were chosen for PAA-mediated delivery as a therapeutic effect is observed when cytosolic access is achieved (chapter 4). The hepatotropic PAAs ISA 1 and 4 were able to deliver both toxins to the cytosol of B16F10 cells, however ISA 22 was not (Pattrick et al, 2001). Reasons for this were unclear, and therefore it was decided to investigate PAA-mediated intracellular membrane destabilisation directly using an isolated rat liver lysosomal suspension as a model (chapter 5). ISA 1 and 22 were unable to disrupt outer lysosomal membranes in response to time or pH *in vitro*. However, when the hepatotropic PAA ISA 1 was administered i.v. to rats, for the first time dose- and time-dependent lysosomal perturbation was demonstrated morphologically and quantitatively at doses > 10mg/kg (Pattrick et al, 2002). To provide further direct evidence for the subcellular trafficking of PAAs and to gain insight into the mechanisms responsible for PAA-mediated toxin delivery, fluorescence microscopy was used to visualise labelled PAAs and gelonin (chapter 6). For the first time, PAA accumulation in non-acidic as well as acidic structures was demonstrated, suggesting endocytic uptake and possible endo/lysosomal rupture. This finding was particularly interesting as fluorescent-labelled PEI demonstrated a similar intracellular localisation (Merdan et al, 2002a). Therefore both polymers may be mediating similar methods of vesicle destabilisation. In addition, visualisation of complexes formed between ISA 1 and gelonin provided a possible mechanism for ISA 1-mediated toxin delivery, by causing enhanced gelonin uptake.

Polymer-physico chemical characteristics have been shown to affect the endosomolytic properties of a polymer. Therefore the effect of different Mw analogues of ISA 23 on membrane activity was examined, with a view to synthesising PAAs with improved endosomolytic ability (chapter 7). No correlation between the degree of membrane destabilisation and ISA 23 Mw was observed, suggesting that the Mw range may have been too narrow.

PAA-toxin constructs as anticancer agents?

To move towards the development of a PAA-toxin construct with anti-tumour activity, the endosomolytic ability of an ISA 1-gelonin conjugate was examined (chapter 7). The ISA 1-gelonin conjugate was not able to cause cytotoxicity to B16F10 cells. This loss in activity could be due to steric hinderance caused by conjugation of gelonin directly to the PAA backbone.

Future work

Although substantial evidence for PAA-mediated endosomolytic ability has been inferred from the experiments outlined in this study, it is important that a model system to directly demonstrate and quantitate their ability to destabilise endosomal membranes is established. As yet, this has not been directly demonstrated for any endosomolytic polymer (Godbey et al, 1999b; Yoo and Juliano, 2000; Zuidam et al, 2000). Mechanistic studies have been performed with the endosomolytic polymer PEAAc to analyse its interaction with calcium and sodium-filled phospholipid vesicles. Results showed that the cooperative protonation of 3-5 carboxylate anions within the polymer coil were required to cause membrane permeabilisation (Thomas and Tirrell, 2000). Likewise, knowledge of the mechanism for PAA-mediated membrane rupture (i.e. pore-formation, α-helix transition, proton-sponge mechanism) would allow design of novel PAAs with the optimum structure for endomembrane lysis.

There are a number of methods which could be used to increase the endosomolytic properties of PAAs. Lackey et al, (1999b) demonstrated that altering the structure of PEAAc to PPAAc to increase hydrophobicity caused an increase in the haemolytic properties of the polymer at pH 6. Therefore it would be interesting to examine whether synthesising PAAs with increased hydrophobicity would also cause enhanced endosomolytic properties. Conjugation of fusogenic peptides to PAAs is also likely to improve efficacy. Transfection efficiency was found to be significantly enhanced after the addition of the fusogenic peptide KALA to (DMAEMA)-co-N-vinyl-2-pyrrolidone-PEG-galactose complexes (Lim et al, 2000). Likewise the inclusion of KALA increased the transfection efficiency of poly-L-lysine-PEG complexes (Lee et al, 2002a).

PAA endosomolyic properties may also be enhanced by increasing PAA cellular uptake. Cationic charge has been shown to promote cellular uptake *in vitro* via electrostatic interactions with the negatively charged cell membrane (reviewed in

Kircheis et al, 2001a). Evidence for this was demonstrated in chapter 4 by toxin delivery experiments, where ISA 1 and 4 promoted toxin delivery due to complex formation and enhanced uptake by absorptive endocytosis. However, cationic molecules are often toxic (chapter 1, table 1.4), and are subject to clearance by the RES after i.v. administration (Verbaan et al, 2001; Lecocq et al, 2000). An alternative method to increase cellular uptake of PAAs is by incorporation of cell-binding ligands causing receptor-mediated uptake of the complex. These can be growth factors, hormones, receptor-ligands, integrins or antibodies. One example of a receptor-ligand used to enhance uptake of PEI is transferrin. This was shown to enhance gene transfer in transferrin expressing cell lines *in vitro*. *In vivo*, targeting of transferrin-PEI complexes was only achieved when complexes were shielded by PEG, or a high density of transferrin molecules (reviewed in Kircheis et al, 2001a). However conjugation of transferrin receptor to HPMA caused complexes to display liver tropism *in vivo* (Flanagan, 1987). For targeting to epithelial cells, intergrin-binding peptides such as RGD may be used for conjugation to PAAs. Conjugation of an RGD sequence to thiol-derivatized PEI-DNA complexes was shown to increase transfection efficiency 10- to 100-fold towards integrin-expressing HeLa cells (Erbacher et al, 1999b). Likewise EGF was also shown to enhance transfection efficiency of PEI-PEG-DNA complexes in an overexpressing EGF receptor cell-line A431 (Lee et al, 2002b). Antibodies can also be used to target specific receptors present on certain cell types. An anti-CD3 antibody (64.1)-streptavidin complex was used to bind biotinylated PPAAc polymer and directed receptor-mediated endocytosis of the ternary complex to a Jurkat T-cell lymphoma cell line. The pH-responsive polymer PPAAc caused subsequent translocation of the complex to the cytosol (Lackey et al, 2002).

The long-term aim of this study was to develop a PAA-toxin construct for i.v. administration and tumour targeting. Conjugation of both a ligand and gelonin to PAAs may increase uptake and subsequently increase endosomolytic ability of the construct. However, as direct conjugation of macromolecules to PAAs resulted in a loss in PAA bioresponsiveness (Khaled et al, 2000; chapter 7), conjugation of molecules to PAAs via a spacer moiety or by streptavidin-biotin binding should be investigated. Also of consideration is which PAA structure is to be used in the resultant complex. ISA 1 and 4 were able to cause cytosolic delivery of toxins in B16F10 cells, however both the ISA 1 and 4 structure displays liver tropism after i.v. administration (Richardson et al, 1999a). Shielding of ISA 1 and 4 with PEG may increase the circulating lifetime of complexes *in vivo*, but may also reduce activity of the polymer. ISA 22 displays a long

circulating lifetime. Although ISA 22 was unable to deliver toxins to the cell cytosol when they were added as a mixture, an ISA 22-gelonin-ligand construct may show activity.

Many different constructs can be designed. The PAA constituent of the construct may form the backbone to which the ligand and toxin molecule are linked (figure 8.2a). This model was initially proposed by Helmut Ringsdorf (Rinsdorf, 1975). Alternatively, the PAA could be attached to an immunotoxin (figure 8.2b). As many immunotoxins are limited in their ability to enter the cytoplasm (Press et al, 1998; reviewed in Rhíová, 1998), PAAs could find an application as agents to enhance cytosolic delivery of immunotoxins. Gelonin molecules could also be entrapped within a PAA nanoparticle containing surface adsorbed ligands (figure 8.2c). Thus gelonin molecules would be protected from degradation in the systemic circulation but released into the cytosol via the endosome after cellular uptake. If an active construct can be synthesised, it would represent an effective, novel alternative to immunotoxins for cancer therapy.

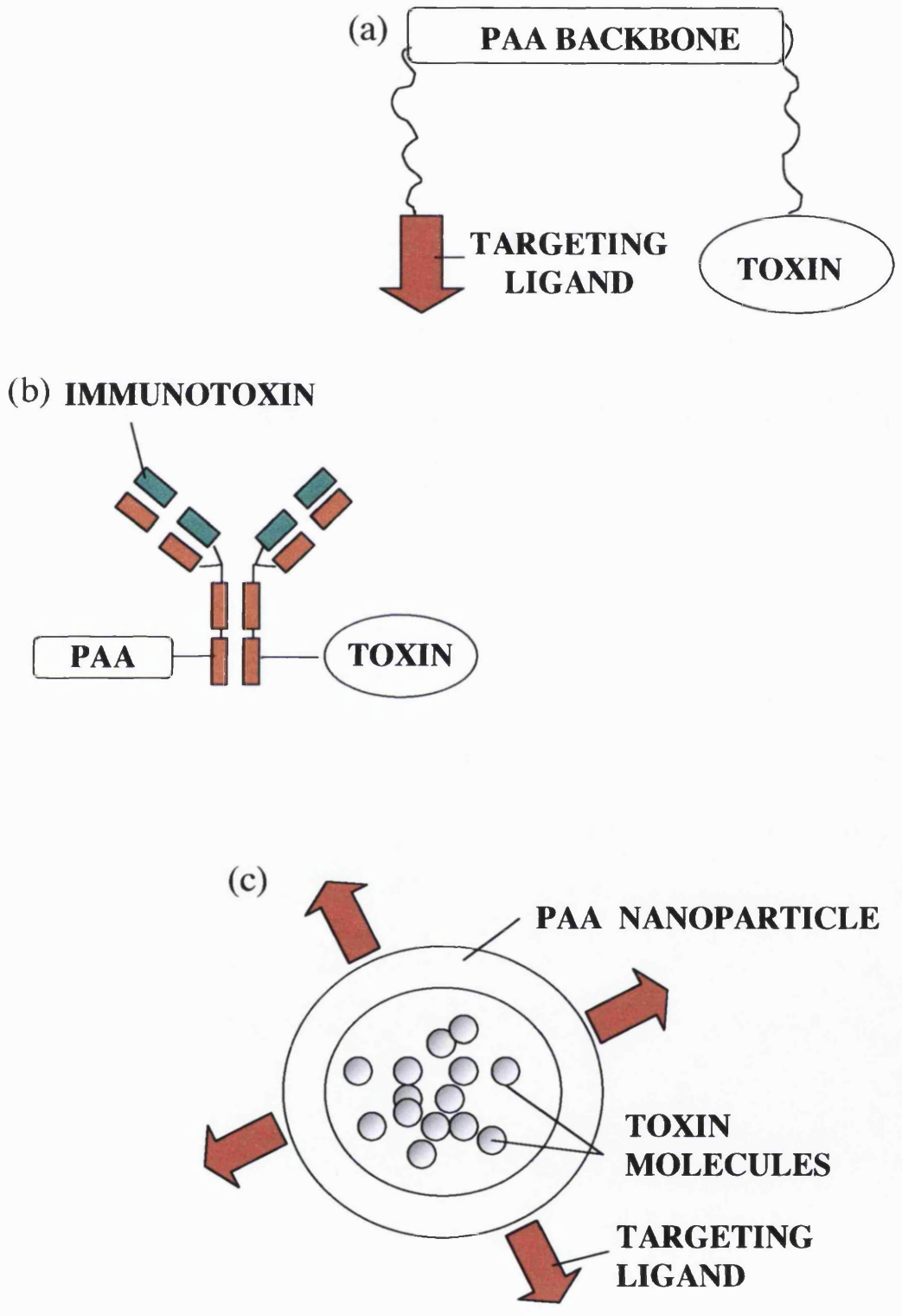

Figure 8.2 Structures of proposed PAA-toxin constructs

REFERENCES

R.H. Argent, A.M. Parrott, P.J. Day, L.M. Roberts, P.G. Stockley, J.M. Lord, S.E. Radford, Ribosome-mediated folding of partially unfolded ricin A-chain, (2000) *Journal of Biological Chemistry*, **275** 9263-9269.

A. Asokan, M.J. Cho, Exploitation of intracellular pH gradients in the cellular delivery of macromolecules, (2002) *Journal of Pharmaceutical Science*, **91** 903-913.

F.M. Ausubel, R. Brent, R.E. Kingston, D.D. Moore, J.G. Seidman, K. Struhl, Preparation and analysis of DNA, In*: Current Protocols in Molecular Biology*, Volume 1, F.M. Ausubel, R. Brent, R.E. Kingston, D.D. Moore, J.G. Seidman, K. Struhl, L.M. Albright, D.M. Coen, A. Varki, V.B. Chanda, Eds., John Wiley & Sons, Inc., USA, 1994 sections 1.2.1-2.5.9.

R. Baluna, E. Coleman, C. Jones, V. Ghetie, E.S. Vitetta, The effect of a monoclonal antibody coupled to ricin A chain-derived peptides on endothelial cells *in vitro*: insights into toxin-mediated vascular damage, (2000) *Experimental Cell Research*, **258** 417-424.

A.J. Barrett and M.F. Heath, Lysosomal enzymes, In: *Lysosomes: a laboratory handbook*, 2nd Edition, J.T. Dingle Eds., Elsevier/North-Holland Biomedical Press 1977 p. 19-146.

W.M. Becker, L.J. Kleinsmith, J. Hardin, Membranes: their structure, function and chemistry, In: *The World of the Cell*, 4th Edition, E. Mulligan. L. Cox, E. Dahlgren, S. Weisberg, L. Kenney, Eds., Addison Wesley Longman, Inc., San Francisco, 2000 p. 163-200.

G. Bellon, L. Michel-Calemard, D. Thouvenot, V. Jagneaux, F. Poitevin, C. Malcus, N. Accart, M.P. Layani, M. Aymard, H. Bernon, J. Bienvenu, M. Courtney, G. Doring, B. Gilly, R. Gilly, D. Lamy, H. Levrey, Y. Morel, C. Paulin, F. Perraud, L. Rodillon, C. Sene, S. So, F. Touraine-Moulin, A. Pavirani, Aerosol administration of a recombinant adenovirus expressing CFTR to cystic fibrosis patients: a phase I clinical trial, (1997) *Human Gene Therapy*, **8** 15-25.

S.J. Bird, J.B. Lloyd, Mechanism of lysosome rupture by dipeptides, (1995) *Cell Biochemistry and Function*, **13** 79-83.

V.A. Bloomfield, DNA condensation by multivalent cations, (1997) *Biopolymers: Nucleic Acid Science,* **44** 269-282.

O. Boussif, F. Lezoualch, M.A. Zanta, M.D. Mergny, D. Scherman, B. Demeneix, J-P. Behr, A versatile vector for gene and oligonucleotide transfer into cells in culture and *in vivo*: polyethylenimine, (1995) *Proceedings of the National Academy of Science of the United States of America,* **92** 7297-7301.

H. Brem, S. Piantadosi, P.C. Burger, M. Walker, R. Selker, N.A. Vick, K. Black, M. Sisti, S. Brem, G. Mohr, P. Muller, R. Morawetz, S.C. Schold, Placebo-controlled trial of safety and efficacy of intra-operative controlled delivery by biodegradable polymers of chemotherapy for recurrent gliomas. The Polymer-brain Tumor Treatment Group, (1995) *Lancet*, **345** 1008-1012.

M.D. Brown, A.G. Schatzlein, I.F. Uchegbu, Gene delivery with synthetic (non viral) carriers, (2001) *International Journal of Pharmaceutics*, **229** 1-21.

P. Casellas, B.J. Bourrie, P. Gros, F.K. Jansen, Kinetics of cytotoxicity induced by immunotoxins. Enhancement by lysosomotropic amines and carboxylic ionophores, (1984) *Journal of Biological Chemistry*, **259** 9359-9364.

P.L. Chang, Calcium phosphate-mediated transfection, In: *Gene Therapeutics: Methods and Applications of Direct Gene Transfer,* J.A. Wolff, Ed., Birkhäuser Boston Press: Massachusetts, USA, 1994 p. 157-179.

J.W. Chen, T.L. Murphy, M.C. Willingham, I. Pastan, J.T. August, Identification of two lysosomal membrane glycoproteins, (1985*) Journal of Cell Biology,* **101** 85-95.

C.Y. Cheung, N. Murthy, P.S. Stayton, A.S. Hoffman, A pH-sensitive polymer that enhances cationic lipid-mediated gene transfer, (2001) *Bioconjugate Chemistry*, **12** 906-910.

Y.H. Choi, F. Lui, J.S. Kim, Y.K. Choi, J.S. Park, S.W. Kim, Polyethylene glycol-grafted poly-L-lysine as polymeric gene carrier, (1998) *Journal of Controlled Release*, **54** 39-48.

J.H. Choi, J.S. Choi, H. Suh, J.S. Park, Effect of poly(ethylene glycol) grafting on polyethylenimine as a gene transfer vector *in vitro*, (2001a) *Bulletins of the Korean Chemical Society*, **22** 46-52.

J.S. Choi, E.J. Lee, H.S. Jang, J.S. Park, New cationic liposomes for gene transfer into mammalian cells with high efficiency and low toxicity (2001b), *Bioconjugate Chemistry*, **12** 108-113.

C.J. Chu, J. Dijkstra, H. Lai, F.C. Szoka, Efficiency of cytoplasmic delivery by pH-sensitive liposomes to cells in culture, (1990) *Pharmaceutical Research*, **7** 824-834.

M. Clague, Molecular aspects of the endocytic pathway, (1998) *Biochemistry Journal*, **336** 271-282.

D.J.A. Crommelin, W.E. Hennink, G. Storm, Drug targeting systems: Fundamentals and applications to parenteral drug delivery, In: *Drug Delivery and Targeting for Pharmacists and Pharmaceutical Scientists*, A.M. Hillery, A.W. Lloyd, J. Swarbrick, Eds., Taylor & Francis Press: London, England and New York, USA, 2001 p. 117-144.

K. Crook, B.J. Stevenson, M. Dubouchet, D.J. Porteous, Inclusion of cholesterol in DOTAP transfection complexes increases the delivery of DNA to cells in vitro in the presence of serum, (1998) *Gene Therapy*, **5** 137-143.

M.P. Curran, K.L. Goa, Pegfilgrastim, (2002) *Drugs*, **62** 1207-1213.

P.R. Dash, M.L. Read, L.B. Barrett, M.A. Wolfert, L.W. Seymour, Factors affecting blood clearance and *in vivo* distribution of polyelectrolyte complexes for gene delivery, (1999) *Gene Therapy*, **6** 643-650.

M.E. Davis, Non-viral gene delivery systems, (2002) *Current Opinion in Biotechnology, 13 128-131.*

C. De Duve, B.C. Pressman, R. Gianetto, R. Wattiaux, F. Appelmans, Tissue fractionation studies, (1955) *Biochemistry*, **60** 604-617.

C. De Duve, R. Wattiaux, Functions of lysosomes, (1966) *Annual Reviews in Physiology*, **28** 435-492.

R.T. Dean, Methods for the isolation of lysosomes, In: *Lysosomes: a laboratory handbook*, 2nd Edition, J.T. Dingle Eds., Elsevier/North-Holland Biomedical Press 1977 p. 1-18.

T. Decharneux, F. Dubois, C. Beauloye, S. Wattiaux-De Coninck, R. Wattiaux, Effect of various flavonoids on lysosomes subjected to an oxidative or an osmotic stress, (1992) *Biochemical Pharmacology*, **44** 1243-1248.

D.E. Discher, P. Carl, New insights into red cell network structure, elasticity, and spectrin unfolding-a current review, (2000) *Cell Molecular Biology Letters*, **6** 593-606.

S. Dokka, Y. Rojanasakul, Novel non-endocytic delivery of antisense oligonucleotides, (2000) *Advanced Drug Delivery Reviews*, **44** 35-49.

G. M. Dubowchik, M.A. Walker, Receptor-mediated and enzyme-dependent targeting of cytotoxic anticancer drugs, (1999) *Pharmacology and Therapeutics*, **83** 67-123.

R. Duncan, Biological effects of soluble synthetic polymers as drug carriers, (1985) *Critical Reviews of Therapeutic Drug Carrier Systems,* **1** 281-310.

R. Duncan, Drug-polymer conjugates: a potential for improved chemotherapy, (1992) *Anti-Cancer Drugs*, **3** 175-210.

R. Duncan, P. Ferruti, D. Sgouras, A. Tuboku-Metzger, E. Ranucci, F. Bignotti, A polymer-triton X-100 conjugate capable of pH-dependent red blood cell lysis: A model system illustrating the possibility of drug delivery within acidic intracellular compartments, (1994) *Journal of Drug Targeting*, **2** 341-347.

R. Duncan, S. Dimitrijevic, E.G. Evagorou, The role of polymer conjugates in the diagnosis and treatment of cancer, (1996) *STP Pharma Sciences*, **6** 237-263.

R. Duncan, Polymer Therapeutics, (2000) *Business Briefing PharmaTech, World Markets Research Centre* p. 178-184.

R. Duncan, S. Gac-Breton, R. Keane, R. Musila, Y.N. Sat, R. Satchi, F. Searle, Polymer-drug conjugates, PDEPT and PELT: basic principles for design and transfer from the laboratory to the clinic, (2001) *Journal of Controlled Release*, **74** 135-146.

Y. Endo, K. Mitsui, M. Motizuki, K. Tsurugi, The mechanism of action of ricin and related toxic lectins on eukaryotic ribosomes. The site and the characteristics of the modification in the 28S ribosomal RNA caused by the toxins, (1987) *Journal of Biological Chemistry,* **262** 5908-5912.

P. Erbacher, T. Bettinger, P. Belguise-Valladier, S. Zou, J.L. Coll, J-P. Behr, J-S, Remy, Transfection and physical properties of various saccharide, poly(ethylene glycol), and antibody-derivatised poly(ethylenimine)s (PEI), (1999a) *Journal of Gene Medicine*, **1** 210-222.

P. Erbacher, J-S. Remy, J-P. Behr, Gene transfer with synthetic virus-like particles via the integrin-mediated endocytosis pathway, (1999b) *Gene Therapy*, **6** 138-145.

P.L. Felgner, T.R. Gadek, M. Holm, R. Roman, H.W. Chan, M. Wenz, J.P. Northrop, G.M. Ringold, M. Danielsen, Lipofection: a highly efficient, lipid-mediated DNA-transfection procedure, (1987) *Proceedings of the National Academy of Science of the United States of America,* **84** 7413-7417.

S. Ferrari, A. Pettenazzo, N. Garbati, F. Zacchello, J-P. Behr, M. Scarpa, Poly(ethylenimine) shows properties of interest for cytstic fibrosis gene therapy, (1999) *Biochimica et Biophysica Acta*, **1447** 219-225.

P. Ferruti, F. Danusso, G. Franchi, N. Polentarutti, S. Garattini, Effects of a series of new synthetic high polymers on cancer metastases, (1973) *Journal of Medicinal Chemistry*, **16** 496-499.

P. Ferruti, Linear amino polymers: synthesis, protonation and complex formation, (1984) *Advances in Polymer Science*, **58** 55-92.

P. Ferruti, M.A. Marchisio, R. Barbucci, Synthesis, physicochemical properties and biomedical applications of poly(amidoamines), (1985) *Polymer*, **26** 1336-1348.

P. Ferruti, Ion chelating polymers for medical applications, In: *The polymeric materials encyclopaedia* Vol. 5 (H-L) J.C. Salamone Ed., CRC Press: Florida USA, 1996 p. 3334-3359.

P. Ferruti, S. Richardson, R. Duncan, Poly(amidoamine)s as tailor-made soluble polymeric carriers, In: *Targeting of Drugs: Stealth Therapeutic Systems*, G. Gregoriadis, B. McCormack, Eds., Plenum Press: New York, 1998 p. 207-224.

P. Ferruti, S. Manzoni, S.C.W. Richardson, R. Duncan, N.G. Pattrick, R. Mendichi, M. Casolaro, Amphoteric linear poly(amidoamine)s as endosomolytic polymers: correlation between physicochemical and biological properties, (2000) *Macromolecules*, **33** 7793-7800.

P. Ferruti, M.A. Marachisio, R. Duncan, Poly(amido-amine)s: Biomedical applications, (2002) *Macromolecules Rapid Communications*, **23** 332-355.

D. Finisinger, J-S. Remy, P. Erbacher, C. Koch, C. Plank, Protective copolymers for non-viral gene vectors: synthesis, vector characterisation and application in gene delivery, (2000) *Gene Therapy*, **7** 1183-1192.

D. Fischer, T. Bieber, Y. Li, H.P. Elsasser, T, Kissel, A non-viral vector for DNA delivery based on low molecular weight, branched polyethylenimine: effect of molecular weight on transfection efficiency and cytotoxicity, (1999) *Pharmaceutical Research*, **16** 1273-1279.

P.A. Flanagan, Evaluation of the pinocytic uptake and cellular processing of antibody-N-(2-hydroxypropyl)methacrylamide copolymer conjugates and estimation of their potential use in "targeted" drug delivery, Ph.D. Thesis, University of Keele, UK, 1987.

O. Fodstad, G. Kvalheim, A. Godal, J. Lotsberg, S. Aamdal, H. Host, A. Pihl, Phase I study of the plant protein ricin, (1984) *Cancer Research*, **44** 862-865.

A.E. Frankel, R.J. Kreitman, E.A. Sausville, Targeted toxins, (2000) *Clinical Cancer Research*, **6** 326-334.

H. Gao, K.M. Hui, Synthesis of a novel series of cationic lipids that can act as efficient gene delivery vehicles through systematic heterocyclic substitution of cholesterol derivatives, (2001) *Gene Therapy*, **8** 855-863.

M.C. Garnett, Gene-delivery systems using cationic polymers, (1999) *Critical Reviews of Therapeutic Drug Carrier Systems,* **16** 147-207.

H. Gershon, R. Ghirlando, S.B. Guttman, A. Minsky, Mode of formation and structural features of DNA-cationic liposome complexes used for transfection, (1993) *Biochemistry*, **32** 7143-7151.

R.V. Giles, D.G. Spiller, J. Grzybowski, R.E. Clark, P. Nicklin, D.M. Tidd, Selecting optimal oligonucleotide composition for maximal antisense effect following streptolysin O-mediated delivery into human leukaemia cells, (1998) *Nucleic Acid Research*, **26** 1567-1575.

P. Glue, R. Rouzier-Panis, C. Raffanel, R. Sabo, S.K. Gupta, M. Salfi, S. Jacobs, R.P. Clement, A dose-ranging study of pegylated interferon alfa-2b and ribavirin in chronic hepatitis C. The Hepatitis C Intervention Therapy Group, (2000) *Hepatology*, **32** 647-653.

W.T. Godbey, K.K. Wu, A.G. Mikos, Poly(ethylenimine) and its role in gene delivery, (1999a) *Journal of Controlled Release*, **60** 149-160.

W.T. Godbey, K.K. Wu, A.G. Mikos, Tracking the intracellular path of poly(ethylenimine)/DNA complexes for gene delivery, (1999b) *Proceedings of the National Academy of Science of the United States of America*, **96** 5177-5181.

W.T. Godbey, A.G. Mikos, Recent progress in gene delivery using non-viral transfer complexes, (2001) *Journal of Controlled Release*, **72** 115-125.

R. Goldman, A. Kaplan, Rupture of rat liver lysosomes mediated by L-amino acid esters, (1973) *Biochimica et Biophysica Acta*, **318** 205-216.

D. Goula, C. Benoist, S. Mantero, G. Merlo, G. Levi, B.A. Demeneix, Polyethylenimine-based intravenous delivery of transgenes to mouse lung, (1998) *Gene Therapy*, **5** 1291-1295.

F. L. Graham, A.J. Van der Eb, A new technique for the assay of infectivity of human adenovirus 5 DNA, (1973) *Virology*, **52** 456-467.

G. Gregoridis, The carrier potential of liposomes in biology and medicine, (1976) *New England Journal of Medicine*, **295** 704-710.

G. Gregoriadis, Immunological adjuvants: a role for liposomes, (1990) *Immunology Today*, **11** 89-97.

S.E. Hamilton, C.G. Simmons, I.S. Kathiriya, D.R. Corey, Cellular delivery of peptide nucleic acids and inhibition of human telomerase, (1999) *Chemistry & Biology*, **6** 343-351.

T. Hari, H. Kunze, E. Bohn, U. Brodbeck, P. Bütikofer, Subcellular distribution of glycosylphosphatidylinositol-specific phospholipase D in rat liver, (1996) *Biochemical Journal*, **320** 315-319.

J.M. Harris, N.E. Martin, M. Modi, Pegylation. A novel process for modifying pharmacokinetics, (2001) *Clinical Pharmacokinetics*, **40** 539-551.

R.P. Haugland, *Handbook of fluorescent probes and research chemicals*, M.T.Z. Spence, Ed., 6th edition, Molecular Probes Inc., USA, 1999.

C. Helene, J.J. Toulme, Specific regulation of gene expression by antisense, sense and antigene nucleic acids, (1990) *Biochimica et Biophysica Acta*, **1049** 99-125.

G.T. Hermanson, The chemistry of reactive groups, In: *Bioconjugate Techniques,* G.T. Hermanson, Ed., Academic Press Inc: California, 1996 p. 137-168.

M.S. Hershfield, R.H. Buckley, M.L. Greenberg, A.L. Melton, R. Schiff, C. Hatem, J. Kurtzberg, M.L. Markert, R.H. Kobayashi, A.L. Kobayashi, Treatment of adenosime deaminase deficiency with polyethyleneglycol-modified adenosine deaminase, (1987) *New England Journal of Medicine*, **316** 589-596.

D.H. Ho, E. Frei, Pharmacological studies of the antitumour agent 6-methylthiopurine ribonucleoside, (1970) *Cancer Research*, **30** 2852-2857.

M.V. Hosur, B. Nair, P. Satyamurthy, S. Misquith, A. Surolia, K.K. Hannan, X-ray structure of gelonin at 1.8 Å resolution, (1995) *Journal of Molecular Biology*, **250** 368-380.

S.J. Hwang, N.C. Bellocq, M.E. Davis, Effects of structure of beta-cyclodextrin-containing polymers on gene delivery, (2002) *Bioconjugate Chemistry*, **12** 280-290.

K. Ichihara, N. Hayase, K. Chiba, H. Parvez, Y. Abiko, Effect of NCO-700, an inhibitor of protease, on lysosomal rupture in the ischemic myocardium, (1991) *Journal of Pharmaceutical Sciences*, **80** 252-254.

K.D. Jensen, P. Kopeková, J.H.B. Bridge, J. Kopecek, The cytoplasmic escape and nuclear accumulation of endocytosed and microinjected HPMA copolymers and a basic kinetic study in HepG2 cells, (2001) *AAPS Pharmaceutical Sciences*, **3** 1-14.

J.H. Jeong, S.H. Song, D.W. Lim, H. Lee, T.G. Park, DNA transfection using linear poly(ethylenimine) prepared by controlled acid hydrolysis of poly(2-ethyl-2-oxazoline), (2001) *Journal of Controlled Release*, **73** 391-399.

L.G. Johnson, J.C. Olsen, B. Sarkadi, K.L. Moor, R. Swanstrom, R.C. Boucher, Efficiency of gene transfer for restoration of normal airway epithelial function in cystic fibrosis, (1992) *Nature Genetics*, **2** 21-25.

M-C. Jones, J-C. Leroux, Polymeric-micelles-a new generation of colloidal drug carriers, (1999) *European Journal of Pharmaceutics and Biopharmaceutics*, **48** 101-111.

N.A. Jones, I.R.C. Hill, S. Stolnik, F. Bignotti, S.S. Davis, M.C. Garnett, Polymer chemical structure is a key determinant of physicochemical and colloidal properties of polymer-DNA complexes for gene delivery, (2000) *Biochimica et Biophysica Acta*, **1517** 1-18.

V.A. Kabanov, A.V. Kabanov, Interpolyelectrolyte and block ionomer complexes for gene delivery: physico-chemical aspects, (1998) *Advanced Drug Delivery Reviews*, **30** 49-60.

H. Kamiya, H. Tsuchiya, Y. Yamazaki, H. Harashima, Intracellular trafficking and transgene expression of viral and non-viral gene vectors, (2001) *Advanced Drug Delivery Reviews*, **52** 153-164.

A. Khaled, Influence of polymer characteristics on biocompatibility and the ability to promote intracytoplasmic delivery, (2000) Final Year Report.

A. Kichler, K. Mechtler, J-P. Behr, E. Wagner, Influence of membrane-active peptides on lipospermine/DNA complex mediated gene transfer, (1997) *Bioconjugate Chemistry*, **8** 213-221.

T. Kielian, W.F. Hickey, Inflammatory thoughts about glioma gene therapy (1999) *Nature Medicine*, **5** 1237-1238.

A.L. Kilbanov, K. Maruyama, V.P. Torchilin, L. Huang, Amphipathic polyethyleneglycols effectively prolong the circulation time of liposomes, (1990) *FEBS Letters*, **268** 235-237.

R. Kircheis, L. Wightman, E. Wagner, Design and gene delivery activity of modified polyethylenimines, (2001a) *Advanced Drug Delivery Reviews*, **53** 341-358.

R. Kircheis, L. Wightman, A. Schreiber, B. Robitza, V. Roessler, M. Kursa, Polyethylenimine/DNA complexes shielded by transferrin target gene expression to tumours after systemic administration, (2001b) *Gene Therapy*, **8** 28-40.

A.R. Klemm, D. Young, J-B. Lloyd, Effects of poly(ethylenimine) on endocytosis and lysosome stability, (1998) *Biochemical Pharmacology*, **56** 41-46.

R.J. Kreitman, Immunotoxins in cancer therapy, (1999) *Current Opinion in Immunology*, **11** 570-578.

R.J. Kreitman, W.H. Wilson, J.D. White, M. Stetler-Stevenson, E.S. Jaffe, S. Giardina, T.A. Waldmann, I. Pastan, Phase I trial of recombinant immunotoxin anti-Tac(Fv)-PE38 (LMB-2) in patients with haematologic malignancies, (2000) *Journal of Clinical Oncology*, **18** 1622-1636.

R.J. Kreitman, W.H. Wilson, K. Bergeron, M. Raggio, M. Stetler-Stevenson, D.J. FitzGerald, I. Pastan, Efficacy of the anti-CD22 recombinant immunotoxin BL22 in chemotherapy-resistant hairy-cell leukaemia, (2001) *New England Journal of Medicine*, **345** 241-247.

T.R. Kyriakides, C.Y. Cheung, N. Murthy, P. Bornstein, P.S. Stayton, A.S. Hoffman, pH-sensitive polymers that enhance intracellular drug delivery *in vivo*, (2002) *Journal of Controlled Release*, **78** 295-303.

C.A. Lackey, N. Murthy, P.S. Stayton, O.W. Press, A.S. Hoffman, D.A. Tirrell, Enhancement of endosomal release and toxic activity of ricin A-chain by a pH-sensitive polymer, (1999a) *Proceedings of the 26th International Symposium of Controlled Release and Bioactive Materials,* Boston, USA. **26**, p. 815-816.

C.A. Lackey, N. Murthy, O.W. Press, D.A. Tirell, A.S. Hoffman, P.S. Stayton, Haemolytic activity of pH-responsive polymer-streptavidin bioconjugates, (1999b) *Bioconjugate Chemistry*, **10** 401-405.

C.A. Lackey, O.W. Press, A.S. Hoffman, P.S. Stayton, A biomimetic pH-responsive polymer directs endosomal release and intracellular delivery of an endocytosed antibody complex, (2002) *Bioconjugate Chemistry*, **13** 996-1001.

U.K. Laemmeli, Cleavage of structural proteins during the assembly of the head of bacteriophage T4, (1970) *Nature*, **227** 680-685.

U.K. Laemmeli, Characterisation of DNA condensates induced by poly(ethylene oxide) and polylysine, (1975) *Proceedings of the National Academy of Science of the United States of America*, **72** 4288-4292.

C. Lamaze, S.L. Schmid, The emergence of clathrin-independent pinocytic pathways, (1995) *Current Opinion in Cell Biology*, **7** 573-580.

D.D. Lasic, N.S. Templeton, Liposomes in gene therapy, (1996) *Advanced Drug Delivery Reviews*, **20** 221-226.

D.D. Lasic, D. Papahadjopoulos, R. Podgornic, Polymorphism of lipids, nucleic acids and their interactions, In: *Self-assembling complexes for gene delivery: From laboratory to clinical trial*, A.V. Kabanov, P.L. Felgner, L.W. Seymour L, Eds., John Wiley and Sons: Chichester, New York, Weinheim, Brisbane, Singapore, Toronto, 1998 p. 27-50.

D.W. Laske, R. Youle, E.H. Oldfield, Tumor regression with regional distribution of the targeted distribution of the targeted toxin Tf-CRM107 in patients with malignant brain tumours, (1997) *Nature Medicine*, **3** 1362-1368.

I. Lebedeva, L. Benimetskaya, C.A. Stein, M. Vilenchik, Cellular delivery of antisense oligonucleotides, (2000) *European Journal of Pharmaceutics and Biopharmaceutics*, **50** 101-119.

M. Lecocq, S. Wattiaux-De Coninck, N. Laurent, R. Wattiaux, M. Jadot, Uptake and intracellular fate of polyethylenimine *in vivo*, (2000) *Biochemical and Biophysical Research Communications*, **278** 414-418.

H. Lee, J.H. Jeong, T.G. Park, A new gene delivery formulation of polyethylenimine/DNA complexes coated with PEG conjugated fusogenic peptide, (2001) *Journal of Controlled Release*, **76** 183-192.

H. Lee, J. H. Jeong, T.G. Park, PEG grafted polylysine with fusogenic peptide for gene delivery: high transfection efficiency with low cytotoxicity, (2002a) *Journal of Controlled Release*, **79** 283-291.

H. Lee, T.H. Kim, T.G. Park, A receptor-mediated gene delivery system using streptavidin and biotin-derivatized, pegylated epidermal growth factor, (2002b) *Journal of Controlled Release*, **83** 109-119.

D.W. Lim, Y.I. Yeom, T.G. Park, Poly(DMAEMA-NVP)-*b*-PEG-galactose as gene delivery vector for hepatocytes, (2000) *Bioconjugate Chemistry*, **11** 688-695.

J.B. Lloyd, Lysosome membrane permeability, (2000) *Advanced Drug Delivery Reviews*, **41** 189-200.

P. Lopez-Saura, A. Trouet, P. Tulkens, Analytical fractionation of cultured hepatoma cells (HTC cells), (1978) *Biochimica et Biophysica Acta*, **543** 430-449.

J.M. Lord, L.M. Roberts, J.D. Robertus, Ricin: structure, mode of action, and some current applications, (1994) *FASEB Journal*, **8** 201-8.

P. Lucas, D.A. Milroy, B.J. Thomas, S.H. Moss, C.W. Pouton, Pharmaceutical and biological properties of poly(aminoacid)/DNA polyplexes, (1999) *Journal of Drug Targeting*, **7** 143-156.

F. Lui, H. Qu, L. Huang, D. Lui, Factors controlling the efficiency of cationic lipid-mediated transfection *in vivo* via intravenous administration, (1997) *Gene Therapy*, **4** 517-523.

J. P. Luzio, B. A. Rous, N.A. Bright, P.R. Prior, B.M. Mullock, R.C. Piper, Lysosome-endosome fusion and lysosome biogenesis, (2000) *Journal of Cell Science*, **113** 1515-1524.

H. Maeda, Polymer conjugated macromolecular drugs for tumour-specific targeting, In: *Polymeric site specific pharmacotherapy*, A.J. Doumb, Ed., John Wiley and Sons Ltd.: Chichester, New York, Weinheim, Brisbane, Singapore, Toronto, 1994 p. 95-115.

H. Maeda, SMANCS and polymer-conjugated macromolecular drugs: advantages in cancer chemotherapy, (2001) *Advanced Drug Delivery Reviews*, **46** 169-185.

H. Maeda, Y. Matsumura, Tumouritropic and lymphotropic principles of macromolecular drugs, (1989) *CRC Critical Reviews of Therapeutic Drug Carrier Systems,* **6** 193-210.

R. I. Mahato, K. Kawabata, T. Nomura, Y. Takakura, M. Hashida, Physicochemical and pharmacokinetic characteristics of plasmid DNA/cationic liposome complexes, (1995) *Journal of Pharmaceutical Sciences*, **84** 1267-1271.

I.T. Mak, H.P. Misra, W.B. Weglicki, Temporal relationship of free radical-induced lipid peroxidation and loss of latent enzyme activity in highly enriched hepatic lysosomes, (1983) *Journal of Biological Chemistry*, **258** 13733-13737.

B. Malgesini, I. Verpilio, R. Duncan, P. Ferruti, Poly(amidoamine)s carrying primary amino groups as side-substituents, (2002) *Macromolecular Chemistry and Physics*, submitted for publication.

N. Malik, R. Wiwattanapatapee, R. Klopsch, K. Lorenz, H. Frey, J.W. Weener, E.W. Meijer, W. Paulus, R. Duncan, Dendrimers: relationship between structure and biocompatibility *in vitro*, and preliminary studies on the biodistribution of ^{125}I-labelled polyamidoamine dendrimers *in vivo*, (2000) *Journal of Controlled Release*, **65** 133-148.

Y.K.S. Man, S.C.W. Richardson, R. Duncan, Characterisation of polymer mediated gene delivery *in vitro*, (1999) Final Year Report.

C.K. Mathews, K.E. Van Holde, Lipids, membranes and cellular transport, In: *Biochemistry*, D. Bowen, S. Weisberg, Eds., The Benjamin/Cummings Publishing Company, Inc. California, Colorado, Massachusetts, New York, Ontario, Wokingham, Amsterdam, Bonn, Sydney, Singapore, Tokyo, Madrid, San Juan, 1990 p. 298-336.

E. Marshall, Gene therapy death prompts review of adenovirus vector, (2000) *Science*, **286** 2244-2245.

K.A. Marx, G.C. Ruben, Evidence for hydrated spermidine-calf thymus DNA toruses organised by circumferential DNA wrapping, (1983) *Nucleic Acids Research* **11,** 1839-1843.

I. Mellman, Endocytosis and molecular sorting, (1996) *Annual Reviews in Cell Developmental Biology*, **12** 575-625.

T. Merdan, K. Kunath, D. Fischer, J. Kopecek, T. Kissel, Intracellular processing of poly(ethylenimine)/ribozyme complexes can be observed in living cells by using confocal laser scanning microscopy and inhibitor experiments, (2002a) *Pharmaceutical Research*, **19** 140-146.

T. Merdan, J. Kopecek, T. Kissel, Prospects for cationic polymers in gene and oligonucleotide therapy against cancer, (2002b) *Advanced Drug Delivery Reviews*, **54** 715-758.

C.E. Meloan, *Chemical Separations. Principles, Techniques, and Experiments*, E. Schofield, Ed., John Wiley & Sons, Inc. New York, Chichester, Weinheim, Brisbane, Singapore, Toronto, 1999.

A. Mhashilkar, S. Chada, J.A. Roth, R. Ramesh, Gene therapy. Therapeutic approaches and implications, (2001) *Biotechnology Advances*, **19** 279-297.

P. Midoux, M. Monsigny, Efficient gene transfer by histidylated polylysine/pDNA complexes, (1999) *Bioconjugate Chemistry*, **10** 406-411.

K.A. Mislick, J.D. Baldeschwieler, J.F. Kayyem, T.J. Meade, Transfection of folate-polylysine DNA complexes: evidence for lysosomal delivery, (1995) *Bioconjugate Chemistry*, **6** 512-515.

K.A. Mislick, J.D. Baldeschwieler, Evidence for the role of proteoglycans in cation-mediated gene transfer, (1996) *Proceedings of the National Academy of Science of the United States of America*, **93** 12349-12354.

J. Mönkkönen, A. Urtti, Lipid fusion in oligonucleotide and gene delivery with cationic lipids, (1998) *Advanced Drug Delivery Reviews*, **34** 37-49.

I. Moret, J.E. Peris, V.M. Guillem, M. Benet, F. Revert, F. Dasí, A. Crespo, S.F. Aliño, Stability of PEI-DNA and DOTAP-DNA complexes: effect of alkaline pH, heparin and serum, (2001) *Journal of Controlled Release*, **76** 169-181.

S. Mukherjee, R.N. Ghosh, F.R. Maxfield, Endocytosis, (1997) *Physiological Reviews*, **77** 759-802.

N. Murthy, J. Robichaud, D. Tirrel, P. Stayton, A. Hoffman, The design and synthesis of polymers for eukaryotic membrane disruption, (1999) *Journal of Controlled Release*, **61** 137-143.

A. Nevo, A. De Vries, A. Katchalsky, Interaction of basic polyamino acids with red blood cells. I Combination of polylysine with single cells, (1955) *Biochimica et Biophysica Acta*, **17** 536-547.

M.L. Nucci, R. Shorr, A. Abuchowski, The therapeutic values of poly(ethylene glycol)-modified proteins, (1991) *Advanced Drug Delivery Reviews*, **6** 133-151.

H. Ohno, J. Stewart, MC Fournier, H. Bosshart, I. Rhee, Interaction of tyrosine-based sorting signals with clathrin-associated proteins, (1995) *Science*, **269** 1872-1875.

M Ogris, P. Steinlein, M. Kursa, K. Mechtler, R. Kircheis, E. Wagner, The size of DNA/transferrin-PEI complexes is an important factor for gene expression in cultured cells, (1998) *Gene Therapy*, **5** 1425-1433.

E. Olsen, M. Duvic, A. Frankel, Y. Kim, A. Martin, E. Vonderheid, B. Jegasothy, G. Wood, M. Gordon, P. Heald, A. Oseroff, L. Pinter-Brown, G. Bowen, T. Kuzel, D. Fivenson, F. Foss, M. Glode, A. Molina, E. Knobler, S. Stewart, K. Cooper, S. Stevens, F. Craig, J. Reuben, P. Bacha, J. Nichols, Pivotal phase III trial of two dose levels of DAB389IL2 (ONTAK) for the treatment of cutaneous T-cell lymphoma, (2001) *Journal of Clinical Oncology*, **19** 376-378.

D. Owen, J.P. Luzio, Structural insights into clathrin-mediated endocytosis, (2000) *Current Opinion in Cell Biology*, **12** 467-474.

N.G. Pattrick, S. Richardson, M. Casolaro, P. Ferruti R. Duncan, Poly(amidoamine)-mediated intracytoplasmic delivery of ricin A-chain and gelonin, (2001) *Journal of Controlled Release,* **77** 225-232.

N.G. Pattrick, S.C.W. Richardson, A. Hann, P. Ferruti, R. Duncan, Quantitating the intracellular fate of poly(amidoamine)s and demonstrating their ability to modulate permeability of the rat liver lysosomal membrane after intravenous administration to rats, (2002) *Proceedings of the 5th International Symposium of Polymer Therapeutics,* Cardiff, UK. **5**, p. 80.

C.M. Perry, B. Jarvis, Peginterferon-alpha-2a (40kDa): a review of its use in the management of chronic hepatitis C, (2001) *Drugs*, **61** 2263-2288.

K.R. Peters, W.W. Carley, G.E. Palade, Endothelial plasmalemmal vesicles have a characteristic striped bipolar surface structure, (1985) *Cell Biology*, **101** 2233-2238.

C. Plank, B. Oberhauser, K. Mechtler, C. Koch, E. Wagner, The influence of endosome-disruptive peptides on gene transfer using synthetic virus-like gene transfer systems, (1994) *Journal of Biological Chemistry*, **269** 12918-12924.

C. Plank, K. Metchler, F.C. Szoka Jr., E. Wagner, Activation of the complement system by synthetic DNA complexes: a potential barrier for intravenous gene delivery, (1996) *Human Gene Therapy*, **7** 1437-1446.

C. Plank, W. Zauner, E. Wagner, Application of membrane-active peptides for drug and gene delivery across cellular membranes, (1998) *Advanced Drug Delivery Reviews*, **34** 21-35.

C. Pouton, Nuclear import of polypeptides, polynucleotides and supramolecular complexes, (1998) *Advanced Drug Delivery Reviews*, **34** 51-64.

L. Prasmickaite, A. Høgset, T.E. Tjelle, V.M. Olsen, K. Berg, Role of endosomes in gene transfection mediated by photochemical internalisation (PCI), (2000) *The Journal of Gene Medicine*, **2** 477-488.

M.K. Pratten, R. Duncan, J.B. Lloyd, Adsorptive and passive pinocytic uptake, In: *Coated Vesicles*, C.D. Ockleford, A. Whyte Eds., Cambridge University Press, Cambridge, New York, Melbourne 1980 p. 179-218.

O.W. Press, J.A. Hansen, A. Farr, P.J. Martin, Endocytosis and degradation of murine anti-human CD3 monoclonal antibodies by normal and malignant T-lymphocytes, (1988) *Cancer Research*, **48** 2249-2257.

P. Prokop, E. Kozlov, W. Moore, J.M. Davidson, Maximising the *in vivo* efficiency of gene transfer by means of nonviral polymeric gene delivery vehicles, (2001) *Journal of Pharmaceutical Sciences*, **91** 67-76.

C.J. Provoda, K-D. Lee, Bacterial pore-forming haemolysins and their use in the cytosolic delivery of macromolecules, (2000) *Advanced Drug Delivery Reviews*, **41** 209-221.

E. Ramsay, J. Hadgraft, J. Birchall, M. Gumbleton, Examination of the biophysical interaction between plasmid DNA and the polycations polylysine and polyornithine, as a basis for their differential gene transfection *in vitro*, (2000) *International Journal of Pharmaceutics,* **210** 97-107.

E. Ranucci, G. Spagnoli, P. Ferruti, D. Sgouras, R. Duncan, Poly(amidoamine)s with potential as drug carriers: degradation and cellular toxicity, (1991) *Journal of Biomaterial Science: Polymer Edition*, **2** 303-315.

V. Raso, J. Lawrence, Carboxylic ionophores enhance the cytotoxic potency of ligand- and antibody-delivered ricin A-chain, (1984) *Journal of Experimental Medicine*, **160** 1234-1240.

J-S. Remy, B. Abdallah, M. A. Zanta, O. Boussif, J-P. Behr, B. Demeneix, Gene transfer with lipospermines and polyethylenimines, (1998) *Advanced Drug Delivery Reviews*, **30** 85-95.

A. Rémy-Kristensen, J-P. Clamme, C. Vuilleumier, J-G. Kuhry, Y. Mely, Role of endocytosis in the transfection of L929 fibroblasts by poly(ethylenimine)/DNA complexes, (2001) *Biochimica et Biophysica Acta*, **1514** 21-32.

J. Renes, E.G. De Vries, P.L. Jansen, M. Muller, The (patho)physiological functions of the MRP family, (2000) *Drug Resistance Updates*, **3** 289-302.

B. Rhíová, Receptor-mediated targeted drug or toxin delivery, (1998) *Advanced Drug Delivery Reviews*, **29** 273-289.

S.C.W. Richardson, N.G. Pattrick, S. Man, P. Ferruti, R. Duncan, Poly(amidoamine)s as potential non-viral vectors: ability to form interpolyelectrolyte complexes and to mediate transfection *in vitro*, (2001) *Biomacromolecules*, **2** 1023-1028.

S.C.W. Richardson, P. Ferruti, R. Duncan, Poly(amidoamine)s as potential endosomolytic polymers: Evaluation *in vitro* and body distribution in normal and tumour bearing animals, (1999a) *Journal of Drug Targeting*, **6** 391-404.

S.C.W. Richardson, Characterisation of poly(amidoamine)s and chitosan as potential intracytoplasmic delivery systems, Ph.D. Thesis, University of London, UK, 1999b.

S.C.W. Richardson, Y.K.S. Man, P. Ferruti, R. Duncan, Poly(amidoamine)s: evaluation as potential endosomolytic polymers, (1999c) *Proceedings of the 26th International Symposium of Controlled Release and Bioactive Materials*, Boston, USA. **26**, p. 434-435.

H. Ringsdorf, Structure and properties of pharmacologically active polymers, (1975) *Journal of Polymer Science., Polymer Symposium*, **51** 135-153.

P.D. Robins, S.C. Ghivizzani, Viral vectors for gene therapy, (1998) *Pharmacology Therapy*, **80** 35-47.

M.A. Rosenfeld, K. Yoshimura, B. Trapnell, K. Yoneyama, E. Rosenthal, W. Dalemans, M. Fukayama, J. Baron, L. Stier, L.D. Stratford-Perricaudet, M. Perricaudet, W. Gaggino, A. Pavirani, J-P. Lecocq, R.G. Crystal, *In vivo* transfer of the human cystic fibrosis transmembrane conductance regulator gene to the air-way epithelium, (1992) *Cell* **68** 143-155.

K.G. Rothberg, J.E. Heuser, W.C. Donzell, Y.S. Ying, J.R. Glenney, R.G. Anderson, Caveolin, a protein component of caveolae membrane coats, (1992) *Cell,* **68** 673-682.

U. Rungsardthong, M. Deshpande, L. Bailey, M. Vamvakaki, S.P. Armes, M.C. Garnett, S. Stolnik, Copolymers of amine methacrylate with poly(ethylene glycol) as vectors for gene therapy, (2001) *Journal of Controlled Release*, **73** 359-380.

E. Rutenber, B.J. Katzin, S. Ernst, E.J. Collins, D. Mlsna, M.P. Ready, J.D. Robertus, Crystallographic refinement of ricin to 2.5 Å, (1991) *Proteins*, **10** 240-250.

K. Sandvig, B, van Deurs, Endocytosis, intracellular transport, and cytotoxic action of shiga toxin and ricin, (1996) *Physiological Reviews*, **76** 949-964.

D.V. Schaffer, D.A. Lauffenburger, Optimisation of cell surface binding enhances efficiency and specificity of molecular conjugate gene delivery, (1998) *The Journal of Biological Chemistry*, **273** 28004-28009.

D.V. Schaffer, N.A. Fidelman, N. Dan, D.A. Lauffenburger, Vector unpacking as a potential barrier for receptor-mediated polyplex gene delivery, (2000) *Biotechnology and Bioengineering*, **67** 598-606.

J.P. Schofield, C.T. Caskey, Non-viral approaches to gene therapy, (1995) *British Medical Bulletin*, **51** 56-71.

P.K. Selbo, K. Sandvig, V. Kireveliene, K. Berg, Release of gelonin from endosomes and lysosomes to cytosol by photochemical internalisation, (2000a) *Biochimica et Biophysica Acta*, **1475** 307-313.

P.K. Selbo, G. Sivam, O. Fodstad, K. Sandvig, K. Berg, Photochemical internalisation increases the cytotoxic effect of the immunotoxin MO31-gelonin, (2000b) *International Journal of Cancer*, **87** 853-859.

L.W. Seymour, P.A. Flanagan, A. Al-Shamkhani, V. Subr, K. Ulbrich, J. Cassidy, R. Duncan, Synthetic polymer conjugates to monoclonal antibodies: vehicles for tumour targeted drug delivery, (1991) *Selective Cancer Therapeutics*, **7** 59-72.

L.W. Seymour, D.R. Ferry, D. Anderson, S. Hesslewood, P.J. Julyan, R. Poyner, J. Doran, A.M. Young, S. Burtles, D.J. Kerr, Hepatic drug targeting: phase I evaluation of polymer-bound doxorubicin, (2002) *Journal of Clinical Oncology*, **20** 1668-1676.

D. Sgouras, The evaluation of biocompatibility of soluble polymers and assessment of there potential as specific drug delivery systems, PhD Thesis, University of Keele, UK, 1990.

D. Sgouras, R. Duncan, Methods for the evaluation of biocompatibility of soluble synthetic polymers which have potential for biomedical use. 1. Use of the tetrazolium-based colorimetric assay (MTT) as a preliminary screen for evluation of *in vitro* cytotoxicity, (1990) *Journal of Material Science, Materials and Medicine*, **1** 61-68.

S. Shaunak, M. Thornton, S. John, I. Teo, E. Peers, P. Mason, T. Krausz, D.S. Davies, Reduction of the viral load of HIV-1 after the intraperitoneal administration of dextrin 2-sulphate in patients with AIDS, (1998) *Aids*, **12** 399-409.

J.C. Simpson, L.M. Roberts, K.Romisch, J. Davey, D.H. Wolf, J.M. Lord, Ricin A-chain utilises the endoplasmic reticulum-associated protein degradation pathway to enter the cytosol of yeast, (1999) *FEBS Letters*, **459** 80-84.

P.K. Smith, R.I. Krohn, G.T. Hermanson, A.K. Mallia, F.H. Gartner, M.D. Provenzano, E.K. Fujimoto, N.M. Goeke, B.J. Olsen, D.C. Klenk, Measurement of protein using bicinchoninic acid, (1985) *Analytical Biochemistry*, **150** 76-85.

B.A. Sosnowski, A.M. Gonzalez, L.A. Chandler, Y.J. Buechler, G.F. Pierce, A. Baird, Targeting DNA to cells with basic fibroblast growth factor (FGF2), (1996) *Journal of Biological Chemistry*, **271** 33647-33653.

P.S. Stayton, A.S. Hoffman, N. Murthy, C. Lackey, C. Cheung, P. Tan, L.A. Klumb, A. Chilkoti, F.S. Wilbur, O.W. Press, Molecular engineering of proteins and polymers for targeting and intracellular delivery of therapeutics, (2000) *Journal of Controlled Release*, **65** 203-220.

E.M. Stier, C.J. Provoda, K-D. Lee, Cytosolic delivery of gelonin to murine melanoma cells using listeriolysin, (2002) *Proceedings of the 29th International Symposium of Controlled Release and Bioactive Materials*, Seoul, Korea. **29**, #035.

F. Stirpe, S. Olsnes, A. Pihl, Gelonin, a new inhibitor of protein synthesis, nontoxic to intact cells. Isolation, characterisation, and preparation of cytotoxic complexes with concanavalin A, (1980) *Journal of Biological Chemistry*, **14** 6947-6953.

Y. Suda, S. Kusumoto, N. Oku, H. Yamamoto, M. Sumi, F. Ito, M. Ottenbrite, Modified polyanionic polymers for enhanced cell membrane interaction, (1992) *Journal of Bioactive and Biocompatible Polymers*, **7** 275-287.

J. Suh, H.J. Paik, B.K. Hwang, Ionisation of poly(ethylenimine) and poly(allylamine) at various pH's, (1994) *Bioorganic Chemistry*, **22** 318-327.

R. Tachibana, H. Harashima, Y. Shinohara, H. Kiwada, Quantitative studies on the nuclear transport of plasmid DNA and gene expression employing nonviral vectors, (2001) *Advanced Drug Delivery Reviews*, **52** 219-226.

B. Tan, D. Piwnica-Worms, L. Ratner, Multidrug resistance transporters and modulation, (2000) *Current Opinion in Oncology*, **12** 450-458.

M.X. Tang, F.C. Szoka, The influence of polymer structure on the interactions of cationic polymers with DNA and morphology of the resulting complexes, (1997) *Human Gene Therapy*, **4** 823-832.

J.L. Thomas, D.A. Tirrell, Polymer-induced leakage of cations from dioleoyl phosphatidylcholine and phosphatidylglycerol liposomes, (2000) *Journal of Controlled Release*, **67** 203-209.

V.V. Tolstikov, R. Cole, H. Fang, S.H. Pincus, Influence of endosome-destabilising peptides on efficacy of anti-HIV immunotoxins, (1997) *Bioconjugate Chemistry*, **8** 38-43.

K. Ulbrich, V. Subr, J. Strohalm, D. Plocova, M. Jelinkova, B. Rhiova, Polymeric drugs based on conjugates of synthetic and natural macromolecules I. Synthesis and physico-chemical characterisation, (2000) *Journal of Controlled Release*, **64** 63-79.

P. Van de Wetering, J-Y. Cherng, H. Talsma, W.E. Hennink, Relationship between transfection efficiency and cytotoxicity of poly(2-(dimethylamino)ethyl methacrylate)/plasmid complexes, (1997) *Journal of Controlled Release*, **49** 59-69.

P. Van de Wetering, E.E. Moret, N.M.E. Schuurmans-Nieuwenbroek, M.J. van Streenbergen, W.E. Hennink, Structure-activity relationships of water-soluble cationic methacrylate /methacrylamide polymers for nonviral gene delivery, (1999) *Bioconjugate Chemistry*, **10** 589-597.

E.J.M. Van Kan, A. van der Bent, R.A. Remel, B. de Kruijff, Membrane activity of the peptide antibiotic clavanin and the importance of its glycine residues, (2001) *Biochemistry,* **40** 6398-6405.

P.A. Vasey, S.B. Kaye, R. Morrison, C. Twelves, P. Wilson, R. Duncan, A.H. Thompson, L.S. Murray, T.E. Hilditch, T. Murray, S. Burtles, D. Fraier, E. Figerio, J. Cassidy, Phase 1 clinical and pharmacokinetic study of PK1 [N-(2-hydroxyproyl)methacrylamide copolymer doxorubicin]: first member of a new class of chemotherapeutic agents: drug-polymer conjugates, (1999) *Journal of Clinical Cancer Research,* **5** 83-94.

F.J. Verbaan, C. Oussoren, I.M. van Dam, Y. Takakura, M. Hashida, D.J.A. Crommelin, W.E. Hennink, G. Storm, The fate of poly(2-dimethyl amino ethyl)methacrylate-based polyplexes after intravenous administration, (2001) *International Journal of Pharmaceutics*, **214** 99-101.

I.M. Verma, N. Somia, Gene therapy-promises, problems and prospects, (1997) *Nature,* **389** 239-242.

J.A. Wagner, P. Gardner, Toward cystic fibrosis gene therapy, (1997) *Annual Review Of Medicine,* **48** 203-216.

E. Wagner, M. Zenke, M. Cotton, H. Beug, M.L. Birnstiel, Transferrin-polycation conjugates as carriers for DNA uptake into cells, (1990) *Proceedings of the National Academy of Science of the United States of America*, **87** 3410-3414.

T.A. Walsh, A.E. Morgan, T.D. Hey, Characterisation and molecular cloning of a proenzyme form of a ribosome-inactivating protein from maize. Novel mechanism of proenzyme activation by proteolytic removal of a 2.8-kilodalton internal peptide segment, (1991) *Journal of Biological Chemistry*, **266** 23422-23427.

K-W. Wan, B. Malgesini, I. Verpilio, P. Ferruti, R. Duncan, The effect of salt form on the membrane activity of endosomolytic poly(amidoamine)s, (2002) *Proceedings of the 29th International Symposium of Controlled Release and Bioactive Materials*, Seoul, Korea. **29**, #179.

R. Wattiaux, M. Jadot, M-T. Warnier-Pirotte, S. Wattiaux-De Coninck, Cationic lipids destabilise lysosomal membrane *in vitro*, (1997) *FEBS*, **417** 199-202.

R. Wattiaux, N. Laurent, S. Wattiaux-De Coninck, M. Jadot, Endosomes, lysosomes: their implication in gene transfer, (2000) *Advanced Drug Delivery Reviews*, **41** 201-208.

S.R. Wedge, Mechanism of action of polymer-anthracyclines; potential to overcome multidrug resistance. PhD Thesis, University of Keele, UK, 1991.

M.A. Wolfert, L.W. Seymour, Atomic force microscopic analysis of the influence of the molecular weight of poly-L-lysine on the size of polyelectrolyte complexes formed with DNA, (1996) *Gene Therapy*, **3** 269-273.

M.A. Wolfert, P.R. Dash, O. Nazarova, D. Oupicky, L.W. Seymour, S. Smart, J. Strohalm, K. Ulbrich, Polyelectrolyte vectors for gene delivery: influence of cationic polymer on biophysical properties of complexes formed with DNA, (1999) *Bioconjugate Chemistry*, **10** 993-1004.

G.Y. Wu, C.H. Wu, Receptor-mediated in vitro gene transformation by a soluble DNA carrier system, (1987) *Journal of Biological Chemistry*, **262** 4429-4432.

G.Y. Wu, C.H. Wu, Receptor-mediated delivery of foreign genes to hepatocytes, (1998) *Advanced Drug Delivery Reviews*, **29** 243-248.
Y. Xu, F.C. Szoka Jr., Mechanism of DNA release from cationic liposome/DNA complexes used in cell transfection, (1996) *Biochemistry*, **35** 5616-5623.

Y. Yang, H.C.J. Ertl, J.M. Wilson, MHC class I-restricted cytotoxic T lymphocytes to viral antigens destroy hepatocytes in mice infected with E1-deleted recombinant adenoviruses, (1994) *Immunity*, **1** 433-442.

H. Yoo and R.L. Juliano, Enhanced delivery of antisense oligonucleotides with fluorophore-conjugated PAMAM dendrimers, (2000) *Nucleic Acids Research*, **28** 4225-4231.

R.J. Young, P.A. Lovell, *Introduction to polymers*, R.J. Young, P.A, Lovell, Ed., Chapman & Hall, London, U.K. 1996

S. Zalipsky, C. Lee, Use of functionalised poly(ethylene glycol)s for modification of polypeptides, In: *Poly(ethylene glycol) Chemistry. Biotechnical and Biomedical Applications*, J.M. Harris, Ed., Plenum Press: New York, USA and London, England, 1992 p. 347-370.

O. Zelphati, F.C. Szoka Jr, Mechanism of oligonucleotide release from cationic liposomes, (1996) *Proceedings of the National Academy of Science of the United States of America*, **93** 11493-11498.

J.Z. Zhang, B.A. Daveltov, T.C. Sudhof, R.G.W. Anderson, Synaptogamin I is a high affinity receptor for claithrin AP-2: implications for membrane recycling, (1994) *Cell*, **78** 739-750.

G. Zuber, E. Dauty, M. Nothisen, P. Belguise, J-P. Behr, Towards synthetic viruses, (2001) *Advanced Drug Delivery Reviews*, **52** 245-253.

N. Zuidam, G. Posthuma, E.T.J. De Vries, D.J.A. Crommelin, W.E. Hennink, G. Storm, Effects of physicochemical characteristics of poly(2-(dimethylamino)ethyl

methacrylate)- based polyplexes on cellular association and internalisation, (2000) *Journal of Drug Targeting*, **8** 51-66.

APPENDIX

List of abstracts and publications

Papers

P. Ferruti, S. Manzoni, S.C.W. Richardson, R. Duncan, N.G. Pattrick, R. Mendichi, M. Casolaro, Amphoteric linear poly(amidoamine)s as endosomolytic polymers: correlation between physico-chemical and biological properties, (2000) *Macromolecules*, **21** 7793-7800.

S.C.W. Richardson, N.G. Pattrick, S. Man, P. Ferruti, R. Duncan, Poly(amidoamine)s as potential non-viral vectors: ability to form interpolyelectrolyte complexes and to mediate transfection *in vitro*, (2001) *Biomacromolecules*, **2** 1023-1028.

N.G. Pattrick, S. Richardson, M. Casolaro, P. Ferruti R. Duncan, Poly(amidoamine)-mediated intracytoplasmic delivery of ricin A-chain and gelonin, (2001) *Journal of Controlled Release,* **77** 225-232.

N.G. Pattrick, S.C.W. Richardson, M. Casolaro, P. Ferruti, R. Duncan, Ability of poly(amidoamine)s to disrupt isolated rat liver lysosomes after administration *in vivo*, 'in preparation'.

Abstracts

N.G. Pattrick, S.C.W. Richardson S. Manzoni, P Ferruti, R. Duncan, Poly(amidoamine)-mediated intracytoplasmic delivery of ricin A-chain and gelonin toxins, (2000) *Proceedings of the 4th International Symposium of Polymer Therapeutics,* London. UK. p. 77.

N.G. Pattrick, S.C.W. Richardson, P. Ferruti, R. Duncan, Poly(amidamine)-mediated intracytoplasmic delivery of ricin A-chain and gelonin toxins, (2000) *Journal of Pharmacy and Pharmacology* **52** (supplement) p 53.

N.G. Pattrick, P. Ferruti, R. Duncan, Demonstration of poly(amidoamine)-mediated lysosomal membrane perturbation after administration to rats *in vivo*, (2001) *Proceedings of the 28th International Symposium of Controlled Release and Bioactive Materials*, San Diego, USA. **28**, p. 864-865.

N.G. Pattrick, S.C.W. Richardson, A. Hann, P. Ferruti, R. Duncan, Quantitating the intracellular fate of poly(amidoamine)s and demonstrating their ability to modulate permeability of the rat liver lysosomal membrane after intravenous administration to rats, (2002) *Proceedings of the 5th International Symposium of Polymer Therapeutics,* Cardiff, UK. 2002 p. 80.